Novel Mechanisms of Glucolipotoxic Pancreatic Beta Cell Death

Katie Hanna

A thesis submitted in partial fulfilment of the requirements of the Nottingham Trent University for the degree of Doctor of Philosophy

Nottingham Trent University

10th July 2018

Copyright Statement

Contents

Data in this thesis has contributed to the following publications;

Bagnati M, Ogunkolade BW, Marshall C, Tucci C, Hanna K, Jones TA, Bugliani M, Nedjai B, Caton PW, Kieswich J, Yaqoob MM, Ball GR, Marchetti P, Hitman GA, Turner MD. Glucolipotoxicity initiates pancreatic β-cell death through TNFR5/CD40-mediated STAT1 and NF-κB activation. Cell Death & Disease. 2016;7:e2329

Cripps MJ, Hanna K, Lavilla C, Sayer S, Caton PW, Sims C, Girolamo LD, Sale C, Turner MD. Carnosine scavenging of glucolipotoxic free radicals enhances insulin secretion and glucose uptake. Scientific Reports. 2017;7:13313. doi:10.1038/s41598-017-13649-w.

Acknowledgements

The work was funded by Diabetes UK and undertaken at Nottingham Trent University.

I would like to thank my supervisor Dr Mark Turner for giving me the opportunity to complete this PhD and offering support and guidance throughout the project.

I would like to thank Akash Singh, Michael Cripps, Tatjani Baranov, and Marta Bagnati for providing data that has been used in this project. Tania Jones for generating MetaCore™ maps and Professor Graham Ball for generating bespoke interaction pathways. I would like to acknowledge other members of the lab for their support including, Charlie Lavilla Jr, Laura Lopez, and especially Dr Sergio Colombo who was a great support in the lab throughout the course of this project and always offered assistance whenever needed.

Clare Coveney and David Boocock for assistance, support and patience with Co-IP and mass spectrometry data generation and analysis.

Simon Hanna for assisting with illustrations.

For the unwavering and unconditional support of my partner, friends and family, especially my parents. Thank you.

List of Figures

List of Tables

Abbreviations

3-NT	3-Nitrotyrosine
4-HNE	4-Hydroxy-2-nonenal
α-KG	Alpha Ketoglutarate
Δ	Delta
ACC	Acetyl-CoA carboxylase
ACLY	ATP-Citrate Lyase
ADP	Adenosine diphosphate
ATP	Adenosine Triphosphate
BSA/BCA	Bovine Serum Albumin/Bovine Calf Albumin
CAT	Catalase
CD40	Cluster of differentiation 40 (AKA TNFR5)
cDNA	Complimentary DNA
Cis	Cystine
CN ½	Carnosinase 1/2
Ct	Cycle Threshold
CTXN-1	Cortexin-1
DD	Death Domain
DMSO	Dimethyl Sulfoxide
ELISA	Enzyme-linked Immunosorbent Assay
ER	Endoplasmic Reticulum
ERGIC	ER-Golgi intermediate compartment
FAS	Fatty Acid Synthase
GDP	Guanosine diphosphate
GTP	Guanosine-5'-triphosphate
GLT	Glucolipotoxic
GPx	Glutathione Peroxidase
GSIS	Glucose Stimulated Insulin Secretion
GTPBP4	GTP Binding Protein 4
HATs	Histone Acetyl Transferases
His	Histidine
HNF4α	Hepatic Nuclear Factor 4 alpha
HNF1 α	Hepatic Nuclear Factor 1 alpha

ID4	Inhibitor of DNA-binding 4
IDH2	Isocitrate dehydrogenase 2
IDH3	Isocitrate dehydrogenase 3
IFNγ	Interferon Gamma
IL-1β	Interleukin 1 Beta
ILVBL	IlvB Acetolactate Synthase Like
iNOS	Inducible Nitric Oxide Synthase
Lys	Lysine
MAF-1	Homolog, Negative Regulator of RNA Polymerase III
MODY	Maturity-Onset Diabetes of the Young
MICAL-1	Microtubule Associated Monooxygenase, Calponin And LIM Domain Containing 1
mRNA	Messenger Ribonucleic acid
MVP	Major Vault protein
NF-κB	Nuclear Factor Kappa B
NO	Nitric Oxide
NOS	Nitric Oxide Synthase
$O_2\cdot$	Superoxide
$ONOO^-$	Peroxynitrite
PDX-1	Pancreas/duodenum homeobox protein 1
qPCR	Quantitative Polymerase Chain Reaction
RCS	Reactive Carbonyl Species
RNA	Ribonucleic acid
ROS	Reactive Oxygen Species
RPMI-1640	Roswell Park Memorial Institute 1640
RT-qPCR	Real Time Quantitative Polymerase Chain Reaction
SC4MOL	Methylsterol Monooxygenase 1
SEM	Standard Error of the Mean
siRNA	Short Interfering Ribonucleic acid
ssRNA	Scramble Sequence Ribonucleic acid
T1D	Type 1 Diabetes
T2D	Type 2 Diabetes
TEMED	Tetramethylethylenediamine
TFAM	Transcription factor A, mitochondrial
TNF	Tumour Necrosis Factor

TNFR	Tumour Necrosis Factor Receptor
TRADD	TNFRSF1A associated via death domain
TRAFs	Tumour necrosis factor receptor-associated factors
Zn	Zinc

Abstract

Glucolipotoxicity (GLT) is the term given to the combined and damaging effect of increased glucose and fatty acid levels on pancreatic beta cells (β-cells) (Poitout et al, 2010). There is mounting evidence that glucolipotoxicity is the cause of the decline in β-cell function found in type 2 diabetes (T2D). T2D is a chronic metabolic disorder characterised by sustained elevated blood glucose and free fatty acids, with a continuously increasing prevalence (Olokoba et al, 2012). It is estimated 415 million people currently are living with diabetes and 193 million are undiagnosed, of those 90% are T2D cases. (chatterjee et al, 2017).

There are multiple aims in this thesis including the identification of GLT-induced inflammatory pathways of the pancreatic β-cell resulting from NF-κB activation. To identify novel transcription factors associated with GLT-induced reduction in insulin secretion and insulin gene expression and whether their expression is associated with the presence CD40. To observe whether the addition of carnosine to cultured cells can prevent/reverse the up-regulation in GLT-induced factors which potentially result in β-cell damage. Finally, to observed whether GLT can induce histone modifications resulting from disruption in the TCA cycle.

To mimic GLT conditions INS-1 rat pancreatic β-cells were cultured in media supplemented with 28mM glucose, 200µM palmitic acid and 200µM oleic acid. The results showed following 5-day incubation ±GLT, there was an increase in TNF receptor CD40 and a CD40-dependent increase in NF-κB. Further to this exposure of INS-1 cells to GLT conditions resulted in a 3.7-fold increase in iNOS mRNA and increased 4-HNE and 3-NT adduct formation (43.4% and 33% respectively) indicating potential GLT-induced β-cell damage. The addition of 10mM carnosine was able to prevent/reverse the up-regulation of GLT-induced NF-κB activity, iNOS protein expression and 4-HNE and 3-NT adduction, identifying it as a potential therapeutic strategy for T2D.

GLT-induced up-regulation of CD40 is also shown to be involved in the modulation of various genes, including insulin. siRNA down-regulation of CD40 resulted in increased insulin gene expression via modulation of ID4. Independent of CD40, a protein usually associated with MODY is observed. GLT results in 33.3% down-regulation of HNF4α, which has a knock-on effect on Rab protein expression resulting in down-regulation of insulin secretion. There by indicating that HNF4α is important in normal insulin secretion.

This research found that GLT can result in acetylation of histones H3 and H4, subsequent to TCA cycle dysregulation and disruption to fatty acid synthesis and cholesterol biosynthesis pathways, indicating that GLT can affect gene transcription.

Chapter 1

Introduction

1.0 CHAPTER 1: Introduction

1.1 Physiology of Pancreatic Islets of Langerhans

The pancreas is located at the rear of the abdomen behind the stomach and is connected to the duodenum via a tube known as the pancreatic duct. The pancreas is unique in that it is possesses both endocrine and exocrine function. It is made up of 95% exocrine tissue and is therefore called an exocrine gland, but it is made up of 5% endocrine tissue (Das et al, 2014). It is comprised of combination of cell types that make up the islets of Langerhans. The islets of Langerhans are made up by 4 cells types; alpha cells, beta cells (β-cells), delta cells and gamma cells (Kulkarni RN, 2004). Alpha cells which account for 20% of total islet cells and are responsible for producing glucagon, which is secreted when blood glucose concentrations fall too low. Glucagon is then converted to glucose to restore glucose homeostasis. Pancreatic β-cells make up most of the cells found in the islet at approximately 70%. Beta cells are responsible for producing insulin. Delta cells making up <10% of total islet cells which produce somatostatin, the function of somatostatin is to inhibit the secretion of both insulin and glucagon. Gamma cells produce pancreatic polypeptide and make up <5% of total islet cells. Together these cells form micro-organs known as islets of Langerhans that are distributed throughout the pancreas, making up 2-3% of the total pancreatic mass (Striegel et al, 2015) and have a key role in glucose homeostasis (Wang et al, 2013). Both insulin and glucagon play pivotal roles in maintaining glucose homeostasis and have important metabolic targets. The major function of insulin and glucagon is to together finely regulate blood glucose concentrations to avoid prolonged hyper or hypoglycaemia. In order to do this insulin inhibits and glucagon stimulates glycogenolysis, gluconeogenesis, lipolysis, and ketogenesis.

Gluconeogenesis occurs in the liver and is the mechanism of the breakdown of glycogen to form glucose which is released into circulation. Gluconeogenesis a biochemical mechanism that synthesises glucose from amino acids. Lipolysis is a process where fatty acids and glycerol are released into circulation from stored triglycerides. Ketogenesis is the synthesis of ketones in the liver that are released into circulation formed from free fatty acids (Robertson and Harmon, 2007).

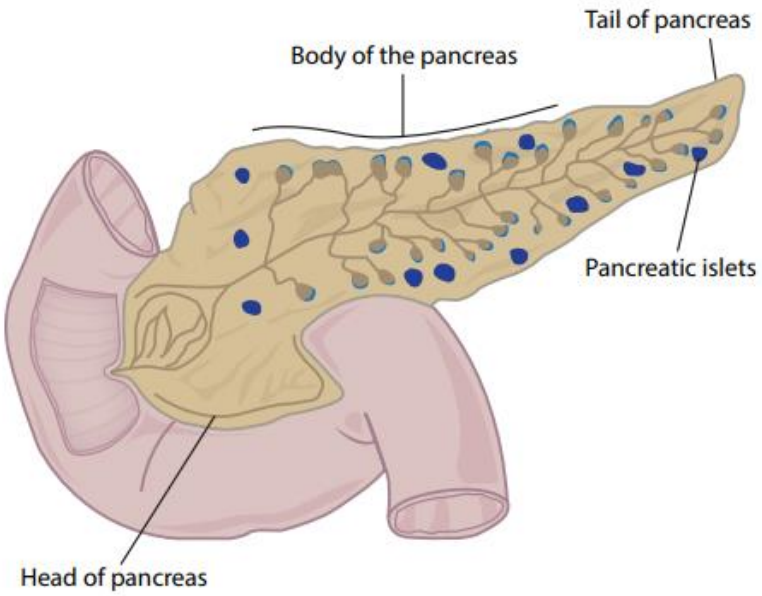

***Figure 1.1 Schematic of Pancreas**. Illustration of Pancreas identifying location of the pancreatic islets. Adpated from Medical Dictionary.*

1.1.1 Insulin biosynthesis

Insulin is a hormone that is synthesised in and secreted from pancreatic β-cells. Insulin has a molecular weight of 5.8kda and is made up of 51-amino acids, the insulin gene however, encodes a precursor of insulin that is constructed of 110-amino acids and is called preproinsulin. The preproinsulin structure contains a hydrophobic N-Terminal signal peptide which interacts with cytosolic ribonuclear-protein signal recognition particles. It is the responsibility of these recognition particles to allow the translocation of preproinsulin across the rough endoplasmic reticulum membrane and into the lumen, via the peptide conducting channel. During this translocation, the N-Terminal signal peptide is cleaved by a signal peptidase resulting in proinsulin. To yield insulin, proinsulin must undergo folding and the formation of three disulphide bonds. Following the bond formation, the folded proinsulin is cleaved resulting in insulin and C-peptide (Fig 1.2). Both insulin and C-peptide are stored in secretory granules (Zhuo et al 2013).

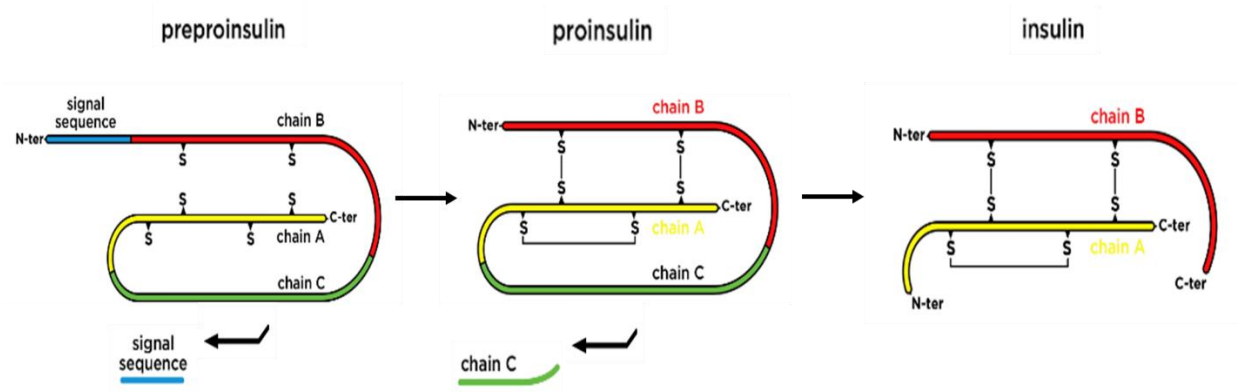

Figure 1.2 Insulin Biosynthesis. *Insulin is initially translated as preproinsulin that contains a hydrophobic amino-terminal signal sequence necessary for entering the ER. In the ER, the preproinsulin signal sequence is proteolytically degraded to form generating proinsulin. Following development of the three-dimensional conformation, the folded proinsulin is translocated from the ER to the Golgi apparatus where proinsulin enters immature secretory vesicles and is cleaved to yield the A chain and B chain of insulin and C-peptide. Figure adapted from Beta Cell Biology Consortium website.*

1.1.2 Insulin secretion

The main stimuli for pancreatic β-cells to secrete insulin is elevated blood glucose concentration following the intake of food. Blood glucose is increased from basal level of 5.0 mM/L, to the post prandial level of approximately 10.4 mM/L following food intake (Rorsman et al, 2000). Circulating blood glucose is taken into the pancreatic β-cell via a transporter that is located on the cell surface. The main rodent β-cell glucose transporter is GLUT2 or SLC2A2 (McCulloch et al, 2011), whereas the main glucose transporters in humans are GLUT1 and/or GLUT3 (De Vos et al, 1995) Subsequent to its up-take, glucose undergoes glycolysis resulting in the generation of adenosine triphosphate (ATP). This alters the intracellular ATP/ADP ratio which in turn causes the closure of the ATP-sensitive potassium channels. When the β-cell is unstimulated the ATP-sensitive potassium channels remain open to ensure the stability and maintenance of resting potential of -70mV by transporting positively charged K^+ ions out of the cell, down its concentration gradient (Rorsman et al, 2000). The closure of the potassium channel and the resulting increase in K^+ ions cause the depolarisation of the cell membrane and the opening of the voltage-dependent L-type calcium channels. The increase in intracellular calcium concentration triggers the fusion of insulin-containing granules with the β-cell membrane and the ultimately the release of insulin (Fig. 1.3) (Röder et al, 2016).

Insulin is secreted in order to maintain glucose homeostasis and stored within the β-cell in pre-formed granules (Cheng et al, 2013).The insulin-containing granules release their contents following fusion with the cell membrane, the key molecules responsible for this fusion are synaptosomal-associated

protein of 25kDa (SNAP-25), syntaxin-1 and synaptobrevins-2 also known as vesicle-associated membrane protein (VAMP2), all of which belong to a superfamily of soluble N-ethylmeleimide-sensitive factor attachment protein (SNAP) receptors (SNAREs). Together with the Sec1/MUNC18-like proteins they form the SNARE complex (Röder et al, 2016). There are two types of SNAREs, categorised based on the membrane in which they are associated; v-SNAREs are found on vesicles and t-SNAREs are located on the target membrane. The formation of the v- and t-SNARE complex is responsible for the docking (Regazzi et al, 1995). To initiate granule fusion with the membrane synaptobrevin-2, a v-SNARE that is integrated in the vesicle membrane fuses with t-SNAREs syntaxin-1 and SNAP-25 which are located in the target cells membrane, with MUNC-18 playing a key role (Röder et al, 2016).

The insulin secretion process is biphasic, and the secretory granules are stored in three separate pools known as the docked, reserve and readily releasable pools. The docked pool is used in the first phase. The first phase peaks at approximately 5 minutes following glucose stimulation and it is in the first phase where most of the insulin is secreted. The second phase occurs considerably more slowly, where the remainder of the insulin is secreted (Röder et al, 2016). The second phase uses the reserve pool of secretory granules and is less robust but can be sustained for a number of hours if elevated blood glucose levels persist (Jewell et al, 2010). The two phases use different pools of insulin containing granules, the first phase uses membrane fused granules known as the readily-usable pool and the second phase uses unfused granules from deeper with in the cell known as the storage pool. The unfused granules in the storage pool replenish the readily-usable pool if they are not used in the second phase (Jewell et al, 2010).

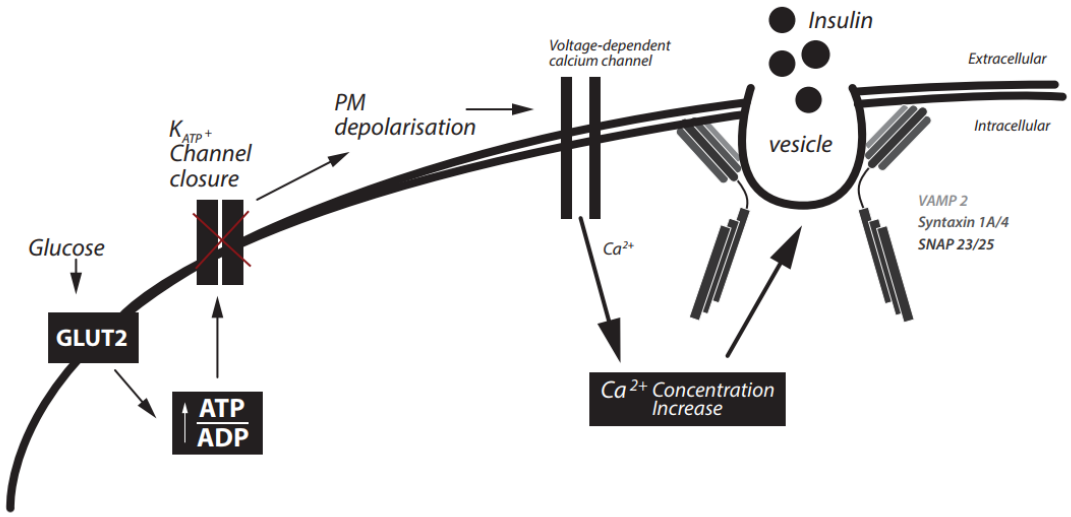

Figure 1.3: Glucose-stimulated insulin secretion from pancreatic β-cell*. Glucose enters the cell via the constitutively active GLUT2 membrane located in the plasma membrane. The glucose gets metabolised which increases the ATP:ADP ratio and leads to closure of the ATP-dependent potassium channel. The closing of the ATP-dependent potassium channels results in depolarisation of the plasma membrane and the opening of the voltage-dependent calcium channel, the opening of this channel allows calcium to influx into the cell resulting in an increase in intracellular calcium concentration levels. Following this, SNARE proteins enable vesicle fusion for insulin release. Adapted from Jewell et al, 2010.*

1.1.3 Insulin Signalling

The hormone known as insulin is able to stimulate glucose uptake into skeletal muscle and adipose tissue, which is pivotal for the maintenance of whole-body glucose homeostasis (Leney et al, 2009). Glucose is transported into muscle cells via facilitated diffusion by the main glucose transporter known as GLUT4. This transporter is a protein that is regulated by a number of factors including insulin, glucose concentration, muscle contraction and hypoxia (Klip et al, 1992). There are currently 13 glucose transporters, GLUT1-12 and HMIT known in the human genome, however GLUT4 is the most highly expressed in skeletal muscle and adipose tissue but not the only expressed GLUT transporter. It is known that in skeletal muscle GLUT5 and GLUT12 may also play a part in glucose up take and GLUT8, GLUT12 and HMIT are also thought to contribute to glucose up take in adipose tissue (Huang et al, 2005).

The tissue that is primarily responsible for post-prandial glucose utilisation is skeletal muscle, which accounts for up to 75% of glucose disposal. In skeletal muscle glucose up take normally occurs in one direction due to rapid intracellular metabolism of glucose into glucose-6-phosphate and subsequent glycolysis (Klip et al, 1992). Glucose is also taken up via insulin signalling in adipose tissue. Mammalian adipose tissue has numerous functions including; insulation and the production of hormones. However, its most important role is to store nutrients in an efficient and compact form and be able to mobilise stored energy for use when needed. Adipocytes have the ability to extract both lipids and sugars from the blood circulation, however, extracting glucose is more highly regulated which means glucose transport is rate limiting. Glucose transport into the adipocyte results in glucose oxidation and ATP production as a result. It is also the basis for fatty acid synthesis and the three-carbon chain that is required for esterification of fatty acids that are extracted from the blood (Summers et al, 2000).

Glucose up take into the cell via GLUT 4 requires the activation of the insulin receptor, tyrosine kinase. This activation then leads to activation of phosphatidylinositol $(PI)^2$ 3-kinase pathway. PI 3-kinase then phosphorylates phosphatidylinositol 4,5 bisphosphate ($PI(4,5)P_2$) and also has the ability to increase the intracellular accumulation of phosphatidylinositol 3,4,5-trisphosphate (PIP_3) at the plasma membrane. It is this accumulation of PIP_3 that results in the activation of Akt via two intermediate kinases known as 3-phosphoinositide-dependentproteinkinase (PDK1) and Rictor/mTOR (Huang and Czech, 2007) which is required for the translocation of GLUT4 to the plasma membrane (Ijuin and Takenawa, 2012).

GLUT4 moves between the cytoplasmic storage site and the plasma membrane where most of the GLUT4 is located intracellularly when insulin signalling is not present, this is because the basal rate of exocytosis is exceeded by the rate of endocytosis. When insulin signalling occurs it significantly increases the rate of exocytosis, which in turn leads to the translocation of up to 50% of all the intracellular GLUT4 protein to the cell surface where it enables the uptake of glucose (Huang and Czech, 2007).

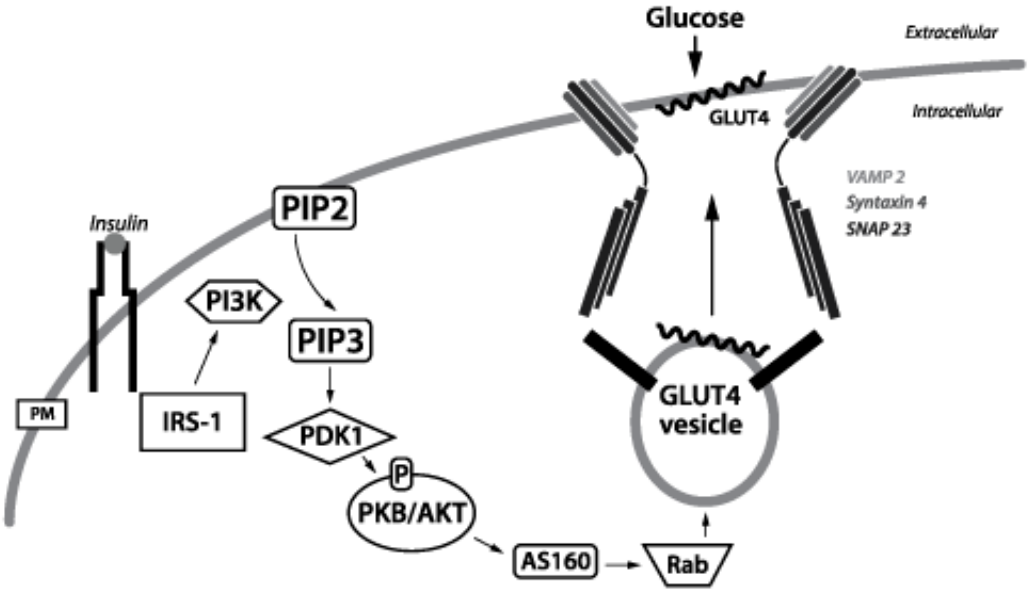

Figure 1.4 Glucose uptake via GLUT4 translocation. *Extracellular insulin binds to the alpha-subunit of the insulin receptor, this results in activation of the beta subunit kinase activity and the recruitment of IRS-1/ IRS-1 recruits PI3K. PI3K employs PDK1 to the plasma membrane where it serves to activate AKT, which in turn phosphorylates PIP2 to generate PIP3, which attracts PDK1 to the plasma membrane, where it activates AKT. The role of AKT is to phosphorylate AS160 which targets Rabs present on GLUT4 containing vesicles. Vesicle fusion occurs via facilitation of SNARE proteins, resulting in GLUT4 incorporation into the plasma membrane for glucose uptake. Adapted from Jewell et al, 2010.*

1.1.4 Insulin degradation

Both insulin uptake and degradation are features of insulin-sensitive tissues. Insulin has a plasma half-life of between 4 and 6 minutes which enables the hormone to respond rapidly to changes in blood glucose concentrations (Duckworth et al, 1998). Under normal conditions almost all the secreted insulin is degraded intracellularly via receptor-mediated internalisation mechanisms. Once insulin is bound to the receptor as part of normal insulin signalling, it can either be recycled to circulation or internalised resulting in insulin degradation (Duckworth et al 1998). During receptor mediated degradation, the insulin receptor binds insulin and internalises it into endosomes. Once formed, endosomes rapidly acidify which results in the dissociation of insulin from the receptor and its degradation. The insulin receptor is then recycled to the cell surface along with either degraded, partially degraded or fully intact insulin (Pivovarova et al, 2015).

A major site for insulin degrading enzyme (IDE)-mediated insulin degradation is the liver, which is responsible for clearing approximately 80% of endogenous insulin. IDE is a zinc-metalloendopeptidase

that can cleave and inactivate insulin and many other peptides involved in regulating blood glucose (Farris et al, 2003). IDE is made up of two domains of equal size, IDE-N and IDE-C that are joined together by a 28-amino acid residue loop (Hulse et al, 2009). The two domains come together to form an enclosed catalytic chamber and engulf the peptide substrate (Tang W, 2016).

1.2 Diabetes

Diabetes is group of diseases associated with metabolic dysfunction, that are all categorised by chronic and continual elevated glucose levels, known as hyperglycaemia. The hyperglycaemia that is found in diabetes results a dysfunction in insulin action, secretion or a combination of both and can lead to long-term complications including kidney damage, retinopathy, nerve damage, amongst others (American diabetes Association). Historically the diagnosis of diabetes was based on fasting blood glucose levels of higher than 7mmol/L, any blood glucose level above 11.1mmol/L, or an abnormal glucose test. However, this has now been modified to include glycated haemoglobin (HbA_{1C}) levels of 6.5% or higher. There are three main type of types of diabetes; Type 1 diabetes, Type 2 diabetes and gestational diabetes (World Health Organisation).

Type 1 diabetes is triggered by an immune-mediated destruction of the insulin producing β-cells, due to the development of islet autoantibodies and accounts for between 5-10% of all diabetic cases (Atkinson et al, 2014 and American association of diabetes). This type of diabetes is one of the most common chronic diseases of childhood, but it can be diagnosed at any age. The peak of diagnosis however is between the ages of 5-7 and at or near puberty (Atkinson et al, 2014).

Type 2 diabetes is the most common form of diabetes and has an increasing prevalence worldwide (Dardano et al, 2014). Type 2 diabetes development is connected with genetic factors and/or environmental factors including life style habits such as a high fat diet and lack of exercise that lead to decreased insulin secretion or insulin resistance and resultant insufficient insulin action (Seino et al, 2010).

Gestational diabetes is a disorder involving glucose metabolism that develops during pregnancy, with up to 5% of pregnancies affected (Seino et al, 2010 and Diabetes UK). Gestational diabetes usually arises in the second or third trimester due the body producing enough insulin to meet the increased demands of pregnancy. The risk factors involved with developing gestational diabetes include excess weight as women who are overweight or obese have a greater risk of gestational diabetes. (Diabetes

UK). Glucose metabolism disorders often return to normal after pregnancy but there is an increased risk in developing type 2 diabetes in the future for both mother and child (Seino et al, 2010).

Type 2 diabetes is the primary focus of this research. Type 2 diabetes accounts for the majority of all cases with 90% of diabetes being type 2 diabetes (diabetes UK).

1.2.1 Type 2 diabetes

Type 2 diabetes (T2D) is characterised by both hyperglycaemia and hyperlipidaemia, which together contribute to the detrimental effect known as glucolipotoxicity. The onset of type diabetes is primarily caused by life style and genetics. The main risk factor associated with type 2 diabetes is being overweight or obese, with obesity accounting for approximately 80-85% of the overall risk (Diabetes UK). In England, data suggests that 90% of people with type 2 diabetes, aged between 16-54 are obese, whereas only 10% of people with type 2 diabetes are a healthy weight or underweight (Public Health England). Life style factors that contribute to the onset of diabetes independently of obesity include being physically inactive, cigarette smoking, excessive alcohol consumption and non-life style dependent factors that can result in T2D include ethnicity and age. (Hu et al, 2001).

As well as a reduced life expectancy by approximately 10 years, there are other complications associated with uncontrolled diabetes. Diabetic retinopathy is currently the leading cause of blindness among adults in the western world and is characterised by the growth of vascular and retinal lesions that is caused by chronic exposure to high blood glucose concentrations. Another common complication cardiovascular disease. Patients with type 2 diabetes have higher atherosclerotic plaque formation, higher atheroma volume, and smaller coronary artery lumen diameter than non-diabetic individuals (Low Wang et al, 2016).

Table 1.1 Risk of complications associated with T2D. *Associated comorbidity and risk of development associated with T2D. Adapted from Public Health England.*

Complication	Additional risk of complication among people with type 2 diabetes
Angina	+76%
Myocardial infarction	+55%
Heart failure	+74%
Stroke	+34%
Renal replacement therapy	+164%
Minor amputation (below ankle)	+337%
Major amputation (above ankle)	+222%

1.2.2 Beta cell compensation

Obesity is characterised by insulin hypersecretion and insulin resistance (Camastra et al, 2005), however, only 15-20% of obese individuals develop type 2 diabetes as euglycaemia, also known as normoglycaemia is maintained by beta cell compensation. Type 2 diabetes develops when β-cells are unable to secrete sufficient insulin to overcome insulin resistance (Terauchi et al, 1997). The amount of insulin that is secreted by β-cells can vary but is dependent stimuli such as glucose concentrations and must meet the insulin demand from target tissues. Euglycaemia is maintained by a feedback loop between insulin sensitivity and insulin secretion. An increase in insulin demand occurs during normal body growth and to meet this demand the β-cell adapts both its mass and function to secrete sufficient insulin to maintain blood glucose homeostasis. The increase in β-cell mass in obesity is a compensatory process, the β-cell masses of obese but non-diabetic or pre-diabetic subjects are larger than lean, normoglycaemic individuals. The β-cell mass of obese individuals is known to increase by 30-40% with insulin secretion increasing by 100% (Plaisance et al, 2014).

Glucose is considered to be the dominant driving force of increased β-cell mass during β-cell compensation with increased glucose glycolysis occurring in the β-cell (Zhang et al, 2016). The enzyme that is responsible for the glycolysis of glucose in the beta cell is glucokinase (Gck), which subsequently leads to the up-regulation of Irs2 expression as a result of increased cytosolic calcium levels. Increased

Irs2 activity has the ability to activate a signalling cascade that enhances β-cell replication, via Fox01 and increases β-cell survival via PKB/Akt (Weir and Weir, 2007).

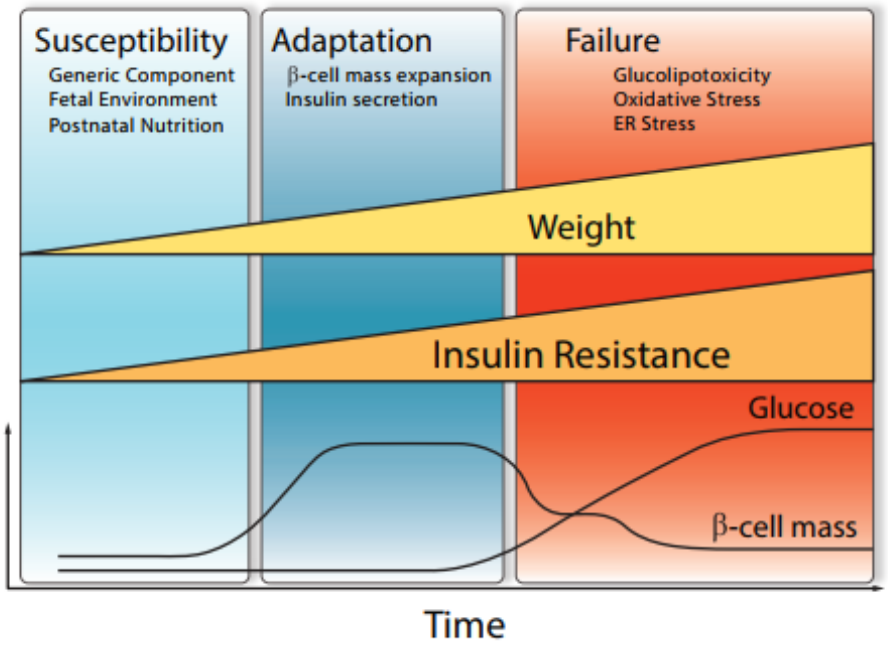

***Figure 1.5 Beta cell adaptation to obesity and onset of diabetes**. Beta cells compensate by increasing in mass and function in response to increases blood levels in obese individuals. However, when compensation fails the onset of hyperglycaemia and diabetes begin, which can result in beta cell failure. Adapted from Alejandro EU, 2015.*

1.2.3 Beta cell mass in type 2 diabetes

A consistent state of glucolipotoxicity results in pancreatic β-cell dysfunction, including impairment of insulin secretion, reduction in insulin gene expression and apoptosis (Samesh et al, 2013). Subsequent to β-cell compensation during obesity and pre-diabetes, patients with type 2 diabetes demonstrate a decrease in beta cell mass of up to 65% by comparison to non-diabetic BMI-matched individuals (Plaisance et al, 2014).

1.2.4 Inflammation in diabetes

An increase in glucose concentration and circulating free fatty acids has the potential to trigger an inflammatory response in many tissues, not only the pancreas. It has been postulated that the initial

inflammatory response is initiated for β-cell repair and regeneration (Donathet al, 2009), but in type 2 diabetes it results in β-cell death. Interleukin-1β (IL-1β) is a proinflammatory cytokine that plays a crucial role in the inflammatory response (Fig. 1.6). IL-1β is known to be induced by elevated glucose levels (Maedler et al, 2002). It is produced by most cell types as an inactive precursor known as pro-IL-1β in response to molecular motifs called pathogen associated molecular patterns (PAMPs) and regulate gene expression pathways via pattern recognition receptors (PRRs). The production of pro-IL-1β is known as the priming step, in order for secretion, the newly primed cell must interact with another PAMP or a danger associated molecular pattern (DAMP) that is released from a cell that has already undergone apoptosis to induce the secretion of active IL-1β (Lopez-Castejon and Brough, 2011). The effects of IL-1 cytokines are regulated by the IL-1 type I receptor (IL-1RI). Together with the IL-1 receptor accessory protein (IL-1RAcP) they combine to initiate signal transduction. The activation of this complex by IL-1 results in the expression of genes that play a further role in inflammation (O'Neill and Adinarello, 2000)

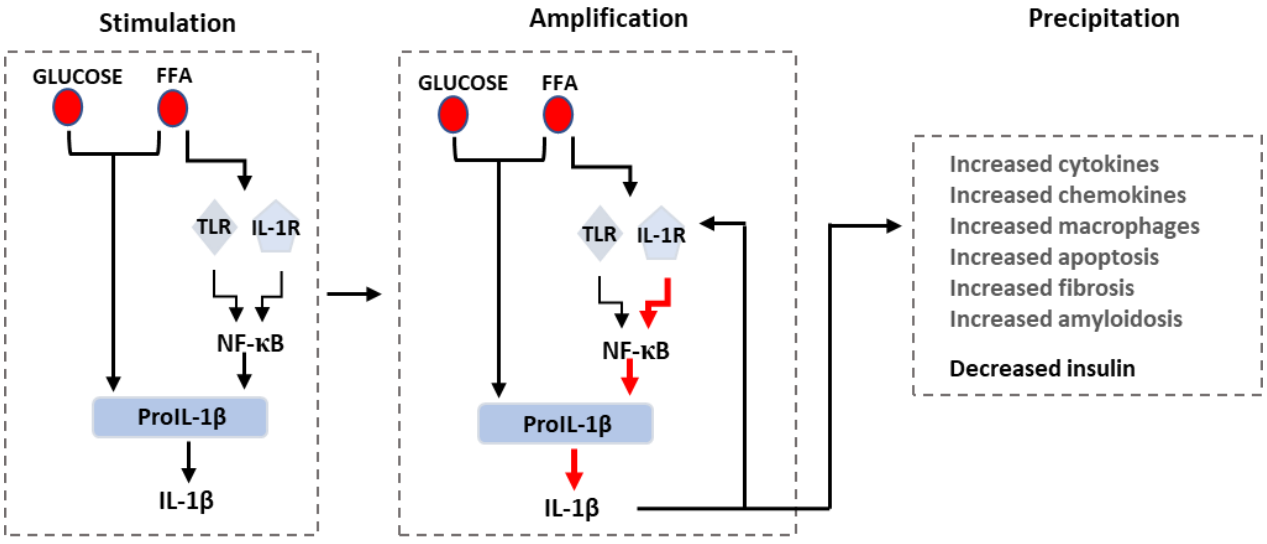

Figure 1.6 Glucose and free fatty acids result in beta cell dysfunction. *Increased glucose and fatty acids result in up-regulation of IL-1β release as part of the adaptive response (Stimulation). Chronic exposure of β-cells to glucose and fatty acids results in activation of IL-1R, which results in further release of IL-1β and activation of NF-κB via an auto stimulatory process (Amplification). The further activation and release of IL-1β results in cytokine and chemokine recruitment which can lead to increased macrophages, apoptosis, fibrosis and amyloidosis and reduction in insulin production. Adapted from Donath et al.2009.*

There are multiple homologues for IL-RI, which has resulted in the formation of a superfamily known as IL-1R/TLR superfamily, in which all members share a highly conserved cytosolic domain (TIR domain). A member of this superfamily is known as MyD88 which operates only in the cytosol and appears to be an adapter protein to members of the superfamily. MyD88 is known to connect the TIR domain of superfamily members to downstream signalling proteins via homotypic interactions (O'Neill and Adinarello, 2000). MyD88 is also a known recruiter and activates TRAF-6 via the recruitment of IRAK-1 and IRAK-2. This in turn can lead to the activation of kinases known as TAB-1 and TAK-2 that activate NIK resulting in the activation of NF-κB (O'Neill and Adinarello, 2000).

IL-1β is able to induce Fas expression (Maedler et al, 2002). Fas also known as CD95 or TNFR6 is a cell-death receptor that is able to induce cell apoptosis via a fas ligand (FasL). FasL are mostly expressed on activated T cells but are also constitutively expressed by beta cells, however beta cells do not express Fas under normal physiological conditions (Darville and Eizirik, 2001). FasL initiates programmed cell death via binding to its receptor and activating caspase-8, which cleaves procaspase-3 resulting in cell death (Jacobsen). It has also been considered that the activation of NF-κB is necessary for Fas activation to occur (Maedler et al, 2002) and in many instances NF-κB has been seen as a signalling mediator for IL-1. The way in which NF-κB becomes activated is by IL-1β interacting with its receptor which results in tyrosine kinase activity which in turn either directly or in directly phosphorylates IKB. The phosphorylated IKB releases NF-κB which translocate to the cytosol (Kwon et al, 1995).

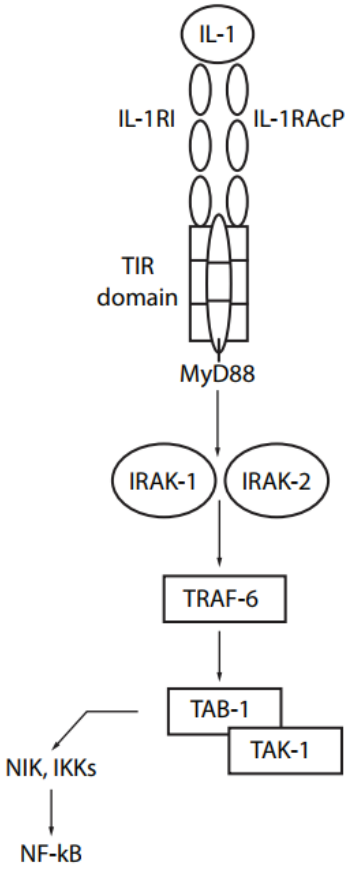

***Figure 1.7 IL-1 induced singnalling pathway**. IL-1 triggers a signalling pathway via a TIR domain and results in the activation of the transcription factor NF-κB. Adapted from O'Neil and Adinarello 2000.*

It is recognised that long-chain fatty acids are also able to stimulate IL-1β expression and induce IL-1-dependent cytokines such as IL-6 and IL-6, which alongside other proinflammatory cytokines such as TNF-α increased expression of various chemokines including; CXCL1 (KC), CXCL2 (MIP-2), MCP-1 and MIP-1α (Donath et al, 2009). CXCL1 and CXCL2 are chemoattractants for neutrophils to the site of inflammation. Neutrophils express the receptor CXR2 and both CXCL1 and CXCL2 both bind to the receptor (Fillipo et al, 2008).

1.3 Current treatments for Type 2 diabetes

Diabetes can be diagnosed based on the symptoms presented by the individual including polyurea, polydipsia, polyphagia and unexplained weight loss. There are also a number of tests that can be

conducted to diagnose prediabetes and diabetes. The diagnosis of prediabetes and type 2 diabetes can be made according to the level of glycated haemoglobin (HbA1c). According to guidelines outlined by the World Health Organisation a result considered non-diabetic is 6% or below (<42mmol/mol), a result considered pre-diabetic is 6-6.4% (42-47mmol/mol) and a result indicating the presence of type 2 diabetes is 6.5% or more (>48mmol/mol). Another test carried out to diagnose type 2 diabetes is the fasting plasma glucose test. This test is carried out following a 10 hour fast from both food and drink and measures the amount of glucose in a sample of blood. The world health organisation defines a non-diabetic result as <6.1mmol/l (110mg/dl), a pre-diabetic result is 6.1-6.9mmol/l (111-125mg/dl) and diabetic result is considered >7.0 mmol/l (>125mg/dl) (Reinehr T, 2013. Rosenbloom et al, 2008). There are currently multiple treatments available for type 2 diabetes that are described below.

1.3.1 Metformin

Metformin is the first line treatment for type 2 diabetes and is the most commonly prescribed type 2 diabetes treatment, taken by approximately 150 million people worldwide. It is also the only drug that can be used to treat pre-diabetes as it able to delay the onset of type 2 diabetes (Marin-Penalver et al, 2016. Pryor and Cabreiro, 2015).

Metformin is hydrophilic and therefore cannot passively diffuse through cell membranes, instead metformin relies upon the organic cation transporter-1 (OCT-1) for its clinical action. Once it has entered the hepatocyte metformin accumulates in the mitochondrial matrix, where it inhibits mitochondrial respiration at the respiratory chain complex-1. Because of this inhibition, ATP levels decrease, and ADP and AMP levels increase. The increase in AMP kinase activity increases insulin action and reduces hepatic gluconeogenesis therefore reducing blood glucose levels (Hostalek et al, 2015. Pryor and Cabreiro, 2015).

1.3.2 Sulphonlyureas

The function of sulphonlyureas is to stimulate release of insulin from pancreatic β-cells by binding to ATP-sensitive potassium channels (Aquilante CL, 2010). They act by binding to the specific sulphonyl receptor on pancreatic β-cells known as sulphonylureas receptor 1 (SUR1), which blocks the channel preventing the influx of potassium ions. The reduction in potassium ions results in membrane depolarisation and the opening of the calcium channel. The influx of calcium subsequently results in the exocytosis of insulin (Sola et al, 2015). Sulphonylurea drugs are only effective when there are

residual pancreatic β-cells present, as their main effect is to increase plasma insulin concentrations directly from the β-cell (Sola et al, 2015).

1.3.3 Gliptins (DPP-4 inhibitors) and Incretin Mimetics

Following the ingestion of food, neuroendocrine cells in the gastrointestinal tract release hormones such as incretins glucagon-like peptide (GLP-1) and glucose-dependent insulinotropic peptide (GIP), which play a part in the increase of nutrient-stimulated pancreatic insulin release, supress glucagon secretion and increase glucose disposal (Duez et al, 2012). However, gliptins also known as DPP-4 are cell surface serine proteases that cleave and inactivate peptides such as GLP-1 and GIP. There by using DPP-4 inhibitors there will be a reduction in the breakdown of GLP-1 and GIP and an increase in nutrient-stimulated insulin release and lower blood glucose (Kim et al, 2014).

1.3.4 GLP-1 agonists

Glucagon-like peptide-1 (GLP-1) is a peptide hormone secreted from endothelial L cells in the intestine following the intake of food. L cells are located in the mucosa of the intestine and function as a nutrient sensor and mediate the release of GLP-1 in response to glucose, fatty acids and amino acids. GLP-1 acts within the intestinal wall to activate reflexes that are a central part of gastric mobility and its role is to slow the gastric emptying, which augments insulin secretion. GLP-1 may also be found in the circulation and acts as a hormone at the islets of Langerhan in the pancreas to stimulate insulin secretion, however, GLP-1 has a short half-life as it is rapidly degraded by DPP-4 (Nadkarni et al, 2014. Heppner et al 2015). The GLP-1 receptor agonists elicit their action by directly interacting with the GLP-1 receptor and work to increase GLp-1 activity, rather than preventing its degradation (Heppner et al, 2015).

1.3.5 Sodium-glucose transporter 2 (SGLT2) Inhibitors

SGLT2 inhibitors act by inhibiting the renal glucose reabsorption resulting in glucose excretion in the urine and subsequent reduction in plasma glucose (Nauck MA, 2014). Glucose reabsorption from the glomerular filtrate occurs in a process that is insulin-independent and is mediated by sodium-glucose co-transporters (SGLT) proteins. SGLTs are membrane bound proteins that actively transport glucose

against its concentration gradient and therefore requires an energy source. Approximately 90% of filtered renal glucose is reabsorbed by SGLT2 which a low-affinity high capacity transporter and the remaining 10% by SGLT1, a high-affinity, low-capacity transporter (Gerich JE, 2010. Triplett CL, 2012).

1.3.6 Acarbose

This treatment is an α-glucosidase inhibitor that prevents the absorption of carbohydrates during digestion in the small intestines, therefore reducing the increase in blood glucose concentrations that occurs after a meal. Acarbose can also decrease HbA1c levels by approximately 0.5% (Gu et al, 2015). Acarbose is thought to regulate glucose homeostasis via the MAPK pathway and suppression of proinflammatory cytokines by releasing miR-10a-5p and miR-664 in the ilium (Zhang et al, 2013).

1.3.7 Thiazolidinediones

Pioglitazone belongs to the Thiazolidinedione class of drugs for type 2 diabetes and is a strong insulin sensitizer. It works by binding to the peroxisome-proliferator activated receptor gamma, which results in enhanced muscle, liver and adipose tissue sensitivity to insulin and also results in a reduction of both fasting and post-prandial blood glucose concentrations (Triplett et al, 2010).

1.3.8 Nateglinide

The function of this class of drugs is to act as an insulin secretagogue and induces rapid insulin secretion synergistically with food intake. This class of drug works in a similar way to sulphonylureas, where its action is mediated via the β-cell potassium ion channel, where the binding of nateglinide results in the closure of the potassium channel and ultimately the release of insulin (Ball et al, 2004).

1.4 Glucolipotoxicity

The term glucolipotoxicity refers to the combination of both high blood glucose (hyperglycaemia) and elevated fatty acid levels (hyperlipidaemia) and the harmful effects that the combination has on pancreatic β-cells regarding both function and survival (Poitout et al, 2010). Individually, raised glucose and free fatty acids elicit negative effects on the β-cell, but in combination both nutrients are

synergistically harmful, which has led to the concept of glucolipotoxicity (Poitout et al, 2010). It is now widely accepted that there must be increased glucose levels to facilitate lipotoxic effects, including inhibition of insulin secretion and apoptosis (Somesh et al, 2013). To replicate Glucolipotoxic conditions cells are exposed to fatty acids and elevated glucose levels. The two fatty acids used are oleate, palmitate, which are the most abundant FFAs in human nutrition and therefore in circulation (Donath et al, 2009). Oleate is the most common unsaturated fatty acid that is found in the diet and is classified as a monounsaturated omega-9. It is found in animals and vegetable fats and oils. Despite being used here as a damaging agent, there is evidence to suggest that oleic acid has anti-apoptotic and anti-inflammatory properties. Palmitic acid is the most common saturated fatty acid found in the diet, it can be sourced from animals, plants and microorganisms. In the diet it can be found in meats and dairy products.

1.4.1 Glucotoxicity

Glucotoxicity is the term given to chronically elevated blood glucose concentrations that ultimately lead to impaired β-cell function and resulting apoptosis. Acutely, an increase in blood glucose concentration has a stimulatory effect on the transcription factors that are involved in encoding preproinsulin (ins) and on insulin release. However, a prolonged exposure the hyperglycaemia reduces the transcription of the *ins* gene and leads to the reduction of insulin secretion following the reduction of Pdx-1 and MafA transcription factors (Ogihara and Mirmira, 2010).

One proposed mechanism of hyperglycaemia-induced β-cell dysfunction is oxidative stress.

Glucotoxicity generates oxidative stress by causing an accumulation of excess reactive oxygen species (ROS). Pancreatic β-cells are vulnerable to oxidative stress which is considered to be the cause of tissue damage that accompanies chronic hyperglycaemia and can induce a reduction in β-cell mass and apoptosis. The vulnerability of pancreatic β-cells to oxidative stress may be due to the lack low levels of antioxidants such as glutathione peroxidase dismutase. Glutathione peroxidase dismutase is an antioxidant enzyme that protects cells from ROS and subsequent downstream damage. The reason for the lack of antioxidants in β-cells is because ROS are constantly present at low levels and β-cells respond to elevated glucose levels via acute regulation of various reactive oxygen species and reactive nitrogen species, therefore ROS are required to be present for glucose homeostasis. However, chronic elevation of ROS can be damaging to the β-cell.

ROS is a collective term given to chemical species that are formed from the incomplete reduction of oxygen, whereas RNS refers to all oxidation states and reactive adducts of nitrogenous nitric oxide

synthase products (Pitocco et al, 2013). The mitochondrial respiratory chain is a main source of ROS. The inner membrane complexes I and III generate highly reactive superoxide ($O_2\cdot$) by the single-electron reduction of oxygen. As this is a charged species it is not able to cross membranes freely. Superoxide is converted to hydrogen peroxide (H_2O_2) which is less reactive. This is able to diffuse across membranes through aquaporins and is then converted to highly reactive hydroxyl radicals ($HO\cdot$) (Gerber and Rutters, 2017).

It's thought that the generation of superoxide is the first step in the ROS-generating cascade that leads to the production of other ROS/RNS. In addition to superoxide forming hydroxyl radicals, it can also react with nitric oxide (NO) to form a highly reactive nitrogen free radical known as peroxynitrite ($ONOO^-$) (Keane et al, 2015).

1.4.2 Lipotoxicity

Lipotoxicity is the term given to describe the dysfunction of non-adipose tissue and cells caused by chronic exposure to elevated free fatty acid levels. When plasma levels of free fatty acids both prandial and postprandial exceed the uptake capacity of adipose tissue, the non-adipose tissue becomes overloaded with lipids. This results in metabolic imbalances, dysfunction and/or disease. (Graier et al, 2009). In normal physiology lipids have multiple biology functions including; being an energy reserve, serving as a signalling molecule and are major membrane components. In β-cells, lipases remove lipids from plasma lipoproteins, the lipids are then converted into long-chain acyl-CoA that can then be transported to the mitochondria and subsequently directed into the β-oxidation pathway to provide energy (Véret et al, 2014). However, in high glucose concentrations β-oxidation is reduced, thus lipid detoxification is reduced, resulting in an accumulation of intracellular long-chain acyl-CoA which mediates the toxic effects of chronically elevated free fatty acids (El-Assaad et al, 2015).

Another possible mechanism by which chronically elevated FFAs has a detrimental effect on pancreatic β-cells is via the induction of uncoupling protein (UCP2). Pancreatic UCP2 has a negative effect on insulin secretion by reducing the increases in ATP production that follows glucose metabolism (Joseph). the presence of glucotoxicity intensifies the negative effects of lipotoxicity (Bachar et al, 2009).

1.4.3 Glucolipotoxicity-induced endoplasmic reticulum stress

A mechanism by which excess free fatty acids and glucose induce β-cell dysfunction and apoptosis is via the activation of an adaptive response known as ER stress. This takes place in the endoplasmic reticulum (ER) which is an organelle involved in transmembrane lipid and protein biosynthesis, and calcium ion signaling and storage (Eizirik et al,2008). Lipotoxicity is the main driver of ER stress but is intensified by the presence of glucose, which combined is known as glucolipotoxicity. Glucolipotoxicity activates a network known as the unfolded protein response (UPR) which has the purpose of restoring regular ER function, degrading proteins that have been misfolded and activating signaling pathways to subsequently upregulate the production of chaperones that are involved in protein folding. (Bachar et al 2009. Cnop et al, 2017).

ER stress results in an increase in binding of misfolded proteins to the ER chaperone known as immunoglobulin heavy-chain binding protein (BiP) resulting in the activation of many ER membrane proteins including PKR-Like ER kinase (PERK) inositol-requiring protein-1 (IRE1) and activating transcription factor 6 (ATF6) (Bachar et al, 2009). These membrane proteins are inactive when bound to the luminal ER chaperone BiP, however they become activated when BiP separates from their luminal side to play a role in protein folding which subsequently initiates ER-chaperone reduction. The function of the PERK is to phosphorylate the translation initiation factor (eIF)2α, thus hindering protein synthesis and decreasing the functional demand on the ER. As well as this, eIF2α phosphorylation increases the translation of ATF6, which is responsible for the transcription of both chaperones and CHOP. CHOP initiates the expression GADD34, that subsequently dephosphorylates PP1 and eIF2α for reduction of translational inhibition. The newly activated IRE1 alternatively splices X-box binding protein 1 (XBP-1) mRNA. Spliced XBP-1 then induces genes that are involved in ER expansion, protein folding and degradation of misfolded proteins. Activated ATF6 translocate to the Golgi and are cleaved from the membrane by proteases known as S1P and S2P, a process responsible for inducing transcription of ER-chaperones such as BiP. When the unfolded protein response fails to relieve glucolipotoxicity-induced ER stress, the cell undergoes apoptosis (Cnop et al,2017. Bachar et al,2009). If the cell cannot resolve the protein-folding defect, cell-death signalling pathways are activated.

1.4.4 Glucolipotoxicity induced JNK activation

Prolonged exposure to glucolipotoxicity-induced ER stress and resulting apoptosis in β-cells is associated with the activation of cJun N-terminal kinase (JNK). JNKs are members of the mitogen-activated protein kinase (MAPK) family (Prause et al, 2014). There are 3 subtypes of JNK, JNK1 and JNK

2 are found ubiquitously whereas JNK3 is expressed only in the brain, testis and pancreatic β-cells (Solinas and Becattini, 2017). The action of JNK varies depending on the apoptotic stimuli. Proinflammatory cytokine-induced β-cell apoptosis results in rapid and transient activation of JNK, whereas glucolipotoxicity-induced ER stress results in a more pro-longed JNK activation. In addition to ER stress JNK activation is initiated by glucolipotoxicity via oxidative stress and ROS formation. However, ER stress is able to associate with the mitochondrial or intrinsic death pathway via the p53-upregulated modulator of apoptosis (puma) and via the JNK-dependent up-regulation of death protein (DP5) in response to GLT.

1.5 Tumour Necrosis Factor Receptors

Tumour necrosis factors are cytokines that mediate multiple effects such as cell proliferation, apoptosis, inflammation, immunomodulation, amongst others (Aggerwal BB, 2000). TNFs are activated by their associated ligands. Ligands are type II membrane proteins that are membrane bound and/or soluble. The role of the TNF ligand is to interact with one or more specific TNF receptor to form a complex that makes up the tumour necrosis factor receptor superfamily (Hehlgans and Pfeffer, 2005).

The tumour necrosis factor receptor (TNFR) superfamily (TNFRSF) is made up of 29 transmembrane receptors. All members of the TNFRSF contain an extracellular domain that is used to bind to ligands and an intracellular domain that is responsible for mediating the activation of downstream pathways (Li et al, 2013). The TNFR cytoplasmic domain can vary in length with between 40-200 residues which are also varied in homology. TNFRs can be broken down into two groups based on whether they contain a 'death domain' (Li et al, 2013). The TNFRs that contain a death domain in the cytoplasmic domain include TNFRSF6/FAS, TNFR1, TRAIL-1, TNFRSF10A/ Death receptor 4, TNFRSF10B/Death receptor 5, TNFRSF10D/TRAIL-R4, TNFRSF25/Death receptor 3 and TNFRSF27. The activation of the death domain containing receptors results in the recruitment of intracellular death domain containing adaptors such as FAS-associated death domain (FADD) and TNFR-associated death domain (TRADD). The recruitment of these molecules subsequently activates the caspase cascade and induce apoptosis (Hehlgans and Pfeffer, 2005).

The TNFR group that doesn't contain a death domain include; TNFRII, TNFRSF7, TNFRSF8, TNFR5, LTβR, OX40, 4-1BB, BAFFR, B-cell maturation antigen (BCMA), TNFRSF11A, transmembrane activator and calcium-signal modulating cyclophilin ligand (CAML) interactor (TACI), Fn14, activation induced TNF-

receptor (AITR), and X-linked EDA-A2 receptor (XEDAR). All the receptors that do not contain a death domain instead contain TNF-receptor associated factor (TRAF) interacting motif (TIM) in the cytoplasmic domain. The activation of TIM subsequently leads to the recruitment of TRAF family members which in turn leads to the activation of various signal transduction pathways, such as NF-κB.

1.5.1 TNFR5/CD40 Structure

TNFR5 also known as CD40 is best known as a costimulatory molecule in B-cells and T-cells (Elgueta et al, 2009) It is a membrane glycoprotein belonging to the tumour necrosis receptor family (TNFR) (Klein et al, 2005). Costimulatory molecules are separated into two broad group based their homologies to original group members. The groups are, the CD28/B7 family and the Tumour necrosis factor receptor family, which CD40 fall into. Other members of the TNFR family are TNFR4 (OX40), TNFR13c (BAFF-R), TNFR13b (TAC1), TNFR17 (BMCA), and TNFR11a (RANK). This group is further subdivided based on function.

CD40 is a type I transmembrane protein with a molecular weight of 48 kDa and contains 193 amino acid extracellular domain. The extracellular domain contains 22 cysteine residues that are conserved between TNFR superfamily members (Elgueta et al, 2009).

CD40 is activated upon binding with its ligand known as CD154 or CD40L. CD40L is a type II transmembrane protein and its molecular weight can vary between 32 and 39kDa due to potential post-translational modifications. CD40L is also a member of the tumour necrosis factor superfamily, it has a characteristic extracellular structure that is made up of an α-helix 'sandwiched' between two β-sheets, which is beneficial for the trimerization of CD40L (Elgueta et al, 2009). CD40 ligation leads to stimulation of several significant signalling molecules including NF-κB, c-Jun kinase (JNK) and p38 (Hostager and Bishop, 2013).

Both CD40 and CD40L expression is most commonly associated with immune cells, as CD40 was initially characterised on B cells and CD40L is expressed primarily on activated T cells and B cells during inflammation, it's now known that CD40 and CD40L are also expressed in non-immune cells including pancreatic duct cells (Barbé-Tuana et al, 2006). The vast expression of both CD40 and CD40L indicates a pivotal role in different cellular immune responses (Elgueta et al, 2009).

1.5.2 CD40 Ligand

The CD40 ligand (CD40L) that is also known as CD154 belongs to the TNF superfamily. CD40L was first identified on activated T cells which induced B cell activation upon binding to CD40 on the B cell surface, resulting in increased proliferation and IgG-class switching (Michel et al, 2017). It has been identified that as well as the full length 33kDa CD40L that forms trimeric complexes on the cell surfaces, a shortened 18kDa version of CD40L exists that lacks the cytoplasmic tail, the transmembrane domain and parts of the extracellular domain. This truncated and soluble version of CD40L (sCD40L) is generated by shedding membrane anchored CD40L by various matrix metalloproteinases (MMPs) and disintegrin metalloproteinases (ADAMs) (Michel et al, 2017). The present study observes the potential activation of CD40 by ligation to CD40L in pancreatic β-cells rather than in T cells, where it is known that CD40L is released from the membrane of T cells by ADAM17 and ADAM10 upon engagement with CD40 (Moss and Minond, 2017). CD40 and its ligand are not only expressed on immune cells but on non-immune cells including platelets, endothelial cells, fibroblasts, pancreatic islet β-cells and pancreatic ductal cells (Seijkens et al, 2012). According to Moss et al, CD40L is shed from the cell surface of any cell type that has ADAM17. A study conducted by Stutzer et al (2012) identified that multiple sheddases are present on the surface of β-cells including beta-site amyloid precursors protein cleaving enzymes 1 and 2 (BACE1 and BACE2) and more importantly members of the 'a disintegrin and metalloproteinase' (ADAM) family.

1.5.3 TRAF recruitment and NF- κB activation

Tumour necrosis factor associated proteins (TRAFs) are cytosolic adapter proteins that work as signaling intermediates for different receptors including; tumour necrosis factor super family receptors, Toll-like receptors, NOD-receptors, and others. TRAF proteins are known to bind to the cytoplasmic domain of CD40 subsequent to its ligation and potentially initiate signal transduction and NF-κB activation. The receptors that TRAF proteins interact with possess no catalytic activity, the activation of downstream pathways such as NF-κB are thought the be controlled predominantly by TRAF proteins, however the exact mechanism by which TRAF proteins regulate such activity remains unknown (Hayem et al, 2014).

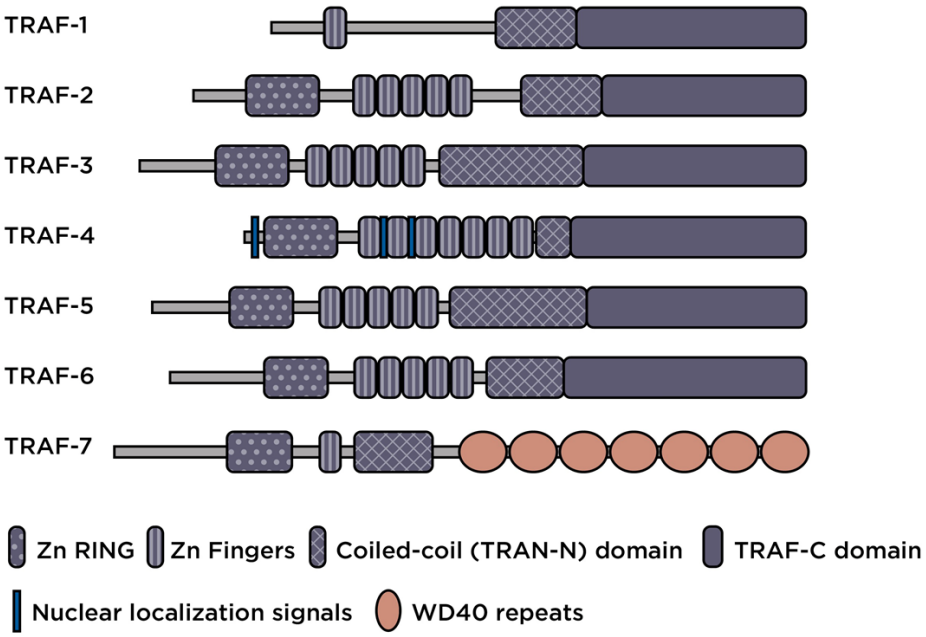

Figure 1.8 Structural composition of TRAFs. *Structural domain of seven TRAFs, identifying Zinc Ring (Zn Ring), Zinc fingers (Zn Fingers), coiled-coil domain (TRAF-N), TRAF-C domain, nuclear localisation signals and WD40 repeats. Adapted from Xie P, 2013.*

There are currently 7 known members of TRAF family and they are all similar in structure (Fig 1.8). The first six TRAFs share a conserved C-terminal TRAF domain and all have an N-terminal. In most TRAFs the N-terminal contains a RING finger motif and a variable range of zinc finger structures that are arranged into CART domains. TRAF7 was more recently identified as a TRAF protein based on its structure possessing a RING and Zinc-finger domain similar to the other TRAF protein, however TRAF 7 doesn't possess a C-Terminal TRAF domain (Hokayem et al, 2017). TRAF1 however does not contain the RING finger motif and the additional zinc finger structures are not arranged into CART domains. TRAF1 is known to directly bind to CD30. CD40 is involved in CD30-mediated NF-kB activation as it contains multiple functional NF-κB binding sites within the promoter (Schwenzer et al, 1999). TRAF2 is spread throughout the cytoplasm of cells when unstimulated but are recruited to the plasma membrane following CD40 ligation (Hostager and Bishop, 2013). The activation of NF-κB occurs via a number of potential mechanisms in both the canonical and non-canonical pathways. The activation of the canonical NF-κB pathway involves TANK (I-TRAF). TANK is a TRAF binding protein that possesses both inhibitory and stimulatory properties. The stimulatory property of TANK is evident in its ability to activate NF-κB in the presence of low levels of TRAF2. This stimulatory action is dependent on the

N-terminal domain of TANK interacting with the TRAF2 (Pomerantz and Baltimore, 1999). TRAF3 is able to bind to the CD40 receptor via the binding toTRAF5 (Leo et al, 1999). Upon binding to TRAF5 it plays a role in initiating the activation of NF-κB (Ni et al, 2000). However, it has also been reported that the up-regulation of TRAF3 blocks the activation of CD40. TRAF4 is both structurally and functionally an atypical member of the TRAF superfamily in that it works to negatively regulate the inflammatory signalling downstream of agonists such as tumour necrosis factors. TRAF4 inhibits the activation of NF-κB by binding to the Nod-like receptor family member, NOD2 (Marinis et al, 2012). TRAF6 is dissimilar to other TRAFs as it can participate in signal transduction from IL-1R/TLR superfamily, whereas the other TRAFs mediate signals from only TNFs. Also, in CD40 signalling, TRAF6 is able to mediate diverse effector functions downstream or is able to collaborate with TRAF2. The mediation elicited by TRAF6 is important for p38 MAP kinase activation, CD40-induced IL-6 secretion and plasma cell survival (Wu and Arron, 2003). TRAF7 is also distinct to the other TRAF members as they interact with protein kinase members via the TRAF domain, instead TRAF7 uses the WD40 repeats-containing region to interact with MEKK3. MEKK3 is a pivotal signaling molecule in TNF-induced NF-κB activation pathway, and the expression of both MEKK3 and TRAF7 results in the activation of p38 MAP kinase and JNK (Zotti et al, 2012).

1.5.4 TNFR5/CD40 and Diabetes

There is increasing evidence linking CD40 and CD40L to inflammation associated with type 2 diabetes. Chronic inflammation is a characteristic of type 2 diabetes and manifests in the pancreas, adipose tissue, liver, vasculature, and the circulation. The inflammatory response is associated with an increase in pro-inflammatory cytokines expression, including IL-1β and IL-6, which are induced and maintained by oxidative stress and glucolipotoxicity. The expression of CD40 on pancreatic β-cells increases in response to proinflammatory cytokines such as IL-1β, TNF-α, and IFN-γ. Whereas the membrane-bound CD40L is expressed on immune cells that infiltrate the diabetic pancreas (Seijkens et al, 2012).

1.6 Nuclear Factor kappa B

Nuclear factor kappa B (NF-κB) is a family of ubiquitously expressed transcription factors that have the primary function of regulating the induction of genes involved in immune and inflammatory cell function (Pomerantz). The NF-κB family includes; NF-κB1 (p50/p105), NF-κB2 (p52/p100), p65 (RelA), RelB, and c-Rel (Tak and Firestein, 2001). All members have the ability to homodimerize and form

distinct heterodimers with other NF-κB family members, with the most common heterodimer being P50 or p52 subunit and p65, these members contain transactivation domains (TAD) which are necessary for gene induction (Tak and Firestein, 2001). Each member has a 300-amino acid Rel homology domain (RHD), this domain has multiple functions including interacting with iκB, dimerization, interacting with DNA and translocation to the nucleus.

In the majority of cell types NF-κB is activated by the canonical pathway (Fig 1.9) where it is sequestered in the cytosol in its in inactive form attached to the NF-κB inhibitor known as iκB (Zhang et al, 2016). The iκB family of inhibitors are related proteins that all of have a core of six or more ankyrin repeats, an N-terminal regulatory domain and C-terminal that contains a PEST motif. The most commonly known member of the iκB family is iκBα, which is known to bind to NF-κB dimers and block their nuclear localisation sequence, resulting in NF-κB being trapped in the cytoplasm. For NF-κB to translocate to the nucleus NF-κB must be activated and the NF-κB-iκB complex disrupted (Karin M, 1999). The activation of NF-κB and its nuclear translocation is known to play a key role in inflammation through its ability to induce transcription of proinflammatory genes (Tak and Firestein, 2001).

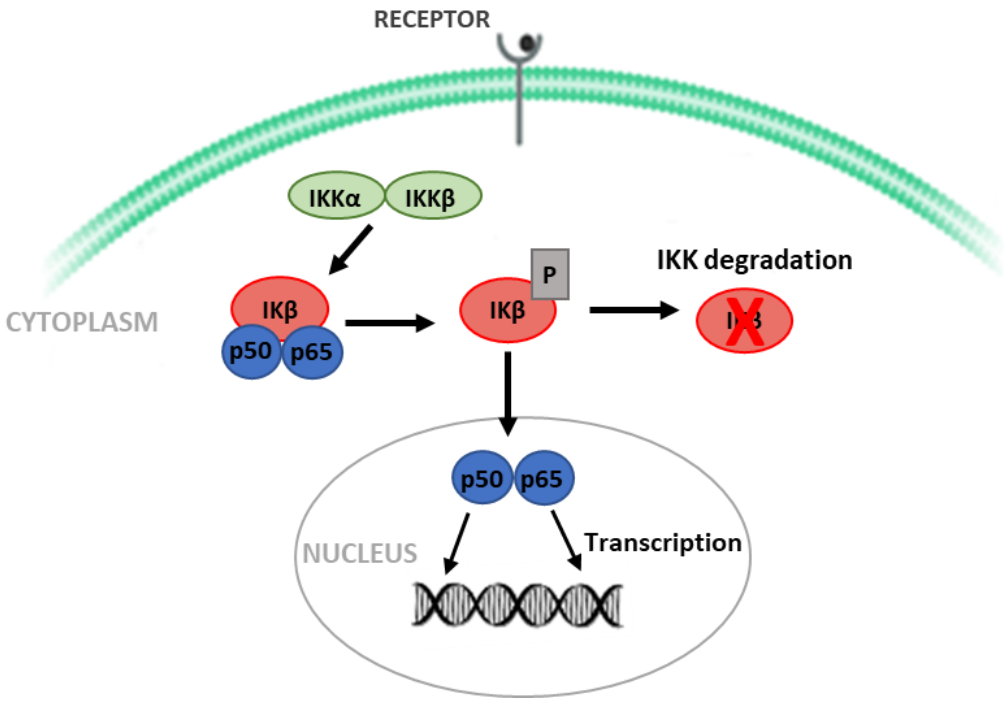

Figure 1.9: Canonical activation of NF-κB*. Activation of NF-κB p50/p65 occurs via the degradation of its inhibitor known as Iκ𝐵. Following the degradation of the inhibitor the NF-κB p50/p65 can translocate the nucleus where it acts as a transcription factor. Abcam.com*

Another mechanism of NF-κB activation is via the non-canonical pathway.

The non-canonical pathway is involved in immune cell differentiation and maturation (Shih et al, 2011). The non-canonical pathway differs from the canonical pathway by using a mechanism that relies on the inducible processing of p100 instead of IKβ degradation (Fig 1.10). Another major difference between the canonical and non-canonical pathway is the mechanism of activation. The canonical pathway responds to stimuli from diverse immune receptors and leads to rapid but transient NF-κB activation whereas the non-canonical NF-κB pathway relies on phosphorylation-induced p100 processing, which is triggered by signalling from a subset of TNFR members, including CD40. This pathway is dependent on NIK and IKKα, but not on the trimeric IKK complex, and mediates the persistent activation of RelB/p52 complex (Sun S, 2011).

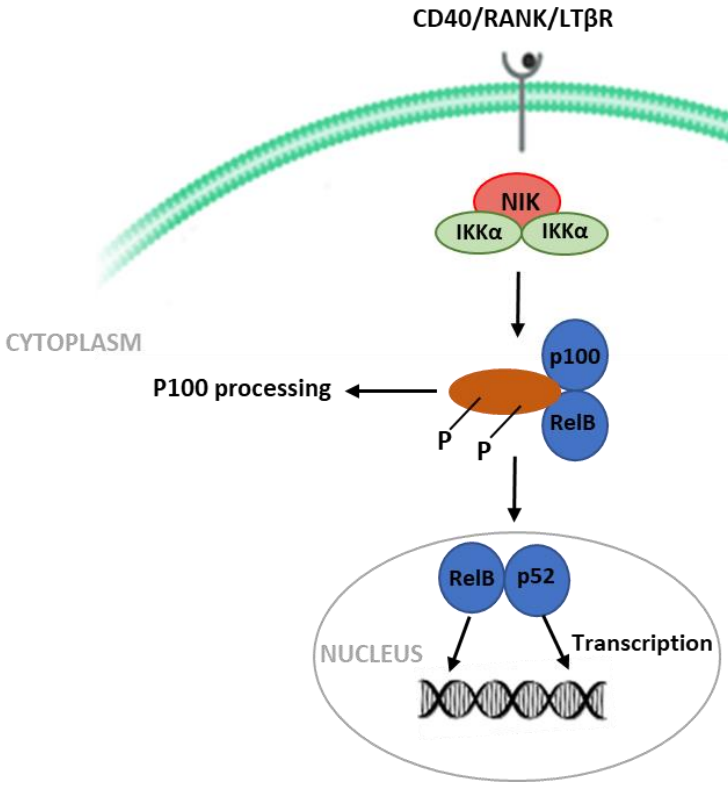

Figure 1.10 Non-canonical Activation of NF-κB*. The non-canonical pathway is activated by members of the TNFR family utilises the phosphorylation induced processing of p100 to activate NF-κB.*

1.7 GLT effect on mitochondria function

This project also focuses on GLT-induced disruption of the citric acid cycle and the resulting effect on fatty acid synthesis, Cholesterol synthesis and histone acetylation.

1.7.1 Citric Acid cycle

The process of respiration occurs in 3 main pathways: glycolysis, the citric acid cycle and electron transport (Fernie et al, 2004). The citric acid cycle is also known as the TCA cycle and the Krebs cycle takes place in the mitochondria of the cell. It is the process that is relied upon by all aerobic organisms to generate NADH and $FADH_2$ that provides the reductive potential that is required to generate ATP (Mailloux et al, 2007). The citric acid cycle occurs directly after glycolysis and is made up of 8 steps. The first step of the cycle is the generation of citrate resulting from the condensation of acetyl-coA with oxaloacetate and is catalysed by citrate synthase. The second step is formation of isocitrate via cis-Aconitate, this reversible step is catalysed by aconitase. The third step results in the formation of α-ketoglutarate and CO_2 which occurs due to the oxidative decarboxylation of isocitrate catalysed by the enzyme isocitrate dehydrogenase. Step four involves α-ketoglutarate undergoing oxidative decarboxylation catalysed by the α-ketoglutarate dehydrogenase complex and results in succinyl-CoA. Following this, succinyl-CoA is converted to succinate by succinyl-coA synthetase. The sixth step involves succinate undergoing oxidation to form fumarate by succinate dehydrogenase. In step seven, L-malate is generated by the reversible hydration of fumarate and is catalysed by L-malate. Finally, L-malate is oxidised to form oxaloacetate by NAD-linked L-malate dehydrogenase (Berg et al,2005).

1.7.2 Histones

Histones are broken into two groups, the first group being the core histones including; H2A, H2B, H3 and H4. All core histones are similar in structure with an unstructured amino-terminal tail and conserved central motif domain that is known as a histone fold. The histone fold is made up of an α-helix with a short helix bordering either side. The core histones all have a N-terminal with a basic region that extends through the DNA and into the space surrounding the nucleosome. The second group are linker histones made up of H1 and H5. Histone H1 and H5 pivotal roles in regulating the structure of chromatin and contributes to linking the chromatin to higher order structures such as fibrils (Lyubitelev et al, 2015) Both linker histones have a conserved structure that is made up a N-terminal tail, a central globular domain and C-terminal tail. It is the role of the globular domain that

binds to the nucleosome core and the role of the C-terminal tail that interacts with linker DNA and is important for higher affinity binding of linker histones to the nucleosome.

The main function of histones is to package DNA into chromatin, which are the basic subunits of nucleosomes. The nucleosome is made up of two copies of each histone, the H2A-H2B form a dimer and H3-H4 for a tetramer. Together the core histones form an octane which is the basic core particle of a nucleosome, around which ~147 base pairs of DNA wrapped in ~1.65 left-handed super- helical turns (Fig 1.11) (Zhou et al, 2015).

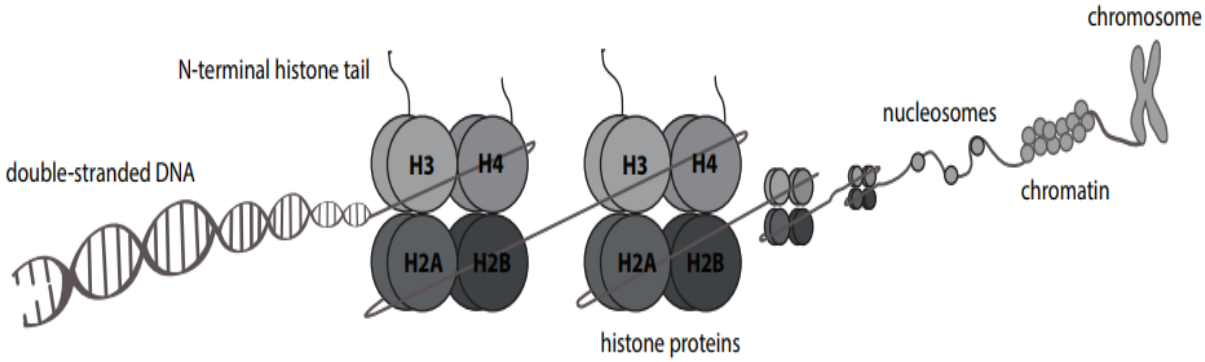

Figure 1.11 Schematic representation of the organisation of genetic material*. Nucleosomes are formed by DNA wrapped around eight histone proteinns, which together form chromatin. whatisepigenetics.com.*

1.7.2.1 Histone Acetylation

The post translational modification to histones known as histone acetylation is associated with altered transcriptional activity in eukaryotic cells. Acetylation of histones occurs at the lysine residue on the amino-terminal tail of the core histones by the addition of an acetyl unit, resulting in the removal of the positive charge of the histone tails and causing a reduced affinity between the histone and DNA. Consequently, histone acetylation alters nucleosomal conformation which can lead to increased accessibility of transcriptional regulatory proteins to chromatin templates (Struhl K., 1998). Histone acetylation is catalysed by a number of different histone acetyltransferases (HATs), which are responsible for transferring the acetyl group from acetyl-CoA to the lysine residue. The HATs work in

complexes with multiple proteins and these complexes regulate specific chromatin targeting. There are three main types of HATs including; Gcn5, MYST, and p300/CBP, all of which share a conserved binding site with acetyl-CoA. The most commonly found HAT is p300/CBP, which has the ability to acetylate all four of the core histones (Ogryzko et al, 1996).

The level of histone acetylation depends on intermediary metabolism in the citric acid cycle for supplying acetyl-coA (Gladieri et al, 2014). Acetyl-coA is produced in the mitochondria of the cell via glycolysis prior to entering the citric acid cycle. Acetyl-coA to be used in fatty acid synthesis, cholesterol synthesis or histone acetylation must leave the mitochondria. However, as there is no transporter to transfer acetyl-coA across the mitochondria membrane into the cytoplasm, acetyl-coA condenses with oxaloacetate to form citrate which is transported out of the mitochondria and subsequently converted to acetyl-CoA and oxaloacetate by ATP-Citrate lyase (Fan et al, 2015. Wellen et al, 2009). This means that acetyl-coA has a key regulatory role and is a pivotal metabolite that connections metabolism with many other functions including; transcription and signaling. This also means that the amount of histone acetylation is dependent on nutritional intake and presence of ATP-citrate lyase, which could be related to obesity-related type 2 diabetes (Wellen et al, 2009).

1.8 Aims and Objectives

1.8.1 GLT induced inflammation

The initial aim of this thesis is to identify activation of inflammatory pathways resulting from INS-1 pancreatic β-cell exposure to glucolipotoxic cell media. The reason for observing the induction of inflammation resulting from GLT is because elevated glucose and fatty acids are considered to be pivotal for the onset of type 2 diabetes (Boden and Laakso, 2004). This is also important based on the knowledge that over 85% of type 2 diabetics are overweight or obese and that overweight and obese individuals have increased blood glucose and circulating free fatty acids (Sepp et al, 2014). To elucidate potential inflammation resulting from exposure to GLT INS-1 cells will be incubated in media supplemented with 28mM glucose, 200µM palmitic acid and 200µM for 5 days, subsequently, alterations in protein, mRNA and activation will be observed and results will highlight potential cell damage inflicted by GLT.

1.8.2 CD40-induced Gene Modulation

Based on a bespoke neural net analysis (NNA) map generated by Professor Graham Ball that identifies genes potentially down regulated in the presence of CD40, an aim in this project is to identify whether GLT-induced up-regulation of CD40 is able to modulate various genes and potentially play a role in the down regulation of insulin that is seen in type 2 diabetes and β-cells exposure to GLT. In order to achieve this CM cells are initially used to validate the findings of the NNA map, subsequent to this INS-1 cells are used as CM cells are unable to function in GLT conditions. After validating the NNA map, the pathway will be further enriched to identify any genes that are associated with CD40 expression that also play a role in insulin secretion or expression. This is important as will identify a novel role for CD40 in insulin expression. The strategy to achieve this aim will utilise siRNA transient knock down technology to determine the effect CD40 has on selected genes and the effect this has downstream on inhibition of binding-4 (ID4) and ultimately on insulin gene expression.

1.8.3 Carnosine as a Potential Therapy

A further aim in this project is to identify whether a dipeptide known as carnosine has the ability to prevent or reverse the potentially damaging effects of GLT. In order to achieve this aim, it will be observed whether the INS-1 pancreatic β-cell contains carnosine synthase and therefore has the ability to generate carnosine naturally in the presence of β-alanine, L-histidine and ATP. Following this, 10mM of carnosine will be added to cell culture media ±GLT to identify whether it has the ability to reverse or prevent the inflammatory process seen in chapter which can potentially cause damage to the β-cell.

1.8.4 GLT-induced effect on HNF4α

HNF4α is commonly associated with a type of diabetes known as MODY caused by a mutation of the HNF4α gene resulting in β-cell dysfunction (Gardener and Tai, 2012). The aim of this chapter is to identify whether exposure of INS-1 cells to GLT for 5 days also has an effect on HNF4α gene expression and whether this has a further effect on insulin secretion via dysregulation of Rabs. The reason HNF4α is of interest is based on enriched MetaCore™ data generated by Dr Tania Jones, which identified HNF4α as a being down regulated following exposure to GLT. This is validated using RT-qPCR. siRNA

knock down technology is used to find any effect that HNF4α has on selected Rab genes and on insulin secretion using an insulin secretion ELISA. The findings in this chapter will highlight whether HNF4α is affected by diet (GLT) rather than, or as well as mutation to have an effect on insulin secretion and that the mechanism for disrupting insulin secretion is via down-regulation of Rab genes.

1.8.5 GLT-induced Histone acetylation

Another aim of this project was to observe whether GLT-induced disruption of the TCA cycle ultimately results in an increase in histone acetylation. In order to determine this, INS-1 cells will be incubated ±GLT for 5 days and metabolites including citrate, IDH2 and IDH3 will measured using RT-qPCR. Subsequent to this ATP-citrate lyase levels will be measured ±GLT which is the enzyme responsible for generating cytosolic acetyl-coA from citrate. The pathways which utilise acetyl-coA will be observed for any disruption in response to GLT by measuring the protein and mRNA of certain components. If disruption is observed, then acetylation of histones will be measured using western blotting in both control and GLT conditions. This chapter will determine whether exposure to GLT is sufficient to cause potential alteration in gene transcription via histone acetylation resulting from disruption of the TCA cycle.

Chapter 2

Materials and Methods

2.0 CHAPTER 2: Materials and Methods

2.1 Materials

All reagents were purchased from Sigma-Aldrich (St. Louis, MO, USA) and all plasticware purchased from ThermoFisher (Waltham, MA, USA) unless otherwise stated.

2.2 Solutions and Buffers

Table 1.1: Compositions of buffers used throughout the project.

SOLUTION	COMPOSITION
RIPA buffer	150mM NaCl, 0.1% Triton X-100, 0.5% sodium deoxycholate, 0.1% SDS, 50mM Tris HCL, H_2O pH 8.0
Sample buffer	40% glycerol, 240 mM Tris HCl, 8% SDS, 0.04% Blue Bromophenol, 5% β-mercaptoethanol, pH 6.8
Lower buffer	1.5 M Tris HCl, 0.4% SDS, pH 8.8
Upper buffer	1.5 M Tris HCl, 0.4% SDS, pH 6.8
Running Buffer	0.25 M Tris HCl, 2.5 M glycine, 1% SDS, pH 8.3
Transfer buffer	60% Biorad transfer solution, 20% ddH_2O, 20% Ethanol
PBS 10X	137 mM NaCl, 2.7 mM KCl, 10 mM Na_2HPO_4, 2 mM KH_2PO_4
Stripping buffer	6.25 ml Tris HCl 0.5M pH 6.8, 5 ml SDS 20%, 347µl β-mercaptoethanol

2.3 Cell culture and cell growth

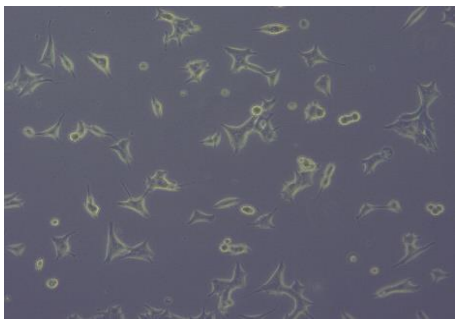

INS-1 cells 24 hour after passage

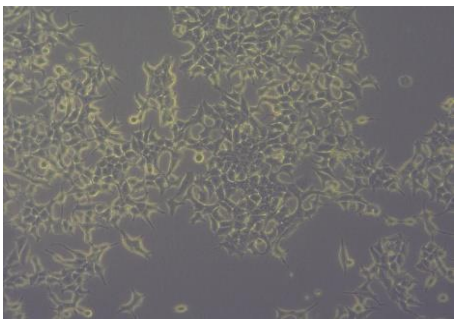

INS-1 cells in RPMI-1640 (5 days)

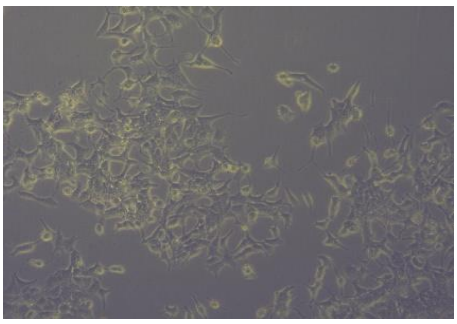

INS-1 cells in GLT media (5 days)

2.4 Cell lines

2.4.1 INS-1 cell line

The cell line used in this project is a rat insulinoma cell line known as INS-1. INS-1 cells display important characteristics of the pancreatic β-cell which includes high insulin content and responsiveness to glucose within a physiological range. INS-1 cells are derived from a rat insulinoma by x-ray irradiation. Despite being able to respond to glucose the cells are still proliferative, but the total amount of insulin is only about 20% of that of the native cells (Skelin et al 2010). This cell line is used based on its ability to display β-cell characteristics however other insulinoma cell line used in β-cell research is RINm5F. This cells line has been reported to possess abnormal properties of glucose transport and inapt glucose sensitivity (Halban et al, 1983).

2.4.2 CM Cell line

The second cell line used in this project is the cell line known as CM. The CM cell line is derived from human pancreatic insulinoma. As it is a beta cell is suitable for this project as it appears to maintain the characteristics of functioning β-cells (Jonnakuty and Gragnoli, 2007).

2.4.3 Cell Culture

INS-1 and CM were both cultured in media with the same composition. The pancreatic β-cells were cultured in RPMI-1640 media (Life Technologies, UK) comprising of 11mM D-glucose and supplemented with 10mM HEPES, 26mM sodium bicarbonate, 50µM β-Mercaptoethanol and adjusted to pH 7.4. The complete medium was supplemented with 10% v/v foetal bovine serum (FBS) (Life Technologies UK), 1% v/v sodium pyruvate (Life Technologies, UK), 1% v/v Penicillin/Streptomycin (Life Technologies, UK). Cells were cultured in T75 flasks and incubated at 37°C and 5% CO_2 and passaged when 80-85% confluent.

2.4.4 Glucolipotoxic Treatment

To create the replica of the extracellular glucolipotoxic environment the RPMI-1640 medium was supplemented with 17mM D-glucose (final concentration 28mM), 200µM sodium oleate (oleic acid)

and 200µM palmitic acid (Bagnati et al; 2016). The stock solutions of the fatty acids were conjugated to BSA, 100mM of oleic acid was dissolved in 50% ethanol and palmitic acid was dissolved in 100% ethanol. The RPMI-1640 was supplemented 2% BSA and filtered, following the addition of the fatty acids the media was incubated in a water bath at 37°C to allow the fatty acids to conjugate to the BSA.

2.4.5 Cyro-conservation and Cell Recovery

INS-1 cells were collected cyro-conservation when they reached 80-85% confluency. The media was aspirated, and the adherent cells washed with sterile phosphate buffered saline (PBS). The cells were detached with the addition of trypsin EDTA and incubated at 37°C for 5 minutes. The cells were harvested in RPMI-1640 media and centrifuged at 400 x g for 5 minutes. The supernatant was aspirated, and the pellet was resuspended in 1ml of synth-a-freeze (life technologies, UK) per one million cells. The cryovial was stored in a suitable container at -80°C for 48 hours and then were moved into liquid nitrogen storage.

2.4.6 Mycoplasma detection and treatments

INS-1 cells were regularly checked for mycoplasma infection using Roche mycoplasma PCR ELISA kit. If mycoplasma infection of cells was detected it was treated using LookOut® Mycoplasma Elimination Kit purchased from Sigma-Aldrich according to the manufacturer's guidelines.

2.5 Preparation of protein samples

2.5.1 Cell lysis

Cells were seeded into 6-well plates and treated with appropriate media. Following the incubation period (usually 5 days) the cells were washed in cold PBS and lysed in RIPA buffer containing 1x protease and phosphatase inhibitor tablet (Roche applied Sciences, Basel, Switzerland) whilst stored on ice. Cell scrapers were used to harvest cells from the surface of the plates and destroy cellular integrity. Lysates were transferred to 1.5ml Eppendorf tubes and kept on ice for 40 minutes and vortexed for 1 minute every 5 minutes. The tubes were centrifuged at 13,000 rpm for 10 minutes to pellet cell debris and the supernatant was transferred to a clean 1.5ml Eppendorf tube and stored at -80°C until used for subsequent analysis.

2.5.2 BCA Assay

The protein concentration of cell lysates was measured using Pierce™ BCA (Bicinchoninic acid) Protein Assay Kit (Thermo Fisher Scientific, Waltham, MA). The principle of this colorimetric assay technique is that peptide bonds present in the proteins can reduce Cu^{2+} ions from cupric sulphate. The amount of reduced Cu^{2+} is proportional to the amount of protein present in the solution forming a purple-coloured product that absorbs light at 562nm. The absorbance is nearly linear over a broad concentration range (20-2000µg/ml) bovine serum albumin (BSA) is included in the kit to create a standard calibration curve for protein quantification.

2.6 Western blot

2.6.1 SDS-PAGE

Acrylamide/bisacrylamide gels were hand poured using the Biorad system. Firstly, a resolving gel was prepared as shown in table 2.2, poured between two glass plates 1mm apart, this was allowed to set with a covering of 70% ethanol. Secondly, a stacking gel was prepared and poured on top of the resolving gel with a ten teeth comb in place, following the removal of the ethanol layer.

Table 2.2: Table showing recipe of 10% SDS-gel used in western blotting

Ingredient for 10% gel	**Resolving gel**	**Stacking gel**
H_2O	6.15 ml	3.07 ml
30% acrylamide/Bisacrylamide 29:1	4.95 ml	670µl
Tris-HCL 1.5M	3.75 ml	-
Tris-HCL 0.5M	-	1.25 ml
APS (10%)	75 µl	25 µl
SDS (20%)	75 µl	25 µl
TEMED	10 µl	5 µl

The prepared gels were placed into electrophoretic tanks and once submerged in running buffer the combs were removed. Between 20-30µg protein were denatured by the addition of 4x laemmli loading buffer (Biorad, Ca, US) and heated to 95°C for 5 minutes. This denatured protein was loaded to the gel alongside a molecular weight marker. The gel was run at a constant voltage 90V for 120 minutes. Subsequently the proteins were transferred to a nitrocellulose membrane using Biorad transfer buffer and a Biorad Transfer unit using a semi-dry transfer for mix molecular weight proteins.

2.6.2 Immunoblotting

Nitrocellulose membranes were blocked with 5% (w/v) non-fat dried milk dissolved in 1x Tris-buffered Saline with Tween (TBST) for 120 minutes at room temperature to prevent non-specific binding. The nitrocellulose membrane was incubated with the primary antibody diluted in 5% (w/v) non-fat dried milk in TBST over night at 4°C on a tube roller. The following day the membrane was washed in TBST 3 times for 10 minutes before being incubated in the correct secondary antibody (anti-mouse or anti-rabbit IgG) for 120 minutes at room temperature. The membrane was then washed in TBST 3 times for 10 minutes before covered in ECL solution (Amersham, GE Healthcare, UK) and the signals exposed using chemiluminescence.

2.7 Real-time qPCR

2.7.1 Primer design

Primers were designed using a combination of NCBI gene search to obtain species specific mRNA sequences, Primer Quest to obtain potential primer pairs and NCBI primer blast to identify specificity of primer pairs. Specific forward and reverse primers were designed of 18-25bp longs, with a GC content no higher than 55% and a melting temperature of 57-62°C. The specificity of the primers was determined by nucleotide blast search and then purchased from Sigma-Aldrich. The primers were verified using PCR.

2.7.2 Primer testing

A Taq polymerase master mix was prepared that contained both forward and reverse primers and the cDNA which was put into the thermo cycler with a denaturing temperature ranging from 58-62.5° (Fig. 2.1). Primers were tested using an agarose gel made up of 1.5% agarose dissolved in 1x TAE buffer. This was heated until the agarose dissolved and poured into a gel cassette and left to set. Loading dye was added to each of the samples prior to being loaded to the gel and they were run alongside a SYBR safe DNA gel stain ladder. The gel was run at 90V for 40 minutes. The gel was then visualised using GeneSnap software.

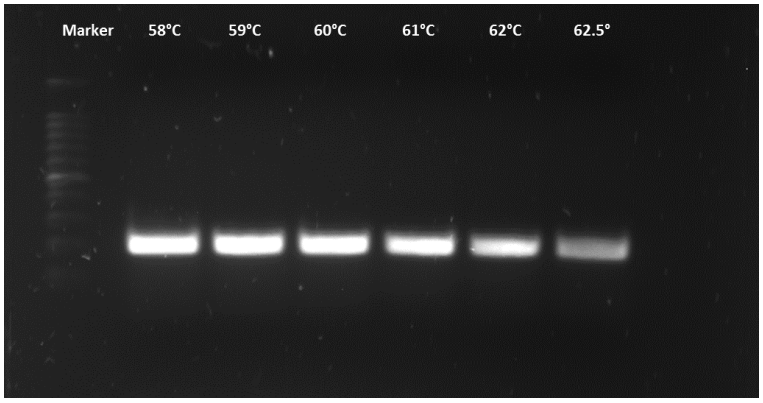

Figure 2.1 Image for optimum PCR denaturing temperature. *Temperatures ranging from 58°C-62.5°C were used to distinguish the optimum annealing temperature that used be used for the specific primers.*

2.7.3 Preparation of sample

INS-1 cells were seeded and treated in either 6-well plates or T75 flasks, following the treatment incubation period the cells were detached using trypsin EDTA (Life technologies, UK). The cells were then centrifuged at 1500 RPM to form a pellet, 1ml of sterile PBS was used to suspend the pellet and a maximum of 5 x 10^5 cells were transferred to a new 1.5ml tube. This was centrifuged at 1500 RPM to form a pellet.

2.7.4 RNA Extraction

To extract RNA from the INS-1 cells a RNeasy® Micro Kit (Qiagen, UK). The supernatant was removed from the cell pellet and 350µl of RLT buffer was added followed by 1 volume of 70% ethanol and mixed well using pipetting. The sample along with any precipitate was transferred to a RNeasy® Mini spin column in a 2ml collection tube and centrifuged for 15 seconds at 8000 x g. The flow through was discarded. To the spin column 350µl of RW1 buffer was added and centrifuged for 15 seconds at 8000 x g. The flow through was discarded. A DNase incubation mix was prepared by mixing 10µl DNase I stock solution with 70µl RDD buffer and added directly to the spin column membrane, this was incubated at room temperature for 30 minutes. Subsequent to the incubation period 350µl of RW1 buffer was added and the spin column was centrifuged for 15 seconds at 8000 x g. The collection tube was discarded. Once in a new collection tube 500µl RPE buffer was added and centrifuged at 8000 x g for 15 seconds. The flow through was discarded. Eighty percent ethanol was added to the spin column and centrifuged for 2 minutes at 8000 x g. The collection tube was discarded and replaced. The spin column was centrifuged with the lid open for 5 minutes at 13,000 x g to dry the membrane. The

collection tube was discarded and replaced with 1.5ml collection tube. To the centre of the membrane 14µl RNase free water was added and centrifuged for 1 minute at 13,000 x g to elute the RNA.

2.7.5 RNA quantification

The RNA extracted was quantified using Nanodrop spectrophotometer technology to determine concentration and quality. The NanoDrop calculates RNA concentration by measuring the absorbance at 260 nm; absorbance correlates with concentration in a linear manner (Beer-Lambert law).

2.7.6 cDNA synthesis and Reverse Transcription

cDNA synthesis was carried out using High Capacity cDNA Reverse Transcription kit (Thermo Fisher Scientific, UK). In each reaction 1.5µg of total RNA was used to be reversed transcribed to cDNA. The reaction was set up as follows:

Table 2.3: Reagents and volumes used in cDNA synthesis prior to RT-qPCR.

Reagent:	**Volume (µl)**
Reverse Transcription buffer	2
dNTPs	0.8
Random Primers	2
Reverse Transcription enzyme	1
RNA	(1.5µg)
Water	(make up to 20µl)

2.7.7 Quantitative PCR

Quantitative PCR (qPCR) measures the amount of PCR product generated in one cycle, using a fluorescence label. During amplification a fluorescence dye binds to the DNA molecules, and fluorescence values are recorded during each cycle of the amplification process. The fluorescence signal is directly proportional to the DNA concentration over a broad range, and the point at which fluorescence is first detected as statistically significant above the background is called the threshold cycle or Ct value. The higher the initial amount of sample DNA, the sooner the accumulated product is detected in the fluorescence plot and the lower the Ct value. Each time a control was run alongside

the samples that was negative for cDNA, therefore if amplification of product was observed it was evidence of contamination.

The reaction for the qPCR was set up as follows:

Table 2.4: Reagents and volumes for mastermix used in RT-qPCR.

Reagent	**Volume (µl)**
SYBR green	8.4
Forward Primer (10µM)	0.8
Reverse Primer (10µM)	0.8
cDNA	(25ng)
Water	(make up to 20µl)

2.7.8 Data Analysis

The qPCR data obtained was analysed using the 2-ΔΔCT method, a relative quantification strategy that calculates a ratio between the target and reference gene. The reference gene used throughout the qPCR experiments was GAPDH. A CT value gained from computer software Rotor Gene Q series was converted into ΔCT to calculate the relative fold change of a sample again the control sample, known as calibrator. The calibrators for the qPCR reactions carried out in this project were the control (untreated samples). The house keeping genes used were, GAPDH, β-actin in INS-1 cells and GAPDH and B2M in CM cells.

The fold change relative to the calibrator sample was calculated as follows:

1. Δ_{CT} = Ct target gene – Ct endogenous control (normalisation to housekeeping gene to minimize sample to sample variations)
2. $\Delta\Delta_{CT} = \Delta_{CT}$ sample - Δ_{CT} calibrator
3. $2^{\Delta\Delta CT}$ = fold change relative to the calibrator sample

2.8 siRNA Transfection

siRNA techniology was used to transiently knockdown cellular proteins. The transient transfections were performed using Lipofectamine RNAiMAX (life Technologies, UK) alongside siRNA (Dharmacon, GE Healthcare, UK). INS-1 cells were seeded into 6-well plates 24 hours before the transfection in order to be 40-50% confluent at the time of transfection. siRNA-Lipofectamine complexes were prepared for each sample to be transfected (one well of the 6-well plate) as follows: in a 1.5ml sterile

tube, 7µl of siRNA (20µM) was diluted in 243µl of Optimem (Invitrogen) without serum and was mixed gently. In a separate sterile tube 7µl of RNAiMAX (Invitrogen) was diluted in 243µl of Optimem without serum and mixed gently. These solutions were incubated at room temperature for 8 minutes before being combined into one tube. The duplex was incubated at room temperature for 25 minutes. Media was removed from the cells and replaced with RPMI-1640 with serum but without antibiotics, subsequently 500µl of the transfection solution was added. Following a 24-hour incubation the transfection solution was removed and complete RPMI-1640 was added and was incubated for 72 hours before knock-down was detected using western blotting.

2.9 Mass Spectrometry

The basic principal of mass spectrometry is the generation of ions from a specific sample. The ions are separated based on their mass-to-charge ratio (m/z) and the relative abundance of each ion is then identified. This is done via the following process; the ions are produced from the sample in the ionisation source. Based on the mass-to-charge ratio the ions are then separated in the mass analyser. Selected ions are then fragmented and analysed again, these are then detected their abundance is measured by a detector that can convert the ions into electric signals. These signals are then processed using a computer (premier biosoft).

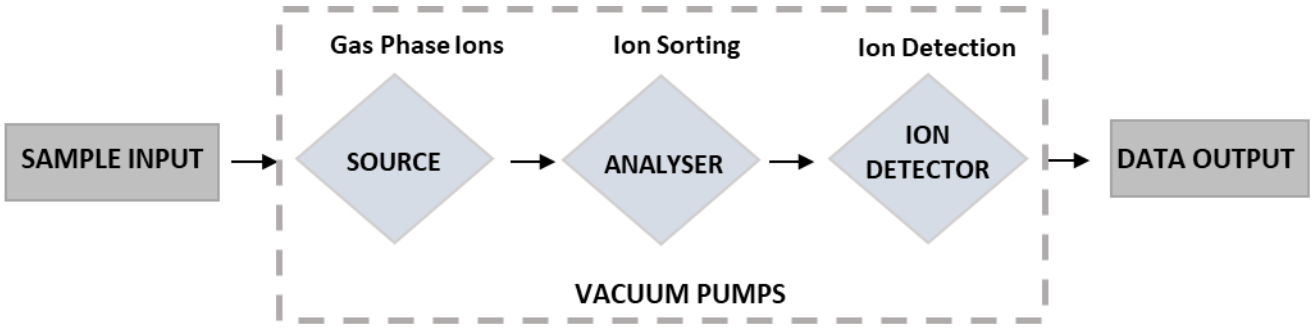

Figure 2.2 Overview of a Mass spectrometer. *A mass spectrometer has three main components; ion source for producing gaseous ions, the analyser for sorting the ions based on their mass-to-ratio and a detector for detecting ions and recording the relative abundance.*

2.9.1 Cell lysis

Cell lysis was used prior to protein quantification using BCA assay. Cells were harvested using Trypsin EDTA, (Gibco life technologies UK) incubated for 5 minutes at 37°C and centrifuged for 5 minutes at 300g. The cell pellet was washed twice in DPBS (Phosphate buffered saline) (Gibco, Life technologies UK) to remove any residual serum. Subsequently 15µl of 8M Urea was added to the pellet followed by 20µl 0.05% ProteaseMAX™ surfactant (Promega). The tube was then vortexed to ensure complete lysis of the cells. Following this 58.5µl of 50mM TEAB (Triethyl ammonium bicarbonate) was added and the tube was incubated on ice for at least 15 minutes. The cells were then centrifuged for 10 minutes at 14,000g and the supernatant was transferred into a fresh tube. To enhance cell lysis, the cell lysate was placed in a water bath sonicator for 5 minutes on full power, then on to ice for 5 minutes, this was repeated 3 times. The cell lysate was the centrifuged again 13,000x g for 5 minutes, the supernatant was transferred to a fresh tube.

2.9.2 Alkylation and Reduction

To the cell lysate 1µl of 0.5M DTT was added and incubated at 56°C for 20 minutes. Following the incubation period 2.7µl of 0.5M IAA was added. This was then mixed using a vortex and incubated at room temperature for 15 minutes in the dark. A protein assay was then carried out.

2.9.3 Trypsinisation protocol

From the cell lysate, 50µg of protein was collected and the volume was made up to 100µl with 50mM TEAB. Alongside this, 20µl of 1mM HCL was added to a vial of Trypsin (sigma), vortexed thoroughly to re-suspend the trypsin and 2µg (2µl) of Trypsin was added to the cell lysate sample, vortexed thoroughly and incubated at 37°C for 12-13 hours. Following the trypsinisation incubation the samples were concentrated to dryness in a speedvac. The samples were then re-suspended in 20µl 5% acetonitrile and transferred to a fresh LC vial. The sample were then analysed using the mass spectrometer.

2.10 Nitrate/Nitrite assay

To determine the levels of nitrite present in the INS-1 cell, a nitrite/nitrate kit was purchased (Sigma-Aldrich). A standard curve was generated, and all buffers were prepared based on manufacturer's instructions. Following the cell growth and treatment period the cell culture media was collected and centrifuged at 1000 x g to remove all insoluble material. The supernatant was collected and

transferred to a clean tube. Appropriate amounts of standard and sample were added to wells of a 96-well plate. Greiss reagent A was added to all wells and the plate was covered and incubated at 25°C for 5 minutes on a horizontal shaker. Greiss reagent B was then added to the wells and the plate was incubated at 25°C for 10 minutes. Following this incubation period, the absorbance was measured at 540nm. The blank measurements were subtracted from the test samples and the standards and the levels of nitrite were determined using the standard curve.

2.11 NF-κB activity

NF- κB activation is measured in this project as it is implicated in to regulation and transcription of multiple genes that are involved in the mediation of immune and inflammatory responses. The principle of the NF- κB transcription factor kits is to detect and quantify transcription factor activation via an ELISA assay.

2.11.1 Nuclear extraction

The nuclear extract is required for the NF-κB Transcription Factor Assay (Active Motif, CA, USA), this was doing using the Nuclear/cytosol extraction kit (Biovision, Milpitas, CA, USA). All buffers were prepared prior the assay according to manufacturer's guidelines. The cells were detached from the plate surface using trypsin EDTA and centrifuged to form a cell pellet. Cytosol extraction buffer-A was added to the pellet and fully resuspended via vortexing. The cells were then incubated on ice for 10 minutes. Following this ice-cold cytosol extraction buffer-B was added and they tube was vortexed for 10 seconds followed by an incubation on ice for 1 minute and the vortexed again for 10 seconds. The tube was centrifuged for 5 minutes at 17,000 x g and the supernatant (cytosolic fraction) was immediately transferred to clean tube and placed on ice. The pellet was resuspended in ice-cold nuclear extraction buffer and vortex for 15 seconds and returned to the ice, this was repeated every 10 minutes for 40 minutes. The tube was then centrifuged at 17,000 x g for 10 minutes. The supernatant (nuclear extract) was transferred to a clean tube and used in the NF-κB activity assay immediately.

2.11.2 NF-κB activity assay

To measure NF-κB activity a kit was purchased, and the manufacturers guidelines were followed. All buffers and reagents were prepared according the manufacturer. To each well 30µl of complete binding buffer was added to each well being used. To the positive test well 20µl of diluted jurkat was added and to the negative wells 20µl complete lysis buffer was added. The plate was covered at incubated at room temperature for 1 hour with mild agitation on a plate rocker. The wells were then washed 3 times with diluted wash buffer. To each well 100µl of diluted NF-κB antibody was added, followed an incubation period of 1 hour at room temperature without agitation. The wells were then washed 3 times with diluted wash buffer. To each well 100µl of diluted HPR-conjugated antibody was added and the plate was covered and incubated at room temperature. after this incubation the wells were washed 4 times with diluted wash buffer followed by 100µl of developing solution added o each well. This was incubated for 3 minutes before 100µl of stop solution was added and the absorbance was measured at 450nm/655nm.

2.12 HNE-assay

To measure the presence of 4-hydroxynonenal (Abbexa, Cambridge, UK) was purchased, and the manufacturers guidelines were followed. The wells were washed prior to use and 50µl of prepared standards were added to the standard well, and 50µl of the diluted sample were added to the test well and 50µl of sample/standard buffer was added to the control wells. This was followed immediately by 50µl of biotin conjugate antibody being added to each well. The plate was covered and incubated at 37°C for 45 minutes. The plate was then washed with diluted wash buffer three times. To each well 100µl of Streptavidin-HRP Conjugate working solution was added and the plate was covered and incubated at 37°C for 30 minutes. Following the incubation period each well was washed five times with diluted wash buffer. To each well 90µl of TMB was added, the plate was then covered and placed in the dark at 37°C for 20 minutes. Subsequently, 50µl of stop solution was added to each well and the absorbance was measured at 450nm.

2.13 Immunoprecipitation

Immunoprecipitation is a technique that is used to separate proteins that are bound to an antibody from the rest of the sample. This is done by coating magnetic beads with a specific antibody prior to

adding the cell lysate. This allows easy removal of the magnetic bead-bound antibody and proteins (Cothall JT, 2014).

2.13.1 Antibody binding to beads

Immunoprecipitation was carried using out using Pierce™ Crosslink Magnetic IP/Co-IP Kit (Thermo Scientific, Waltham, MA, USA) Any required buffers were prepared according to manufacturer's guidelines.

To each tube being used 25µl of vortexed magnetic beads was added and placed on magnetic stand for 1 minute. The bead storage solution was discarded, leaving only the beads in the tube. To each tube 500µl of prepared 1x modified coupling buffer was added. The contents of the tube were mixed and incubated at room temperature for 1 minute on a rotating platform. The beads were collected using the magnetic stand the supernatant was removed and discarded. Antibody was diluted 1:20 and added to the magnetic beads. The beads were incubated in the antibody solution for 1 hour, vortexing every 10 minutes. The beads were collected using the magnetic stand and the supernatant was removed and discarded. Following this, 100µl of prepared 1x modified coupling buffer was added to the beads, the tube was gently inverted, and the beads were collected, and the supernatant removed and discarded. The final step was 300µl of 1x modified coupling buffer being added to the beads, gently inverted to mix. The beads were collected using the magnetic strip and the supernatant removed and discarded. This step was repeated.

2.13.2 Antibody Cross-linking

The provided disuccinimidyl suberate (DSS) blister pack was prepared according to the manufacturer's guidelines. The prepared DSS was then diluted 1:100 in DMSO. To the bead 2.5µl 20x coupling buffer, 4µl DSS and 43.5µl water was added. This cross-linking reaction was incubated for 30 minutes at room temperature, vortexing every 10 minutes. The beads were collected, and the supernatant was removed. The beads were then ready to be incubated with the cell lysate.

2.13.3 Cell lysis and incubation with antibody cross-linked beads

The INS-1 adherent cells were detached from the flask surface using trypsin. The cells were centrifuged into a pellet and washed with cold PBS. Ice cold lysis buffer provided in the kit was added to the cells according to the manufacturer's guidelines. The pellet was resuspended on incubated on ice for 5

minutes with periodic mixing. The lysate was transferred to a microcentrifuge tube and centrifuged at 13,000 x g for 10 minutes to pellet the cells. The supernatant was then transferred to a clean tube prior to protein determination and incubation with the antibody-bound cross-linked beads. The appropriate amount of cell lysate was added to the magnetic beads and stored at 4°C overnight. The following day the beads were stored in 50mM TEAB prior to trypsinisation.

2.13.4 Trypsinisation

The immunoprecipitation samples were then trypsinised. (section 2.7.3). The following day the magnetic beads were removed, and the supernatant was analysed using SWATH-MS.

2.14 Citrate Assay

Citric acid is an important intermediate in the mitochondrial citric acid cycle and is generated by the addition of oxaloacetate to acetyl CoA that results from the glycolytic pathway. Citrate can be transported out of the mitochondria and converted back to oxaloacetate and acetyl CoA where it can then be used for cholesterol synthesis, fatty acid synthesis and histone acetylation. The principle of the citrate kit is a colorimetric assay. The citrate assay kit quantifies citrate in a sample by converting citrate to pyruvate via oxaloacetate. The newly formed pyruvate is able change the colour of a probe and the optical density is measured (Abcam, Cambridge, UK).

2.14.1 Citrate assay sample preparation

INS-1 cells were harvested and centrifuged to form a cell pellet. The pellet was washed with cold PBS and resuspended in 100µl of assay buffer. A cell pellet was reformed by centrifugation at 13,000 g for 5 minutes at 4°C. The supernatant was collected and transferred to a clean prior to the start of the citrate assay kit protocol (Abcam, UK). A standard curve was prepared according to the manufacturer's guidelines.

2.14.2 Deproteinisation step

The sample was added to a 10 kD Spin Column (ab93349) and centrifuged 3 x 10 minutes at 13,000g in order to collect the deproteinised sample used for the assay procedure.

2.14.3 Citrate assay procedure

A standard curve was prepared was prepared according to the manufacturer's guidelines. To each of the standard wells 50µl of standard was added and to the test wells 50µl of diluted sample was added and this was repeated for the background samples.

A reaction mix was prepared as below;

Table 2.5: Reaction mix for test, standard and background samples.

Reagent	Volume for test and standard samples (µl)	Volume for background well (µl)
Assay buffer	44	46
Enzyme mix	2	0
Developer	2	2
Citrate probe	2	2

To the corresponding well 50µl was added. The plate was incubated at room temperature for 30 minutes prior to the absorbance being measured at 570nm.

2.15 Insulin Secretion ELISA

Insulin secretion from INS-1 pancreatic β-cells was measured using an ELISA assay purchased from Mercodia, Uppsala, Sweden. The ELISA was carried out according to the manufacturer's guidelines. INS-1 cells were seeded into 6-well plates and treated ± GLT for 5 days. The following buffers were prepared immediately prior to the start of the ELISA assay.

Table 2.6: Krebs ringer-hepes buffer recipe.

Reagent	**Concentration**
Sodium Chloride	125mM
Potassium Phosphate monobasic	1.2mM
Potassium Chloride	5mM
Magnesium Sulphate	2mM
Calcium Chloride	1mM
Glucose	1.67mM
Hepes	25mM
BSA	0.1%
	pH 7.4

Table 2.7: Secretagogue Cocktail.

Reagent	**Concentration**
Tolbutamide	1mM
Leucine	10mM
Glutamine	10mM
PMA	1µM
Isobutylmethyxantine	1mM
Glucose	10mM

To appropriate wells, 1ml of Krebs ringer-hepes buffer or secretagogue was added and incubated at 37°C for 2 hours. Subsequent to the incubation period the cell medium was collected into clean 1.5ml Eppendorf tubes and centrifuged at 900 rpm for 2 minutes. The supernatant was collected and placed into fresh Eppendorf tubes. Sample and calibrators (10µl) were pipetted into a pre-coated 96-well plate in duplicate, to this 50µl of enzyme conjugate was added. The plate was covered and placed on a plate shaker for 2 hours at room temperature shaking 900 rpm, in order for any insulin present to bind to the antibodies on the pre-coated plate. The reaction volume was discarded, and the wells were washed 5 times using 350µl wash buffer per well. To each well 200µl substrate TMB was added to each well and incubated at room temperature for 15 minutes followed by 50µl stop solution. The optical density was read at 450nm.

2.16 Statistical Analysis

To determine statistical significance of results gained in this thesis statistical analysis using a two-tailed, unpaired T-test for analysis of two conditions or ANOVA for analysis of or more conditions were carried out using Microsoft Excel. A p-value of <0.05 was considered to be significant. Results are expressed

as mean ± standard error of the mean (SEM). All results expressed are from three or more independent experiments.

Chapter 3

Glucolipotoxic-induced Beta Cell Inflammation

3.0 CHAPTER 3: Glucolipotoxic-induced Beta Cell Inflammation

3.1 Introduction

Type 2 diabetes is a chronic metabolic disorder with increasing prevalence worldwide (Kennedy-Martin et al, 2017) and is characterised by β-cell dysfunction, insulin resistance and ultimately beta cell death (Ortega et al, 2017). Excess body weight and the associated changes in metabolism that occurs as a result of a high energy diet including increased glucose and circulating free fatty acids is the main risk factor of developing type 2 diabetes (Golson et al, 2010). Type 2 diabetes is the most common type of diabetes with type 2 diabetes accounting for approximately 91% off all diabetic cases (Ortega et al, 2017). It is known that over 80% of type 2 diabetic patients are obese and that glucose and free fatty acid levels are often increased in obesity. Fatty acids can induce insulin secretion and long chain fatty acids, however increased fatty acid levels associated with obesity can result in impaired insulin secretion and development of T2D via oxidative stress and inflammation (Ježek et al, 2018). Beta cell dysfunction in type 2 diabetes could potentially result from multiple causes including, ER stress, oxidative stress, lipotoxicity, and glucotoxicity, which elicit an inflammatory response (Nordmann et al, 2017). Inflammation is a manifestation of a disease which initially has beneficial effects such as encouraging regeneration or preventing spread of infection, however prolonged or chronic inflammation may intensify disease via tissue destruction which is likely to be the case in type 2 diabetes (Donath et al, 2009). Inflammatory responses are likely to result in the activation of nuclear factor kappa B (NF-κB) (Nordmann et al, 2017).

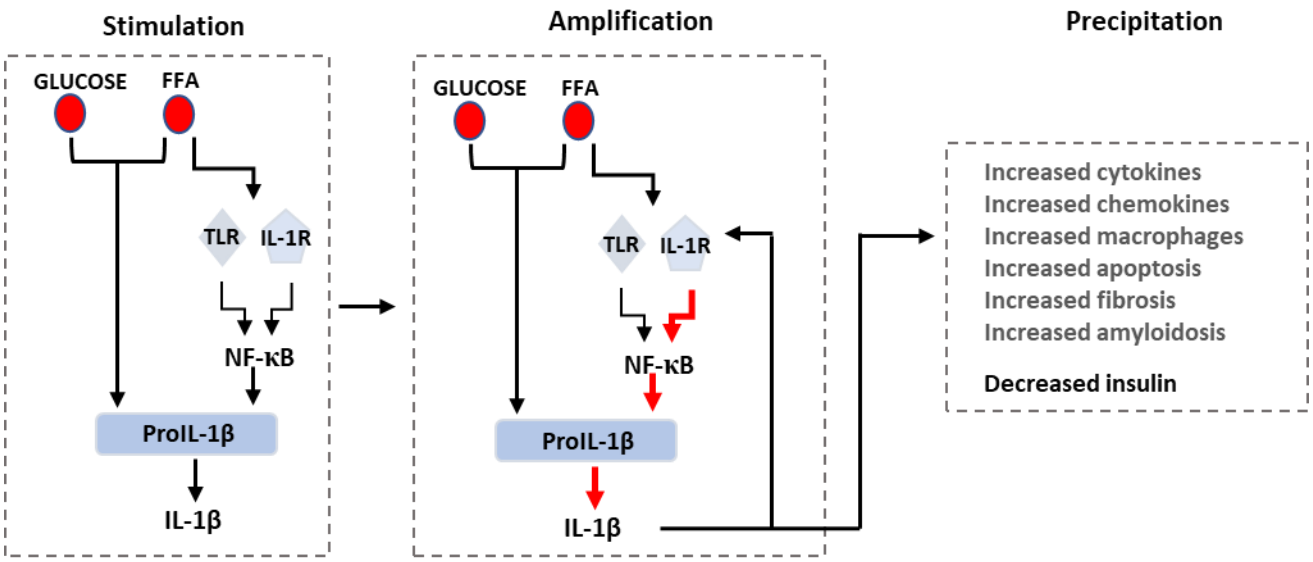

Figure 3.1 Effects of glucose and fatty acids on pancreatic β-cell. *The exposure of β-cells to GLT initially results in the expression of cytokines such as IL-1, resulting from the adaptive cellular response. Chronic exposure to GLT results in the auto stimulatory activation of IL-1RI and further production of IL-1 and IL-1-dependent cytokine and chemokine release in the amplification stage. The precipitation stage results in a broad inflammatory response via activation of the paracrine and autocrine (Donath et al, 2009).*

3.1.1 Nuclear factor kappa B

NF-κB is a family of inducible transcription factors that are found ubiquitously. The family is made up of 5 members including; Rel (c-Rel), RelA (p65), RelB, NF-κB1 (p50/p105) and NF-κB2 (p52/p100) that are able to associate with each other to form homo- and heterodimer (Oeckinghaus and Ghosh,2009). All of which have a conserved Rel homology domain (RHD) that is made of up of approximately 300 amino acids, which is responsible for its interaction with other NF-κB family members, inhibitory proteins and DNA. In non-stimulated cells NF-κB are bound to ankyrin-rich regions the inhibitor IκB and NF-κB is sequestered in the cytoplasm, in stimulated cells the IκB inhibitor is phosphorylated, meaning NF-κB is free to enter the nucleus, where it is able to bind to the κB sites in the promoter regions of target genes and induces transcription of pro-inflammatory mediators such as iNOS, COX-2, IL-1β, IL-6, amongst others (Shin et al, 2012. Lorenzo et al, 2011).

NF-κB has long been considered a prototypical proinflammatory signalling pathway, largely based on the activation of NF-κB by proinflammatory cytokines such as interleukin 1 (IL-1) and tumour necrosis factor α (TNFα), and the role of NF-κB in the expression of other proinflammatory genes including cytokines, chemokines, and adhesion molecules (Lawrence T, 2009).

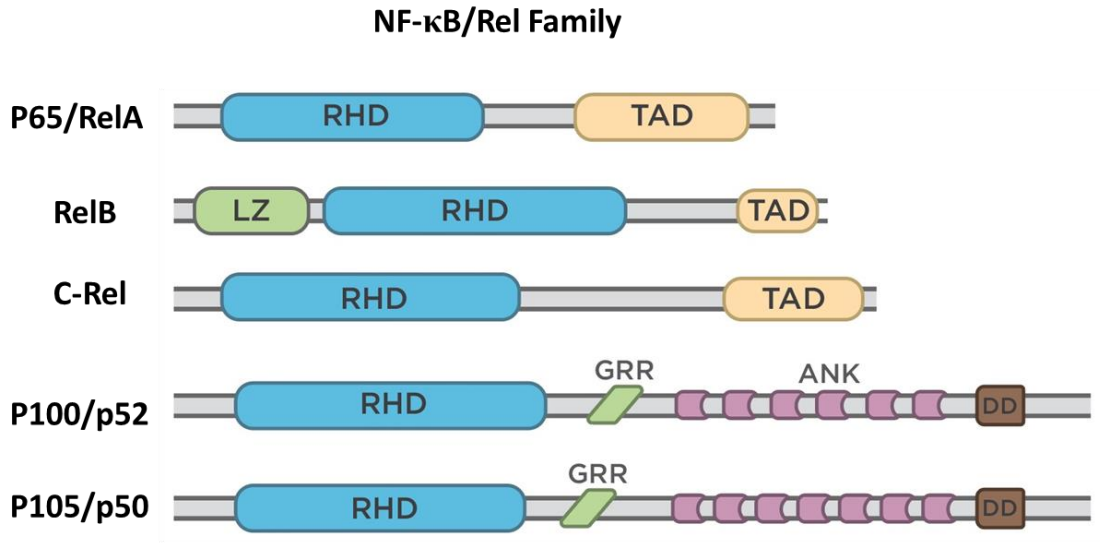

***Figure 3.2 NF-κB family members**. Schematic image showing the structure of the NF-κB family members. Adapted from Oeckinghaus and Ghosh, 2009.*

3.1.2 Cluster of differentiation (CD40)/ Tumour Necrosis Factor Receptor 5 (TNFR5)

As already discussed in chapter 1 section 1.5, CD40 also known as TNFR5 is a membrane glycoprotein belonging to the tumour necrosis factor receptor super family and is expressed in many cell types. Its natural ligand CD40L (CD154) is part of the TNFα protein family and is a type II transmembrane protein (Barbé-Tuana et al, 2005). The interaction between CD40 and CD40L has been reported to coordinate the inflammatory process through secondary messengers. CD40-CD40L initiates the release of various cytokines and chemokines and activate multiple transcription factors, one of which may be NF-κB (Tone et al, 2001. Rizvi et al, 2008).

3.1.3 Inducible Nitric Oxide Synthase

Nitric oxide synthase (NOS) metabolises L-arginine to OH-L-arginine which is then oxidised to L-citrulline and nitric oxide (NO). There are three types of NOS, all of which contain haem and bind with calmodulin. Endothelial NOS (eNOS) which are expressed in endothelial cell and have a role in maintaining blood vessel dilation, controlling blood pressure and vaso-protective properties. Neuronal

NOS (nNOS) that is expressed in peripheral neurons and functions in maintaining synaptic plasticity in the central nervous system, vasodilation and central regulation of blood pressure. This project is concerned with inducible NOS (iNOS), which unlike nNOS and eNOS is not constitutively expressed and expression is induced in stimulated cells by various inflammatory stimuli (Simon et al, 2015). iNOS is expressed in a number of cell types both immune and non-immune cells and its induction contributes to the pathophysiology of inflammatory diseases (Förstermann and Sessa, 2012).

3.1.4 Nitric Oxide

NO is a free radical and a gaseous signalling molecule that is required for pancreatic physiology. NO is produced by the enzyme NOS, of which are 3 isoforms. The isoform of interest in this project is iNOS, because it is the NOS isoform that is chiefly responsible for the role of NO in inflammation, via NF-κB-dependent transcription (Zamora et al, 2000). iNOS is involved in nitic oxide (NO) formation by catalysing the transformation of L-arginine to L-citrulline, where L-arginine concentrations are rate limiting in this process (Keklikoglu and Akinci, 2013). The increased levels of NO resulting from the transformation of L-arginine to L-citrulline could potentially result in increased levels of peroxynitrite ($ONOO^-$) to such an extent that it could interact with signalling pathways in the region which its produced. NO is able to interact with superoxide in a number of physiological situations, including inflammation (Wolin et al, 2002). Superoxide is reactive oxygen species ROS, which are generated when glucose undergoes oxidative phosphorylation in the mitochondria. ROS was originally considered to be a useless by-product of metabolism in the mitochondria which had damaging effects on biological systems but there is increasing evidence to suggests that the generation of ROS is essential for various processes (Pi et al, 2007) such as, in cellular respiration increased superoxide is found to be required in decreasing ADP concentration, supplying substrates and increasing intracellular Ca^{2+} concentrations. Superoxide is highly reactive but can be converted to a less reactive molecule known as H_2O_2 by superoxide dismutase (SOD), which can then be converted to water and oxygen by enzymes catalase (CAT), glutathione peroxidase (GPx) and peroxiredoxin. Pancreatic β-cells possess low levels of anti-oxidant enzymes to overcome the constant production of superoxide, they are equipped with moderate SOD, but insufficient levels of H_2O_2 inactivating enzymes CAT and GPx, possessing around 5% GPx compared to expression in the liver. The vast imbalance between superoxide and H_2O_2 breakdown could mean that pancreatic β-cells are vulnerable to H_2O_2 build up (Pi et al, 2007).

3.1.5 Reactive carbonyl species

Reactive carbonyl species (RCS) are made up of biological compounds that are formed via membrane lipid oxidation by reactive oxygen species and possess carbonyl-conjugated C-C bonds. By comparison to free radicals, RCS are more stable and are able to freely diffuse in and out of the cell, meaning they can attack targets away from the area of formation making them mediators of oxidative stress and tissue damage. An increase in ROS can be associated with the progression of various diseases via the increase in RCS, which can then employ their detrimental effects by increasing ROS production and resulting in the formation of a vicious cycle of ROS and RCS production (Vidal et al, 2014). Following their production, RCS are highly reactive due to their electrophilic nature and easily react with nucleophilic amino acids such as Lys, His and Cys which results in protein adduct formation. The formation of carbonyl species adducts is reported to cause irreversible cellular damage (Hwang et al, 2016).

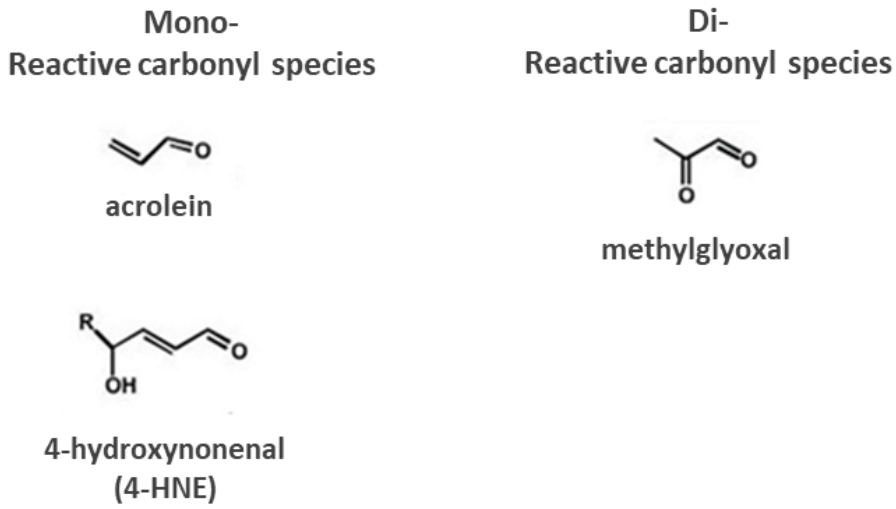

Figure 3.3 Carbonyl species and adducts. *Schematic image of the most abundant carbonyl species. Adapted from Tian et al, 2014.*

Of the carbonyl species the α,β-unsaturated aldehydes known as 4-hydroxynonenal (4-HNE) and acolein and the dicarbonyl known as methylglyoxal are the most abundant and toxic lipid derived RCS (Vidal et al, 2014). As such, this project 4-hydroxynonenal (4-HNE), which is a small electrophilic, mono-reactive carbonyl species that is a major by-product of lipid peroxidation (Tian et al, 2014). ROS that is produced by the mitochondrial transport chain is the major source of 4-HNE and because there

is a basal concentration of ROS that is inherent to aerobic life, there should be a basal concentration of 4-HNE. The physiological concentration of 4-HNE in plasma is 0.3-0.7µM, therefore if the concentration of the RCS doesn't exceed this then this could be beneficial for the cell, as in low concentrations 4-HNE plays important roles in various cellular functions including, cell growth, proliferation, differentiation and apoptosis (Tian et al, 2016. Semchyshyn HM, 2014. Dallaeu et al, 2013).

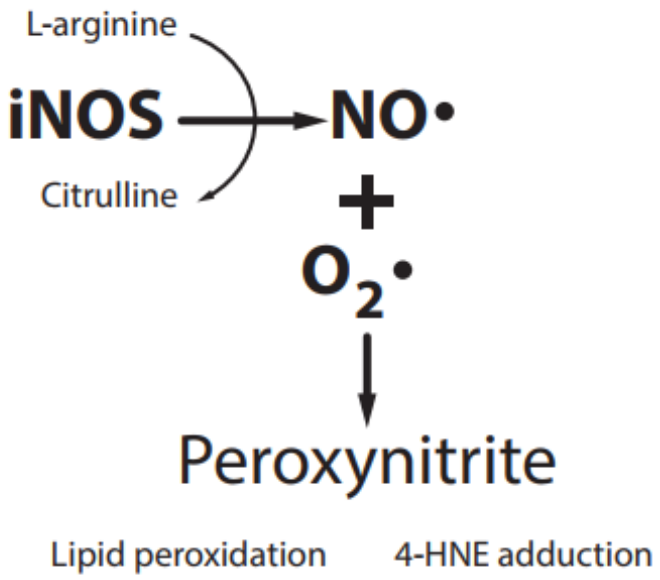

Figure 3.4 Pathway demonstrating how iNOS results cell damage. *iNOS converts L-arginine to citrulline and produces simultaneously produces NO in the process. When NO is upregulated it more likely to encounter superoxide (O_2•). The combination of NO and O_2• results in the production of peroxynitrite and lipid peroxidation and HNE adducts as by products (Pacher et al, 2007)*

3.2 Chapter Aim

This project focusses on the dysfunction of pancreatic β-cells resulting from inflammatory process induced by the exposure to glucolipotoxicity. Glucolipotoxicity is the term given to the deleterious effects of the combination of both elevated glucose and free fatty acid levels (Poitout et al, 2010). The aim of this investigation was to identify inflammatory processes resulting from the exposure to INS-1 and CM cell to high glucose and free fatty acid levels down stream of CD40, that could potentially lead to β-cell damage.

3.3 Results

In order to investigate the effects of both high glucose and high fatty acids on inflammation in pancreatic beta cells, a rat insulinoma cell line was used known as INS-1. To replicate chronic glucolipotoxic conditions the INS-1 cells were incubated in either control conditions (11mM glucose) or glucolipotoxic conditions (GLT) (27mM glucose, 200µM palmitic acid and 200µM oleic acid) for 5 days, prior to cell death. The initial results below demonstrate that a day treatment induces phenotypical changes of INS-1 cells without significantly decreasing cell viability (Fig 3.6) and prolonged exposure to GLT conditions results in cell death (Fig 3.5). Further to this 5-day exposure of INS-1 cells to GLT reduces insulin secretion by 30% (p=0.00037) indicating that chronic exposure to high glucose to fatty acids disrupts β-cell function (Fig 3.7).

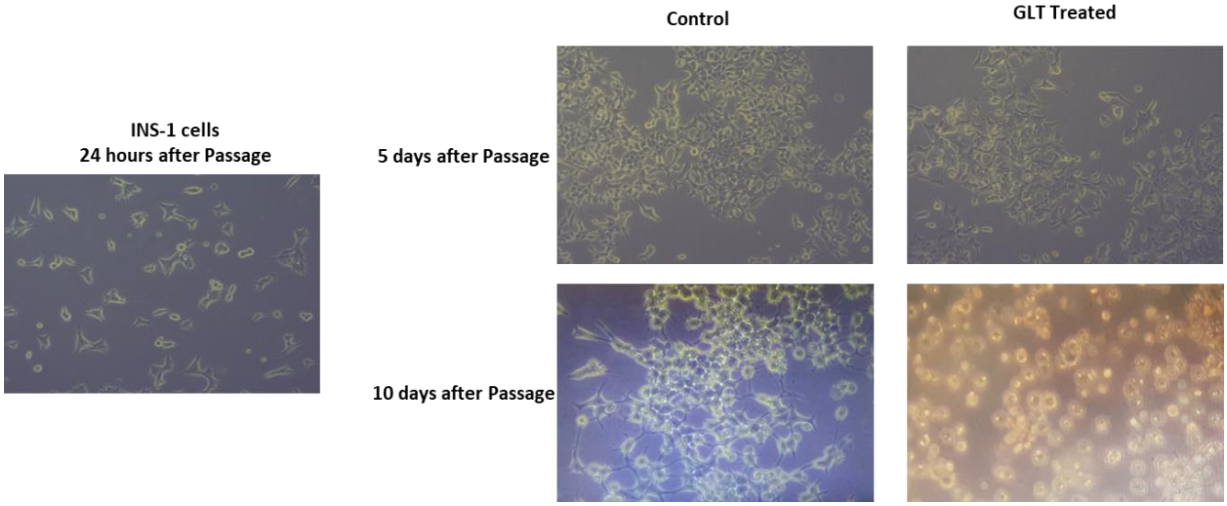

Figure 3.5 INS-1 cells at different time points in control and GLT conditions. *The GLT treatment is added 24 hours after passage and experimental procedures carried out 5 days later. As the photos indicate the cells are still viable at 5 days in*

control and GLT conditions and demonstrate phenotypic differences. Ten days post treatment the GLT treated cells are no longer living.

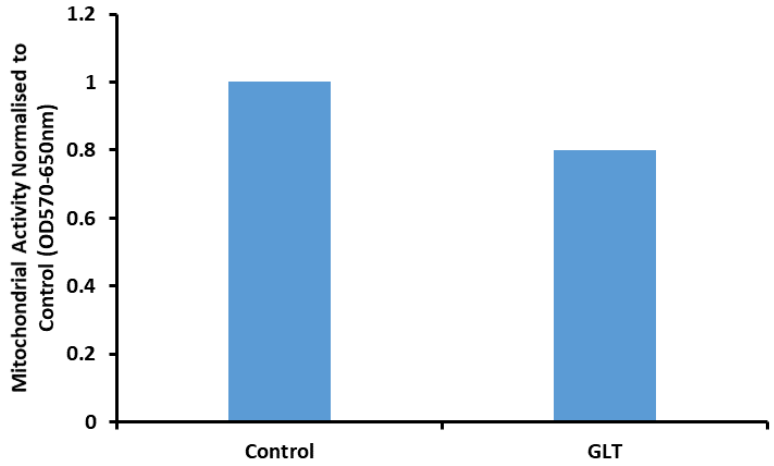

Figure 3.6 Effect of GLT on mitochondrial activity. *INS-1 cells were incubated 5-days ±GLT and cell viability was determined via MTT assay. Data shows absorbance values 570nm – 650nm. The data shown is the mean ± SEM of three independent experiments.*

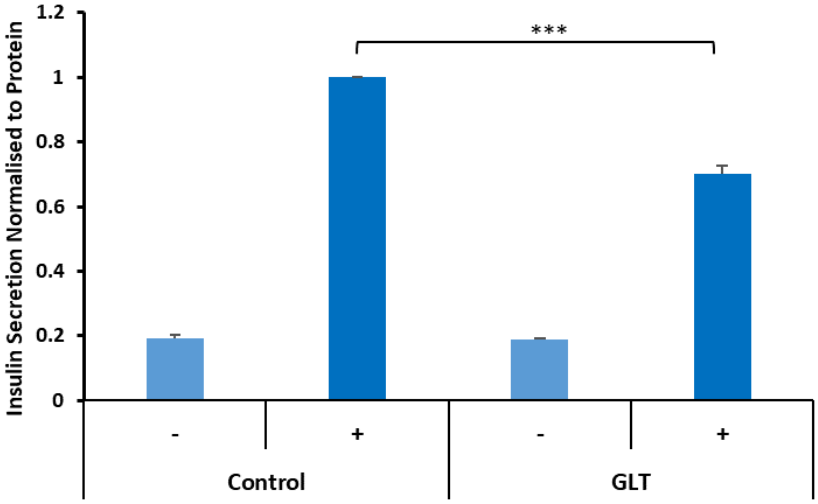

Figure 3.7 Insulin secretion following 5-day incubation ±GLT. *INS-1 cells were incubated for 5-days ±GLT. Cells were then subjected to secretagoge incubation for one hour prior to insulin secretion analysis using ELISA testing (Mercodia, Uppsala, Sweden). The data shown is the mean ± SEM of three independent experiments.*

3.3.1 Effect of GLT on CD40 and NF-κB

CD40/TNFR5 belongs to the tumour necrosis factor receptor superfamily (Tone et al, 2001) and is expressed in a number of cell types. The ligand of CD40 known as CD40L is primarily associated with immune cells but is present in other cell types including pancreatic β-cells. The reason for observing the effects of the TNFR5 member of the super family is based on Affymetrix data and PCR that showed TNFR5/CD40 is the most up-regulated of family members affected by GLT (Table 3.1).

Table 3.3: TNFR super family member expression. *Analysis of individual expression data for TNFR superfamily members TNFRSF1, TNFRSF5, TNFRSF6 and independent RT-qPCR analysis. Data are shown from three individual experiments. Experiments were performed by Dr Marta Bagnati. Bagnati et al, 2016.*

	TNFR1	TNFR5	TNFR6
Affymetrix	———	2.23 (p=<0.0001)	1.59 (p=<0.05)
PCR	2.23 (p=NS)	3.62 (p=<0.05)	1.19 (p=NS)

To identify interactions of CD40, MetaCore™ was used to generate a non-biased network by Dr Tania Jones, from microarray data that was gathered by Dr Marta Bagnati. MetaCore, from Thomson Reuters, is an analysis programme for interpreting functional information from lists of regulated genes. It produces relevant pathways, diseases and networks associated with the specific genes of interest.

CD40L signalling through CD40 resulted as the top-ranked of all up-regulated networks in GLT conditions. The analysis showed that both NF-κB and JAK/STAT signalling networks were up-regulated in response to GLT.

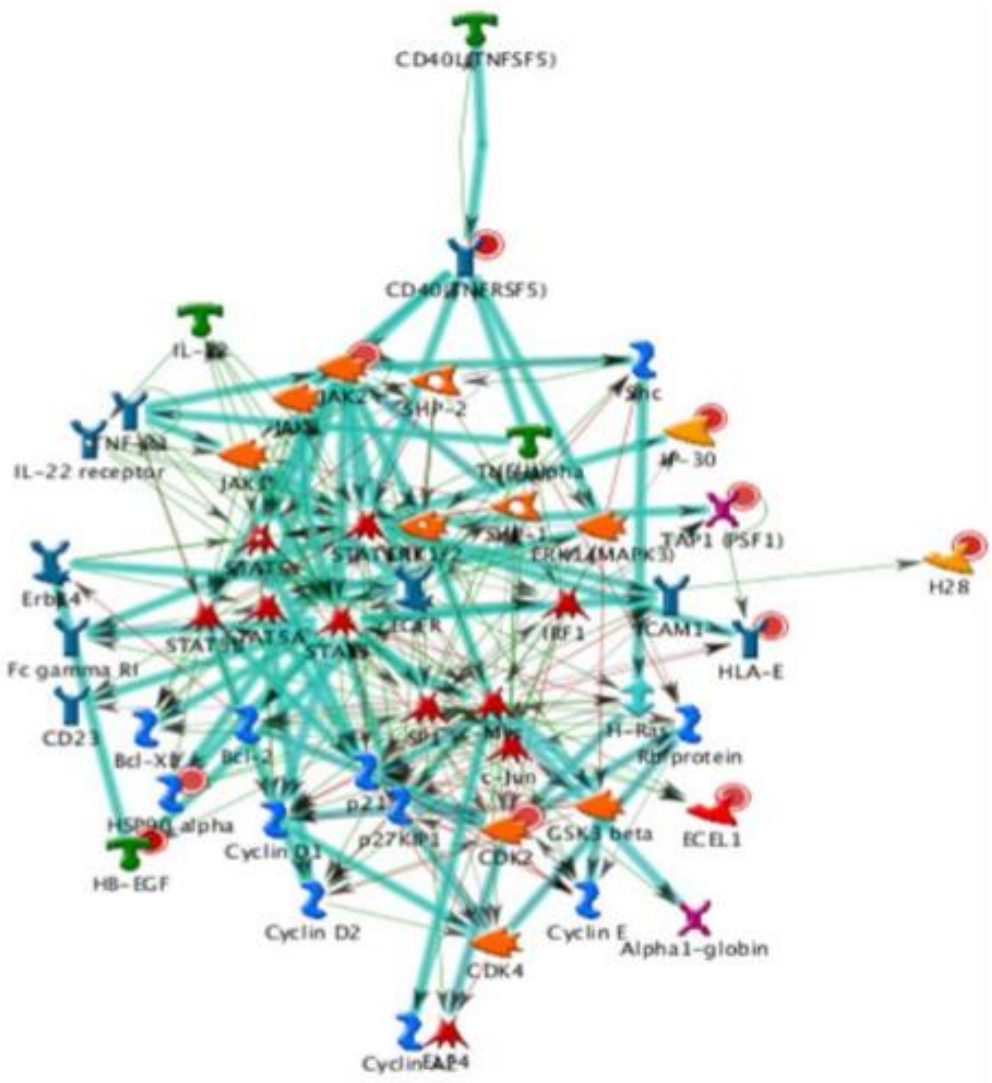

Figure 3.8 MetaCore™ Network Analysis. *Unbiased network analysis of a microarray data set ±GLT generated by Dr Tania Jones.*

In order to observe the effects that GLT conditions has on the expression of the CD40 and NF-κB gene, INS-1 cells were incubated for 5 days in media containing 200µM palmitic acid, 200µM oleic acid and 27mM glucose, the cells were lysed, and total RNA was extracted (Qiagen, Hilden, Germany). The level of CD40 mRNA was measured by RT-qPCR using CD40 specific primers. The data demonstrated an increase in the CD40 gene by 5.65-fold ($p<0.00072$). CD40 protein expression ±GLT was also measured using western blotting and despite the increase in protein expression being more modest than that of mRNA expression, CD40 protein expression was still significantly increased following 5-day GLT incubation.

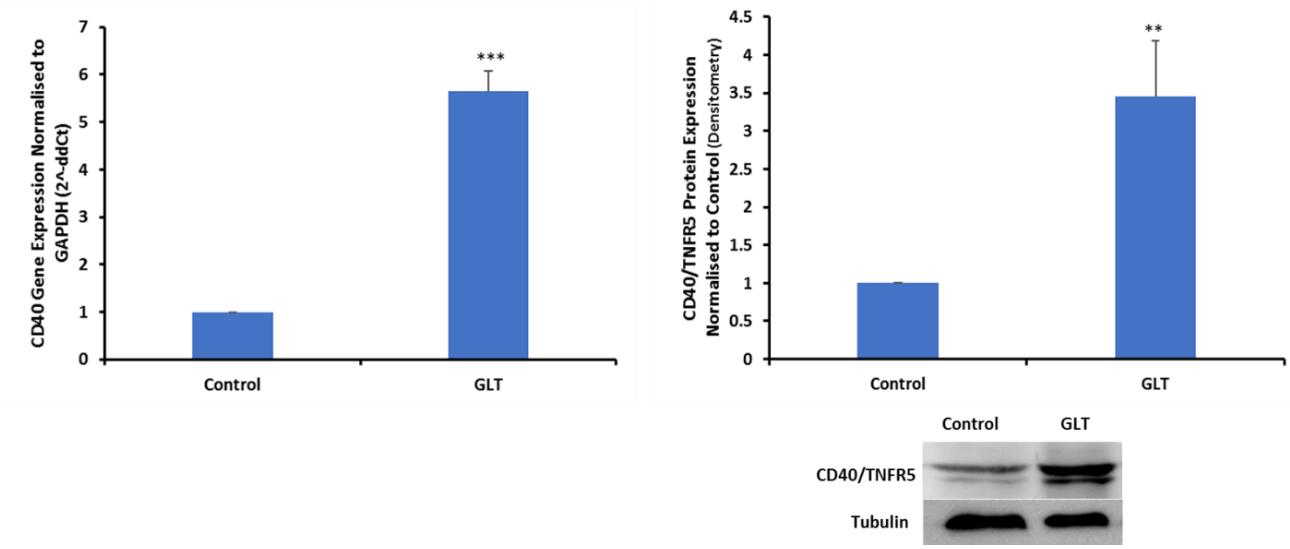

Figure 3.9 TNFR5/CD40 mRNA and Protein Expression. *INS-1 cells were incubated ±GLT for 5 days. Cells were subsequently lysed and either total RNA was extracted or RIPA was used to extract proteins. RT-qPCR was used to measure mRNA, using specific CD40 primers and data represent ΔΔCt expressed as fold change compared to the untreated control. Protein lysates were loaded to a 10% acrylamide gel and separated using SDS-PAGE. Proteins were transferred to a nitrocellulose membrane and immunoblotted using CD40 specific antibody. Data shown is normalised to tubulin and expressed as fold change compared to the untreated control Data shown as mean ±SEM in three independent experiments.*

It was also of interest to observe whether NF-κB activation is directly affected by GLT. The level of NF-κB mRNA expression was measure using NF-κB specific primers and the results demonstrated that exposure to a high glucose and fatty acid environment induced an increase in NF-κB expression by 5.59-fold (p=0.00021). NF-κB activation was also measured using an NF-κB activation ELISA kit (Active motif, Carlsbad, CA, USA). INS-1 cells were incubated ±GLT for 5 days and the nuclear compartment was subsequently extracted, using nuclear/cytosol fractionation kit (Biovision, Milpitas, CA, USA). The data obtained showed that there is an increase in NF-κB activation resulting from exposure to glucolipotoxic conditions of 2.01-fold increase (p=0.0002). This data indicates that the presence of high glucose and high fats is able to induce an increase gene expression of both CD40 and NF-κB.

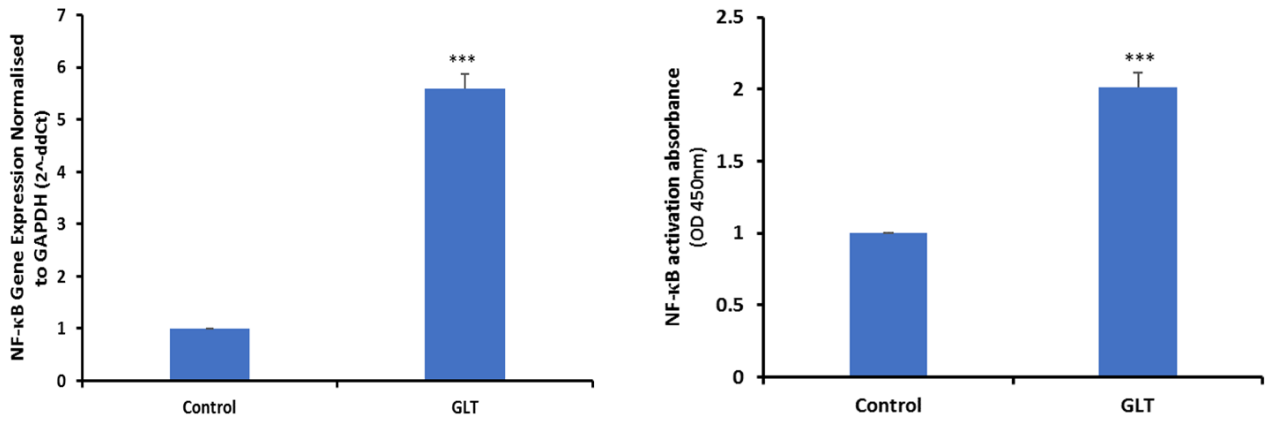

Figure 3.10 NF- κβ mRNA expression and activity. *INS-1 cells were incubated ±GLT for 5 days. Cells were subsequently lysed and total RNA was extracted prior RT-qPCR analysis to measure mRNA, using specific NF-κβ primers. Data represent ΔΔCt expressed as fold change compared to the untreated control. For measuring NF-κβ cells were lysed and measures using NF-κβ TransAm NF-κβ kit (Active Motif, CA, USA). Data shown is mean ±SEM of three independent experiments.*

3.3.2 Effect of CD40 on NF-κB

As observed in the figure above (Fig 3.10) the replication of chronic glucolipotoxic conditions in INS-1 cells has an effect on both CD40 and NF-κB gene expression in pancreatic beta cells. It was important to investigate whether CD40 expression might influence NF-κB activity. To determine this, a transient knockdown of CD40 was carried out using siRNA. The INS-1 cells were subject to ssRNA/siRNA for 24 hours, subsequently incubated ±GLT media for 72 hours and the nuclear extracted was obtained (Biovision, Milpitas, CA, USA). The NF-κB activity of the INS-1 nuclear extracts were measured using an NF-κB activity ELISA kit (Active Motif, CA, USA). The data obtained showed that following CD40 knock down (58.3% $p<0.0423$) there was a reduction in NF-κB activation (46.7% $p<0.0385$).

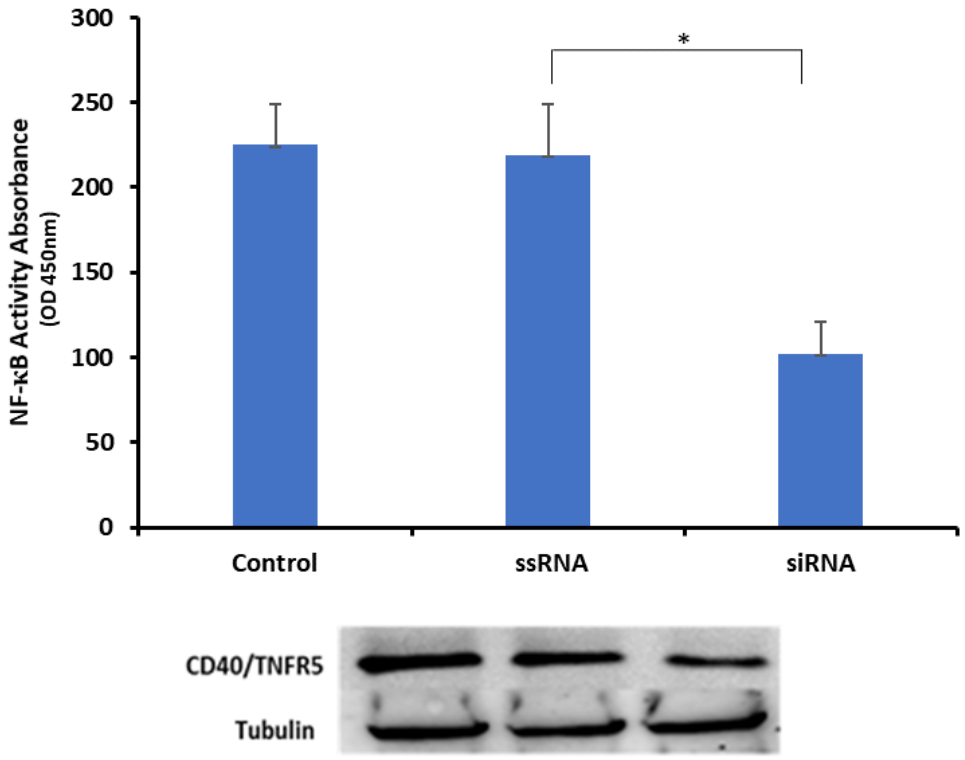

***Figure 3.11 NF-κβ activity following CD40 knock down**. Knock down of CD40 was carried out using siRNA (Dharmacon, GE Healthcare, UK). Cells were treated ±siRNA ±ssRNA for 24 hours and subsequently incubation in RPMI-1640 media ±GLT for 72 hours. Following CD40 knock down the effect of diminished CD40 expression on NF-κβ activity. NF-κβ activity was determined using TransAm NF-κβ kit. Data shown is mean ±SEM of three independent experiments.*

3.3.3 NF-κB p65 is a transcription factor for iNOS

Nuclear Factor Kappa B is a family of transcription factors that are known to play a pivotal role in inflammation via its ability to induce transcription of proinflammatory genes. The NF-κB family include NF-κB1 (p50/p105), NF-κB2 (p52/p100), RelB, c-Rel and p65. This research project focused on NF-κB p65, because as well as being the most commonly activated form of NF-κB it also contains the transactivation domain that is necessary for gene induction (Tak). NF-κB p65 specifically binds to the κB-binding site of target genes located in either the promoter or enhancer region to initiate transcription. Consistant with the other NF-κB family members, p65 contains a Rel homology domain (RHD), which is responsible for recognising DNA sequences of target genes as well forming heterodimers with other members of the NF-κB family (Lecoq et al, 2017).

Following on from the identification that GLT-induced CD40 upregulation is involved in NF-κB activation, we next wanted to determine whether iNOS was also affected by a high glucose and high fat diet. INS-1 cells were incubated for 5 days ±GLT, the cells were lysed in RIPA buffer and the proteins were separated on a 7.5% SDS-PAGE gel, transferred onto a nitrocellulose membrane and were immunoblotted with anti-iNOS monoclonal antibody (Abcam, Cambridge, UK). The results showed that exposure to GLT caused an up-regulation in iNOS protein expression (3.7-fold p=0.0075).

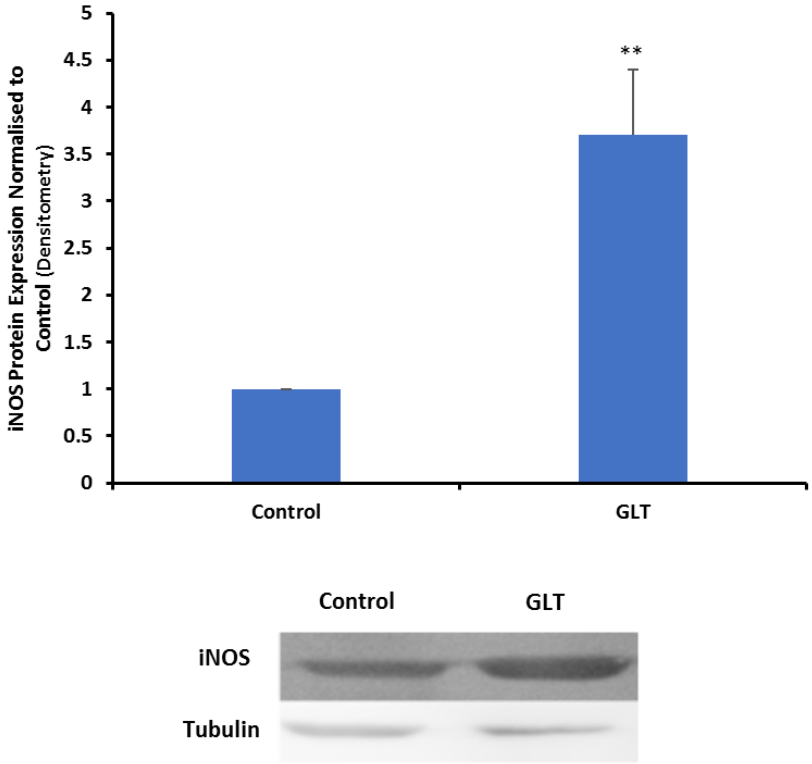

Figure 3.12 iNOS Protein Expression*. INS-1 cells were incubated ±GLT for 5 days prior to lysing using RIPA buffer. Proteins were quantified using BCA assay and loaded to 7.5% acrylamide gel and separated using SDS-PAGE. Proteins were transferred to nitrocellulose and gel and immunoblotted using iNOS specific antibodies. Data is normalised to tubulin and expressed as fold change compared to the untreated control. Data shown is mean ±SEM of three individual experiments.*

3.3.4 Nitric Oxide is produced via two distinct mechanisms in pancreatic beta cells

Nitric oxide is a free radical that is produced in many tissue types, it is known to be responsible for multiple regulatory functions and plays a role in the pathogenesis of cellular injury. NO can be generated from a Nitric oxide synthases (NOSs) (Li et al, 2008).

3.3.4.1 Nitric oxide is produced from L-arginine

In this project, it was observed that iNOS increases in response to GLT conditions. To identify whether nitric oxide is formed enzymatically in β-cells in GLT, it was observed whether L-arginine was being broken down to form citrulline and NO when iNOS expression increases, by measuring the expression of arginosuccinate. INS-1 cells were incubated ±GLT for 5-days, lysed and total RNA was extracted. RT-qPCR was used to measure levels of the gene argininosuccinate synthase (ASS1), which is the enzyme that catalyses the reformation of L-arginine following its initial conversion to citrulline and was measured to see if the up-regulation of iNOS (Fig 3.8) resulted in a greater turnover of L-arginine, in turn meaning an increase in NO. The results demonstrate that the mRNA levels of ASS1 increase in GLT which suggests that citrulline is being formed by the breakdown of L-arginine during the formation of NO.

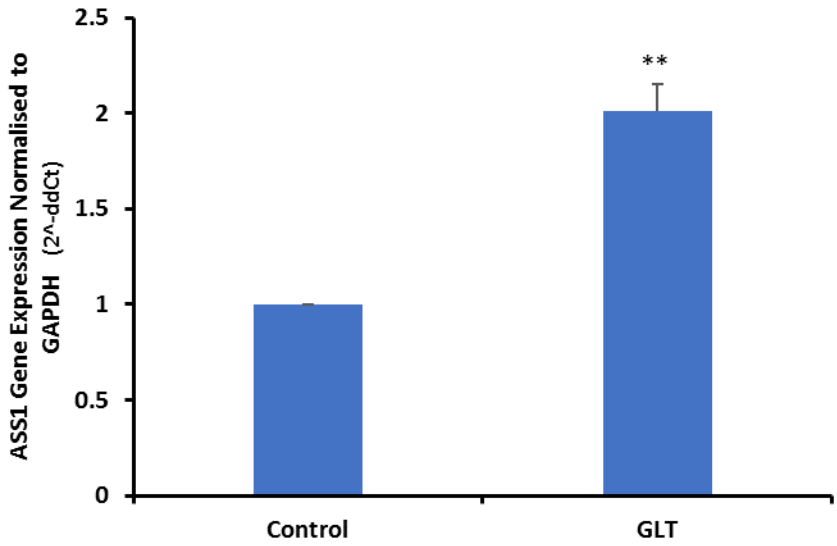

Figure 3.13 Arginosuccinate synthase mRNA expression. *INS-1 cells were treated ± GLT for 5 days. Cells were subsequently lysed and total RNA was extracted, reverse transcribed to generate cDNA and analysed using RT-qPCR using arginosuccinate synthase primers. Data represent ΔΔCt expressed as fold change compared to the untreated control. Data shown is mean ±SEM from three independent experiments.*

3.3.4.2 Is Nitric Oxide is produced from Nitrite

Nitrite is thought to be a mechanism of storing NO in a physiologically stable condition. Nitrite can be converted to NO in certain conditions such hypoxia, by the enzyme nitrate reductase. Nitrite was measured in this experiment to determine whether the pools of stable NO increased in GLT conditions. INS-1 cells were incubated ±GLT for 5-days prior to being used in the Nitrite Assay kit (Sigma-Aldrich, St.Loius, MO, USA).

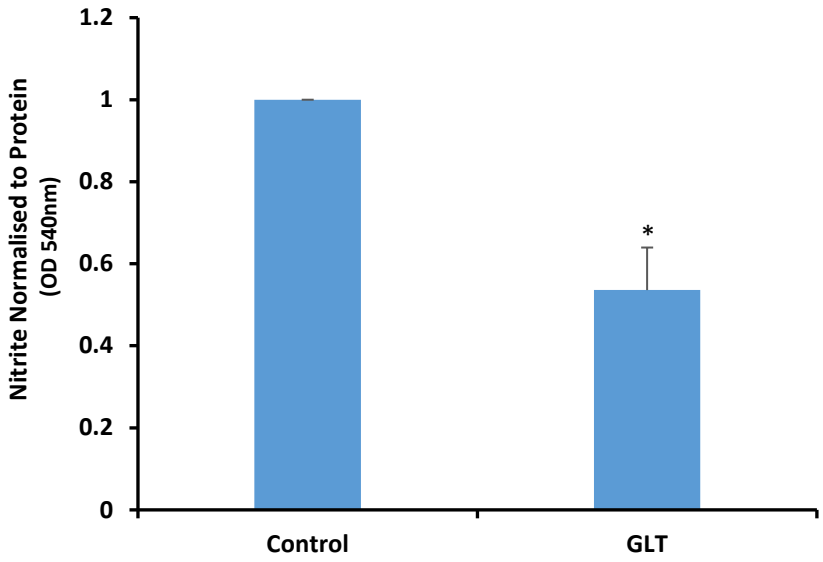

***Figure 3.14 Nitrite in response to GLT**. Cells were incubated ±GLT for 5 days. Cells were lysed and used in the Nitrite colorimetric assay (Sigma-Aldrich). Data represents nitrite compared to the untreated control Data shown is the mean ± SEM of four independent experiments.*

3.3.5 Nitric oxide results in HNE adduction and 3-NT

The reason HNE and 3-NT was included in this investigation is because the most common source of 4-HNE is from reactive oxygen species and 3-NT is a marker of lipid peroxidation, that results from an increase in NO (Cruz and Fardilha, 2016). These species were observed as the results in Fig 3.11 did not indicate an increase in NO, however, the increase in HNE and 3-NT suggests that NO does increase in GLT conditions and results in cell damage. To identify whether HNE and 3-NT increased in response to GLT conditions, INS-1 cells were incubated for 5 days ±GLT media and 4-HNE formation was determined by ELISA (Abbexa, Cambridge, UK) and the absorbance was read at 450nm. The results demonstrated that exposure of the pancreatic β-cell to GLT for 5-days increased 4-HNE formation by 43.4%. 3-NT species were determined by ELISA (Abcam, Cambridge, UK) and the absorbance was read at 450nm. The results showed an increase in 3-NT species by 33%. 3-NT analysis was carried out by Michael Cripps.

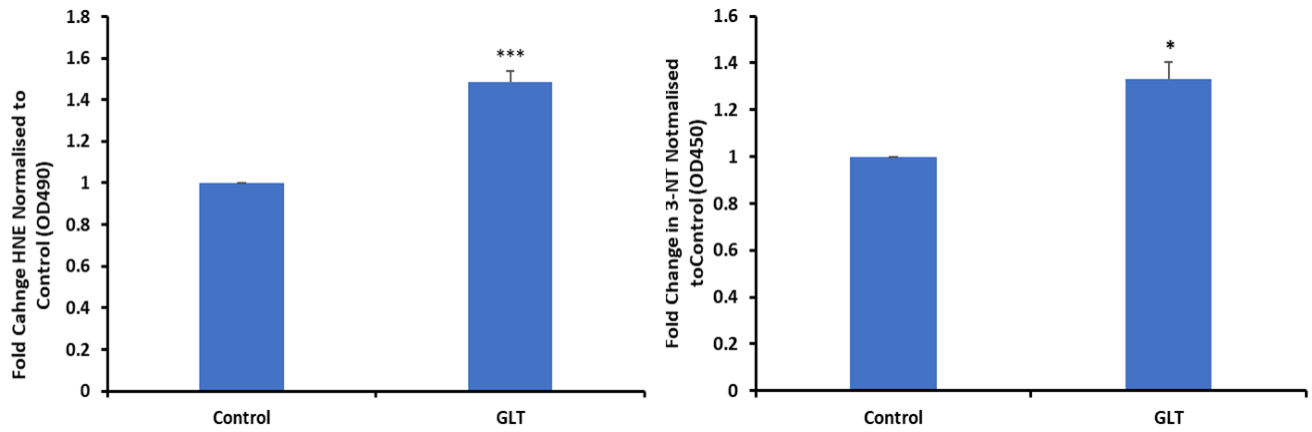

Figure 3.15 4-HNE adducts and 3-NT in response to GLT. *Cells were incubated ± GLT for 5 days. 4-HNE formation was determined by ELISA (Abbexa, Cambridge, UK) and absorbance measured at 490 nm. 3-NT formation was determined by ELISA (Abcam, Cambridge, UK), with absorbance measured at 450 nm. Data are expressed as mean ± SEM from 3 independent experiments.*

3.3.6 Effect of CD40 on interferon gamma induced proteins

The unbiased network analysis performed on microarray data of INS-1 cells ±GLT showed major involvement of the JAK/STAT signalling pathway (Fig 3.4). To validate this finding independent RT-qPCR was used to measure the expression changes of six interferon gamma (IFN-γ) genes, that were present in the original microarray data set. The reason for observing changes in expression of IFN-γ is because they are associated with stimulating the initiation of the JAK/STAT pathway and initiating an immune response (Horvath CM, 2004). The cells were treated ± GLT for 3-days prior to RNA extraction (Qiagen, Hilden, Germany), reverse transcribed to generated cDNA (ThermoFisher, Waltham, MA, USA) and analysed using RT-qPCR using IFN-γ specific primers. The results showed that all 6 of the tested IFN-γ genes were significantly up-regulated in response to GLT.

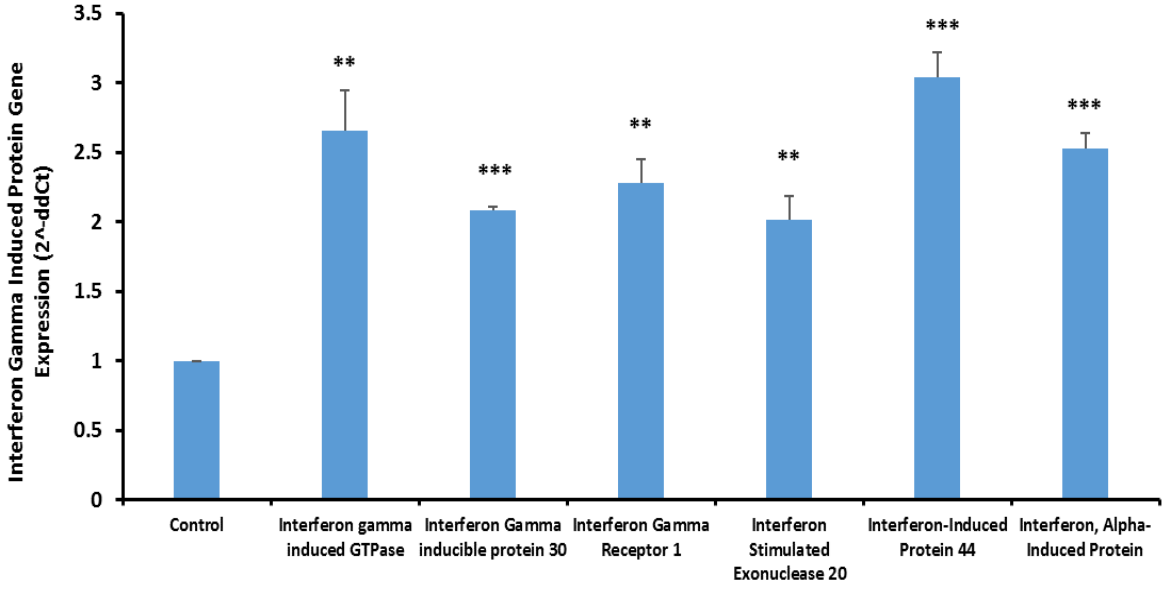

Figure 3.16 IFNγ mRNA Expression*. Cells were incubated ± GLT for 5 days. Total RNA was extracted from cells and reverse transcribed to generate cDNA and subsequently analysed using RT-qPCR using specific IFNγ primers. Data represent ΔΔCt expressed as fold change compared to the untreated control. Data shown is mean ± SEM from three independent experiments.*

3.4 Discussion

The damaging effects of elevated glucose combined with elevated free fatty acids on the function of pancreatic β-cells is termed glucolipotoxicity. Glucolipotoxicity negatively effects β-cell function, particularly insulin production and secretion. In human circulation, palmitic, oleic and stearic are the most common fatty acids making up approximately 80% of the total circulating fatty acids, with oleic acid being the most prominent free fatty acid found in the human pancreas.

Type 2 diabetes is caused largely by factors associated with life style and genetics. A number of life style factors contribute to the onset and development of type 2 diabetes, with chronic over nutrition combined with lack of exercise the main cause of increasing prevalence of overweight and obese individual. In the UK, approximately 86% of type 2 diabetic patients are overweight or obese (Olokoba et al, 2012. Kempf et al, 2006. Al-shafari and Gunaid, 2014).

CD40/TNFR5 is a cell surface receptor and belongs to the tumour necrosis factor receptor superfamily. It is a type 1 transmembrane protein with four extracellular cysteine rich domains that are important for it to bind to its ligand, CD40L. CD40 is mainly associated with the initiation and progression of adaptive immune responses including T cell-dependent immunoglobulin class switching, memory B

cell development and germinal centre development but both CD40 and its ligand have been found in multiple cell types and its therefore now accepted that the CD40-CD40L interaction is associated with more general immune regulation, and CD40-mediated signalling is involved in many pathways including NF-κB, STAT3 and MAPK (Van Kooten and Banchereau, 2000. Yao et al, 2016).

Based on Affymetrix and PCR data obtained by Marta Bagnati it apparent that CD40/TNFR5 was the most up-regulated of the observed TNFR family members. Additionally, MetaCore™ analysis of genes identified using microarray analysis ± GLT, identified CD40 as a major regulatory pathway. MetaCore™ is an integrated software that is used for functional analysis for experimental data. It is based on a collection of data of human protein-protein, protein-DNA interactions, transcription factors, effects of bioactive molecules and signalling and metabolic pathways. MetaCore™ can be used for functional analysis of proteomics, metabolomics, gene expression, siRNA, and others (MIT Libraries). The software for this investigation was beneficial as it identified that CD40 potentially signals via NF-κB.

The results obtained in this project demonstrated that CD40/TNFR5 gene and protein expression increased in response to elevated glucose and fatty acids. The results showed that CD40 gene expression increased significantly by 5.65-fold and the protein expression increased by 3-fold. This investigation is based on results obtained and published by Bagnati et al, 2016 who identified that a number of tumour necrosis factor receptors that were associated with inflammation and apoptosis and of these CD40/TNFR5 was the most affected in response to GLT. Bagnati et al found an increase in CD40 gene expression of 2.23-fold, which is much less than the current study. Bagnati et al also identified an increase in CD40 protein expression by 2-3-fold, which again is less than the current study. A reason that Bagnati et al identified a lower increase in CD40 gene and protein expression could be because they incubated the INS-1 cells in media supplemented with high glucose and fatty acids for 72 hours rather than 5-days, that was used in the present investigation. This suggests the chronic exposure of INS-1 to GLT media intensifies over time prior to causing apoptosis.

INS-1 incubation in GLT media also had an effect on the expression and activation of NF-κB, which is a family of inducible transcription factors and are activated by a number of different stimuli (Hayden and Ghosh, 2014). NF-κB gene expression was increased significantly by 5.59-fold in response to GLT and NF-κB activity was also up-regulated in response to INS-1 incubation in GLT media by 2.01-fold. The next step of the investigation was to determine whether CD40 signalling has an effect on NF-κB activation and expression. This again builds upon published work by Bagnati et al, who found and published that NF-κB protein expression was up-regulated by an average of 73% following 72-hour incubation in glucolipotoxic media. This finding was followed by the observation that the increase and

activation of NF-κB is in fact associated with the increase in CD40. Firstly, evidence for this is shown in the Bagnati et al paper that presented that in the presence of the CD40 ligand known as CD40L, there was an increase in the translocation of NF-κB from the cytoplasm to the nucleus suggesting that it was no longer being sequestered by its inhibitor and was now active. Subsequent to this, our current investigation used siRNA to transiently knock down CD40 and observe the effects this had on NF-κB activation or mRNA expression. The results showed that despite a modest knock down of 58.3 ±16.9%, NF-κB activation was reduced by 46.7 ±8.2%, which is published in the Bagnati et al 2016 paper. This suggests that CD40 is an upstream activator of NF-κB.

The transcription factor family, NF-κB is central to iNOS regulation (Vanini et al 2015). This investigation sought to identify whether glucolipotoxic conditions had an effect on iNOS expression. iNOS expression is important because it's thought to be one of the direct consequences of an inflammatory process and is responsible for the production of nitric oxide (NO). NO is an uncharged and unstable free radical molecule that functions as a mediator in many tissue types. Due to its small size and it being uncharged, NO can diffuse out of the cell where it was produced and into nearby target cells (Augusti et al, 2004. Collin-Osdoby et al, 1995). Low concentrations No is essential for cell maintenance however, if concentrations become too high it can have cytotoxic effects on the cells (Augusti et al, 2004).

The results showed that iNOS expression was significantly increased in response to GLT. iNOS protein expression increased by 3.7-fold in GLT conditions compared to the untreated control. This is a significant finding as it demonstrates that a high glucose and fatty acid environment results in inflammation, as iNOS is the main producer of NO.

The next part of the investigation was to measure argininosuccinate synthase (ASS1) mRNA levels in response to GLT incubation. The reason for this was to identify whether the increase in iNOS would result in NO production, as iNOS is responsible for catalysing the reaction of L-arginine to L-citrulline that results in NO production. The reason ASS1 was measured is because it is the enzyme required for converting L-citrulline back to L-arginine once following the catalysis of iNOS (Haines et al, 2011). The results indicated that ASS1 mRNA levels increased by almost exactly 2-fold, supporting the suggestion that that NO production is increased in GLT conditions following the increase in iNOS induction.

The effect of glucolipotoxic conditions on nitrite was also observed. The reason that nitrite was factored into this investigation is because it is a stable product of NO, as NO itself is only short-lived due to scavenging reactions. Nitrate can be formed from the reduction of nitrate, but the majority of nitrite is derived from the oxidation of NOS-generate NO (Tiso and Schlechter, 2015. Lundberg et al, 2008). The results however were unexpected and showed that nitrate production was down-regulated

following INS-1 exposure to GLT conditions. Nitrite was down-regulated by 46.5% in GLT conditions compared to the untreated control. This result was unexpected as it was rational to consider that if NO levels increase, as suggested by the increasing iNOS expression, it would result in an increase in NO oxidation and therefore an increase in nitrite. A source of nitrite is from the oxidation of nitric oxide. This means that nitrite could be formed from NO that is originally generated from iNOS (Lundberg et al, 2008). However, it has been identified in this study that when INS-1 cells are exposed to GLT media there is increase in HNE, which suggests that the NO resulting from increased iNOS expression, is reacting with superoxide to form peroxynitrite rather than being oxidised. Peroxynitrite is produced from the diffusion-limited reaction of NO with superoxide and is an important intermediate in the pancreatic beta cell inflammatory response (Jourd'heuil et al, 2001).

HNE is the most abundant product of lipid peroxidation that results from omega-6 (ω-6) polyunsaturated fatty acids. HNE is known to be increased in oxidative stress related diseases including obesity and diabetes (Li et al, 2013). HNE have damaging effects resulting from its high reactivity based on its strong electrophilic functional group; 2,3-double bond close to the hydroxyl group on C4 and the carbonyl group on C1 (Li et al, 2012). There are apparently two main factors that affect HNE concentration, the first is up-stream metabolism of HNE, as high levels of lipid peroxidation resulting in HNE is the hallmark of increased levels of oxidative stress. The second factor is down-stream of HNE metabolism and is the disposal of HNE which includes; conjugation to glutathione, cysteine and carnosine. It also includes reduction to DHN by cytosolic aldehyde reductase and finally oxidation to 4-hydroxynonanoic acid that can be catalysed to form acetyl-CoA and propionyl-CoA that enters the citric acid cycle. Disturbance of the balance between metabolism and disposal of HNE can lead to the accumulation in HNE causing protein, lipid, and/or DNA damage by modifications. A significant study observed the effects of 4 diets (standard chow, low fat, ketogenic and high fat) on HNE concentrations in mouse liver cells. The results showed that HNE and its analogue known as ONE were found in the highest concentrations in liver cells that were exposed to the high fat diet. They also proved that conjugation to of HNE to glutathione is a major HNE disposal pathway in the liver. However, they didn't explore HNE disposal in other pathways such as cysteine or carnosine conjugation.

The reason the study conducted by Li et al, 2012 is significant is because they have demonstrated that diet can influence HNE concentration which is down stream of NF-κB, iNOS and NO which this current investigation is concerned with. However, the current investigation builds upon the study by Li et al, 2012 by looking at more relevant fatty acids and glucose. The results found in the present investigation is that HNE increases on average by 43.4% when the INS-1 cells are incubated in media containing elevated glucose, oleic and palmitic acid. The study by Li et al uses linoleic and linolenic acid to generate the 4 different diet types being tested. Linoleic and linolenic acid are ω-6 and ω-3 fatty acids,

that are found in vegetable oils and fish oils respectively. Both of which are polyunsaturated essential fatty acids. However, the main dietary fatty acids are oleic acid and palmitic acid, which are used in the present investigation. Oleic acid is the most abundant fatty acid in nature and is an ω-9 monounsaturated fatty acid that is found in plant oils. Palmitic acid is a common saturated fatty acid that is found in plant and animals (PubChem). The relevance of the finding that HNE increases in INS-1 β-cells following incubation in GLT media for 5 days is that it demonstrates directly that diets is responsible for damage to β-cells in conditions that are representative of obesity and type 2 diabetes, despite neither of the fatty acids used being an ω-6 fatty acid.

As well as lipid peroxidation causing an increase in HNE, the increase may also result from lack of scavenging. It was demonstrated by Li et al, that glutathione conjugation was the major source of HNE disposal, however it is known that pancreatic islets have less glutathione peroxidase and it has even been shown to be completely absent in a pancreatic β-cell line (Tiedge et al, 1997). Glutathione peroxidase is an enzyme that is present in the ROS degradation pathway to protect cells from increased hydrogen peroxide concentrations and lipid peroxides, however, it is thought to be expressed in much lower concentrations in β-cells because it is required for insulin secretion (Robertson and Harmon, 2007. Pi et al, 2007). Therefore, without the protection of glutathione peroxidase it is likely that HNE would accumulate more in pancreatic beta cells than in other cell types, in stressful conditions resulting in beta cell damage. Another study that was investigating the effect of a high fat diet on HNE concentration in adipose tissue supported this hypothesis. Again, the study used linoleic fatty acid in the high fat diet as this is the most commonly found fatty acid in adipose tissue and their results showed that lipid peroxidation and HNE is increased in high fat conditions in epididymal adipose tissue, however the same result wasn't identified in subcutaneous adipose tissue. They also found that glutathione peroxidase was down regulated in mouse epididymal adipose tissue following the high fat diet but the enzyme was not affected in subcutaneous adipose, this again supports the idea that glutathione peroxidase conjugation is a major disposal pathway for HNE and is the reason that HNE was increased in subcutaneous adipose tissue following the high fat diet (Long et al, 2013). Therefore, this again supports the theory that pancreatic β-cells are more susceptible to HNE accumulation based on their lack of glutathione peroxidase and that the CD40-induced NF-κB pathway results in HNE accumulation and ultimately β-cell damage.

Another part of investigation into the CD40/TNFR5 signalling pathway and its association with other genes. A programme known as MetaCore™ was used to build a network of signalling that were significantly up-regulated following INS-1 exposure to GLT. The primary signalling network that up-regulated by GLT was the JAK/STAT signalling pathway. This was validated by measuring IFNγ genes that are reported to initiate the pathway and up-regulate cytokine action in the immune response.

This finding may suggest a possible role for pancreatic β-cell damage in the onset of T2D induced by the JAK/STAT pathway

3.5 Conclusion

In conclusion the results shown in this chapter indicate that an up-regulation in CD40 is induced by elevated levels of glucose and fatty acids and it suggests that CD40 plays a role in glucolipotoxic-induced inflammation that is found in diabetes. The results also indicate that the glucolipotoxic-induced increase in CD40 expression is linked to an increase in NF-κB activation and downstream inflammatory pathways culminating in the production of 4-HNE in pancreatic beta cells, summarised in Figure 3.17.

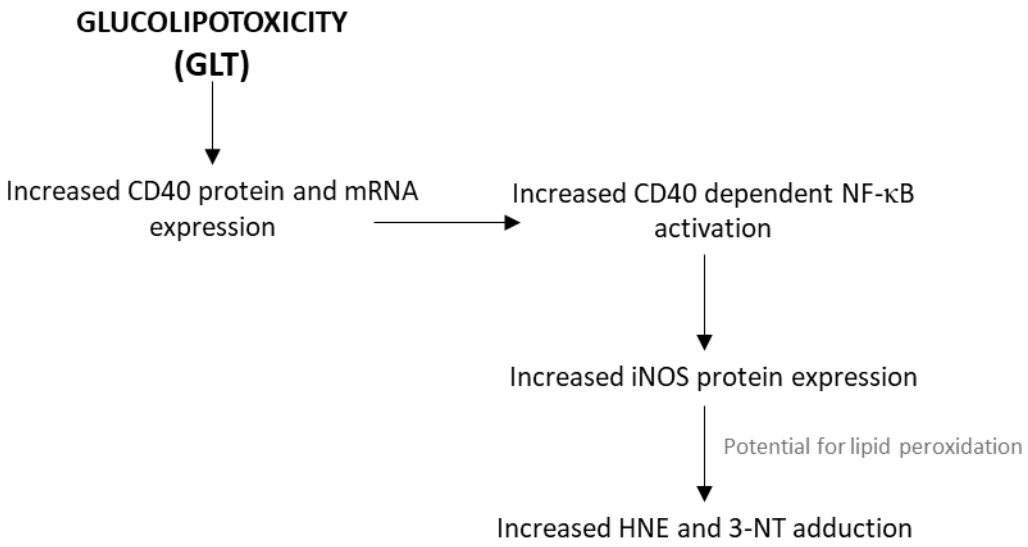

Figure 3.17: Summary of results. *Summary of chapter 3 results that identified GLT resulted in an increase of CD40 protein and mRNA, leading to increased NF-κB activity. NF-κB is a transcription factor of iNOS which also increased following exposure to GLT and finally an increase in markers of lipid peroxidation, HNE and 3-NT adducts.*

Chapter 4

Modulation of Gene Expression by CD40/TNFR5

4.0 CHAPTER 4: Modulation of Gene Expression by CD40/TNFR5

4.1 Introduction

As discussed in chapter 3 of this thesis, CD40 is up-regulated in INS-1 cells following exposure to glucolipotoxic (GLT) conditions. As shown in chapter 3 this results in a cascade that of up-regulation of genes and proteins that are potentially involved in inflammation. This chapter further examines how CD40 is able to modulate various genes to disrupt normal beta cell function.

4.1.1 Tumour necrosis factor super family

There are currently 19 ligands and 29 receptors that make up the tumour necrosis factor superfamily (TNFSF) (Xu et al, 2017). The superfamily plays a role in activating signalling pathways that are involved in cell survival, proliferation, or apoptosis. The tumour necrosis factor receptors (TNFRs) can be broken down into two groups depending on whether they possess an intracellular death domain (DD). The DD results in cell apoptosis via activation of caspases through contribution of adapter proteins FADD (Fas-associated death domain) and TRADD (TNF receptor associated death domain). The second group of TNFSFRs signal via TNF receptor-associated proteins (TRAFs) only. However, DD-containing receptors can also operate via this pathway. TRAFs are able to bind directly to TRADD or to the cytoplasmic portion of the receptor to initiate a response (Ślebioda and Kmieć, 2014).

CD40 is a cell surface receptor and a member of the TNFR super-family and has the alias TNFR5. It was first identified and characterised on B lymphocytes, however, it has since been found on multiple other cell types (Van Kooten and Banchereau, 2000). CD40 is a type I transmembrane protein with a molecular mass of 48kDa and is made up of an extracellular domain, a leader sequence, a transmembrane domain and an intracellular domain. Within the extracellular domain there are 22 cysteine residues that are conserved between TNFR super family members (Elgueta et al, 2009). The ligand for CD40 is known as CD40L or CD154, and is a type II transmembrane protein, with a molecular weight between 32 and 39kDa, CD40L has a variable molecular weight due to post translational modifications. The ligand for CD40 is also part of the TNF superfamily and is characterised by its 'sandwich' structure. CD40L is composed of a α-helix loop located between two β-sheets, which allows for its trimerization (Elgueta et al, 2009).

It is known that CD40 is a key activation receptor via its interaction with CD40L resulting in the production in many proinflammatory cytokines including IL-1, IL-6 and IL-8. The signal transduction

mechanism of CD40-CD40L has been shown to be mediated by the transcription factor Nuclear Factor Kappa B (NF-κB). Several proinflammatory cytokines have NF-κB binding sites in their promoter region and are therefore potential targets of CD40 engagement (Phipps R, 2000). Regarding pancreatic cells specifically, results in chapter 3 of this thesis and data published by Bagnati et al, indicate that it is pancreatic up-regulation of CD40 that leads to the activation of both NF-κB and STAT1 that initiates islet inflammation and eventually β-cell death by increasing transcription of inflammatory mediators (Turner MD, 2017).

4.1.2 Inhibitor of DNA binding proteins

There are four inhibitor of DNA binding proteins, also commonly known as inhibitor of differentiation proteins (ID1-4), that are part of the helix-loop-helix (HLH) family of transcriptional regulatory proteins that act as dominant negative regulators and repress transcription of bHLH transcription factors. All four of these ID proteins have a homologous helix-loop-helix domain which is highly conserved and is made up 2 amphipathic helices on either side of a loop that controls homo- and hetero-dimerisation but lack the basic DNA binding domain (Han et al, 2017). ID proteins dimerise with their partner basic HLH (bHLH) transcription factors in a dominant negative manner to prevent them binding DNA (Han et al, 2017). The bHLH dimers bind to the E-box DNA consensus, represented by the sequence CANNTG present in a wide variety of tissues, via a group of positively charged amino acids (Sharma et al, 2016). The binding is repressive as it is the E-box that mediates transcription. It is known that E-box elements are present in promoter and enhancer regions that regulate pancreas-specific gene expression. A number of genes that are only found located in the pancreas, such as insulin and somatostatin genes, require E-Box sites to be expressed sufficiently. Insulin and somatostatin promoter sites contain E-box sites that when multimerized are adequate enough to regulate pancreatic β-cell specific gene expression (Massari and Murre, 2000).

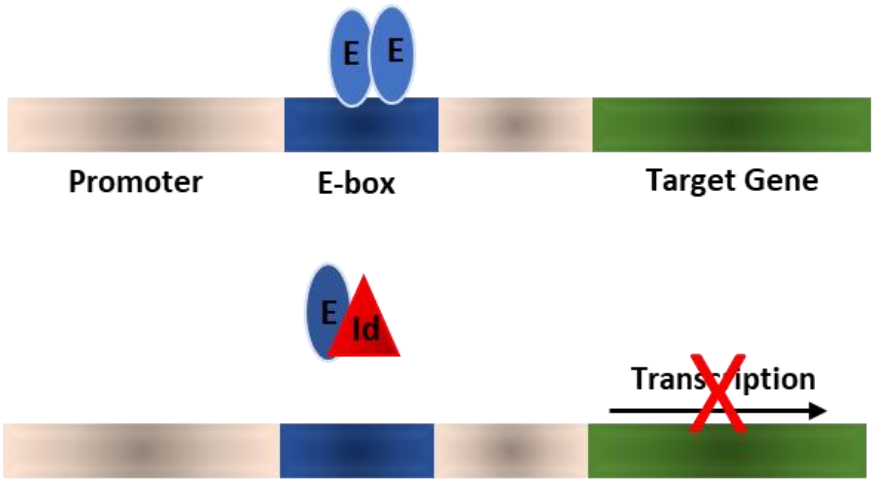

Figure 4.1 Schematic image of how id proteins bind to E-proteins to prevent transcription. *Adapted from Engel and Murre, 2001.*

ID proteins have a wide variety of roles in physiological development processes and also in pathology, however, biological effects of ID4 appear to the opposite of the other bHLH dimers. ID1-3 are considered to play a role in regulation of the cell cycle and differentiation and as their expression is commonly found in various cancer types, ID1, ID2 and ID3 are considered to be tumour enhancers/ oncogenes where as ID4 has emerged as a potential tumour suppressor, as it appears to be silenced in many cancers.

4.1.3 Insulin synthesis and Secretion

Insulin gene expression only occurs in beta cells of the endocrine pancreas in response to increased glucose concentrations (German and Wang, 1994). The insulin gene promoter is regulated by the binding a specific transcription factors to its promoter region such as PDX-1, MAF-A and HNF-1 amongst others (Melloul et al, 2002). Insulin gene transcription is controlled by the interaction of regulatory proteins known as trans-activating factors with specific DNA sequences known as cis-elements. The most important cis-element that regulates transcription is the insulin control element (ICE), which operates via both positive and negative-acting transcription factors (Melloul et al, 2002). The transacting activators of ICE expression are thought include E, A and C1/RIPE3. E boxes bind proteins of the basic helix-loop-helix (bHLH) family which function as potent transcription activators by forming heterodimers with bHLH family members. A-boxes bind to a well-known insulin transcription factor known as pancreatic duodenal homeobox-1 (PDX-1) to initiate insulin gene

transcription. PDX-1 is involved in the early conversion of primitive gut cells to pancreatic beta cells and also in the maturation of beta cells. PDX-1 is a major trans activator of the insulin gene, and islet specific genes such as GLUT2, glucokinase and somatostatin (Stein et al, 1994. Melloul et al, 2002).

The reason for observing transcription factors in this chapter is to determine whether CD40 might modulate gene expression beyond inflammation (detailed in Chapter 3). A former member of the Turner lab observed four well known insulin gene transcription factors; PDX-1, MAF-A, HNF-1 and TFAM for alterations following CD40 transient knock down using siRNA. However, none were affected by the absence of CD40, although crucially this knock-down resulted in increased insulin expression.

4.2 Aim

It has been observed in the previous chapter that CD40 expression increases when the pancreatic beta cell is exposed to GLT, resulting in an increase in genes involved in inflammation, however the aim of this chapter was to determine whether the presence of CD40/TNFR5 was able to result in the suppression of gene expression in pancreatic beta cells, therefore altering function and also to identify a repressor of insulin gene transcription that is mediated by CD40.

4.3 Results

A concentration of 10mM carnosine was used to investigate its ability to prevent or reverse the up-regulation of various proteins and genes resulting from INS-1 exposure to GLT. This concentration was determined as being the most effective and least damaging to the INS-1 cells compared to other concentrations (1mM, 20mM 50mM and 100mM, data not shown). Cell culture media ±GLT was supplemented with 10mM and incubated for 5 days.

4.3.1 CD40 inhibits transcription in human CM cell line

This chapter of the thesis utilised a human cell line known as CM. The CM cell line is derived from a human pancreatic insulinoma and it was used in this project as a model for β-cells and to study the effect of CD40 on various genes. Importantly, CM have been reported been reported to maintain many of the primary characteristics of β-cells (Jonnakuty and Gragnoli, 2007). The reason the human CM cell

line is used here is because human data was used to generate the bespoke CD40 regression analysis pathway (Fig 4.2). The use of a second cell line also added validity to the project.

Utilising unique neural net algorithms (generated by Professor Graham ball, NTU) a bespoke CD40 regression analysis pathway was generated. This demonstrated the negative effect of CD40 on the interaction between numerous genes. It has already been demonstrated in chapter 3 that CD40 is up-regulated when INS-1 cells were exposed to high glucose and fatty acid media. From the genes that were predicted to be inhibited by the presence of CD40/TNFR5, six were selected based on their physiological role and their position as hubs in the interactions (Figure 4.2).

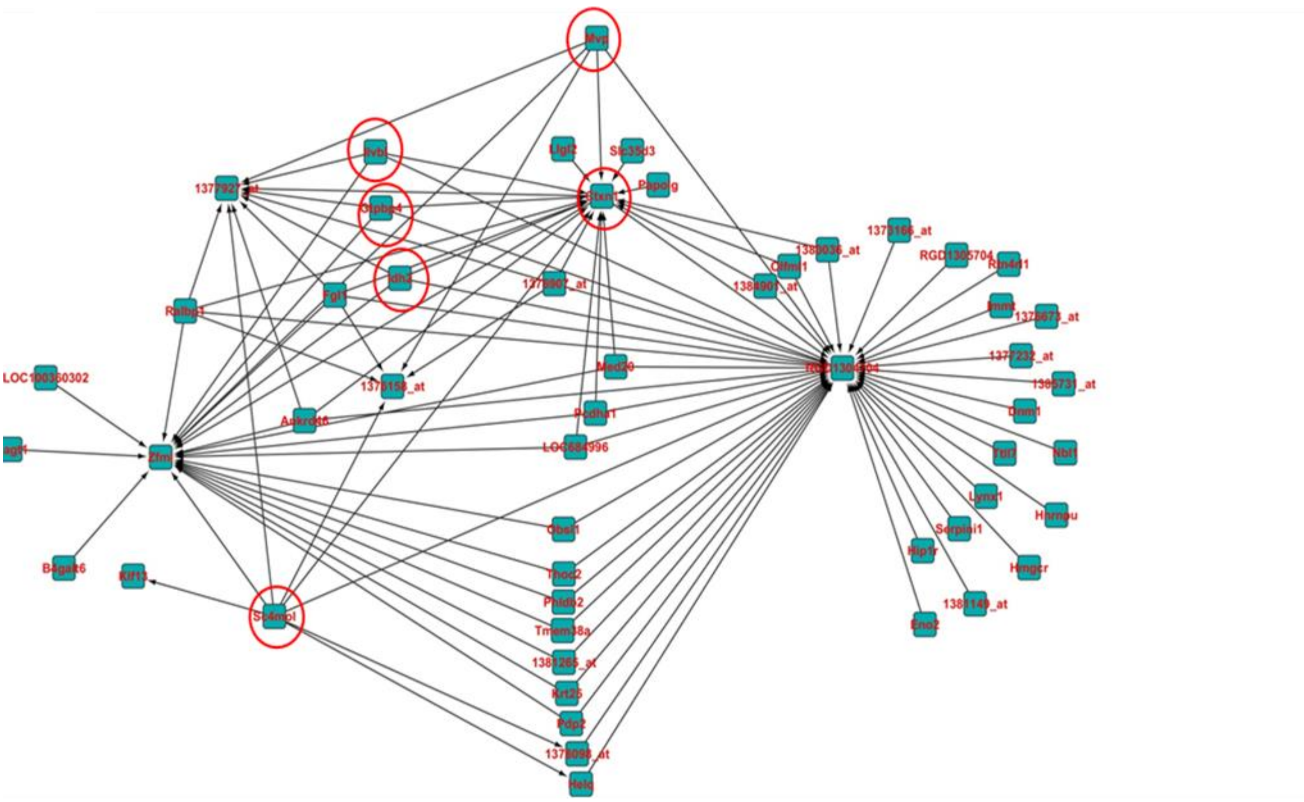

Figure 4.2 Bespoke CD40 regression analysis pathway. *Generated by Professor Graham Ball. Shows pathway as generated by Professor Ball and highlights selected genes for further analysis.*

Table 4.1 Six selected genes identified as negatively regulated in the bespoke CD40 regression analysis and their corresponding function.

Gene	Function
GTP-binding protein 4 (GTPBP4)	GTP-binding proteins are GTPases and function as molecular switches that can flip between two states: active, when GTP is bound, and

	inactive, when GDP is bound. 'Active' in this context usually means that the molecule acts as a signal to trigger other events in the cell.
ILVB acetolactate like gene (ILVBL)	A protein encoding gene that plays a role in catalysing the first step in branched amino acid synthesis.
Isocitrate dehydrogenase 2 (IDH2)	Catalyses the oxidative decarboxylation of isocitrate to α-ketoglutarate and synthesis NADPH in the mitochondrial TCA cycle.
Major vault protein (MVP)	Required for normal vault structure. Vaults are multi-subunit structures that may act as scaffolds for proteins involved in signal transduction. Vaults may also play a role in nucleo-cytoplasmic transport.
Sterol-C4-methyl oxidase like (SC4MOL)	Encodes the protein sterol-C4- methyl oxidase (SMO), which is involved in catalysing the demethylation of C4-methysterols in the cholesterol synthesis pathway.
Cortexin-1 (CTXN)	Encodes a protein that is found located in precursors of neurons and is involved in the mediation of intra and extra-cellular signalling of cortical neurons during brain development.

CM cells were transiently transfected with siRNA for 24 hours to knockdown CD40/TNFR5 expression (Dharmacon, GE Healthcare, UK). Following 24 hours incubation in transfection reagent cells were washed with PBS and incubated in 0.8mM glucose RPMI-1640 for 72 hours. Subsequent to the knockdown procedure, cells were lysed and captured in a pellet. The pellet was then split in order to be used for both western blot technology and PCR analysis. Prior to western blot analysis protein was extracted from the cells using RIPA buffer and quantified by a BCA assay. Equal amounts of protein were loaded to a 10% SDS-Page gel and the proteins were separated using electrophoresis. The proteins were then transferred to a nitrocellulose gel and immunoblotted using specific antibodies. The results demonstrated a significance in analysis of variance (0.00001) and that CD40/TNFR5 was knocked down in the siRNA treated cells by 85% compared to the control ($p=0.000038$) and CD40/TNFR5 was down regulated in the siRNA treated cells by 79.2 % by comparison to the scrambled sequence treated cell (ssRNA) ($p=0.000097$).

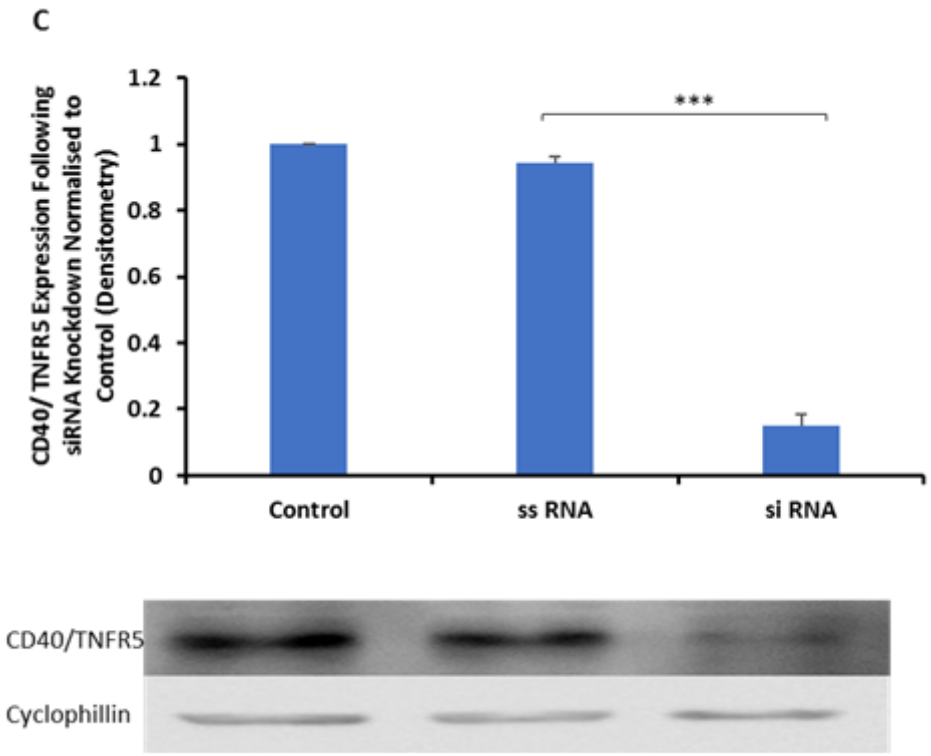

Figure 4.3 CD40 knock down in CM cells. *CD40 was transiently knocked down in human CM using siRNA. siRNA transfection solution was applied to cells for 24 hours. Subsequently, CM cells were incubated in 0.8mM glucose RPMI-1640 for 72 hours. Cells were lysed using RIPA buffer and quantified using BCA assay. Proteins were loaded to a 10% acrylamide gel and separated using SDS-PAGE. Proteins were transferred to nitrocellulose membrane and immunoblotted using CD40 specific antibodies.*

The pellet obtained as explained above was used to extract RNA using an RNA extraction kit (Qiagen), reverse transcribed and used in qPCR analysis. Specific primers were used for the genes observed (GTPBP4, ILVBL, IDH2, MVP, SC4MOL, and CTXN).

The results demonstrated 85% knockdown of CD40 in siRNA treated cells. This resulted in increased expression of all genes identified in the bespoke regression map, apart from MVP. The cells that underwent transient knockdown of CD40 using siRNA showed an increased expression of GTPBP4 by 3.84-fold ($p=0.009$), 5.83-fold increase of ILVBL gene expression ($p=0.048$), 3.44-fold increase in IDH2 gene expression ($p=0.0084$), 3.8-fold increase in SC4MOL gene expression ($p=0.0086$) and a 4.69-fold increase in CTXN1 gene expression ($p=0.037$) by comparison to the untreated control cells. However, there was no significant change in gene expression of MVP. These results confirm the validity of the predicted interactome, with the presence of CD40 able suppress expression of various functional genes.

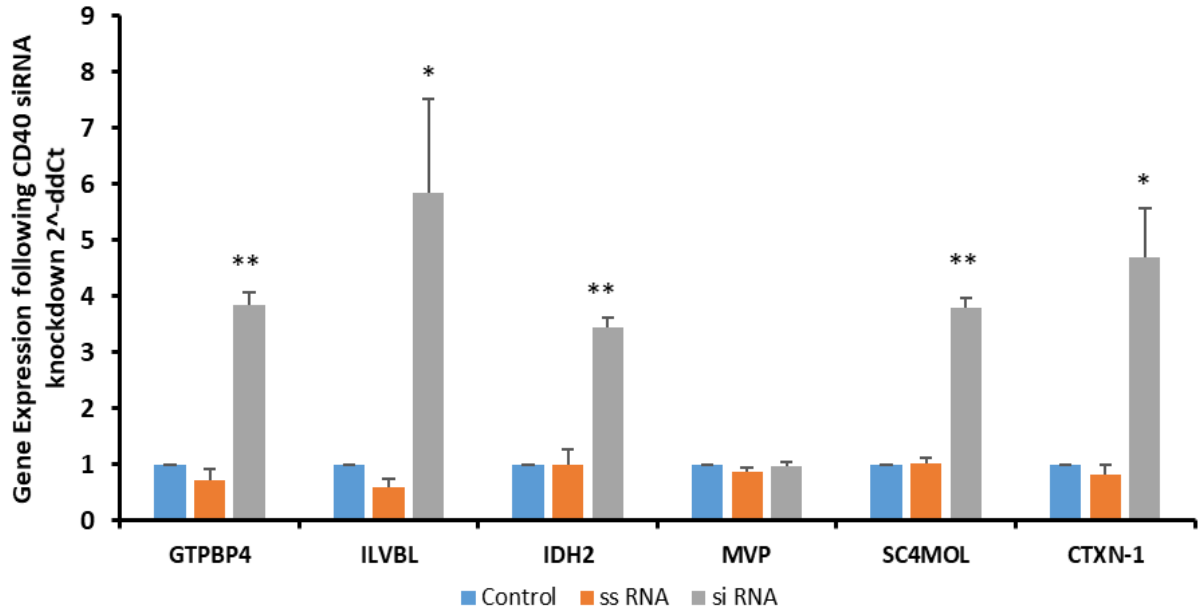

Figure 4.4: Gene expression following CD40 knockdown in CM cells*. Subsequent the CD40 knockdown in human CM cells, total RNA was extracted (Qiagen, Hilden, Germany), reverse transcribed (Thermofisher, Waltham, MA, USA) and analysed using RT-qPCR with specific primers. Results are shown as ΔΔCt expressed as fold change compared to the control. Results shown are mean ± SEM of four independent experiments.*

Previous results were supported by identifying whether the same reduction in expression was experienced in GLT conditions at protein level. The INS-1 cell line was utilised for further investigation as CM cells do not function in GLT conditions. INS-1 cells were incubated ±GLT for 5 days. After the incubation period, protein was extracted using RIPA buffer and quantified by a BCA assay. Equal amount of protein for each condition was loaded to 10% SDS-Page gels and the proteins were separated using electrophoresis. The proteins were then transferred to nitrocellulose membranes and immunoblotted with either IDH2 or SC4MOL specific antibodies. The results showed that exposure to GLT resulted in a reduction of IDH2 protein expression by 24% (p=0.00014) and a reduction in SC4MOL protein expression by 55.6 (p=0.0003).

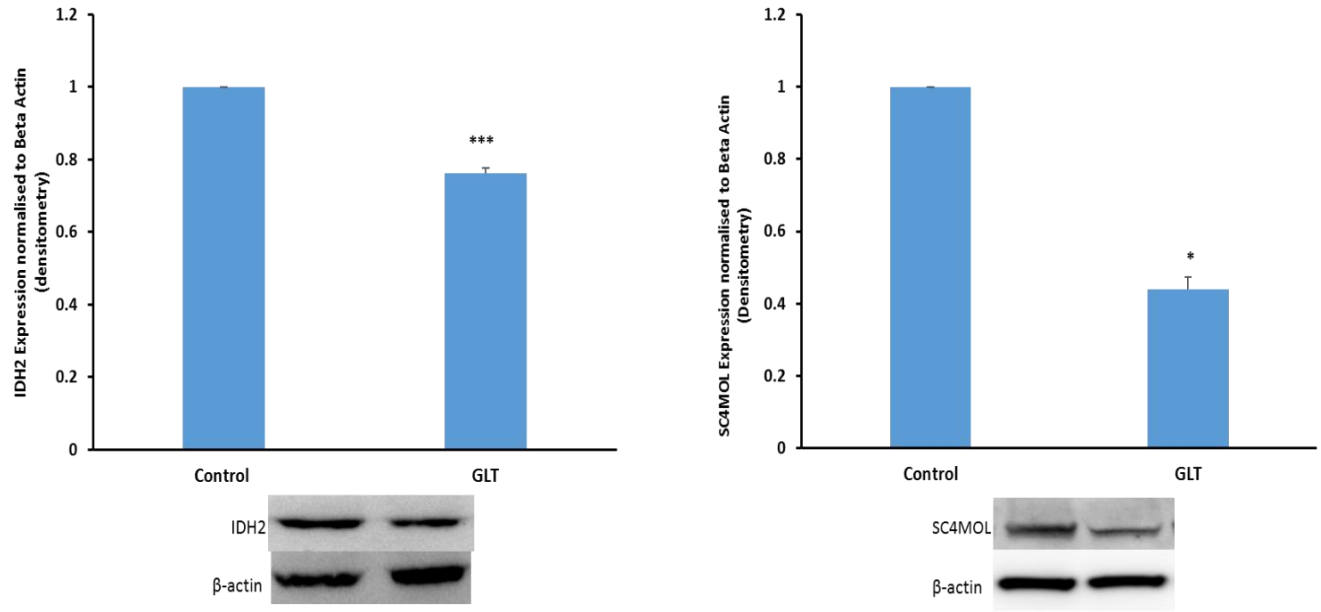

Figure 4.5 IDH2 and SC4MOL protein expression in response to GLT*. INS-1 cells were incubated ± GLT for 5-days. Proteins were lysed used RIPA buffer and quantified using BCA assay. Proteins were loaded to acrylamide gels and separated using SDS-PAGE. Proteins were transferred to nitrocellulose membranes and immunoblotted using specific antibodies.*

4.3.2 GLT reduces insulin gene transcription

It is well known that chronic exposure to high glucose and fatty acid concentrations reduces insulin gene expression. The aim of this section was to determine whether novel genes could be identified that participate in this process, and hence that might play a role in reducing insulin secretion.

4.3.2.1 Time lapse insulin gene expression

INS-1 cells were incubated ±GLT media for 24, 72 or 120 hours. Following the incubation period, total RNA was extracted from the cell using an RNA extraction kit (Qiagen), reverse transcribed and ultimately used in qPCR analysis, using specific primers for the insulin gene. The results showed that there was gradual decline in insulin gene expression as the time points progressed compared to control. Analysis of variance demonstrated there was a significant reduction in insulin expression between time points ($p=0.042$).

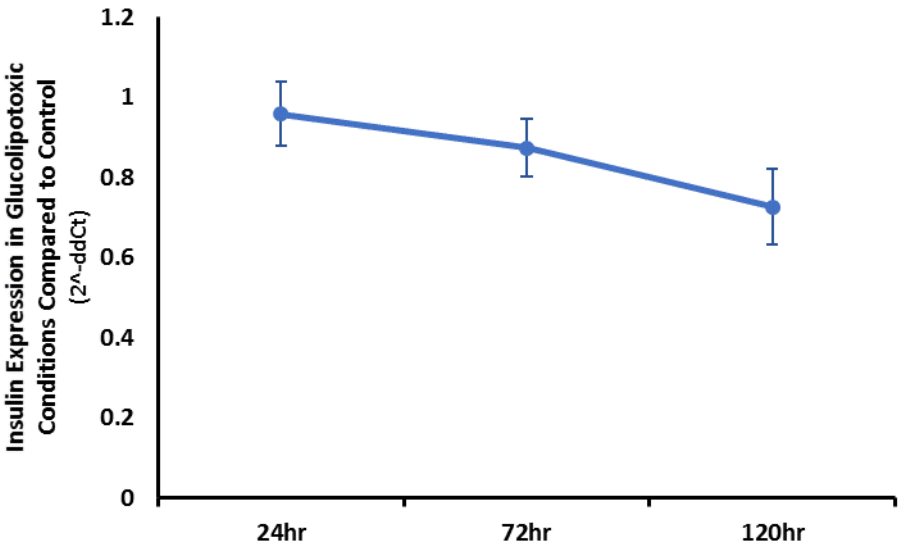

Figure 4.6 Insulin gene expression in response to GLT. *INS-1 cells were incubated ± GLT for either 24 hours, 72 hours or 120 hrs. Prior to incubation total RNA was extracted (Qiagen, Hilden, Germany), reverse transcribed (Thermofisher, Waltham, MA, USA) and analysed using RT-qPCR with insulin specific primers. Results are shown as ΔΔCt expressed as fold change compared to the control. Results shown are from three independent investigations.*

Following the observation that insulin gene expression is reduced in INS-1 β-cells, RT-q PCR analysis was undertaken to determine whether the gene for the insulin degrading enzyme (IDE) was increased. IDE is a zinc metalloproteinase which was first observed for its ability to degrade insulin (Tundo et al, 2012). Cells were incubated ± GLT for 5 days prior to RT-qPCR analysis being performed using specific IDE primers. The results (Fig. 4.7) shows that despite IDE expression being moderately increased in response to GLT, was not statistically significant.

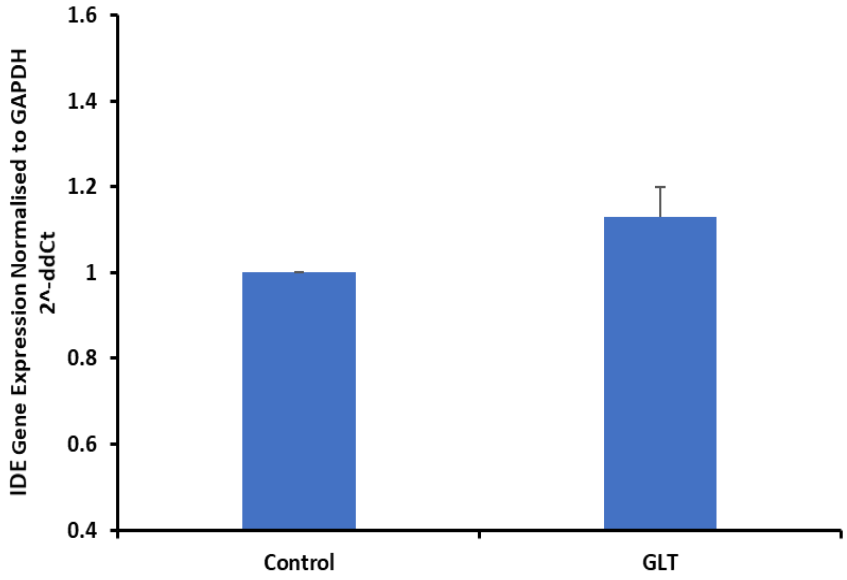

Figure 4.7 IDE Gene expression in response to GLT. *INS-1 cells were incubated ± GLT 5 days. Total RNA was extracted (Qiagen, Hilden, Germany), reverse transcribed (Thermofisher, Waltham, MA, USA) and analysed using RT-qPCR with IDE specific primers. Results are shown as ΔΔCt expressed as fold change compared to the control. Results shown are mean ± SEM from three independent investigations.*

4.3.3 GLT increases potential insulin inhibition gene

Further neural net analysis was performed with enriched analysis for CD40 interaction with transcriptional regulators. Of those showing a positive interaction with CD40, inhibition of DNA-binding 4 (ID4), a transcriptional repressor was the top hit. Therefore, in order to determine whether the presence of CD40 influenced the reduction of insulin gene expression through modulation of ID4 I first sought to determine whether ID4 expression changes in response to GLT conditions. INS-1 cells were incubated ± GLT for 5 days, subsequent to the incubation period total RNA was extracted (Qiagen), reverse transcribed (Invitrogen) and analysed using qPCR with primers specific to ID4. The results showed (Fig 4.8) ID4 gene expression was significantly increased by 2.23-fold (p=0.003) following 5 days incubation in GLT media.

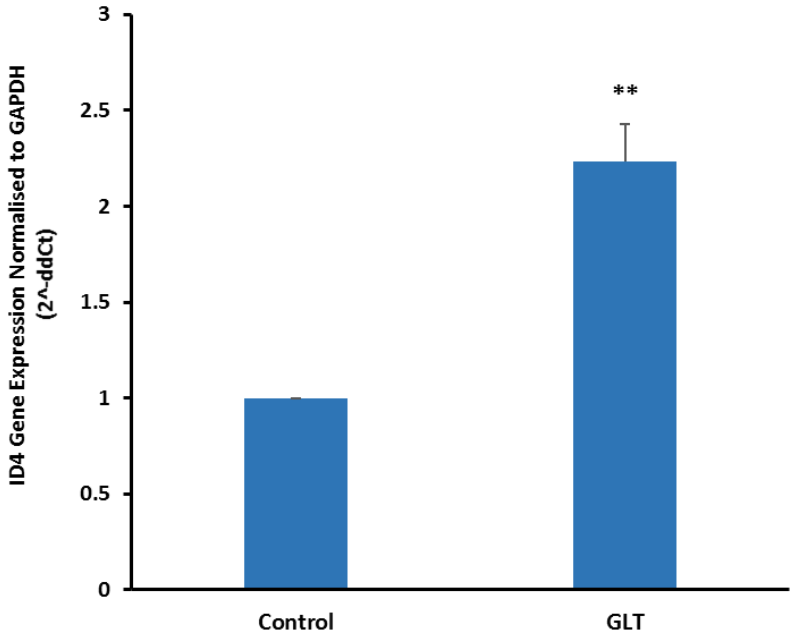

Figure 4.8 ID4 gene expression in response to GLT. *INS-1 cells were incubated ± GLT 5 days. Total RNA was extracted (Qiagen, Hilden, Germany), reverse transcribed (Thermofisher, Waltham, MA, USA) and analysed using RT-qPCR with ID4 specific primers. Results are shown as ΔΔCt expressed as fold change compared to the control. Results shown are mean ± SEM from three independent investigations.*

As ID4 gene expression is increased by GLT, I then sought to determine whether up regulation of ID4 affected the down regulation of insulin observed in the same conditions.

INS-1 cells were subjected to siRNA transfection to knock down expression of ID4 for 24 hours, then transfection media replaced with RPMI-1640 media ±GLT for 72 hours. Following the 72-hour incubation the cells were lysed with RIPA buffer, separated into two tubes and then either prepared for western blotting to detect the level of ID4 knockdown or for PCR analysis to measure the change in insulin gene expression. The initial result (Fig 4.9) confirmed previous data in this chapter, in that insulin gene expression was down regulated by 52.6% (p=0.016) in GLT treated cells compared to control. The results also showed that following siRNA transient knockdown of ID4, in non-GLT treated cells ID4 protein expression was reduced by 87.1 resulting in a 42.2 (p=0.006) increase in insulin gene expression in siRNA treated cells compared to non-GLT treated ssRNA cells. In GLT treated cells there was a reduction in ID4 protein expression by 92% resulting in an increase in siRNA treated cells in insulin gene expression by 26.4% (p=0.034) compared to ssRNA treated cells.

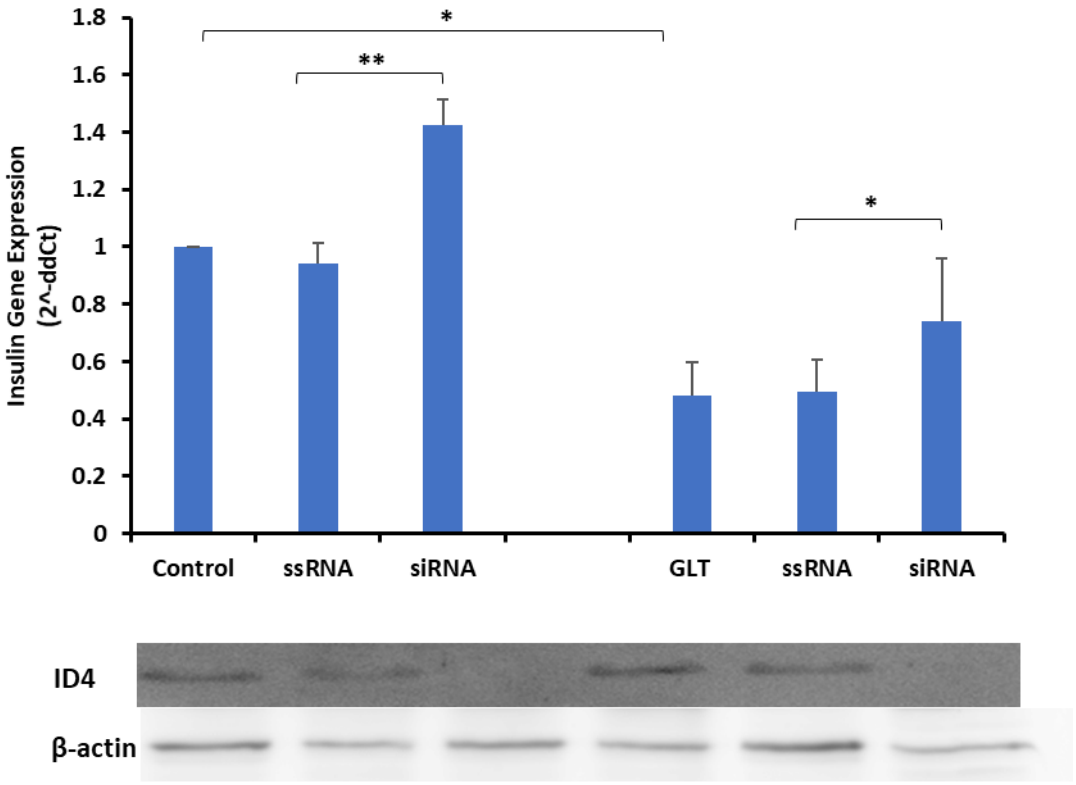

Figure 4.9 Insulin gene expression following ID4 knockdown. *ID4 was transiently knocked down using siRNA for 24 hours followed by 72 hours incubation ± GLT. Total RNA was then extracted (Qiagen, Hilden, Germany), reverse transcribed (Thermofisher, Waltham, MA, USA) and analysed using RT-qPCR with insulin specific primers. Results are shown as ΔΔCt expressed as fold change compared to the control. Results shown are mean ± SEM from three independent investigations.*

To determine whether CD40 was the driving force responsible for the up-regulation of ID4 witnessed in GLT conditions and the subsequent reduction of insulin gene expression, a transient knockdown of CD40 was carried out. I then determined the effect on ID4 expression (Fig 4.10).

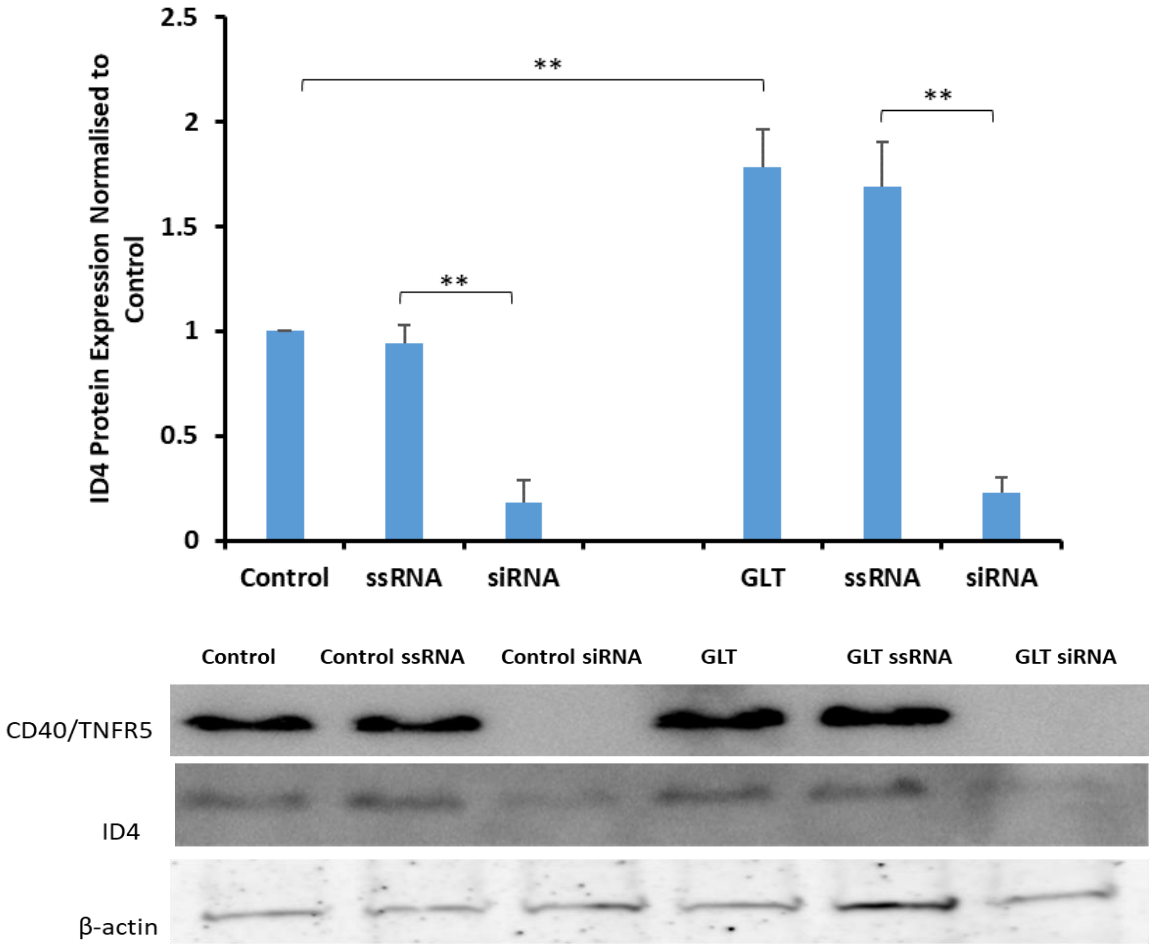

Figure 4.10 Effect of CD40 knockdown on ID4 protein expression. *CD40 was transiently knocked down using siRNA for 24 hours followed by 72-hour incubation ± GLT. Proteins were extracted using RIPA buffer and quantified using BCA assay. Proteins were loaded to acrylamide gels and separated using SDS-PAGE. Proteins were transferred to nitrocellulose membrane and immunoblotted using specific antibodies.*

4.4 Discussion

Cluster of differentiation 40 (CD40) belongs to the TNF receptor family and is involved in the development of various inflammatory diseases (Portillo et al, 2014). The reason for investigating CD40 in this chapter was to determine whether the increase in CD40 expression, that was previously shown to result from exposure to GLT, was able to modulate expression of genes associated with β-cell function. Using a bespoke interactome network map genes were identified that were predicted to be negatively regulated by CD40. Each gene is presented as a node and the link between the genes is symbolised as by an arrow to indicate the directional effect from the 'source node' to the 'target node' and this is used to demonstrate interactions between biological components (Tong et al, 2014).

From the genes in the regression interactome (Fig. 4.2A), where all the genes identified were shown to be negatively regulated by CD40, six were selected for testing (Fig. 4.2B). Evidence of CD40 activation resulting in cellular dysfunction was demonstrated. From six genes tested, five were negatively regulated by CD40 in human CM cells. This was determined by transient knock down of CD40 using siRNA. Following a knock down in CD40 of 85% compared to the untreated control and 79 compared to the scrambled sequence control, PCR was used to determine the change in gene expression of the selected genes. GTPBP4 (GTP-binding protein 4) is a GTP-ase and functions as a molecular switch that alternates between the active and inactive GDP-bound form. When in the GTP-bound active form, it can function as a trigger to initiate other cellular events. Following the knock down of CD40, GTPBP4 is increased 3.84 compared to control ($p=0.0012$), and 5.29 compared to the scrambled sequence control ($p=0.0011$). The next gene to be tested was ILVBL (ILVB acetolactate like gene) is a protein encoding gene that plays a role in catalysing the first step in branched amino acid synthesis. Subsequent to the knock down of CD40, ILVBL gene expression is increased 5.83-fold compared to control ($p=0.046$), and 9.79-fold compared to the scrambled sequence control ($p=0.039$). IDH2 (isocitrate dehydrogenase 2) is found in the mitochondria and catalyses the oxidative decarboxylation of isocitrate to α-ketoglutarate and synthesis NADPH (Han et al, 2017). IDH2 gene expression increased by 3.44-fold compared to untreated control and 3.44-fold compared to the ss control. MVP (Major vault complex) showed no changed in expression in response to the reduction in CD40 protein expression. SC4MOL (sterol-C4-methyl oxidase like) gene encodes the protein sterol-C4-methyl oxidase (SMO), which is involved in catalysing the demethylation of C4-methysterols in the cholesterol synthesis pathway (He et al, 2011) was up regulated by 3.8-fold in response to the transient knock down of CD40 compared to the untreated control and was up regulated by 3.7-fold compared to the ss control. Finally, CTXN (cortexin-1) gene encodes a protein that is found located in precursors of neurons and is involved in the mediation of intra and extra-cellular signalling of cortical neurons during brain development (Watson et al, 1994).

These results therefore demonstrate that CD40 stimulation via GLT exposure is able to result in the suppression of various genes and is likely to influence multiple cellular functions in β-cells. These findings are consistent with a report on B cells where systematic screening showed there are many unrecognised targets of CD40 including transcription factors, signalling molecules, proapoptotic molecules, cytokines and others. Importantly the study found that a number of genes were down regulated in response to CD40 stimulation including 18 transcriptional regulators (Dadgostar et al, 2002).

In order to validate the findings of Figure 4.4, protein expression of IDH2 and SC4MOL was measured

to confirm whether these proteins are reduced in GLT conditions, where it is known that CD40 activation is increased. The results confirmed the findings of Figure 4.4 and showed that IDH2 protein expression was reduced by 24% and SC4MOL was reduced by 55.6%. IDH2 is located in the mitochondria, where it functions as an enzyme in the citric acid cycle. Its role is to consume $NADP^+$ and provides NADPH by catalysing the oxidative decarboxylation of isocitrate to α-ketoglutarate (Smolkova and Jezek, 2012. Medeiros et al, 2017). GLT-induced damage of the mitochondria would be expected as it known that it is a major source of ROS and a primary site for ROS-induced oxidative damage and apoptosis. A recent study found that a reduction in IDH2 resulted in decreased cell viability and mitochondrial respiration rates where as a complete loss of IDH2 led to oxidative damage and apoptosis in HEI-OC1 cell, a mouse inner ear cell line (White et al, 2018).

As previously mentioned SC4MOL is involved in the demethylation of C4-methysterols in the cholesterol synthesis pathway. A similar study examining the effects of high glucose on pancreatic β-cells found that HMGCoA was significantly reduced which is a rate limiting enzyme in cholesterol synthesis and its function is to catalyse mevalonate from 3-hydroxyl-3-methylglutaryl Co enzyme A and a reduction in cholesterol content (Somanath et al, 2009). This is consistent with the results shown in the present study and suggest that the driving force behind the alterations to the mitochondria, cholesterol synthesis and other mechanisms in the pancreatic β-cell that are caused by GLT are likely due to, at least in part due to activation of CD40.

Consistent with my ID4 data presented in this chapter, a former member of the Turner lab group identified that by knocking down CD40 using siRNA, a 1.7-fold increase in insulin mRNA could be achieved in control conditions (data not shown). This finding suggests a novel role for CD40 in transcriptional regulation beyond just the inflammatory pathway in β-cell function. Therefore, the aim of this chapter is to identify the transcriptional machinery regulated by CD40 activation that results in the loss of insulin gene expression in GLT conditions. Multiple publications have demonstrated that insulin secretion is reduced in high glucose or fatty acid environments, however publications usually either show the effects of glucotoxicity or lipotoxicity, rarely combined, as demonstrated in this research project. It is well known that prolonged exposure of β-cells to glucotoxic environments diminishes insulin secretion (Dubois et al, 2007), and hyperglycaemia results in the reduced capacity of β-cells to secrete insulin (Kawahito et al, 2009). A suggested explanation for the loss of insulin secretion following exposure to the fatty acid palmitate is because it impairs the activity of the insulin promoter, but the same study identified that the addition of palmitate did not affect the stability of the preproinsulin gene (Kelpe et al, 2003).

Insulin degrading enzyme (IDE) is a zinc metallopeptidase that can degrade peptides including insulin. IDE is reported to be localised mainly in the cytosol of the cell but is also found in the mitochondria, peroxisomes and endosomes (Song et al, 2018). The results showed that in response to GLT, expression levels of the IDE gene increased by 13±6%. Despite an increase in the peptidase which is able to degrade insulin, the increase was not considered significant ($p=0.09$), and therefore isn't the reason for the significant reduction of insulin gene expression that results from INS-1 cell exposure to GLT conditions.

ID4 is identified as a stress-induced protein in β-cells that is significantly up-regulated in response to GLT conditions in INS-1 cells. The results showed that ID4 is up regulated by 2.23-fold in GLT conditions compared to control untreated cells. This finding is supported by Bensallam et al (2015), who identified that all members of the ID family were up regulated in diabetic mouse islets and builds upon another study that identified that both ID1 and ID3 are up-regulated in response to glucose and other insulin secretagogues (Wice et al, 2001). However, neither of these publications investigated ID4 in pancreatic β-cells.

The results presented in this chapter identify ID4 as a novel modulator of insulin gene expression. The results showed that following the transient knock down of ID4 there is an increase in insulin gene expression in both control and GLT conditions, identifying that ID4 plays a role in the suppression of insulin gene expression that is observed in GLT conditions. However, this seemingly contradicts previously published data that stated that all four members of the ID family did not alter insulin secretion in physiological concentrations (Wice et al, 2001). However, it has already been observed that exposure of the INS-1 cells to GLT conditions was able to significantly up regulate ID4 gene expression above the control level. The findings by Wice et al (2001) also suggest that the up regulation of ID1 and ID3 in response to glucose actually promotes insulin secretion rather than inhibit synthesis as seen by ID4 in this project (Wice et al, 2001). The reason for ID4 responding in the opposite manner to other ID members is explained in a study that examined expression patterns of the ID protein family during mouse embryogenesis. The study identified that there was a difference in expression patterns of ID1-3 and ID4 which could suggest the dominant negative transcriptional activity of the proteins may lead to different physiological consequences (Jen et al, 1996).

Therefore, the increase in ID4 might result in suppression of insulin gene expression due to ID4 inhibiting the actions of the other members of the ID family. Consistent with this hypothesis a study has identified that the presence of ID4 was able suppress the effect of proteins ID1-3 in human prostate cancer cells lines (Sharma et al, 2015). This determination could also be relevant in pancreatic β-cells and the same phenomenon could be occurring, as Wice et al stated that ID1-3 could be

beneficial for insulin secretion, but in stress conditions such as GLT, ID4 is up regulated and it may be that this inhibits ID1-3, in turn suppressing insulin gene expression. This theory also expands upon further findings of Bensallam et al, who identified that when ID1 and ID3 were inhibited there was a resulting increase in reactive oxygen species (ROS). This is supported by results in the current research project that has identified a concomitant increase in ID4 gene expression and ROS when INS-1 were exposed to GLT. The results in this chapter also identified that CD40 is the driving force behind ID4 up regulation in response to GLT. As it is shown in this chapter that ID4 is responsible for suppressing insulin gene expression ID4 is therefore identified as a novel negative regulator of insulin gene expression. The results demonstrate a clear connection between CD40 knockdown using siRNA and a resultant loss in ID4 expression.

Chapter 5

Potential Therapeutic Effects of Carnosine

5.0 CHAPTER 5: Potential Therapeutic effects of Carnosine

5.1 Introduction

Carnosine is a physiological dipeptide that is synthesised from L-histidine and β-alanine in the presence of ATP. It is present in mammalian tissue and is found in abundance mostly in skeletal muscle tissue, heart muscle and the central nervous system (Harris et al, 2012). Beta-alanine is considered to be the rate limiting step in carnosine formation as it has been demonstrated that by increasing the availability of β-alanine via supplementation, there is an increase concentration of carnosine in muscle tissue (Cuthbertson et al, 2010). Carnosine synthase, which belongs to the ATP-grasp family is also known as ATPGD1 and is the ATP-dependent ligase responsible for the formation of carnosine from its components L-histidine and β-alanine. (Drozak et al, et al 2010. Veiga-da-Cunha et al, 2014). The dipeptidase known as carnosinase (CN) is responsible for the degradation of histidine containing dipeptides including carnosine. There are two types of CN, CN1 which hydrolyses carnosine in plasma and CN2 which hydrolyses carnosine in the cytoplasm of cells (Peters et al, 2018. Otani et al, 2008).

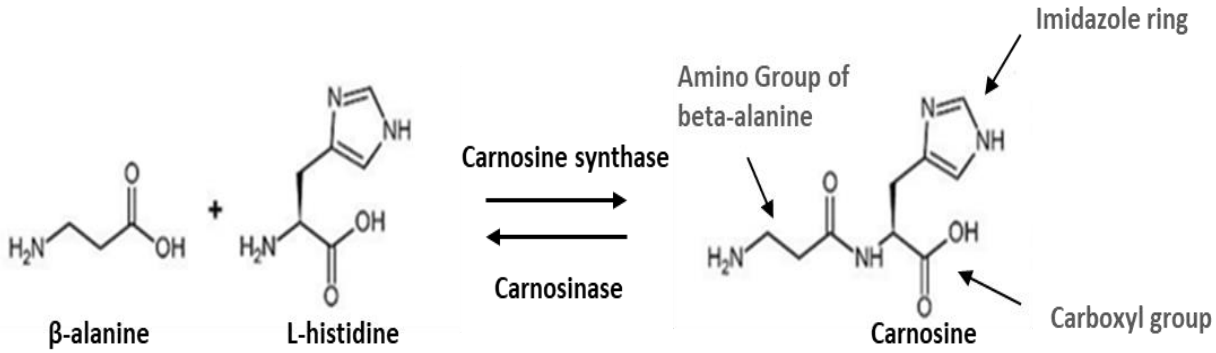

Figure 5.1: Structure of carnosine, Beta-alanine and L-histidine. *Schematic image illustrating the formation of carnosine from β-alanine and L-histidine (Superfoodly.com).*

5.1.1 Functions of Carnosine

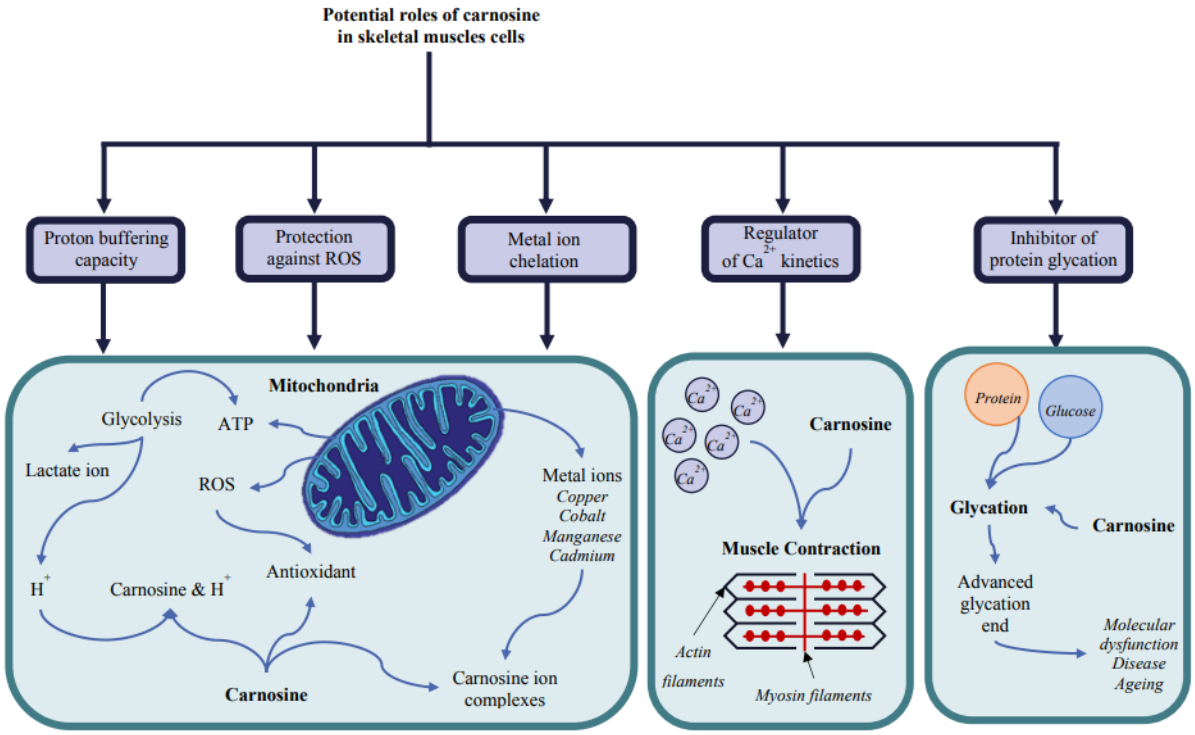

Figure 5.2 Potential functions of carnosine. *Schematic of the potential roles of carnosine within skeletal muscle. (Generated by Jones R, 2017).*

Carnosine is a water-soluble dipeptide that is characterised by three ionisable groups; the carboxylic group (pKa 2.76), the amino group of the β-alanine (pKa 9.32) and the imidazole group/ring (pKa 6.72). The imidazole ring is located on the histidine residue of the dipeptide, it contains two nitrogen atoms and functions as the driver in a number of carnosine's functions. (Culbertson et al, 2010).

Carnosine is an antioxidant, which broadly means that it is able protect lipids, protein, DNA and other macromolecules from oxidative damage. The antioxidant properties possessed by carnosine are mediated by mechanisms including metal ion chelation and scavenging of reactive oxygen species and reactive carbonyl species. The antioxidant activity exhibited by carnosine is based on the functions of the imidazole ring. It has been shown that imidazole alone reduces oxidation to lipids by 39% and that histidine-containing dipeptides such as carnosine that were lacking the proton on the nitrogen of the imidazole ring showed very little antioxidant activity (Kohen et al, 1988).

One mechanism by which antioxidants protect their target from oxidative stress is via metal ion chelation (Kohen et al, 1988). There is a lot of evidence to suggest that carnosine forms complexes

with metals of the first transition metal series including Cu^{2+}, Co^{2+}, Cd^{2+}, Zn^{2+}. Of these, the complexes of carnosine with Cu^{2+} and Zn^{2+} are the most studied and understood due to their physiological relevance and potential pharmaceutical applications. It has been proposed that metal ions bind with the imidazole ring, amino and peptide nitrogen atoms to form two-membered chelate rings. In normal physiological conditions reactive oxygen species (ROS) have role in maintaining regulatory functions. However, if there is an uncontrolled increase in expression of ROS they can interact with biomolecules and resulting in oxidative modifications and stress, which prevents them undertaking their functional regulatory roles. The markers of oxidative modifications and oxidative stress include glycated proteins and products of lipid peroxidation (Prokopieva et al, 2016). ROS is able to react with a biomolecule known as superoxide, which can result in downstream lipid peroxidation, HNE adduct and 3-nitrotyrosine formation, which are major biomarkers of oxidative stress and cell damage (Weber et al, 2013). However, at physiological concentrations carnosine has been found to directly interact with superoxide via a 'charge-transfer' complex which alters the reactivity of superoxide, therefore preventing the downstream cellular damage (Boldyrev et al, 2013). Carnosine is also reactive carbonyl species (RCS) scavenger. RCS can be divided into 3 groups, α,β-unsaturated aldehydes such as HNE, ketoaldehydes and dialdehydes (Hwang et al, 2016).

Carnosine is also used to inhibit protein glycation. Glycation of proteins lead to the generation of a heterogenous group of adducts known as advanced glycation end products (AGE). The primary mechanism of glycation -induced damage involves the cross-linking between proteins and/or DNA modifying or destroying their functional properties (Pepper et al, 2010). It has been suggested that the presence of carnosine abolishes protein cross-linking resulting from glycation. A possible mechanism for this is the amino group or imidazole group on the carnosine binds to reactive dicarbonyls. An alternative possibility that has been suggested is that the proteins become 'carnosinylated' at carbonyl groups and this may protect them from being degraded or cross-linked (Pepper et al, 2010).

Carnosine also has pH buffering abilities. A buffer is a compound that is able to resist large changes in pH even in low concentrations (Decker et al, 2001). In skeletal muscle it has been identified that carnosine has the ability to stabilise pH levels and it is the function of the imidazole group located on the L-histidine residue to buffer pH. This is because they have a pK value similar to the intracellular pH, thus one of the two nitrogens in the imidazole group can be protonated within the physiological range (Abe, 2000).

Another potential function of carnosine is the regulation of calcium ion (Ca^{2+}) concentrations. In muscles during contraction and relaxation, Ca^{2+} exchange is primarily controlled by Ca^{2+} ATPase. Ca^{2+}

ATPase is involved in the accumulation of Ca^{2+} during muscle relaxation and Ca^{2+}-channels which allow the release of Ca^{2+} into the cytoplasm during muscle contraction (Batrukova and Rubtsov, 1997). Carnosine has the potential to assist in cytoplasmic regulation of Ca^{2+} and H^{+} coupling as it able to bind to both ions (Jones et al, 2017). Published data has also shown that the presence of carnosine improves the efficiency of Ca^{2+} pump by increasing the Ca/ATP coefficient. The mechanism by which it does this is thought to be via binding to the saturable binding sites (Batrukova and Rubtsov, 1997). Evidence has also shown that components of carnosine have effects on Ca^{2+} channels. Beta-alanine is able to enter the cells along with depolarising Na^{+} ions which results in the opening of voltage-activated L-type Ca^{2+} channels and L-histidine as a cationic amino acid is able to cause gating of voltage-sensitive Ca^{2+} channels resulting from depolarisation if the plasma membrane (Albrecht et al, 2017).

5.1.2 Factors Affecting Carnosine Concentration

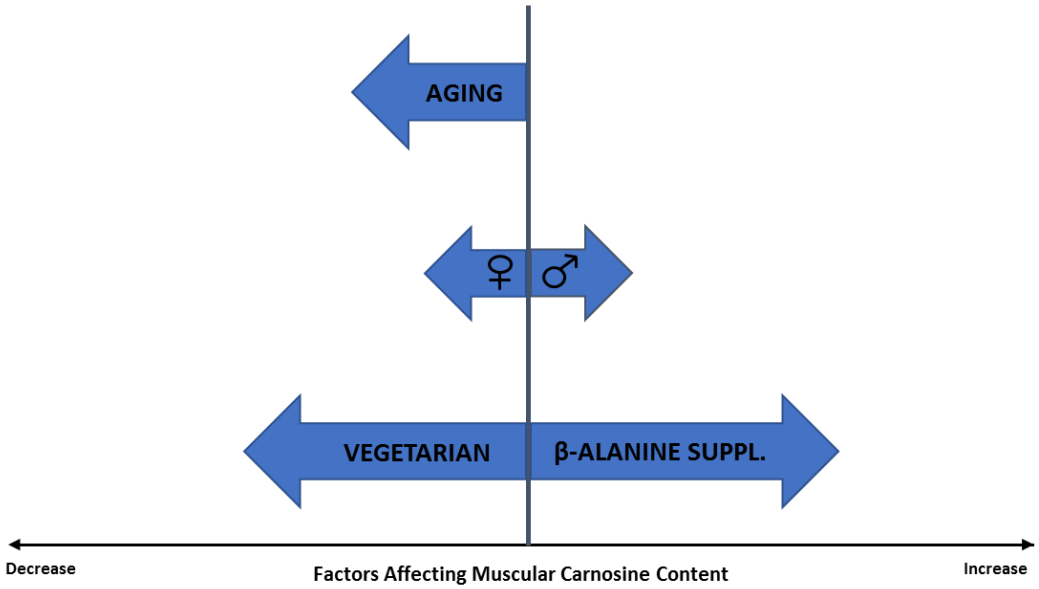

Figure 5.3 Potential factors affecting carnosine content. *The image shows that aging, being female and following a vegetarian diet are likely to reduce skeletal muscle carnosine content, whereas males and individuals who follow an omnivorous diet or supplement their diet with β-alanine are likely to high increased levels of carnosine in the skeletal muscle. Adapted from Derave et al, 2010.*

There are multiple factors that can impact carnosine content in muscles. Diet influences carnosine levels and meat intake is considered to be the primary supply of carnosine in humans. Dietary carnosine is able to cross the intestinal lumen barrier and appear intact in the plasma if it hasn't been

hydrolysed by carnosinase. Based on the rapid hydrolysis of carnosine it is considered to be a bioactive food component. Following meat ingestion there has also been an increase in urinary carnosine shown (Gardener et al, 1991). Evidence that meat is a primary source of carnosine has been documented. Females who were chronic vegetarian (vegetarian for 8 years +) showed a 20% reduction in muscular carnosine compared to omnivorous counterparts. Another study that measured carnosine content in calf muscle found that vegetarian men had 26% less carnosine that omnivorous subjects (Everaert et al, 2010). However, it has been debated that a vegetarian life style must be chronic in order to affect carnosine levels, short term vegetarianism is not sufficient to show a reduction in muscular carnosine (Baguet et al, 2011).

Another factor affecting carnosine content is gender, where men appear to have higher concentration of carnosine in skeletal muscle than women. A study conducted by Everart et al, concluded that men have up to 82% more muscular carnosine than women in various skeletal muscles. The reason for this appears to be the difference in muscle type between men and women, men have a higher percentage of type II muscle fibres than women who are reported to have type I muscle fibres. There is between 30-100% more carnosine in type II muscle fibres than type I (Varanoske et al, 2017). Another major factor that affects carnosine concentration is age. As the aging process takes place muscle undergo alterations which include reduction in strength and mass. Peripheral muscle strength reduces by 20% between the ages of 20 and 70, which corresponds with the reduction in mass. Carnosine also has muscle-independent effects on inflammatory processes, wound healing and tissue protection, therefore it may be possible that age-related inflammation and delayed wound healing are also associated with a reduction in carnosine as individuals age (Stuerenberg and Kunze, 1999).

5.2 Aims

1. To identify whether pancreatic β-cells possess carnosine synthase, the enzyme required to generate carnosine from β-alanine and L-histidine in the presence of ATP.

2. To identify whether carnosine synthase concentrations are affected by GLT, thereby affecting the ability of the β-cell to generate carnosine.

3. To see if the effects of GLT on carnosine synthase concentrations can be reversed or prevented by the supplementation with carnosine, β-alanine and or/ L-histidine.

4. To observe whether the supplementation of ±GLT media with 10mM carnosine is able to reverse/prevent cytotoxic damage that is caused by high glucose and high fatty acid media. If so, this has the potential to be developed in line with therapeutic strategies based around carnosine.

5.3 Results

5.3.1 Beta cells are able to generate Carnosine

The initial part of the investigation involved incubation of the rat pancreatic INS-1 cells ± GLT, ±GLT and 10mM carnosine and ± GLT supplemented with 10mM of the components of carnosine (β-alanine and L-histidine), as well as ± carnosine and ± carnosine components alone for 5 days. The reason for this was to determine whether pancreatic β-cells possess sufficient active enzyme to generate carnosine from β-alanine to L-histidine. Following the incubation period, the cells were lysed, and proteins were extracted using RIPA buffer and the protein was determined using BCA assay. Equal amounts of protein were loaded to an SDS-Page gel and were separated using electrophoresis. The proteins were transferred to a nitrocellulose membrane immunoblotted using a carnosine synthase specific antibody. The results initially demonstrate that carnosine synthase is in fact present in pancreatic β-cells. The results also demonstrate that the addition of GLT induced a significant decrease in carnosine synthase by 23.8% ($p=0.035$). The addition of 10mM carnosine was able to able to return the level of carnosine back to basal level. The supplementation of RPMI-1640 with 10mM carnosine was able to increase the level of carnosine synthase by 10% compared to the control level (not significant increase). The results also demonstrated that the addition of GLT ± L-histidine/β-alanine was also able to significantly decrease carnosine synthase levels by 27.3% and 33.4% respectively. When used to supplement RPMI-1640 media both L-histidine and β-alanine were able to push carnosine synthase levels above control.

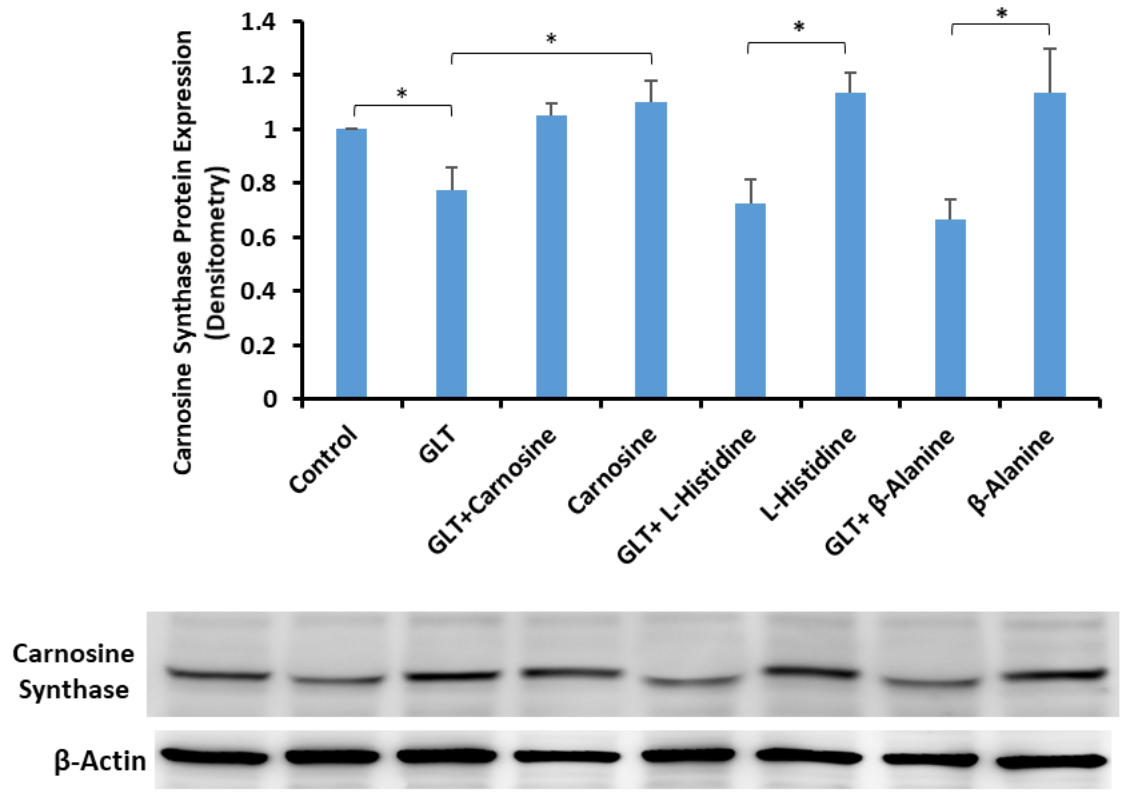

Figure 5.4: Effect of GLT on carnosine synthase expression. *INS-1 cells were incubated ±GLT, supplemented with either carnosine, L-histidine, β-alanine for 5 days prior to protein lysis, protein was quantified using BCA assay and equal amount of protein were loaded to a 10% acrylamide gel and separated using SDS-PAGE. Proteins were transferred to a nitrocellulose gel and immunoblotted using ATPGD1 antibody.*

5.3.2 Carnosine reverses GLT-induced up-regulation of molecules potentially involved in β-cell inflammation

The second part of the investigation involved incubating INS-1 cells ±GLT ± carnosine for 5 days to observe whether the addition of carnosine was able to prevent or reverse the potentially damaging effects elicited by GLT via up-regulation NF-κB, iNOS, 4-hydroxynonenal (4-HNE) and 3-nitrotyrosine (3-NT), shown in chapter 3.

To observe the effects of carnosine on NF-κB activation ±GLT, cells were incubated either in control RPMI-1640 media ± carnosine, or GLT media ± carnosine for 5 days. Nuclear extract was then isolated using the Nuclear/cytosol extraction kit (Biovision, Milpitas, CA, USA) and utilised in the Transcription Factor assay (Active Motif, Carlsbad, CA, USA). The results indicated that there was a factor of variance between the samples (P=0.0062). The results showed (Fig.5.5A) that GLT was able to induce NF-κB activation by 2.6-fold and that addition of 10mM carnosine was able to reduce this increase in

activation to 35% above control level (p=0.039). The addition of 10mM carnosine to control reduced NF-κB activity by 15.4% below control level (although not significantly different).

For iNOS analysis, protein was extracted from INS-1 cells using RIPA buffer and determined by BCA assay (ThermoFisher, Waltham, Ma, USA). Protein was loaded onto a 7.5% gel and separated using SDS-PAGE. Protein was transferred onto a nitrocellulose membrane using a Trans-Blot®Turbo™ transfer system (Bio-Rad, Hercules, CA, USA) immunoblotted using an iNOS specific antibody (Abcam, Cambridge, UK). Analysis of variance indicated a significant difference between the means of the samples (p=0.0052). iNOS protein expression was shown (Fig.5.5B) to increase by 3.7-fold in response to GLT (p=0.0075). By contrast, the addition of 10mM carnosine to the GLT media was able to reduce the increase in iNOS expression to only 55% higher than control level (p=0.017). The supplementation of 10mM carnosine to RPMI-1640 control media reduced iNOS protein expression to 19% below basal level (although not statistically significant).

In order to determine the effects on 4-HNE, an ELISA kit was utilised (Abbexa, Cambridge, UK), following a 5-day ± GLT, ± carnosine incubation period. ANOVA identified a significant difference between the sample means (p=0.0034). The results showed that 4-HNE species increased in response to GLT by 43.46% (p=0.00098). The addition of 10mM carnosine to the GLT media was able to reduce the up-regulation of 4-HNE species to a 16.67% increase (p=0.048). Similarly, an ELISA assay (Abcam, Cambridge, UK) was used to determine the effect on 3-NT adduct formation, where the analysis of variance was significant (p=0.0056). The results demonstrated that GLT was able to induce an increase in 3-NT adduct by 33%, and the addition of carnosine to the GLT media was able to almost completely eradicate the increase in 3-NT adduct formation, resulting in 3-NT adducts only 5% higher than the control level.

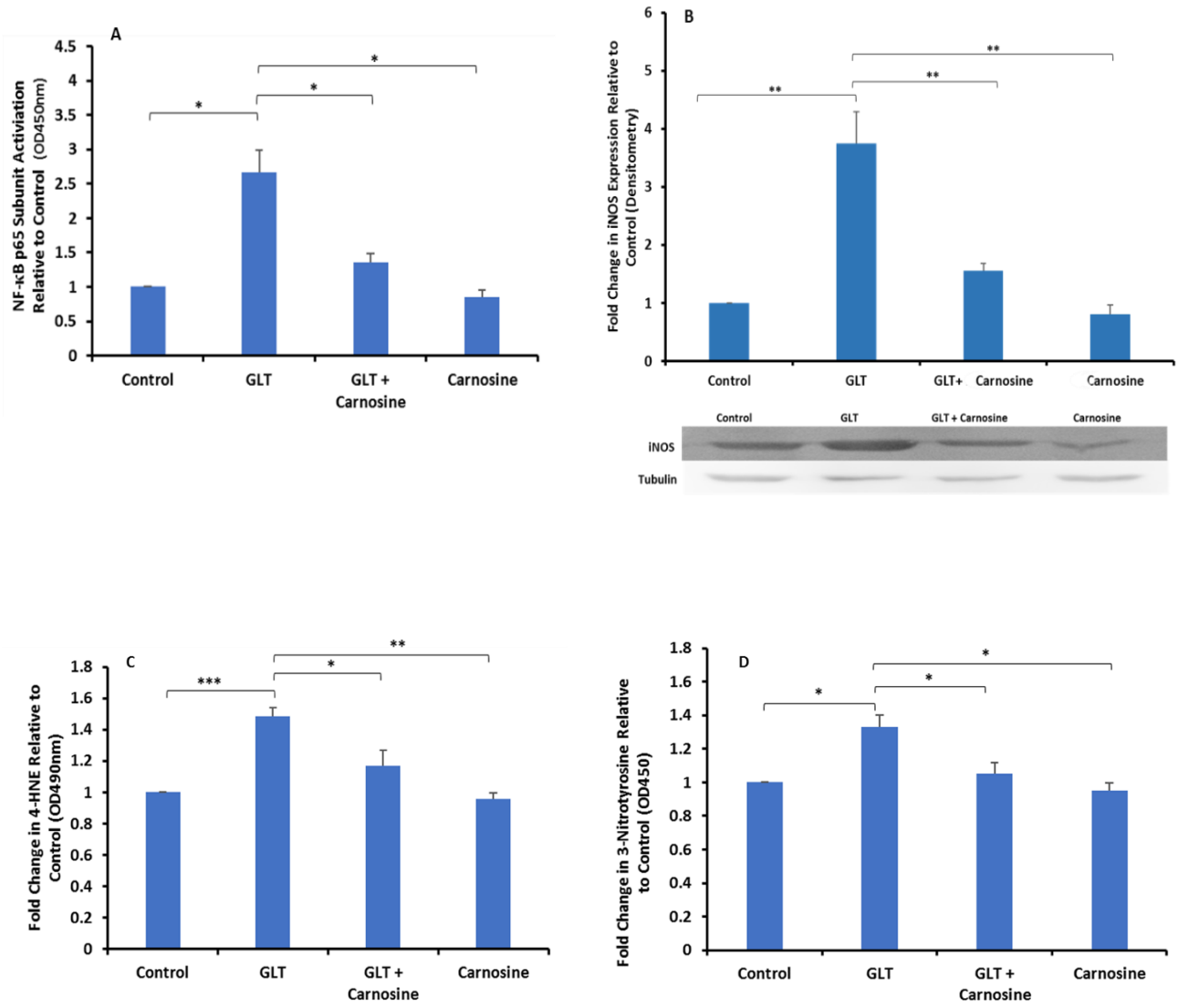

Figure 5.5: Effects of Carnosine supplementation. *INS-1 cells were incubated ±GLT ±carnosine for 5-days. A. cells were lysed and NF-κβ activity was measured using TransAm NF-κβ kit (Active Motif, CA, USA). Absorbance was read at 450mM. B. protein were collected and quantified using BCA assay. Proteins were loaded to 7.5% acrylamide gel and separated using SDS-PAGE. Proteins were transferred to nitrocellulose membrane and immunoblotted using iNOS specific antibody. C. Cell lysates were collected and analysed for the presence of HNE using ELISA (Abbexa, Cambridge, UK) absorbance was measured at 490nm. D. Lysates were collected and analysed for 3-NT species using ELISA (Abcam, Cambridge, UK). Absorbance was measured at 450nm. All data presented is mean ±SEM from 3 or more experiments.*

To identify proteins that were adducted in GLT conditions but didn't show adduction in control or carnosine conditions, cells were incubated for 5 days ± GLT ± Carnosine and analysed using co-immunoprecipitation and mass spectrometry.

Table 5.1: Proteins that develop HNE adducts or form 3-NT species in GLT conditions, but which are reversed by the addition of 10mM carnosine. Identified using co-immunoprecipitation from three independent experiments. Cells were incubated ± GLT ±Carnosine for 5 days prior to Co-IP and mass spectrometry. Data shown is from three individual experiments.

HNE adducts	3-NT species	3-NT species cont.
Protein phosphatase 1 regulatory subunit 1A	Actin-related protein 2/3 complex subunit 5	Protein YIPF4
Isopentenyl-diphosphate Delta-isomerase 1	Clathrin light chain A	Microtubule-associated proteins 1A/1B light chain 3B
Nucleoprotein TPR	CD2-associated protein	Translation initiation factor eIF-2B subunit alpha
Sequestosome-1	Fuctinin-3 (Fragment)	Deoxyhypusine synthase
Mitochondrial 2-oxoglutarate/malate carrier protein	Immediate early response 3-interacting protein 1	GRIP1-associated protein 1
Phosphatidylinositol 5-phosphate 4-kinase type-2 gamma	Malignant T-cell-amplified sequence 1	Adenosine kinase
Aldehyde dehydrogenase, mitochondrial	Sterol-4-alpha-carboxylate 3-dehydrogenase, decarboxylating	von Willebrand factor A domain-containing protein 5A
GrpE protein homolog 1, mitochondrial	E3 ubiquitin-protein ligase NEDD4	Sorting nexin-1
Mitochondrial-processing peptidase subunit beta	Mitochondrial import receptor subunit TOM40 homolog	Dynein light chain Tctex-type 1
Alpha-adducin	Golgi resident protein GCP60	Transmembrane emp24 domain-containing protein 5
Phosphotriesterase-related protein	Retinoid-inducible serine carboxypeptidase	Nicastrin
Tumor susceptibility gene 101 protein	Transmembrane protein 33	DNA polymerase alpha catalytic subunit (Fragment)
C-terminal-binding protein 1	Choline/ethanolamine kinase	Putative GTP cyclohydrolase 1 type 2 Nif3l1
Cathepsin B	Class I histocompatibility antigen, Non-RT1.A alpha-1 chain	Islet cell autoantigen 1
Lysosome-associated membrane glycoprotein 2	3-hydroxyisobutyrate dehydrogenase, mitochondrial	Sideroflexin-3
L-lactate dehydrogenase B chain	Reticulon-3	Testin
Endothelin-converting enzyme 1	Nucleoside diphosphate-linked moiety X motif 19, mitochondrial	Vacuolar protein sorting-associated protein 26A
5'-AMP-activated protein kinase subunit gamma-1	Ras-related protein R-Ras	
5'-AMP-activated protein kinase subunit gamma-1	Cysteine and histidine-rich domain-containing protein 1	
Protein farnesyltransferase/geranylgeranyltransferase type-1 subunit alpha	ADP-ribosylation factor-like protein 2	
Oxygen-dependent coproporphyrinogen-III oxidase, mitochondrial	Fatty acid-binding protein, heart	
Beta-catenin-like protein 1 OS=Rattus norvegicus	Alcohol dehydrogenase class-3	
Beta-catenin-like protein 1	Stromal interaction molecule 1	
1,2-dihydroxy-3-keto-5-methylthiopentene dioxygenase	Cell differentiation protein RCD1 homolog	
Synaptobrevin homolog YKT6	Protein TSSC4	
UBX domain-containing protein	Basal cell adhesion molecule	
Xaa-Pro dipeptidase OS=Rattus norvegicus	Dual specificity mitogen-activated protein kinase kinase 2	
Protein pelota homolog	Ubiquinol-cytochrome-c reductase complex assembly factor 2	
Isochorismatase domain-containing protein 1	ADP-ribosylation factor 6	
COBW domain-containing protein 1	Serine/threonine-protein phosphatase 2B catalytic subunit alpha isoform	
Proteasome subunit beta type-7	Importin subunit alpha-5	
Opioid growth factor receptor	Putative phospholipase B-like 2	
Acyl-protein thioesterase 2	Importin subunit alpha-6	
Ankyrin-3	Golgi integral membrane protein 4	
GTPase NRas		
Isopentenyl-diphosphate Delta-isomerase 1		

Data obtained from mass spectrometry was analysed using Panther Classification System to identify the proteins protein class and biological functions of the proteins that are adducted in GLT conditions but adducts are not present in control, control + carnosine or carnosine conditions.

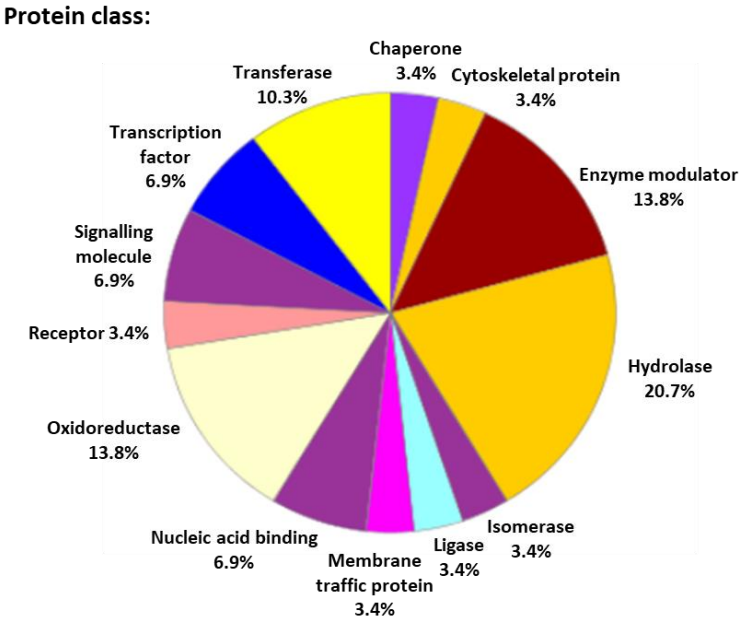

Figure 5.6 Protein class of 4-HNE adducted proteins*. Chart represents proteins that form adducts in response to GLT but is able to be prevented or reversed by the addition of 10mM carnosine. Generated using Panther Classification system.*

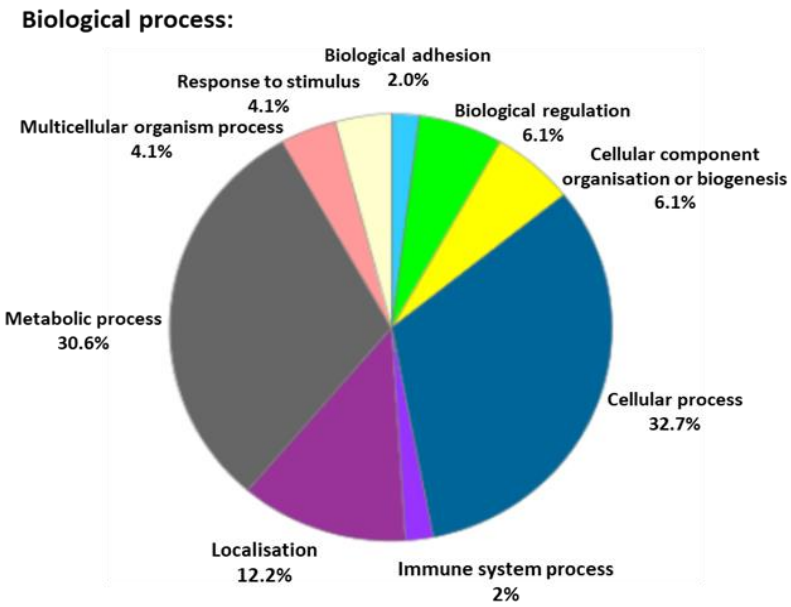

Figure 5.7 Biological process of 4-HNE adducted proteins. *Chart represents the biological functions of the proteins that are adducted with 4-HNE in GLT conditions which is reversed/prevented by the addition of 10mM carnosine. Generated using Panther Classification system.*

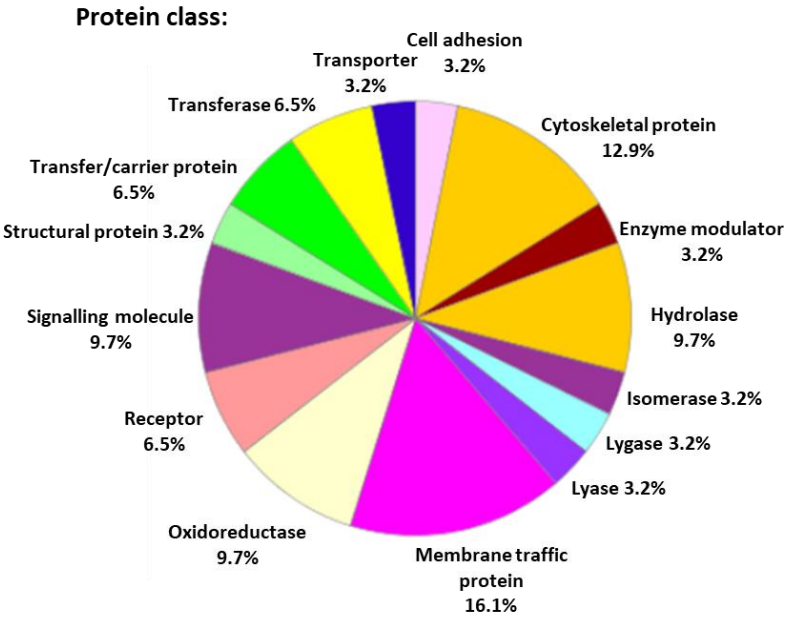

Figure 5.8 Protein class of proteins that generate 3-NT. *Chart shows function of proteins that form adducts in response to GLT but is able to be prevented or reversed by the addition of 10mM carnosine. Generated using Panther Classification system.*

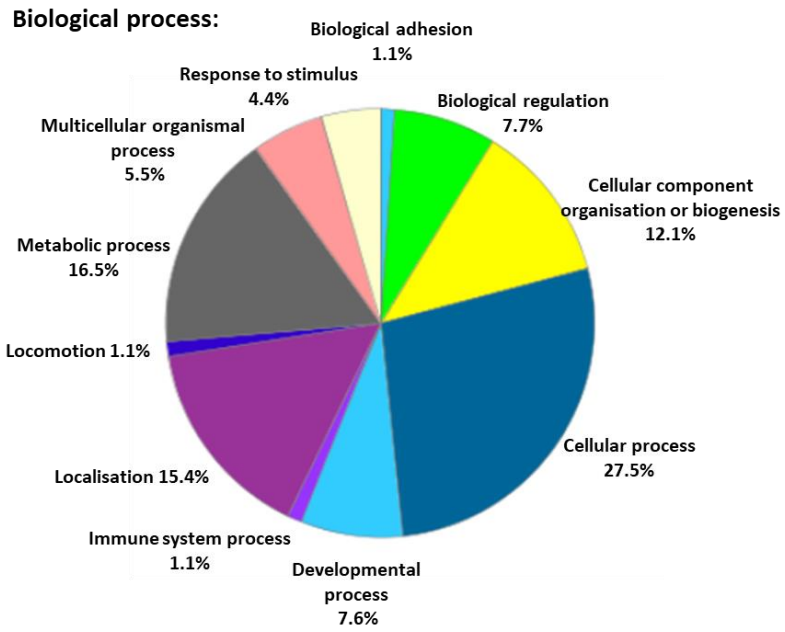

Figure 5.9 Biological process of proteins that generate 3-NT. *Chart represents the biological functions of the proteins that are generate 3-NT in GLT conditions which is reversed/prevented by the addition of 10mM carnosine. Generated using Panther Classification system.*

5.3.3 Carnosine is able to reverse/prevent GLT induced reduction in insulin secretion

The final part of investigation in this chapter was to determine whether the addition of 10mM carnosine to cell media ±GLT was able to reverse or prevent the GLT-induced reduction in insulin secretion as already described in Chapter 3 and 4.

INS-1 cells were incubated in media ± GLT ± 10mM carnosine for 5 days prior to being exposed to a secretagogue cocktail for one hour and insulin being measured using an ELISA assay (Mercodia, Uppsala, Sweden). The results show that the exposure of pancreatic β-cells to GLT conditions is able to down regulate insulin secretion by 30% ($p=0.00037$), however the addition of 10mM carnosine to GLT supplemented cell media, is able to reverse the GLT down-regulation of insulin secretion to 50% above control level ($p=0.0009$) and a similar increase is observed by supplementing the cell media with 10mM of carnosine alone.

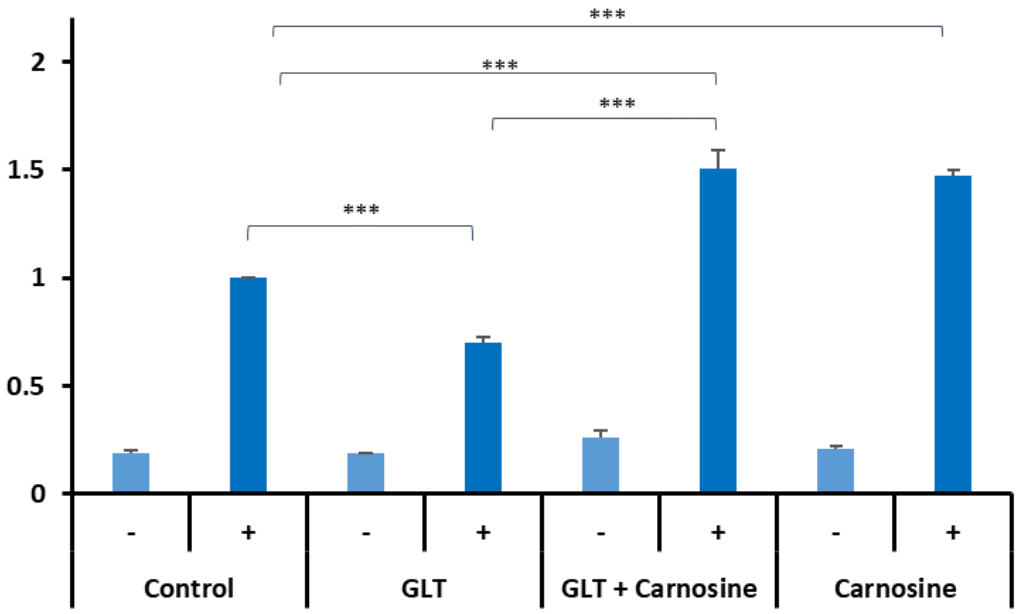

Figure 5.10 Effect of carnosine on insulin secretion. *INS-1 cells were incubated ±GLT and ±carnosine for 5 days cells were then subjected to secretagogue incubation for one hour prior to insulin secretion analysis using ELISA testing (Mercodia, Uppsala, Sweden). The data shown is the mean ± SEM of three independent experiments.*

5.4 Discussion

Carnosine is a naturally occurring dipeptide that is synthesised from β-alanine and L-histidine, catalysed by carnosine synthase in the presence of ATP. The initial aim of this chapter was to identify whether carnosine synthase was present in the INS-1 β-cell line in order to determine whether pancreatic β-cells have the potential to synthesise carnosine. Firstly, as the results of the western blot in Figure 5.5 demonstrates, pancreatic β-cells do contain carnosine synthase. Based on literature searches this appears to be the first time that this enzyme has been identified in β-cells. This finding suggests that β-cells do in fact have the potential to generate carnosine in the presence of β-alanine, L-histidine and ATP. The figure also shows that levels of carnosine synthase are reduced in rat β-cells, when cells are exposed to glucolipotoxic (GLT) conditions for 5 days. This finding progresses upon a study conducted by Gualano et al (2012) which found that individuals with type 2 diabetes had approximately 45% less carnosine in the gastrocnemius muscle which is located in the calf. The reason suggested for this reduction was that carnosine is protected by a limited pool of anti-cytotoxic mediators which decline in conditions that are found in diabetes such as hyperglycaemia, oxidative and carbonyl stress (Gualano et al, 2012). The results found in this chapter build upon the Gualano et al study to identify that cells have a reduced ability to generate carnosine under stress induced by

exposure to high glucose and fatty acid conditions. Therefore, in combination it can be assumed that during the onset of type 2 diabetes, carnosine stores are reduced, and the replenishment is hindered by a reduction in carnosine synthase.

The next part of the investigation involved identifying whether supplementation with carnosine had any beneficial effects following the damage to INS-1 pancreatic β-cell initiated by exposing them to GLT conditions. Nuclear factor kappa B (NF-κB) is a ubiquitous transcription factor that regulates expression of multiple proinflammatory genes and is a known regulator of iNOS expression and is therefore strongly associated with inflammation. NF-κB is sequestered in the cytoplasm in an inactive form when associated with the inhibitor IκB. The activation of NF-κB is dependent on the phosphorylation and degradation of IκB, which allows NF-κB to translocate to the nucleus and act as a transcription factor. Initially the findings in this chapter echo the results of chapter 3 that showed an up-regulation of NF-κB activity in GLT conditions. However, as the results demonstrate in Figure 5.5A, supplementation of media with carnosine had inhibitory effect on the activation of NF-κB. The supplementation of GLT to the cell culture media significantly increased the activation of NF-κB by 2.66-fold ($p=0.014$), whereas the addition of 10mM carnosine to the cell media supplemented with GLT showed an increase of only 35%. The addition of 10mM carnosine to cell culture media not supplemented with GLT reduced NF-κB activation by 16% below control (basal level). This therefore, demonstrates that despite not completely eradicating the up-regulation in NF-κB induced by GLT, the addition of carnosine is able to significantly reduce NF-κB activation and potentially prevent the initiation of an inflammatory response resulting from exposure to high glucose and fatty acids.

Previous work conducted by Odashima et al (2006) highlighted that L-carnosine in combination with zinc was a potential treatment for inflammatory bowel disease and acetic acid induced lesions. The results of their study identified that treatment with zinc carnosine was able to significantly reduce NF-κB in colonic mucosa whilst simultaneously inducing HSP72 which plays a crucial role in the cytoprotective effects of digestive organs (Odashima et al, 2006). The results in this chapter identify carnosine alone as a potential therapy for GLT-induced inflammation whereas the study conducted by Odashima et al, used a combination of zinc and carnosine. Carnosine may be a more beneficial therapeutic strategy as despite zinc also being part of a healthy diet and associated with anti-inflammatory action in the intestine, excessive zinc has been linked impaired immunity in healthy individuals. Increased zinc intake is also linked to side effect symptoms including nausea, vomiting, gastic pain and fatigue, which are not associated with carnosine alone and therefore will not cause ill effect as a supplement in addition to dietary carnosine intake (Chandra et al, 1984. Fosmire GJ, 1990).

Although there is limited mechanistic data published on the effects of carnosine on β-cells, a study was recently published in 2018 that supports the findings in this chapter and showed that following stress induced by H_2O_2, the addition of carnosine was able to significantly reduce both the translocation and expression of NF-κB in pancreatic INS-1E cells (Miceli et al, 2018). Together, the findings in this chapter and the data published by Miceli et al, gives rise to the question of whether carnosine strengthens the association between NF-κB and IκB or else prevents the phosphorylation and degradation of IκB thereby preventing the activation and translocation of NF-κB in order to elicit the therapeutic effects.

Inducible nitric oxide (iNOS) expression is induced by activated NF-κB and is a primary enzyme in generating nitric oxide from L-arginine (Lechner et al, 2005). The results in Figure 5.5B, identify that when exposed to GLT conditions for 5 days rat pancreatic β-cells show a significant increase in inducible nitric oxide synthase (iNOS) expression, whereas the addition of 10mM carnosine prevents GLT up-regulation of iNOS expression, therefore indicating that carnosine is able to inhibit NO formation. This finding both supports and expands upon findings published by Urazaev et al, 1998 who concluded that imidazole, which is found in the histidine residue of carnosine has multiple beneficial effects, including being able to inhibit nitric oxide (NO) synthase in skeletal muscle. A reason for this could be based on the structural similarity between imidazole and 7-nitro indazole, a known NO inhibitor. Whereas imidazole contains two nitrogen atoms located on positions 2 and 4, the NO inhibitor has two nitrogen atoms located on positions 3 and 4 (Urazaev et al, 1998). Despite the similarity, the two are not identical and could be the reason why carnosine is not completely efficient at eliminating NO synthase. This does however exhibit the beneficial effects of carnosine which contains the active imidazole ring and identifies potential protective effects as damage can result down stream of NO synthase. This finding is significant because in normal physiology NO plays a role in cellular function therefore it is important that is concentration is maintained, however, NO can become cytotoxic which is dependent on its combination with superoxide to form peroxynitrite (Ormerod et al, 1999). This combination inactivates NO, therefore disrupting its normal function and creates a potent oxidant (Förstermann and Sessa, 2012). It is therefore important that the supplementation with carnosine is able to inhibit the production of excess NO but also not to down regulate the production of NO below basal level as this may also disrupt cellular function.

4-hydroxynonenal adducts are an α,β-aldehyde that are formed during lipid peroxidation (Barrera et al, 2015). The results in Figure 5.6C demonstrate that the addition of 10mM carnosine to control media was able to reduce HNE below basal level by 3%. The addition of 10mM carnosine to GLT media was able to prevent or reduce the induction of HNE caused by GLT. These results demonstrate that the addition of carnosine to INS-1 cell media reduces cytotoxicity. This is supported by a study conducted

by Liu et al (2003) who found that carnosine was capable of inhibiting protein cross linking that was induced by HNE at a physiologically relevant concentration. The reason for this inhibition was the formation of stable HNE-carnosine bonds. The inhibition of cross-linking also demonstrates the ability of carnosine to intercept intermediates in the reaction of HNE on the protein surface before the intermediates permanently cross-link. This may involve carnosine displacing bound HNE from the protein surface or it may involve the covalent binding of carnosine into the monovalent HNE adducts (Liu et al, 2003). Another study found that when carnosine binds with HNE it prevents or diminishes the cytotoxic effects of HNE in macrophages (Barski et al, 2014).

The generation of 3-nitrotyrosine (3-NT) is catalysed by a class of peroxidases that utilise nitrite and hydrogen peroxide as substrates (Ahsan H, 2013). The results in this chapter show that exposure of INS-1 cells to GLT for 5 days increased 3-NT species by 33%, importantly, the addition of 10mM carnosine was able to prevent 3-NT adduct formation completely ($p=0.0076$) (Cripps et al, 2017).

A study designed to observe nitrosative stress associated with neurological disorders published data identifying that NO, peroxynitrite and 3-NT were all up-regulated in astrocytes exposed to LPS- and INF-γ-induced nitrosative stress, which is similar to the findings of this current project which has identified the up-regulation of NO, HNE and 3-NT. The same published study also demonstrated that treatment with carnosine was able to reduce 3-NT levels (Calabrese et al, 2005). The study identifies the initiation of same inflammatory pathway identified in chapter 3 of this project, which is also either attenuated or prevented by the addition of 10mM carnosine. This suggests that carnosine has therapeutic potential against inflammation found in the onset of type 2 diabetes as well as other pathologies including neurological disorders.

Co-immunoprecipitation (Co-IP) was executed to determine the presence of the post-translational modifications 4-HNE and 3-NT in the pancreatic β-cell line INS-1. The combination of mass spectrometry and Co-IP allows the identification of specific isolated members of a protein complex and is also used to identify interactions between proteins (Free et al, 2009). Figure 5.5 and 5.6 represent the protein class and biological process of the proteins that were adducted by 4-HNE in GLT conditions and not affected in control, carnosine or control + carnosine conditions. Figure 5.7 and 5.8 represent the protein class and biological process in proteins that gained 3-NT in GLT conditions where 3-NT was not present in control, carnosine or control + carnosine conditions. This reiterates the potential benefits of carnosine supplementation. The panther analysis identified clear differences between the location and function of proteins that were adducted. Proteins affected by 4-HNE adduction were primarily enzymes and proteins associated with mitochondrial function whereas the proteins that were adducted with 3-NT were protein involved in trafficking and the cytoskeleton. This

may be identified as a novel therapeutic strategy if the same pattern of adduction extends to other tissues and cells, molecules could be identified as prognostic markers of type 2 diabetes.

Lack of carnosine may result in the increased number of individuals with type 2 diabetes. In 2007 it was reported by the United Nations Food and Agricultural Organisation (UNFAO) that India had the lowest meat consumption compared to other countries throughout the world and a report in 2014 identified that India had the highest rate of vegetarianism with over 1/3 of the population following a lactovegetarian diet, other studies have stated the percentage of vegetarians to be as high as 41% (Devi et al, 2014). Coincidently, in 2000 India had the highest prevalence of diabetes ranging between 5-17% with higher numbers found in the southern part of the country and urban areas (Kaveeshwar and Cornwall, 2014). The high prevalence of diabetes is reported to be based on genetics, and cultural and social factors such as aging population and increased urbanisation (Tripathy et al, 2017). However, based on the reported link between vegetarianism and lack of carnosine in skeletal muscle (Gardener et al, 1991, Everaert et al, 2010) the onset of type 2 diabetes and resulting inflammation-induced cellular damage could be associated with the reduction in cytoprotective properties of carnosine, as vegetarian individuals are not obtaining sufficient carnosine intake via their diet. Another group where the decline in carnosine concentration may result in a decrease in the cytoprotective properties of carnosine is in the elderly. A study conducted in 2016 identified the incidence of type 2 diabetes increased with age and peaked between the ages of 70 and 79 (Sharma et al, 2016). To support this, an age-related decline in carnosine has also been reported. Free carnosine levels reduced by 63% between the ages of 10 and 70, which is thought to be due to a reduction in muscle mass and function (Stuerenberg HJ, 1999). Therefore, the reduction in carnosine concentration that occurs naturally with age could mean the individual is susceptible to inflammation related diseases such as diabetes. However, an age-related decline in pancreatic β-cell carnosine is yet to be determined.

Despite the promising therapeutic potential of carnosine, its use is limited due to its instability in human plasma. Carnosine is rapidly degraded by carnosinase which is a specific dipeptidase that catalyses the hydrolytic cleavage of carnosine (Vistoli et al, 2009). For future work it may be more relevant to look at inhibiting carnosinase function in human plasma rather than increasing carnosine levels. Vistoli et al (2009), observed carnosine derivatives and found that by exchanging L-histidine for D-histidine resulted in a higher selectivity for aldehydes and increased plasma stability and therefore a more efficient RCS quencher. It may therefore be beneficial to supplement the human diet with D-carnosine rather than L-carnosine or as it's rapidly degraded, it may be advantageous increase inhibition of carnosinase to increase the plasma content of carnosine.

Chapter 6

Role of HNF4α in the Regulation of Insulin Secretion of Pancreatic β-cells, and Dysregulation by Glucolipotoxicity

6.0 CHAPTER 6: Role of HNF4α in the Regulation of Insulin Secretion of Pancreatic β-cells, and Dysregulation by Glucolipotoxicity

6.1 Introduction

Chapter 4 discussed how insulin gene expression is reduced as a result of GLT-induced CD40 up-regulation, whereas this chapter examines whether HNF4α plays a role in altering insulin secretion independent of CD40 up-regulation in response to GLT conditions. This chapter examines the effect GLT has on HNF4α and Rab proteins and whether this has any implication on insulin secretion.

6.1.1 Hepatic nuclear factor 4 alpha (HNF4α)

Hepatic nuclear factor 4 alpha (HNF4α) is part of the steroid and thyroid superfamily of transcription factors, which are highly conserved and in adults are primarily found in the liver, gut, kidney and pancreatic islets, including the beta cell (Stoffel and Duncan, 1997). It is considered to be one of multiple transcription factors necessary for the maintenance of the adult β-cell as disruption of this gene leads to impaired glucose tolerance resulting from a reduction in glucose-stimulated insulin secretion (Gupta et al, 2007).

HNF4α has two distinct promoter regions known as P1 and P2. The P1 promoter region is utilised by hepatocytes and used to transcribe exon 1A, whereas pancreatic β-cells use promoter P2 and transcribe exon 1D. In total thirteen exons have been identified in HNF4α, and alternative splicing of these exons results in nine isoforms of HNF4α. Transcription of three of these isoforms, HNF4α 7-9 is driven by the promoter P2, that primarily drives transcription in pancreatic β-cells (Bagwell et al, 2005). HNF4α has a number of functional domains these include N-terminal A/B domain that is associated with the transactivation domain AF-1, a C domain that is responsible for binding DNA, an E domain that is functionally complex as a ligand binding domain, a dimerization platform and a transactivation domain (AF-2), and finally an F domain that has a negative regulatory function (Fig.6.1) (Yagamata K, 2014).

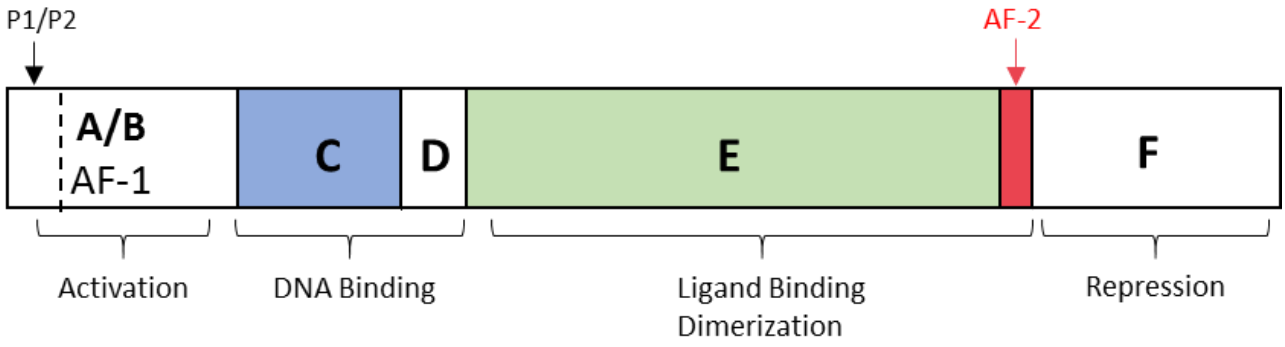

Figure 6.1. Schematic image of HNF4α structure. *Adapted from Jiang et al, 1995.*

HNF4α is synthesized in the cytoplasm and migrates to the nucleus where it interacts with regulatory elements in promoter regions and enhancers. This results in products with various function including the metabolism of fatty acids, amino acids and glucose and is also involved in liver differentiation and development (Ogata et al, 2012. Stoffel and Duncan, 1997). As HNF4α has no known ligand, it is referred to as an orphan receptor however it is considered the activity of HNF4α is controlled by fatty acyl-coenzyme (CoA) thioesters, which can function as both agonists and antagonists and by protein kinase A-mediated phosphorylation, suggesting that HNF4α plays a role in metabolism homeostasis (Hayhurst et al, 2001).

6.1.2 HNF4α and its role in diabetes

HNF4α has been linked to a form of type 2 diabetes known as maturity onset diabetes of the young (MODY) as the HNF4α gene is located within the type 2 diabetes-linked region on chromosome 20q12-q13.1 (Bagwell et al, 2005). MODY1 is a genetically heterogenous monogenic disorder characterised by early onset, usually being diagnosed during adolescence and is caused by an autosomal dominant mode of inheritance, and impaired glucose-stimulated insulin secretion (Miura et al, 2006). MODY is considered to be very rare, accounting for approximately 2-5% of all diabetes cases (Gardner and Tai, 2012). MODY is known to result from a mutation of 6 different genes, the gene that is of interest in this project is HNF4α resulting in MODY1. Other mutations include; a mutation of the gene encoding glucokinase resulting in MODY2, HNF1α resulting in MODY3, PDX-1/ resulting in MODY4, HNF1β and NeuroD1 resulting in MODY5 and 6 respectively (Gupta et al, 2005). HNF4α contains two promoter regions, the first promoter known as P1 is liver specific and drives the expression of HNF4α 1-6 transcripts (Ellard et al, 2006). Whereas the second promoter P2, is located up-stream of transcription

start site is responsible for the expression of transcripts HNF4α 7-9 (Ellard et al, 2006). Transcripts of the P2 promoter have been detected in insulinoma INS-1 cells and in mouse and human pancreatic islets, leading to the conclusion that the P2 promoter is responsible for HNF4α transcription in the endocrine pancreas (Eeckhoute et al, 2003). Clinical studies have demonstrated that MODY1 is characterised by abnormal glucose-stimulated insulin secretion but the MODY1 individuals show normal insulin sensitivity, suggesting that pancreatic β-cell dysfunction rather than insulin resistance is the primary defect in this disorder resulting from abnormal gene expression (Stoffel and Duncan, 1997. Yamagata et al, 1996).

6.1.3 HNF4 alpha effect on trafficking molecules in the insulin secretory pathway

Insulin secreting β-cells store insulin in membrane-bound granules and it is known that these β-cell granules also contain high concentrations of divalent cations including Ca^{2+}. Ca^{2+} is a crucial intracellular signal in the regulation of insulin secretion from pancreatic β-cells. Secretagogue-initiated insulin secretion is dependent on an influx of Ca^{2+} across the plasma membrane, through L-type voltage dependent Ca^{2+} channels. The calcium-sensing receptor (CaR), is a G-protein coupled receptor that senses extracellular levels of Ca^{2+} and maintains Ca^{2+} homeostasis and is a receptor that is found in both pancreatic α- and β-cells. (Zhuang et al, 2010).

HNF4α is known to directly induce the transcription factor x-box binding protein 1 (XBP1) which controls the development and maintenance in multiple secretory cell lines. Loss of function of XBP1 can have a toxic effect on β-cells during the ER stress response where XBP1 plays a role in the unfolded protein response (UPR). UPR typically follows ER stress, UPR is facilitated by three transmembrane stress sensor protein known as PERK, IRE1, and ATF6. IRE1 cleaves unsliced XBP1 which results in the active spliced form XBP1s. XPB1s is responsible for the ER biogenesis and promotes the activation of ER chaperone genes necessary for the folding and trafficking of secretory proteins (Akiyama et al, 2013). A decrease in XBP1 can result in the decrease in production of the ER chaperone Bip. This can occur with or without ER stress (Kirkpatrick et al, 2011.). Importantly, in HNF4α knockdown/knockout models there is a decrease in XBP1 and subsequently reduced cellular ER networks, including Ca^{2+} signalling. This is significant as glucose stimulated insulin release is dependent on ER Ca^{2+} signalling (Moore et al, 2016).

HNF4α is also involved in the regulation of GLUT2 genes. It has been reported that HNF4α is an essential positive regulator of HNF1α which is necessary for GLUT2 glucose transporter expression and L-type pyruvate kinase gene expression in pancreatic β-cells (Párrizas et al, 2001).

6.1.4 Rab Proteins

Rab proteins belong to the Ras superfamily, of small monomeric GTPases that are located on the cytoplasmic surfaces of certain membrane bound organelles (Chen et al, 2014). Their main function is to facilitate the attachment of vesicles to their target membrane (Xiong et al, 2017), but Rabs have also been associated with other aspects of vesicle transport including vesicle formation, motility and docking (Woodman P, 1998). Rabs continuously cycle between a GTP (Guanosine-5'-Triphosphatate)-bound active form and a GDP-bound inactive form. The GTP-bound form interacts with downstream effector proteins and guides transport vesicles from the donor membrane to the target membrane. At the plasma membrane this occurs with assistance of an anterior SNARE fusion complex, which triggers release of inhibiting factors to convert the active Rab complex to its inactive form (Xiong et al, 2017). The switch between the active and inactive form occurs due to GTP-hydrolysis that is facilitated by GDPase activating protein and the Rab-GDP complex then separates from the vesicle. After the conformational switch the newly inactive Rabs interact with a GDP dissociation inhibitor that has the ability to remove the Rabs from the membrane and support them in the cytosol. To switch back to the GTP-bound form the GDP dissociation inhibitor-Rab complex must be recognised by a guanine nucleotide exchange factor (GEF), that removes the GDP dissociation inhibitor and replaces GDP with GTP (Alverez). In unison with this process several accessory proteins associate with the anterior fusion complex and with ATP enzyme, NSF, which hydrolyses ATP and triggers the fusion of vesicles with their target membranes. Transport vesicles/granules are only able to form when they contain specific Rabs and SNARES (Xiong et al, 2017).

6.1.5 Rab1B role in vesicle transport

Rab1B is located in both the ER and the Golgi compartments in eukaryotic cells and is an essential protein for transport between the ER and Golgi and between different Golgi compartments. As Rab1B is found in 2 different stages of vesicle transport it may play a key role in the assembly and disassembly of machinery found in both vesicle fission and vesicle fusion during the early stages of the secretory pathway (Plunter et al, 1995). The effector proteins of Rab1B are, p115, GM130, Golgin84, MICAL-1,

Iporin, and Giantin. Of these it is known that both p115 and GM130 are essential for ER to Golgi transport (Monetta et al, 2007). Studies have also identified that Rab1B has a role in calcium-sensor receptor trafficking from the endoplasmic reticulum to the Golgi, that regulates receptor cell surface expression and thereby cell signalling responsiveness to extracellular calcium (Zhuang et al, 2010).

6.1.6 Rab2A role in vesicle transport

Rab2A is required in the early stages of the secretory pathway in the ER-Golgi intermediate compartment (ERGIC). The ERGIC is made up of a 53-kDa membrane protein and COPI subunit known as COP-β, a tubular vesicular membrane cluster that connects the ER and Golgi. This is also the site of segregation the anterograde and retrograde paths and therefore important in early secretion (Tisdale et al, 2004).

A mechanism that regulates COPI-mediated anterograde and retrograde transport from the ERGIC is the sorting by Rabs using effector proteins. There are 2 Rabs that associate with ERGIC, the first is Rab1B. As already mentioned Rab1B is involved in membrane tethering in anterograde transport. The other Rab is Rab2A that acts in together with an atypical kinase C and GAPDH in order to stimulate COPI vesicle formation enriched in recycling proteins. GAPDH is an effector protein of RAB2A and also a glycolytic enzyme that is regulated by poly (ADP-ribose) polymerase (PARP)-dependent poly (ADP-ribosylation, although the trafficking doesn't require the glycolytic activity of GAPDH (Sugarwara et al, 2014).

6.1.7 Rab4B role in recycling

Rab4B is a key player in the endocytic recycling. It is associated with early endosomes and recycling endosomes and regulates the recycling of membranes and proteins from these compartments back to the plasma membrane. There are 2 isoforms of Rab4 that are highly homologous; Rab4A and Rab4B which are localised in the same compartments and are believed to have very similar functions (Krawczyk et al, 2007).

6.1.8 Role of Rab10 in GLUT4 trafficking

Rab10 is a regulator of insulin-stimulated GLUT4 translocation to the plasma membrane in adipose cells. GLUT4 is a glucose transporter that plays a key role in maintaining glucose metabolism. In non-

insulin-stimulated conditions GLUT4 is sequestered either in the GLUT4 storage vesicles or in the perinuclear storage compartments. Insulin signalling stimulates the GLUT4 storage vesicle recruitment and fusion with the plasma membrane. Insulin binding to the receptor on cell surface initiates a signalling cascade which results in the phosphorylation of the GTP-ase activating protein known as AS160 and the Rab proteins no longer being repressed in the GDP-bound inactive form. Rab10 is known to be the primary Rab protein in regulating GLUT4 storage vesicle translocation downstream of AS160 (Sadacca et al, 2013).

6.2 Aims

The aim of this chapter is to identify whether exposure of INS-1 cells to GLT for 5 days has a negative effect on HNF4α gene expression. This will show that diet (high glucose and fatty acids) has an inhibitory effect on the gene during the onset of type 2 diabetes, as well as gene mutations which occur in MODY. Further to this it will be of interest whether the effect of GLT on HNF4α has an effect on insulin secretion via the dysregulation of Rab genes.

6.3 Results

6.3.1 Effect of glucolipotoxicity on HNF4 alpha gene expression

MetaCore™ was used to build an unbiased network to identify proteins that are affected by glucolipotoxicity. The MetaCore™ network identified that HNF4α is down regulated in response to GLT and is shown by the blue circle. The grey arrows leading to the proteins identify that there is a directional association between HNF4α the other detected genes.

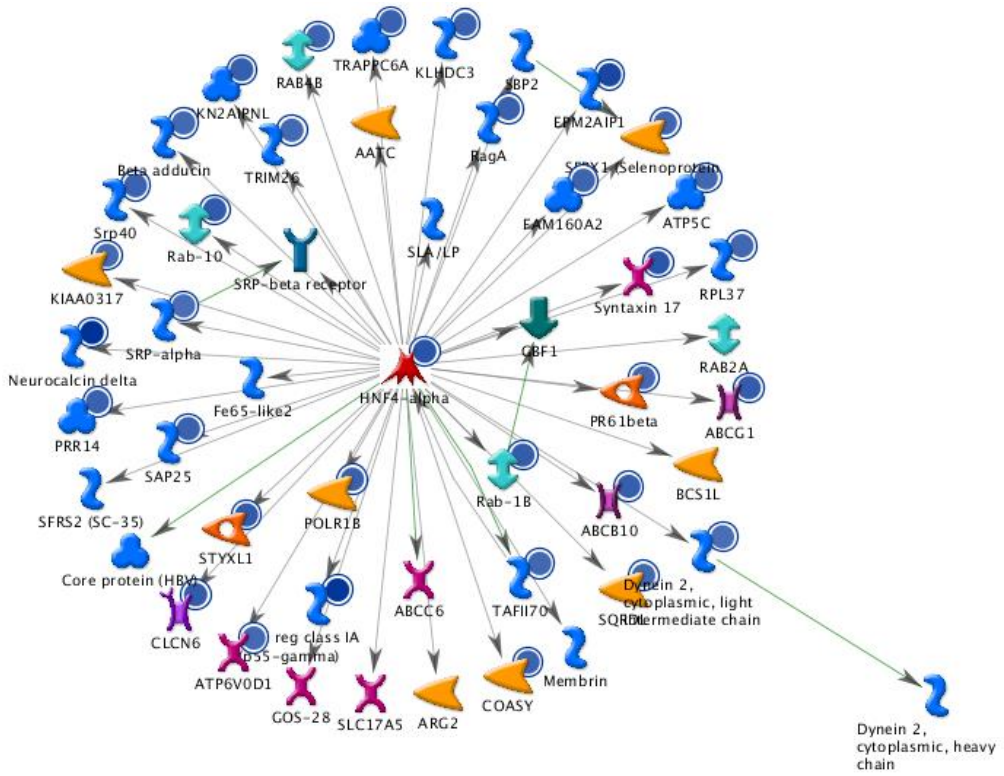

Figure 6.2 MetaCore™ network*. An unbiased interaction network was developed that identified genes affected by glucolipotoxicity. The map shows that genes are negatively regulated by GLT by the blue circle. The main 'hub' shown was HNF4α which is one of the highest ranked down regulated networks. The arrows between hubs are to demonstrate the directional association.*

HNF4α is a transcription factor which is elicits its effects primarily in the liver but is also found in the kidney and pancreatic β-cells. The MetaCore™ unbiased network analysis of the effects of GLT, identified HNF4α as a 'top hit' for down regulation (Fig.6.2), it was then of interest as to whether HNF4α was affected by GLT in pancreatic β-cells.

The INS-1 cells were incubated ± GLT media for 5 days and total RNA was extracted. The levels of HNF4α mRNA was measured using qPCR and HNF4α specific primers. The data showed that HNF4α is significantly down regulated when INS-1 cells are exposed to GLT. The results showed an average 33.3% down regulation of HNF4a ($p=0.0099$).

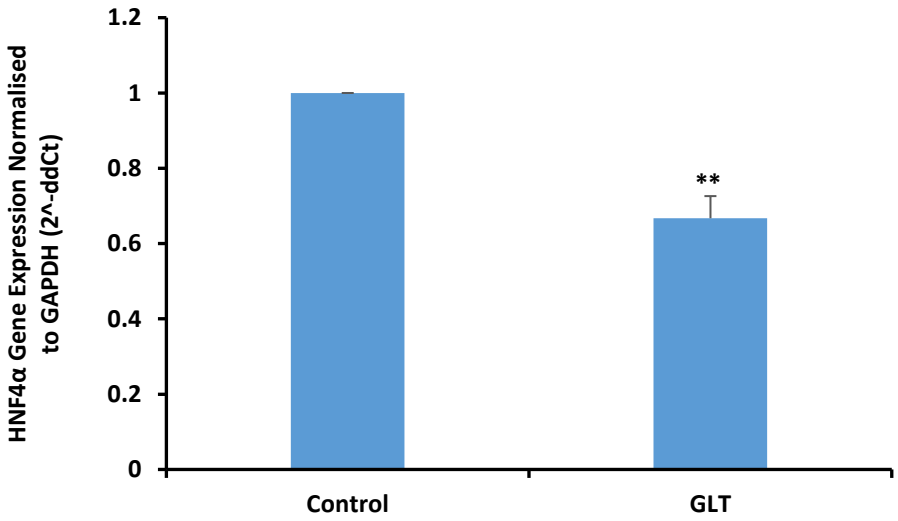

Figure 6.3 Effect of GLT on HNF4α gene expression. *INS-1 cells were incubated ±GLT for 5-days. RNA was extracted (Qiagen, Hilden, Germany), reverse transcribed and analysed using qPCR with HNF4α specific antibodies. Data shown is the mean ± SEM of three independent experiments*

6.2.2 Effect of HNF4α knockdown on Rab expression and insulin secretion

In order to observe any functional effects of HNF4α, it was transiently knocked down using siRNA. Following the knock down using siRNA, cells were incubated ± GLT for 72 hours prior to being lysed using RIPA buffer. Proteins were then separated using a 10% SDS-Page gel, transferred onto a nitrocellulose membrane and immunoblotted with anti-HNF4α monoclonal primary antibody (Abcam, Cambridge, UK) and a secondary mouse antibody. Using analysis of variance it was found there was significant differences between the sample means (p=0.0032).The data indicates that in the RPMI-1640 untreated cells a knock down of 44% compared to the scrambled sequence and 43% compared to untreated control was achieved and 43.58% knock down compared to the scrambled sequence and 45.8% compared to the GLT treated control was achieved.

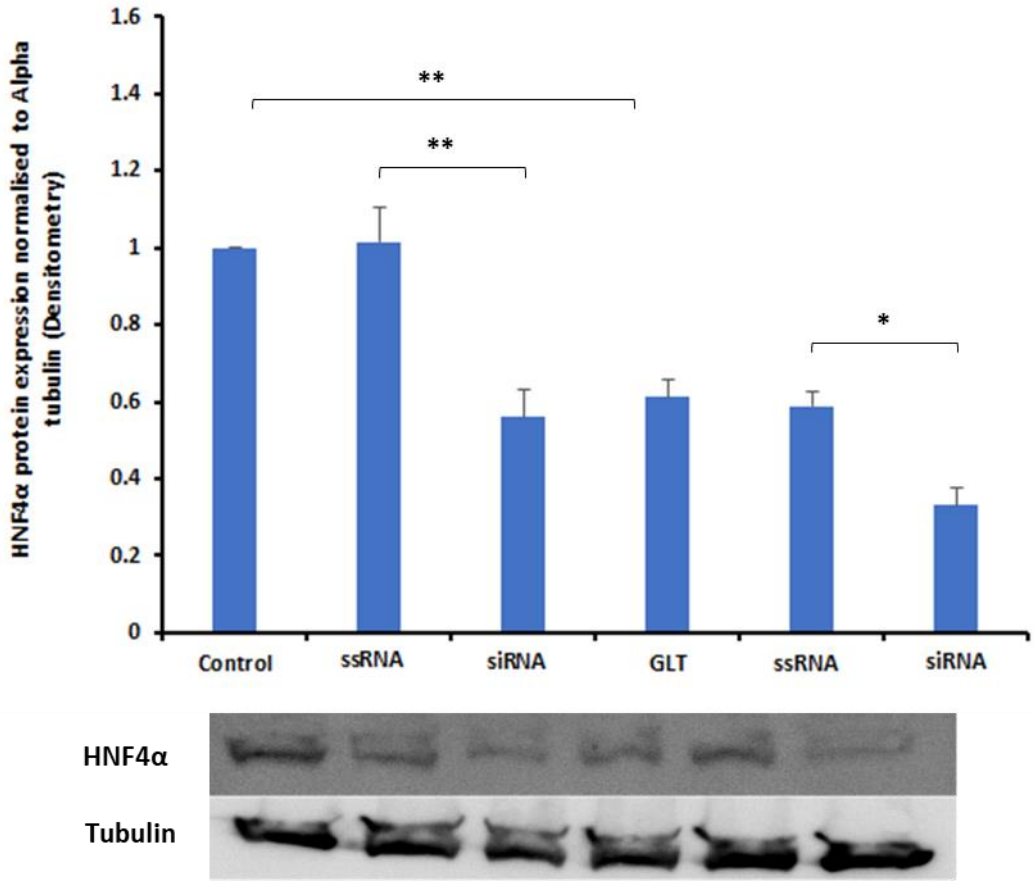

Figure 6.4 Transient knock down of HNF4α. *HNF4α was knocked down using siRNA. Cells were incubated ± HNF4α siRNA, ± ssRNA for 24 hours at 37°C, 5% CO_2. Cells were then incubated ± GLT for 72 hours 24 hours at 37°C, 5% CO_2. Subsequently, cells were lysed and pelleted. This pellet was then halved, for use in protein and mRNA analysis. For protein analysis, protein was quantified using BCA assay (ThermoFisher, Waltham, CA,USA). Protein was loaded to a gel and separated using SDS-PAGE. The protein was then transferred to a nitrocellulose and immunoblotted using HNF4α specific antibodies.*

To identify whether the knock down of HNF4α has any implications on trafficking, the Rab proteins identified by the MetaCore™ network were selected and their gene expression was examined using RT-qPCR. HNF4α was transiently knocked down using siRNA for 24 hours and subsequently incubated in GLT media for 72 hours. Total RNA was extracted (Qiagen, Hilden, Germany) and mRNA levels were measured by RT-qPCR using Rab specific primers. The data showed significant analysis of variance and all four Rabs tested were significantly reduced when HNF4a was knocked down compared to the scrambled sequence treated cells (ssRNA) and all Rabs apart from Rab4B were also significantly reduced in GLT conditions when compared to the control.

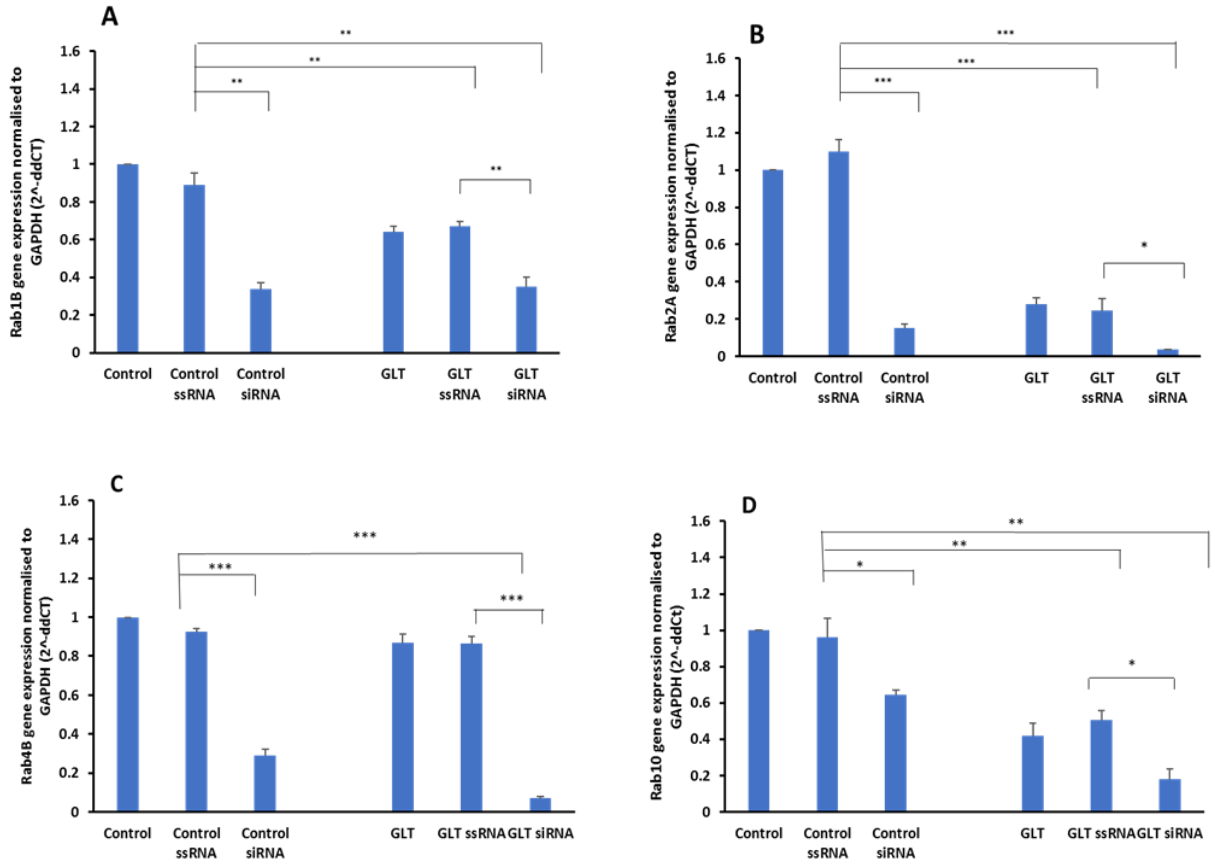

Figure 6.5 Effect of HNF4α knock down on Rab gene expression. *INS-1 cells were transfected ± ssRNA/ HNF4α siRNA and incubated ±GLT for 72 hours prior to RNA extraction, cDNA synthesis and qPCR using Rab specific primers. The extent of HNF4α knock down is shown in figure 6.4.*

Rab1B was reduced by 67% following HNF4a knock down in control cells by comparison to the control ssRNA treated cells (p= 0.0087) and was decreased by 63% following HNF4α knockdown compared to the untreated control (p=0.0076) (Data not shown in Fig.6.5 A). When incubated in GLT conditions the expression of Rab10 was reduced 47.77% compared to GLT ssRNA treated cells (p=0.0065) and was reduced by 45.32% compared to the GLT treated control cells (p=0.0053). It was also observed that Rab10 was decreased when exposed to GLT conditions by comparison to untreated cells by 64.97% (p=0.0034) (Data not shown in Fig.6.5A).

Rab2B was also down regulated following the knockdown of HNF4α by 86.16% in control condition compared to the control ssRNA (p=0.0003) and was down regulated by 84.8% following HNF4α knock down compared to the untreated control (p=0.000006) (significance data not shown in Fig.6.5 B).

Rab2B was also down regulated following HNF4α knock down in GLT conditions, Rab2B was down regulated by 85.73% compared to the GLT ssRNA treated cells (p=0.0264) and was down regulated by 87.5% compared to the GLT control (p=0.004) (significance data not shown in Fig6.5B). There is also a significant reduction in Rab2B expression resulting from GLT conditions, Rab2 expression is decreased by 71.9% following a 5-day incubation in GLT media (p=0.00007) (significance data not shown in Fig.6.5B).

Following HNF4α knock down Rab4B showed a reduction of 68.89% (p=0.00028) when compared to the ssRNA treated cells and 71.18% when compared to RPMI-1640 control (p=0.000068) (significance data not shown in Figure 6.5C). In GLT conditions, following HNF4α knock down Rab4B was reduced 88.55% ±3.49% compared to GLT ssRNA treated cells (p=0.000043) and Rab4B was reduced 88.63% ±3.69% compared to the GLT treated cells (p=0.00012) (significance data not shown in Figure.6.5C). The results also demonstrated that exposure to GLT conditions independent of HNF4α knock down also reduce Rab expression however, GLT inhibited Rab4B by 12.94% compared to control, which was not statistically significant (p=0.069).

Subsequent to HNF4α knock down rab10 was inhibited 32.66% ±1.5% when compared to the ssRNA treated control (p=0.049) and was inhibited by 35.38% compared to the untreated control (p=0.041) (significance data not shown in Figure.6.5 D). In GLT conditions following the knockdown of HNF4α, Rab10 expression was decreased by 64.39% compared to the GLT ssRNA treated cells (p=0.487) and 57.07% compared to the GLT control (p=0.044) (significance data not shown in Fig.6.5D).

As Rabs are involved in vesicle transport and the fact that the Rabs are down regulated when HNF4a expression is decreased, the next step was to identify whether the lack of HNF4a had an impact on insulin secretion. INS-1 cells underwent a transient knockdown of HNF4α using ssRNA/siRNA for 24 hours followed by 72 hours incubation ±GLT. The cells were then subjected to an insulin secretion assay (Mercodia, Uppsala, Sweden). The results showed that reduction in HNF4α does influence insulin secretion. The results showed that following transient HNF4α siRNA knockdown insulin secretion was significantly reduced. In the RPMI-1640 treated cells insulin secretion was decreased 44.6% compared to the ssRNA control cells (p=0.046) and insulin secretion decreased by 47.8% compared to the untreated control (p=0.036). The same pattern was observed in the GLT treated cells where insulin secretion was down regulated 40.9% in GLT-incubated and HNF4α siRNA treated cells compared to the GLT -incubated ssRNA treated cells (p=0.012) and was down regulated 49.1% compared to the GLT incubated control cells (p=0.0066) (significance data not shown in Fig.6.6).

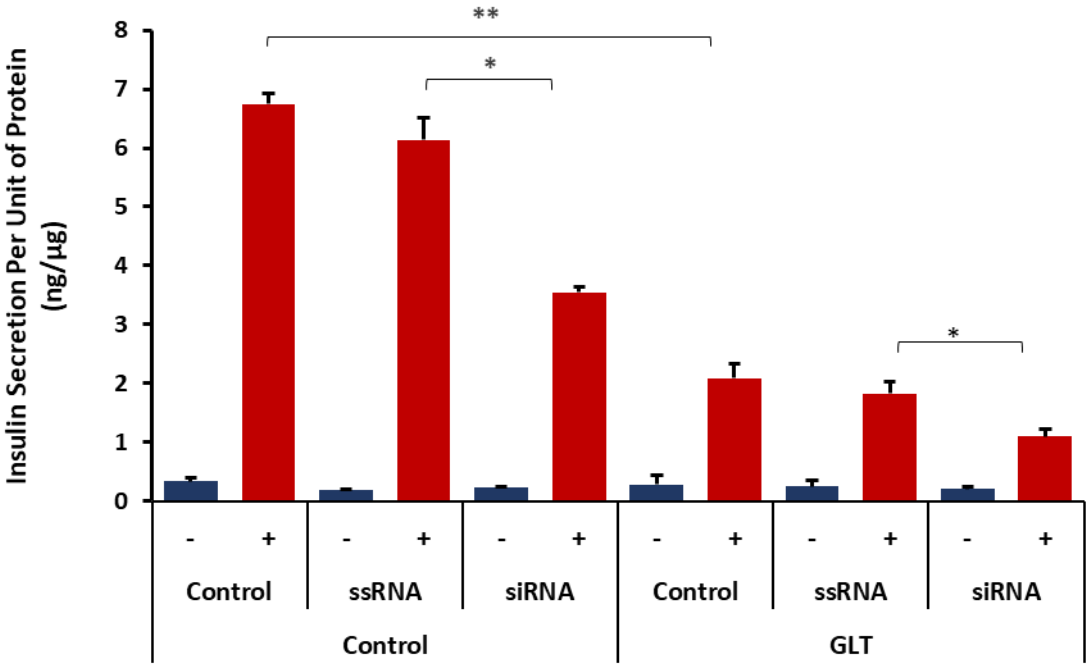

Figure 6.6 Effect of HNF4α knock down on insulin secretion. *INS-1 cells were transiently transfected ± HNF4α siRNA, ± ssRNA for 24 hours at 37°C, 5% CO_2. Cells were then incubated ± GLT for 72 hours at 37°C. Cells were then subjected to secretagogue incubation for one hour prior to insulin secretion analysis using ELISA testing (Mercodia, Uppsala, Sweden). The data shown is the mean ± SEM of three independent experiments.*

In support of the insulin secretion ELISA assay data which demonstrated that insulin secretion was significantly reduced following HNF4a knockdown, RT-qPCR was carried out to identify whether insulin gene expression is also down regulated as a result of HNF-4α knock down. HNF4α was knocked down as described above and treated ±GLT for 72 hours prior to RNA extraction, cDNA synthesis and RT-qPCR with insulin gene specific primers. The results obtained supported that of the insulin secretion ELISA and showed that insulin gene expression is also down regulated. Insulin gene expression was down regulated in the RPMI-1640 control samples following HNF4α knock down by 74.47% compared to the ssRNA treated cells (p=0.0098) and decreased by 70.2% compared to the untreated control cell (p=0.0004) (significance data not shown in Fig.6.7). The GLT treated cells also showed significant reduction in insulin gene expression following HNF4α knock down. Following HNF4α transfection insulin gene expression reduced by 73.39% in GLT compared to the GLT ssRNA treated cells (p=0.0086) and by 75.23% compared to the GLT control cells (p=0.0086) (data not shown in Figure 6.6).

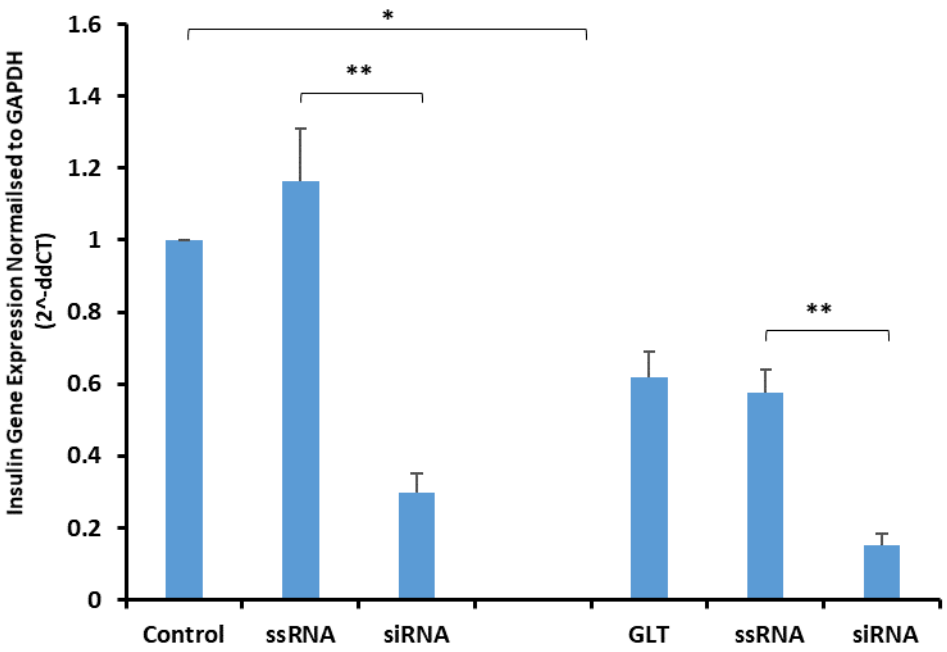

Figure 6.7 Effect of HNF4α knock down on insulin gene expression. *Subsequent to HNF4α knock down using siRNA/ssRNA and 72-hour incubation ±GLT. RNA was extracted from INS-1 (Qiagen, Hilden Germany), reverse transcribed to generate cDNA (ThermoFisher, Waltham, CA, USA) and analysed using qPCR with specific insulin primers. The data shown is the mean + SEM of three independent experiments.*

6.2.3 Effect of glucolipotoxicity on HNF1α expression

Hepatic nuclear receptor 1 alpha (HNF1α) is another protein that is associated with sub type of type 2 diabetes and is considered to be regulated by the binding of HNF4α. To identify whether HNF1α was affected by glucolipotoxic conditions, INS-1 cells were incubated ±GLT media for media for 5 days prior to RT-qPCR. The results identified that, similar to HNF4α, HNF1α was also significantly down regulated by 65.9% (P=0.000924).

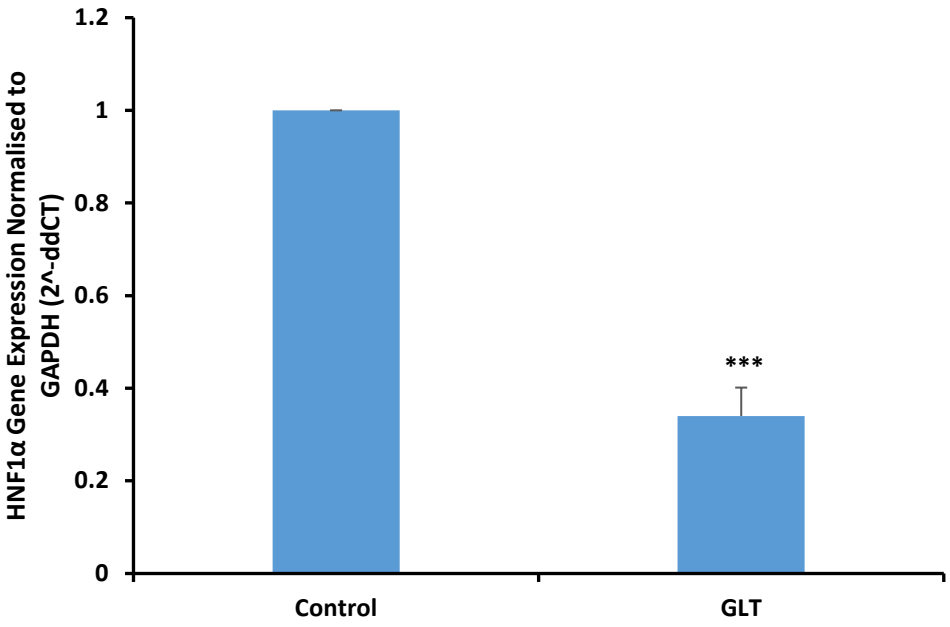

Figure 6.8 Effect of GLT on HNF1α gene expression. *Ins-1 cells were incubated for 5 days ± GLT prior to RNA extraction (Qiagen, Hilden Germany), cDNA synthesis (ThermoFisher, Waltham, CA, USA) and qPCR analysis using HNF1α specific primers. Results shown are the mean + SEM of three independent experiments.*

6.3.4 Effect of HNF4α knock down on HNF1α gene expression

To identify whether the expression of HNF1α genes is reliant upon the presence of HNF4α, the gene expression of HNF1α was measured after HNF4α siRNA knock down. The results demonstrated that when HNF4α is knocked down, the expression of HNF1α is reduced. The reduction in HNF1α gene expression following HNF4α knockdown is significant in both control and GLT treated cells. In the control cells following the 45% knockdown of HNF4α there is a resulting 87.0% reduction in HNF1α gene expression ($p=0.003$). The reduction in HNF1α gene expression is also significant in the GLT treated cells where a 42% knock down of HNF4α was achieved has resulted in a 60% reduction in HNF1α gene expression.

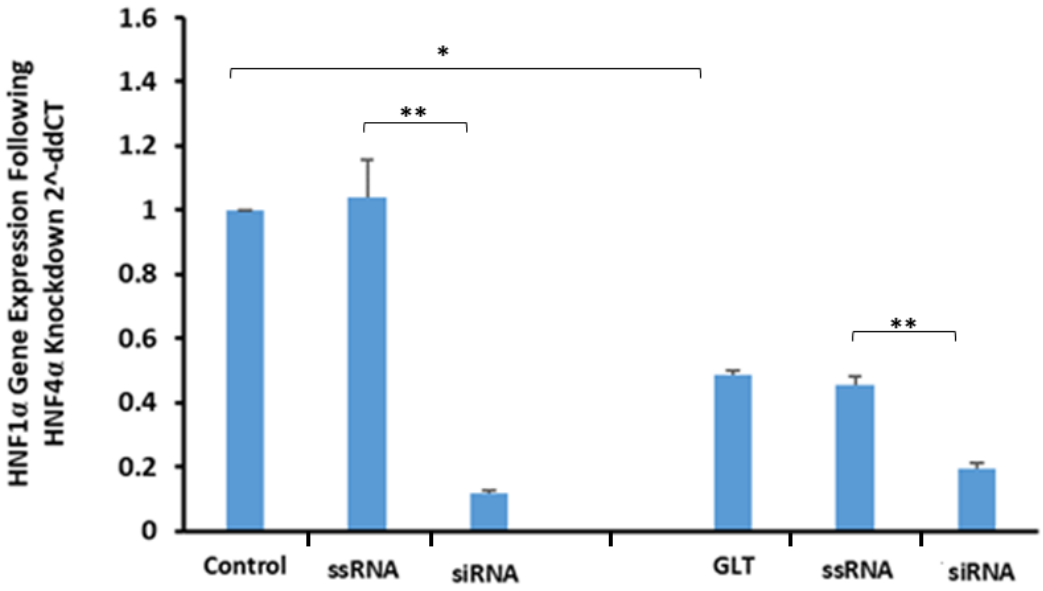

Figure 6.9 Effect of HNF4α knock down on HNF1α gene expression. *INS-1 cells were transiently transfected ± ssRNA/ HNF4α siRNA for 24 hours and incubated ±GLT for 72 hours prior to RNA extraction (Qiagen, Hilden, Germany), cDNA synthesis (ThermoFisher, Waltham, CA, USA) and RT-qPCR with HNF1α specific primers. Results are shown as mean + SEM of three independent experiments.*

6.4 Discussion

Hepatocyte nuclear factor 4 alpha (HNF4α) (NR2A2) is a conserved member of the steroid and thyroid superfamily of transcription factors that is mostly associated with mutations resulting in maturity-onset diabetes of the young (MODY). It is known that HNF4α mutates in the MODY diabetes subtype, but the results of this project build upon this knowledge by demonstrating that exposure of the rat pancreatic INS-1 cell to glucolipotoxic conditions lead to a significant 33.3% reduction in HNF4α gene expression (Fig.6.3), suggesting that HNF4α may be involved in the onset of type 2 diabetes, as MODY is only associated with increased birth weight and not increased glucose or free fatty acid levels, as seen in type 2 diabetes (Gardener and Tia, 2012). The MetaCore™ network (Fig.6.2) that predicted a negative association between GLT and HNF4α was correct. This finding suggests that the expression of HNF4α is disrupted during the high glucose and high fat environment that is found during the onset of type 2 diabetes and that HNF4α may be a gene involved in maintaining normal glucose homeostasis. Data published by Nikolaidou-Neokosmidou et al, (2006) touched upon the inhibition of HNF4α by NF-κB in liver cells. The research of Nikolaidou-Neokosmidou et al (2006) found that the activation of the

NF-κB subunit p65 is necessary for the inhibition of HNF4α. Thereby suggesting the reason for reduced HNF4α in GLT conditions could be due to GLT-induced ER stress. It has been shown earlier in this thesis (chapter 3) that GLT induces inflammation and resulting cell damage, and NF-κB activation is dependent on CD40, which is up-regulated in GLT conditions. In addition, according to Bagnati et al, ER stress is likely to be a consequence of increased islet inflammation.

A network was generated using MetaCore™ which identifies biological molecular interactions. In the network generated for this project, it identified that HNF4α is down regulated following exposure to GLT, which has been positively identified above (Fig.6.2), it also identified that there was an association between HNF4α and other proteins including Rab-GTPases. The network identified that Rab1B, 4B and 10 were also down regulated in GLT but didn't identify any directional change for Rab2A. Rab proteins serve as vesicle trafficking molecules with upstream regulators and downstream effectors, coupled with GTP-binding and hydrolysis they are involved ubiquitously throughout vesicle transport (Xiong et al, 2017). The results presented here demonstrated an association between HNF4α and the expression of Rab genes. The MetaCore™ network identified a negative interaction between HNF4α in GLT conditions and Rab expression. This was confirmed following HNF4α knock down, that resulted in a reduction of Rabs 1A, 2B, 4B and 10. These Rab genes are also decreased when the INS-1 cells are exposed the glucolipotoxic conditions, as suggested by the MetaCore™ network and is complementary to the changes in insulin secretion following GLT exposure for 5 days. This indicates that HNF4α plays a pivotal role in the expression of Rab genes as indicated in the MetaCore™ network in Fig.6.2.

There has been no reported relationship between HNF4a and Rab activity in the literature so far, but this finding builds upon published data that found Rab2A knockdown inhibits glucose stimulated insulin secretion in min-6 cells (Sugarwara et al, 2014). The study found that glucose-stimulated insulin secretion that was induced by elevated glucose levels of 25mM was inhibited by the knockdown of Rab2A. This would be expected from both Rab1B and Rab2A as they are both involved in trafficking from the ERGIC to the Golgi. However, the knockdown resulted in a 90% decrease in Rab2A but only lead to a moderate decrease in insulin secretion (Sugarwara et al, 2014). This suggests that glucose stimulated insulin secretion is only partially dependent on the amount of preproinsulin newly transported from the ERGIC to the Golgi but is also reliant on the insulin granules stored post-Golgi which are not transported by Rab2A.

Data presented here shows for the first time an association between HNF4α, Rab proteins and insulin secretion. Rab2A was the most effected by knock down of HNF4α with an observed reduction of 86.16% in control and 84.8% reduction in GLT treated INS-1 cells (Fig. 6.5B). The reported results of Sugarwara

et al is consistent with data found in this project, however, the inhibition of Rab2A here was a consequence of HNF4α knock down which lead to a decrease in insulin secretion. Therefore, Rab2A clearly plays a role in insulin secretion down stream of HNF4α.

Rab1B has also been reported to plays a role in insulin secretion by aiding in the conversion proinsulin to insulin prior to its secretion via interacting with Golgi membrane protein known as golgin-84. A study conducted by Liu et al found that in INS-1E cells there was a reduction in conversion of proinsulin to insulin following Rab1b knockdown (Liu et al, 2016). From the results in this project it has been determined that Rab1B is regulated downstream of HNF4α.

The majority of literature for both Rab4B and Rab10 expression focuses on skeletal muscle, adipocytes, and cardiomyocytes, and their involvement in insulin-stimulated trafficking of GLUT4 rather than in β-cell insulin secretion. Rab4b is reportedly found in both early endosomes and in the GLUT4 sequestration compartment, which could therefore mean that it is involved in trafficking between the two. A study conducted by Kaddai et al, identified that following the down regulation of Rab4B in adipose tissue there is a negative alteration in GLUT4 translocation and an increase in glucose uptake.

The research of Chen et al found that the role of rab10 predominately follows insulin secretion and is involved in the trafficking of GLUT4 storage vesicles, they found that following Rab10 knockdown there was a significant reduction in insulin-stimulated GLUT4 translocation to the plasma membrane (Chen et al, 2013). However, the data obtained in this research project identifies that Rab10 is present in pancreatic β-cells and is regulated to a certain extent by HNF4α. Evidence for this is shown in Figure.6.5D where rab10 is significantly reduced following the knockout of HNF4α in control and GLT conditions. A reason for Rab10 reduction following the decrease in HNF4α could be because it is up-regulated following insulin secretion, rather than playing a role in insulin trafficking prior to its secretion. This is supportive of previous work that identified HNF4α plays a pivotal role in glucose stimulated insulin secretion.

Expanding on the finding in Figure 6.3 that showed HNF4α is decreased in GLT conditions, it was observed that reduction of HNF4α resulted in a significant decreased in insulin secretion and insulin gene expression in both control and glucolipotoxic conditions. This is a significant finding as reduced insulin secretion in response to elevated glucose and fatty acids is a characteristic of type 2 diabetes, thereby suggesting that HNF4α has an important role in β-cells and the evidence that HNF4α regulates Rab expression suggests a novel role for HNF4α in ER trafficking. Despite the reduction in HNF4α in this study being GLT-induced, which suggests a link to type 2 diabetes, it has been previously reported

that HNF4α MODY is also linked to insulin secretion. Clinical studies have demonstrated reduced GSIS in patients with pre-diabetes of HNF4α MODY, suggesting that β-cell dysfunction is the primary defect in the disorder (Arya et al, 2014). The reason for the decrease in insulin gene expression and insulin secretion resulting from reduced HNF4α could be ER stress. Early stage insulin biosynthesis occurs in ER (Harding and Ron, 2002), which could be disrupted by GLT-induced reduction of HNF4α, which lies up-stream of ER-Golgi trafficking Rabs.

Hepatic nuclear factor alpha (HNF1α) is most commonly associated with maturity onset diabetes of the young type 3 (MODY3). MODY3 is caused by heterozygous mutations in the gene encoding homeodomain-containing transcription factor HNF1α. As can be seen in Figure.6.8 there is a down regulation of the HNF1α gene in response to 5-day GLT treatment by an average of 65.9%, which is vastly more than the reduction of HNF4α in the same conditions. This identifies that HNF1α is also affected during the onset of type 2 diabetes where elevated glucose levels and circulating fatty acids are found and it is more strongly down regulated than HNF4α. The next step of the investigation was to identify whether there was a link between the down regulation of HNF4α and the gene expression levels of HNF1α.

Hepatic nuclear receptor 1 alpha (HNF1α) which contains a homodimer is highly expressed in the liver but is also expressed in the kidney, intestines and the pancreatic islets (Uchizono et al, 2009) Like HNF4α, HNF1α also belongs to the steroid/thyroid hormone receptor superfamily. There is evidence to suggest that both of these transcription factors work together in a transcription factor network where HNF4α controls the activity of HNF1α (Kyither et al, 2013). In the liver its thought that HNF4α acts upstream of HNF1α and it has been hypothesised that HNF4α increases mRNA levels indirectly by increasing HNF1α levels. The results shown in Figure.6.9 identifies that expression HNF1α is at least partially reliant on HNF4α expression. This is clear based on the 64% down regulation of HNF4α using siRNA transfection resulting in the subsequent 87% down regulation in HNF1α expression in RPMI-1640 control conditions and a 43.4% knock down of HNF4α resulted in a 60% reduction in HNF1α in GLT conditions. The results of this project build on existing knowledge by identifying that HNF1α is also significantly decreased in rat pancreatic beta cells when exposed to high fatty acids and high glucose, suggesting that this protein is affected via HNF4α during the onset of type 2 diabetes and not only mutated resulting in MODY3, a subtype of type 2 diabetes. This finding is supported by a study that found HNF4α controls the transcriptional activity of HNF1α in HeLa cell with cooperation with cofactor P300 (Eeckhoute et al, 2004). This supports the idea that HNF4α only partially controls HNF1α transcription, as in the present investigation HNF1α was down regulated to a larger extend than HNF4α. Other studies have found supporting evidence that when HNF1α is disrupted there is a

reduction in insulin secretion, a recent study found that by replacing the first axon of HNF1α with a β-galactosidase coding sequence and a neomycin expression cassette there were significant alterations to both glucose- stimulated and amino acid stimulated insulin secretion. Therefore, these finding and reports from other research groups place HNF1α down stream of HNF4α.

6.5 Conclusion

The results of this project have determined that high glucose and high fats are able to down regulate HNF4α expression which leads to impaired insulin secretion. These results suggest that HNF4α is negatively affected during the onset of type 2 diabetes and this has repercussions on its role in maintaining normal β-cell function and glucose homeostasis. The MetaCore™ network identified that HNF4α is an upstream transcription factor of various Rab-GTPases as their expression was decreased following HNF4α knock down. This indicates that they are involved in regulating aspects of the insulin secretory pathway. Muira et al, (2006), reported that the role for HNF4a in pancreatic β-cells is unclear, however the result gathered in this chapter suggest that HNF4a regulates Rabs involved in insulin gene expression and insulin secretion which is disrupted by GLT, possibly via ER stress.

Chapter 7

Role of Glucolipotoxicity in Mitochondrial Dysfunction and Histone Acetylation

7.0 CHAPTER 7: Role of Glucolipotoxicity in Mitochondrial Dysfunction and Histone Acetylation

7.1 Introduction

The previous chapters have examined how GLT alters gene and protein expression, which may have the potential to negatively affect β-cell function, however this chapter observes how exposure of INS-1 cells to GLT conditions may affect metabolism and result in epigenetic changes, by disrupting the citric acid cycle and increasing histone acetylation.

7.1.1 The importance of the citric acid cycle

The citric acid cycle (also known as the Krebs cycle and TCA cycle) is the most important metabolic pathway for generating energy (Akram M, 2014). The citric acid cycle occurs in the mitochondria, which have important roles in energy metabolism. The function of the mitochondria is to change organic material into ATP energy (Nazaret et al, 2009). The citric acid cycle is made up of 8 steps. In brief, the first step is the formation of citrate which occurs due to the condensation of acetyl-CoA with oxaloacetate where the methyl carbon of the acetyl unit is connected to the carbonyl group of oxalacetate, a process that is catalysed by citrate synthase. During this reaction Citroyl-CoA is formed transiently and rapidly undergoes hydrolysis to yield free CoA and citrate. The second step is the formation of isocitrate via cis-Aconitate, in the step an enzyme known as aconitase catalyses citrate to isocitrate, which is a reversible step. This is done via the formation of the tricarboxylic acid, cis-aconitate. The third step involves oxidative decarboxylation of isocitrate to α-ketoglutarate and CO_2, a reaction catalysed by isocitrate dehydrogenase. The fourth step involves oxidative decarboxylation again, this time of α-ketoglutarate which is converted to succinyl-CoA and oxygen by the α-ketoglutarate dehydrogenase complex. The next step is the conversion of succinyl-CoA to succinate catalysed by succinyl-CoA synthetase. In step six the succinate formed from succinyl-CoA is oxidised to form fumarate by succinate dehydrogenase which is a flavoprotein and is the only enzyme in the citric acid cycle that is membrane-bound. In step seven the enzyme fumarase catalyses reversible hydration of fumarate to L-malate. In the final step L-malate is oxidised to oxaloacetate, by NAD-linked L-malate dehydrogenase (Berg et al, 2005).

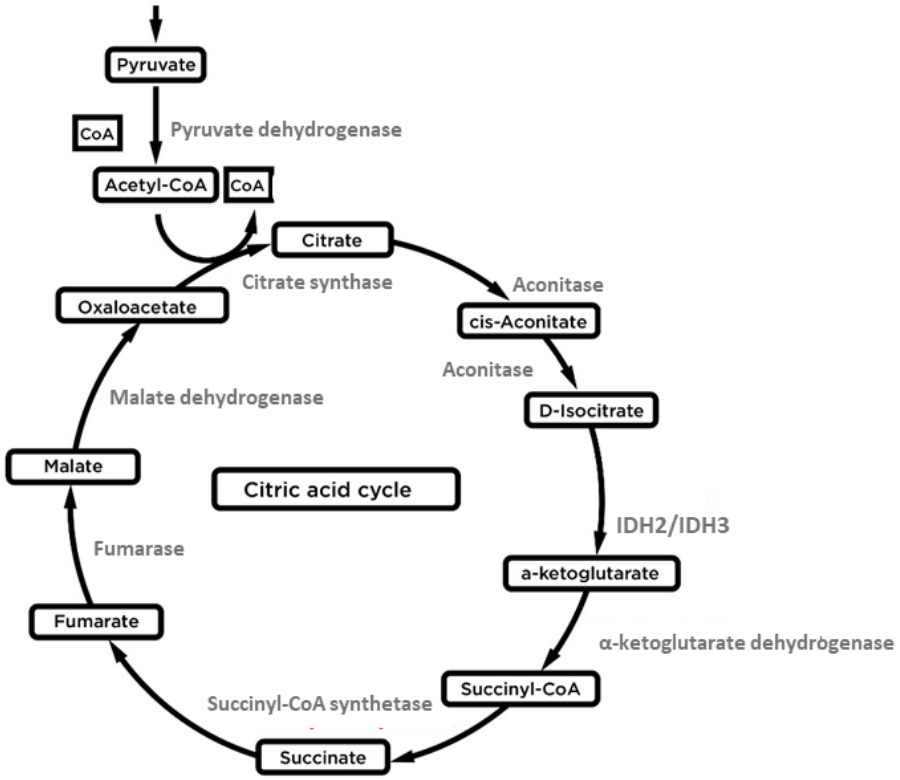

Figure 7.1 Citric acid cycle. *Schematic image of basic events that occur during the mitochondrial citric acid cycle. Adapted from Kruse et al, 2017.*

Pathways that are fed from metabolites branching from the citric acid cycle include fatty acid and cholesterol synthesis and histone acetylation. A molecule involved in both fatty acid and cholesterol synthesis and histone acetylation is acetyl-CoA. In the mitochondria oxaloacetate generates citrate, which is then transported to the cytosol and broken down the acetyl-CoA via ATP-citrate lyase (ACLY) (Chen et al, 2017).

The breakdown of citrate to acetyl-CoA, catalysed by ACLY, triggers fatty acid and cholesterol synthesis. The synthesis of both fatty acids and cholesterol requires acetyl-CoA and NADPH, and both are formed in processes that require the reductive polymerisation of acetyl-CoA and they are also both essential structural components of cell membranes (Gibbons, 2003). The overproduction of both fatty acids and cholesterol can be toxic, which means the levels of these lipids present in cells needs to be controlled. This is achieved by a feedback regulatory system that moderates the transcription of lipogenic enzyme

genes. These moderators belong to a family of transcription factors known as regulatory element-binding proteins (SREBPs) (Ye and DeBose-Boy. 2011).

The difference in the structure of fatty acids and cholesterol is the result of the different pathways used in the reductive polymerisation of acetyl-CoA. During fatty acid synthesis acetyl-CoA is converted to malonyl-CoA, catalysed by acetyl-CoA carboxylase, and results in straight chain products (Somesh et al., 2013. Gibbons GF, 2003). The pathway involved in cholesterol synthesis generates branched chain intermediates known as HMG-CoA, which is then reduced by NAPDH resulting in mevalonic acid. Mevalonic acid is the precursor of the isoprene unit, isopentyl pyrophosphate (Gibbons GF, 2003). The isoprene units are then condensed to form a 30-carbon squalene molecule. Squalene is a precursor for all steroids and in order to generate cholesterol, squalene must be transformed to lanosterol and finally to cholesterol (Cerqueira et al, 2016).

The DNA of eukaryotes is assembled into nucleosomes, where 146 base pairs of DNA are wrapped 1.65 times around a histone octamer. There are four core histones, H2A, H2B, H3 and H4 and the octamer is made up of two H2A–H2B dimers and one H3–H4 tetramer and this complex forms the repeating unit of chromatin (Gardener et al, 2011). All the core histones have a lysine-rich N-termini which is positively charged and binds with negatively charged DNA (Guo et al, 2006). Histones are present throughout the entirety of eukaryotic DNA and their function is to prevent access to genetic information to prevent unwanted transcription or replication (Guo et al, 2006). Histone acetylation is a modification that can occur on any of the core histones and is important for maintaining normal cell cycle progression, gene expression and DNA repair. The enzyme family primarily responsible for catalysing histone acetylation are the histone acetyl transferases (HATs) which use acetyl-CoA as an acetylation donor (Galdieri and Vancura, 2012). As with fatty acid and cholesterol synthesis the level of acetyl-CoA available is dependent upon ACYL, which has been shown to regulate histone acetylation and influence gene expression in a wide range of mammalian cell types (Carrer et al, 2017). Acetylation of histones occurs on specific lysine residues at the N-terminus which reduces the affinity of DNA and histones by reducing the positive charge for each acetyl group added the overall positive charge is reduced by 1 (Turner BM, 1991). The decrease in affinity of histone and DNA means that transcription factors can easily access the promoter region and alter gene transcription, in addition to this, acetylated histones are known to form recognition sites for bromodomain-containing proteins which further enhances gene transcription as bromodomain-containing protein are found in transcriptional co-regulators (Peleg et al, 2016). The rate of histone acetylation is dependent on intermediary metabolism for supplying acetyl-CoA to the nuclear cytosolic compartment. In mammalian cells the

major source of acetyl-CoA used for histone acetylation is ATP-citrate lyase (Galdieri and Vancura, 2012).

Post translational modifications have previously been linked to diabetes, where studies have demonstrated that diabetic stimuli such as high glucose can alter levels of key histone modifications including both acetylation and methylation.

7.2 Aim

The aim of this investigation was to observe whether a high glucose and high fatty acid environment, replicating chronic hyperglycaemia and lipidaemia that is found in type 2 diabetes could alter the metabolic pathway by disrupting the citric acid cycle and to identify whether this had an effect on gene transcription via histone acetylation. The reason for this investigation is based on the fact that histone acetyl transferases use acetyl-CoA as an acetyl-unit donor which links mitochondrial metabolism to histone acetylation and gene expression (Takahashi et al, 2006).

7.3 Results

Mitochondrial citrate can be transported out to the cytoplasm where it can subsequently be used to generate acetyl-CoA which is the donor of an acetyl group in histone acetylation (Wellen et al, 2009) The first step taken in identifying whether the citric acid cycle is affected by glucolipotoxicity was to measure cellular levels of citrate using a citric assay kit (Abcam, Cambridge, UK). The results (Fig. 7.2) demonstrated that there was a significant increase of 3.1-fold in GLT conditions compared to control ($p=0.00027$).

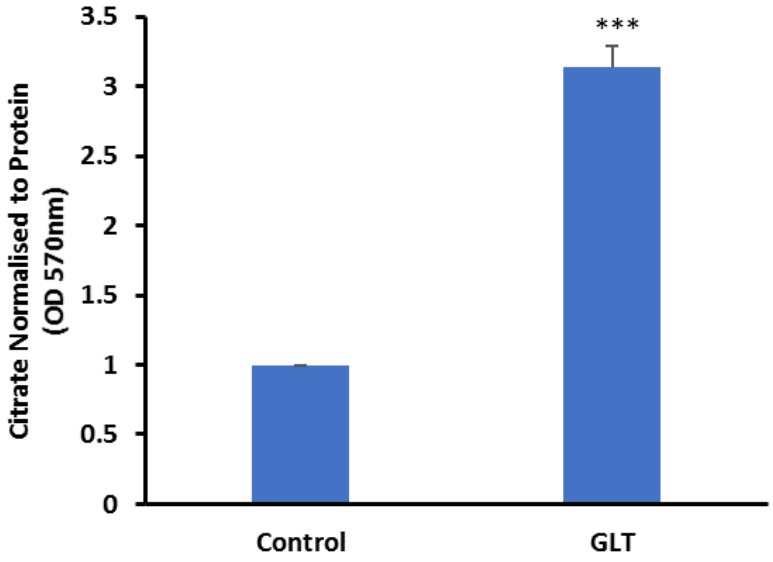

Figure 7.2 Effect of GLT on citrate levels*. Cells were incubated ± GLT for 5 days prior to analysis using citrate assay kit (Abcam, Cambridge, UK). Absorbance was measured at 570nm. Results are expressed as mean ± SEM of three individual experiments.*

The next part of the investigation involved looking at ATP production and whether this was affected by glucolipotoxic conditions. ATP content was observed using a kit supplied by Perkin Elmer, Massachusetts, US. The results showed that following incubation of INS-1 cells ± GLT for 5 -days there was a significant decrease in ATP content by 42.1% (p=0.005).

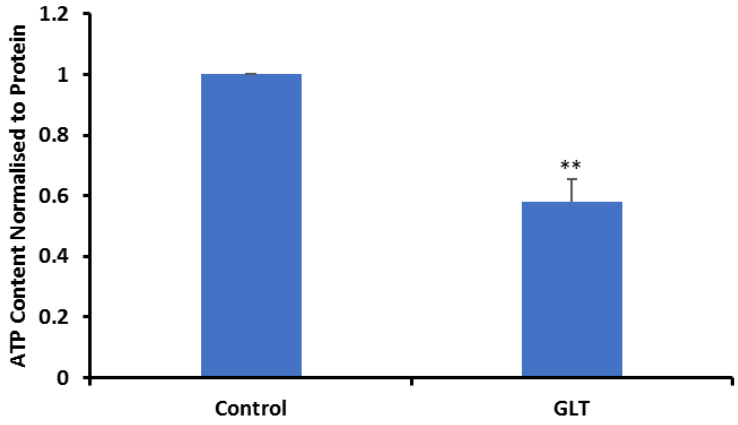

Figure 7.3 Effect of GLT on ATP content*. INS-1 cells were incubated ± GLT for 5 days prior to analysis using ATP assay kit (Perkin Elmer, Waltham, MA, USA). Results are expressed as mean ± SEM of three independent experiments. Analysis following incubation was carried out by Akashdeep Singh.*

After identifying that ATP production is disrupted in glucolipotoxic conditions it was clear that there is a disruption in the citric acid cycle. To identify whether IDH2 is affected by glucolipotoxic conditions, western blot and RT-qPCR assays were conducted following the incubation of INS-1 cells ±GLT media. The results demonstrated that IDH2 is significantly down regulated following cellular exposure to GLT. IDH2 gene expression was decreased by 41.7% (p=0.0074) and IDH2 protein expression was reduced to a lesser extent by 24% (p=0.00014).

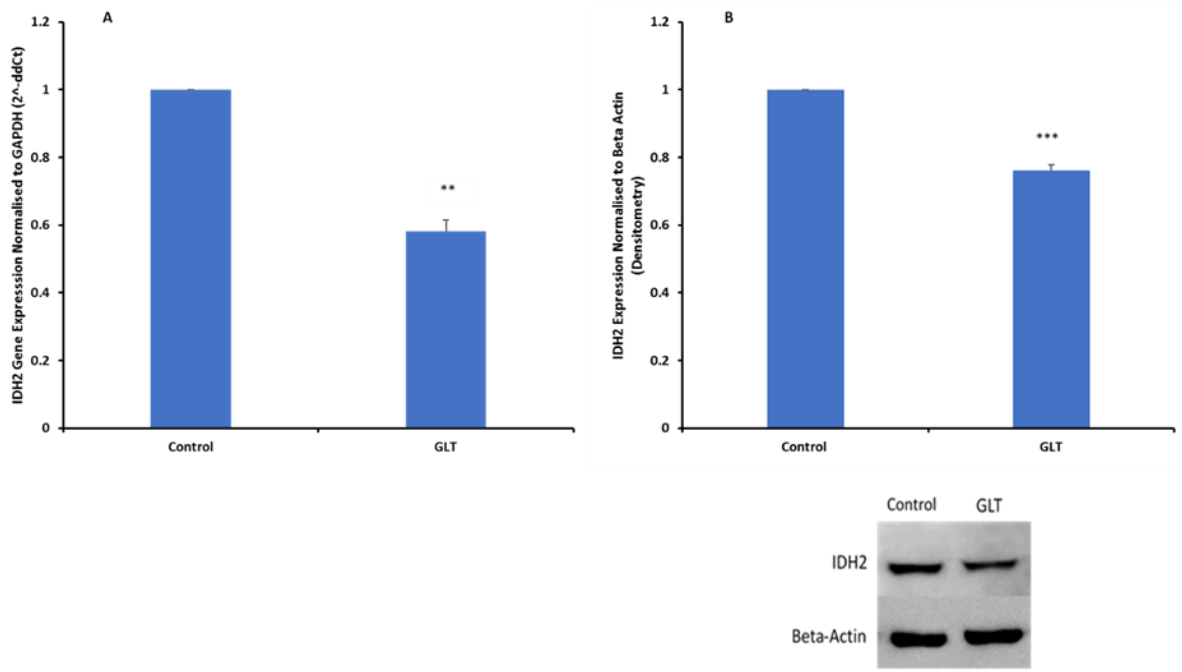

Figure 7.4 Effect of GLT on IDH2 gene and protein expression. *INS-1 cells were incubated ± GLT for 5 days prior to collection using Trypsin EDTA and centrifuged to collect a cell pellet. The pellet was halved and used in either qPCR analysis or western blot technology. For RT-qPCR, total RNA was extracted (Qiagen, Hilden Germany, CDNA transcribed (ThermoFisher, MA, USA) and analysed by RT-qPCR using IDH2 specific primers. Results are shown as ΔΔCt expressed as fold change compared to control. The INS-1 cells collected for western blot was lysed using RIPA buffer to extract protein. Protein was quantified using BCA assay and protein was loaded to 10% acrylamide gel, separated using SDS-PAGE and transferred to a nitrocellulose membrane. Membranes were immunoblotted using IDH2 specific primers. Results shown are mean ± SEM of three independent experiments.*

Following on from the observation that IDH2 was reduced in GLT conditions it was important to observe whether IDH3 was also affected. The results demonstrated that using RT-qPCR following a 5-day incubation ±GLT, the INS-1 cells also showed a significant down regulation in IDH3. RT-qPCR results showed a similar down regulation to that of IDH2 at 36.9% (p=0.0017). Western blot data demonstrates that IDH3 protein expression was decreased by 24.4% (p=0.0009).

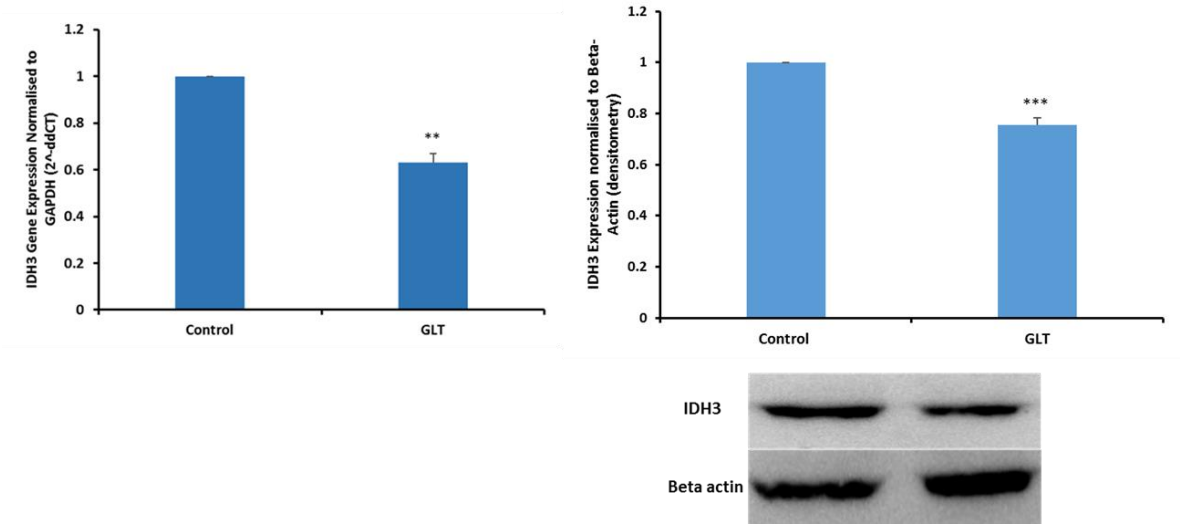

Figure 7.5 Effect of GLT on IDH3 gene and protein expression. *INS-1 cells were incubated ± GLT for 5 days prior to collection using Trypsin EDTA and centrifuged to collect a cell pellet. The pellet was halved and used in either qPCR analysis or western blot technology. For RT-qPCR, total RNA was extracted (Qiagen, Hilden Germany, CDNA transcribed (ThermoFisher, MA, USA) and analysed by RT-qPCR using IDH3 specific primers. Results are shown as ΔΔCt expressed as fold change compared to control. The INS-1 cells collected for western blot was lysed using RIPA buffer to extract protein. Protein was quantified using BCA assay and protein was loaded to 10% acrylamide gel, separated using SDS-PAGE and transferred to a nitrocellulose membrane. Membranes were immunoblotted using IDH3 specific primers. Results shown are mean ± SEM of three independent experiments.*

The next metabolite to be investigated was acetyl-coA carboxylase, the enzyme responsible for catalysing acetyl-CoA to malonyl-coA. INS-1 cells were incubated ± GLT for 5-days prior to RNA extraction, cDNA synthesis and RT-qPCR with acetyl-CoA carboxylase specific primers. The results showed a significant increase in acetyl-CoA carboxylase by 3.9-fold (p=0.013).

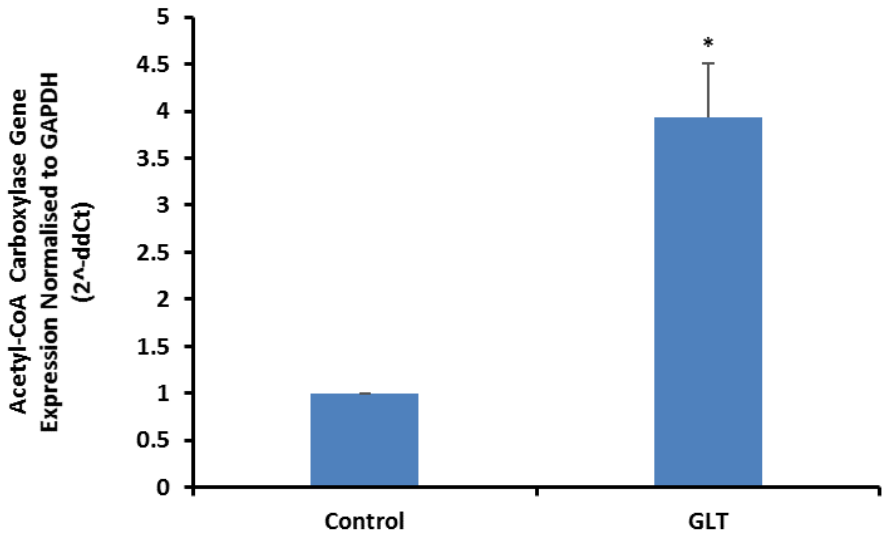

Figure 7.6 Effect of GLT on Acetyl-CoA carboxylase gene expression. *INS-1 cells were incubated ± GLT for 5-days. Total RNA was extracted (Qiagen, Hilden, Germany). Reverse transcribed to obtain cDNA (ThermoFisher, Waltham, MA, USA) and analysed using RT-qPCR with acetyl-coA specific primers. Results are shown as ΔΔCt expressed as fold change compared to the control. Results shown are mean ± SEM of three independent experiments.*

ATP-citrate lyase (ACLY) is an enzyme that converts citrate to acetyl-coA and oxaloacetate. INS-1 cells were incubated ±GLT for 5-days prior to RNA extraction, cDNA synthesis and RT-qPCR with ACLY specific primer. The results showed exposure to GLT conditions increased ACLY expression by 2.5-fold (p=0.034). A similar fold increase was achieved when observing protein expression. GLT increased ACLY by 2.49-fold. ACLY was also observed using proteomics, the results obtained were supportive of the RT-qPCR data and identified that ACLY proteins increased in GLT (data not shown).

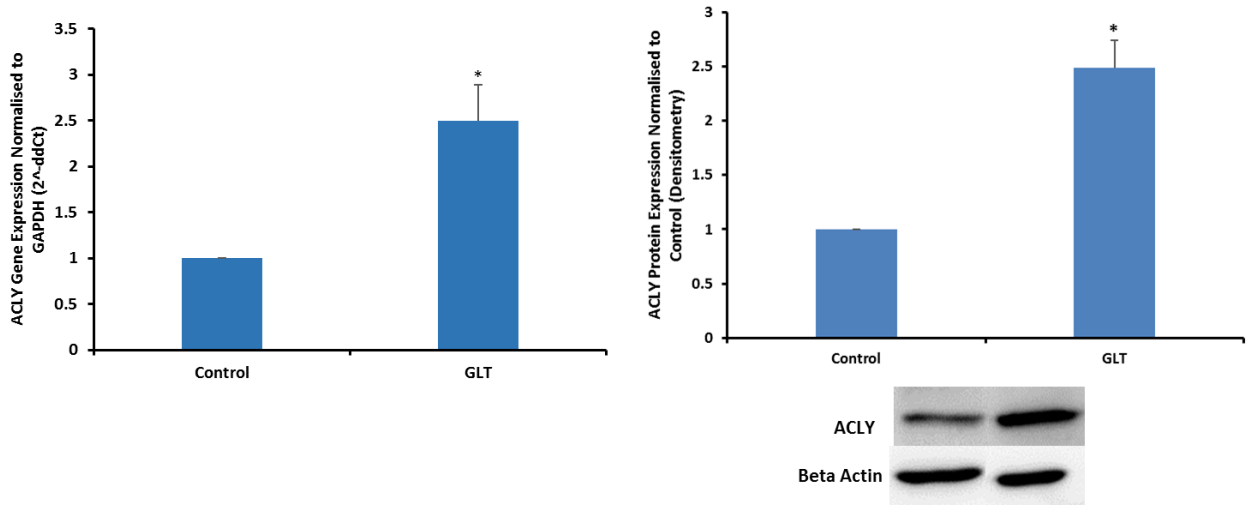

Figure 7.7 Effect of GLT on ATP-citrate lyase. *INS-1 cells were incubated ± GLT for 5 days. For RT-qPCR analysis total RNA was extracted (Qiagen, Hilden, Germany), cDNA was synthesis (ThermoFisher, Waltham, MA, USA) and used for RT-qPCR analysis using ATP-citrate lyase specific primers. Results are shown as ΔΔCt expressed as fold change compared to the control. For western blot analysis cells were lysed using RIPA buffer and the extracted protein was quantified using BCA assay. Proteins were loaded to 10% acrylamide gel and separated using SDS-PAGE. Proteins were transferred to a nitrocellulose membrane and immunoblotted using ATP-citrate lyase specific enzymes Western Blot data supplied by Tatjana Baranov. Data shown is mean ± SEM of three independent experiments.*

As the previous results demonstrate that there is a disruption in the citric acid cycle caused by the exposure to high glucose and fatty acids and there is an increase in acetyl-coA departing the citric acid cycle in the mitochondria as citrate and travelling to the cytosol. It was of interest to see what effect this was having on other processes that utilise acetyl-CoA. It is known that fatty acid synthesis takes place in the cytosol and acetyl-CoA carboxylase is considered to be a crucial enzyme in this process. As it has already been seen in figure 7.6, acetyl-coA carboxylase is increased in GLT conditions. The next step of this investigation was to identify whether the excess acetyl-CoA was being employed for fatty acid synthesis. INS-1 cells that had been incubated ± GLT for 5-days were utilised for RNA extraction, cDNA synthesis and RT-qPCR with fatty acid synthase specific primers or were lysed using RIPA buffer to generate a whole cell lysate prior to western blotting. The results showed that despite the excess acetyl-CoA carboxylase gene expression in GLT conditions there was a reduction in fatty acid synthase gene expression by 56.9% (p=0.0018) and a reduction in fatty acid synthase protein expression by 52% (p= 0.043).

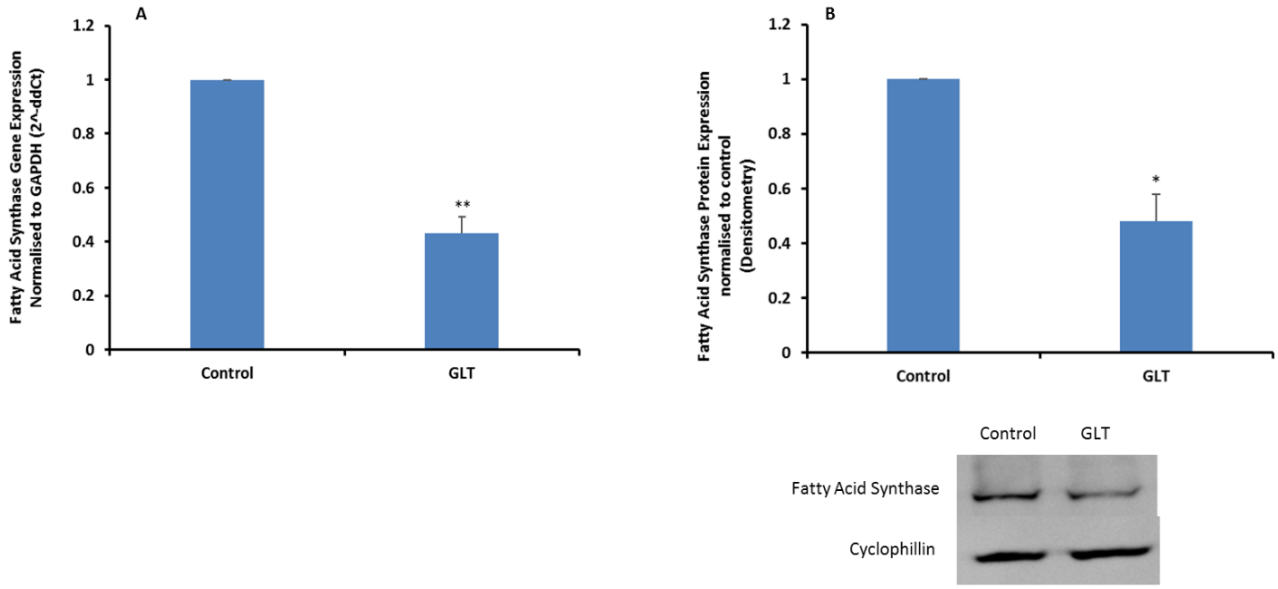

Figure 7.8 Effect of GLT on fatty acid synthase gene expression and protein expression. *INS-1 cells were incubated ± GLT for 5 days prior to collection using trysin EDTA and centrifuged to collect a cell pellet. The pellet was halved and used in either qPCR analysis or western blot technology. For RT-qPCR, total RNA was extracted (Qiagen, Hilden Germany, CDNA transcribed (ThermoFisher, MA, USA) and analysed by RT-qPCR using FAS specific primers. Results are shown as ΔΔCt expressed as fold change compared to control. INS-1 cells collected for western blot was lysed using RIPA buffer to extract protein. Protein was quantified using BCA assay and protein was loaded to 10% acrylamide gel, separated using SDS-PAGE and transferred to a nitrocellulose membrane. Membranes were immunoblotted using FAS specific primers. Results shown are mean ± SEM of four independent experiments.*

An alternative pathway that could potentially make use of the excess acetyl-CoA in the cytosol is cholesterol synthesis which employs acetyl-coA to begin the pathway. SC4MOL plays a role in the cholesterol synthesis pathway and observed using both RT-qPCR and western blot technology following 5-days ±GLT. The results showed that following exposure to GLT the expression of the SC4MOL gene was reduced by 55.6% (p=0.00017) compared to the untreated and SC4MOL protein expression was reduced by 41.2% (p=0.0003).

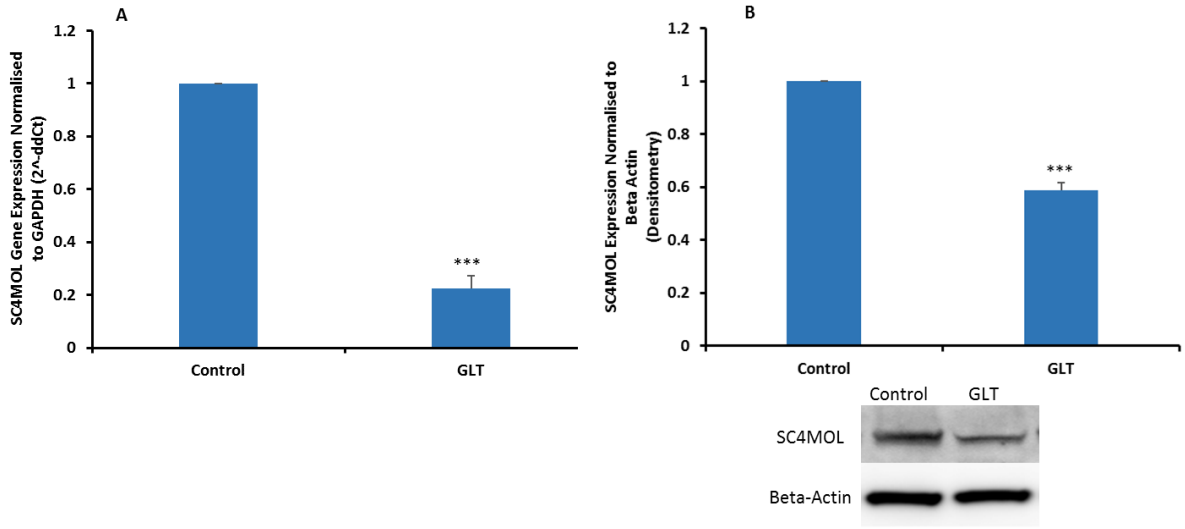

Figure 7.9 Effect of GLT on SC4MOL gene expression and protein expression. *INS-1 cells were incubated ± GLT for 5 days prior to collection using trypsin EDTA and centrifuged to collect a cell pellet. The pellet was halved and used in either qPCR analysis or western blot technology. For RT-qPCR, total RNA was extracted (Qiagen, Hilden Germany, CDNA transcribed (ThermoFisher, MA, USA) and analysed by RT-qPCR using SC4MOL specific primers. Results are shown as ΔΔCt expressed as fold change compared to control. The INS-1 cells collected for western blot was lysed using RIPA buffer to extract protein. Protein was quantified using BCA assay and protein was loaded to 10% acrylamide gel, separated using SDS-PAGE and transferred to a nitrocellulose membrane. Membranes were immunoblotted using SC4MOL specific primers. Results shown are mean ± SEM of three independent experiments.*

The schematic in figure 7.10 demonstrates the changes to the citric acid cycle that are caused by glucolipotoxicity. As the results so far in this chapter have suggested, the exposure of INS-1 cells to GLT cause a disruption in both the fatty acid synthesis and cholesterol pathways despite the abundance of acetyl-CoA. It is therefore demonstrated in this chapter that GLT which is characteristic of type 2 diabetes likely results in histone acetylation and potential epigenetic change by blocking alternative pathways and utilising acetyl groups of the acetyl-CoA as donors for acetylation.

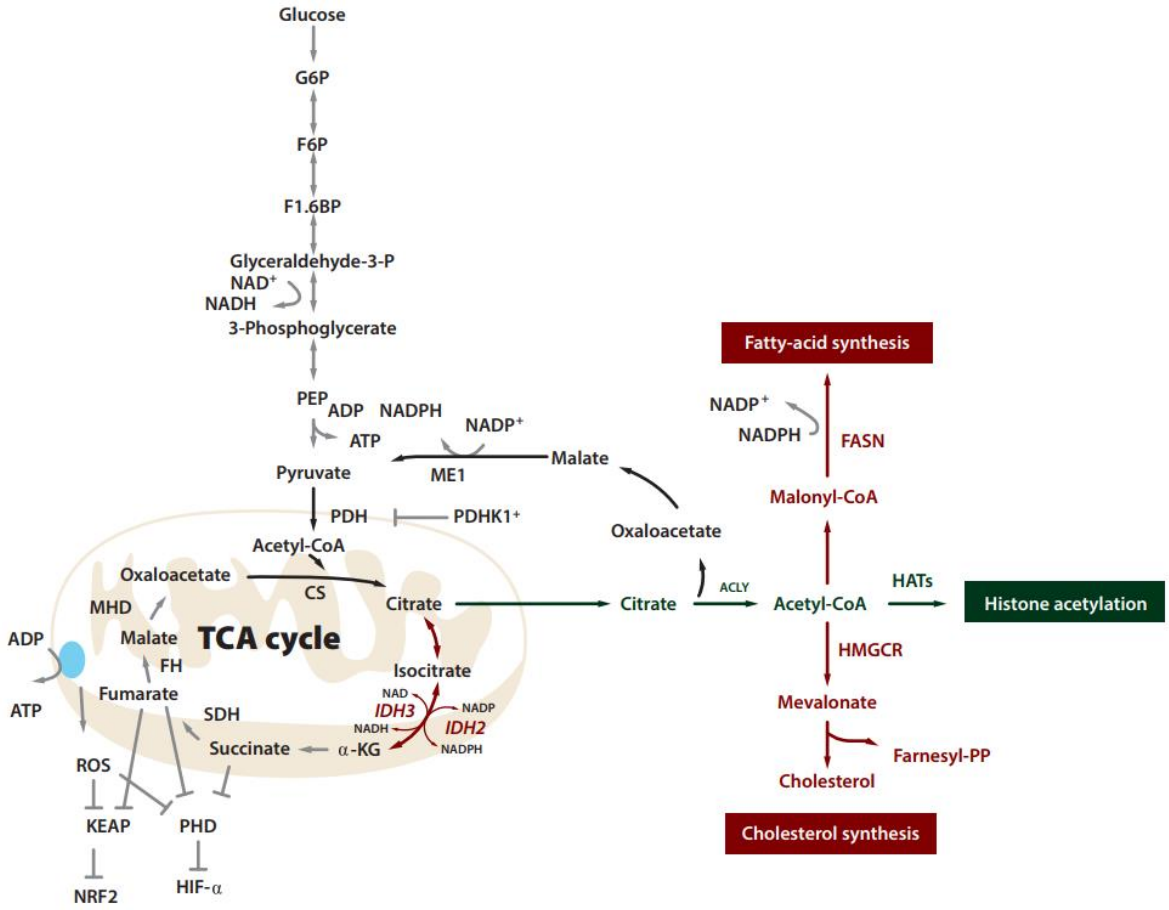

Figure 7.10 Schematic showing the effect of GLT on the TCA cycle, fatty acid synthesis, cholesterol synthesis and histone acetylation.

Based on the finding that the increase in citrate, resulting in acetyl-CoA was not being used in fatty acid synthase or cholesterol synthesis it was important to look at histone acetylation. Histone acetylation is a process where the lysine residue of the N-terminal becomes acetylated and alters gene transcription. The results demonstrate that of the four core histones both histone H3 and Histone H4 have increased acetylation in GLT conditions. The INS-1 cells were incubated ±GLT for 5-days prior to protein extraction using RIPA buffer and used in western blot analysis. Figure 7.11 shows that histone H3 acetylation was increased by 2.53-fold ($p=0.031$) and histone H4 acetylation was increased 2.8-fold ($p=0.042$).

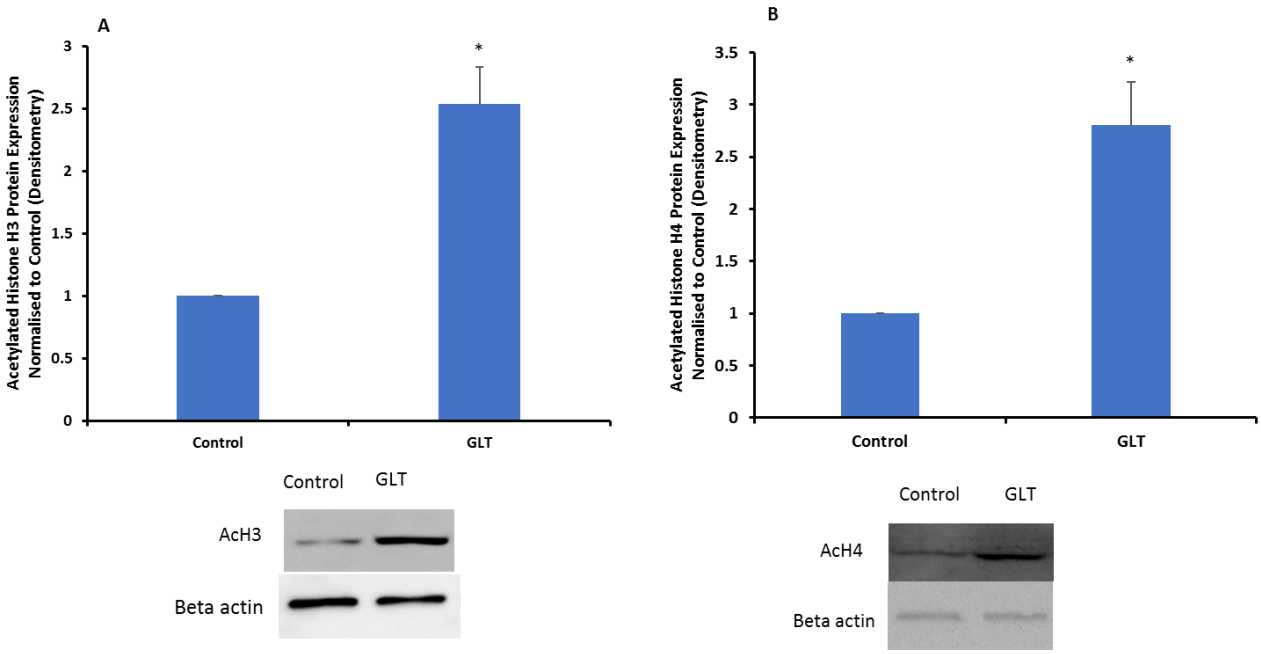

Figure 7.11 Effect of GLT on histone acetylation of histones H3 and H4. *INS-1 cells were incubated ± GLT for 5-days prior to being lysed using RIPA buffer. Extracted proteins were quantified using BCA assay (ThermoFisher, Waltham, MA, USA). Proteins were loaded to a 15% acrylamide gel and separated using SDS-PAGE. Proteins were transferred to a PVDF membrane and immunoblotted using acH3 or acH4 antibody. Results are shown as mean ± SEM of four individual experiments.*

7.4 Discussion

Acetylation is a well-studied post-translational modification that can occur on histones. This project examined the link between metabolic stress resulting from high glucose and fatty acids and potential epigenetic alterations resulting from histone acetylation. The metabolite acetyl-CoA is considered to be a key metabolite in the connection between the citric acid cycle and epigenetic changes. Acetyl-CoA can be produced via numerous mechanisms, both catabolic and anabolically. The main mechanism is the conversion of pyruvate into acetyl-coA by pyruvate dehydrogenase in the mitochondria during glucose oxidation (Kaelin and Mcknight, 2013). In mitochondria, acetyl-CoA is produced from pyruvate that is generated during glycolysis prior to the citric acid cycle, via oxidative

decarboxylation. There is no transporter molecule to guide acetyl-coA to the cytoplasm, instead acetyl-CoA is transferred into citrate by condensing with oxaloacetate, this is then transported out of the mitochondria and subsequently converted back to oxaloacetate and acetyl-coA by ATP-citrate lyase. It is also possible for acetyl-CoA to be formed in the cytoplasm from acetate by cytosolic acetyl-coA synthetase, however, metazoans are only exposed to low levels of acetate and therefore use glucose as their main source of acetyl-CoA following glycolysis (Fan et al,2015, Wellen et al, 2009). Results in figure 7.2 demonstrate that exposure of the rat islet cell line, INS-1 to high glucose and fatty acids results in an increase in citrate levels measured using a citrate assay kit (Abcam, Cambridge, UK). The increase seen in citrate is a 3.1-fold increase compared to control, this is a substantial finding as citrate is converted to acetyl-CoA once out of the mitochondria and therefore is reason to believe that the levels of acetyl-CoA and available acetyl groups are therefore increased.

The initial result in the project suggested that citrate is increased in response to GLT, the next task was to determine whether the overall citric acid cycle was affected by the exposure to glucolipotoxic conditions by measuring ATP content. The results in this project showed that ATP content was reduced by 42.1% in GLT conditions compared to the control, which demonstrates that the overall citric acid cycle is disrupted by pancreatic beta cell exposure to GLT conditions. A potential cause of ATP reduction is oxidative stress which has been found in high fat diet induced obesity in both humans and rodents. A study conducted by Rogers et al, 2014 found that prolonged exposure to lipotoxicity resulted in mitochondrial crisis in preadipocyte cells via a transient increase in ROS and lipid peroxides, decreases in ATP capacity and ultimately cell death. The Rogers et al study exposed the cells to a fatty acid concentration of 600µM of free fatty acids made up of oleic acid, palmitic acid, linoleic acid and stearic acid, which resulted in an accumulation of mitochondrial ROS. The results obtained in this current study build upon a recent publication that found that oxidative stress results in pancreatic β-cell dysfunction and reduction in ATP production (McEvoy et al, 2015). The present study is more relevant as the study conducted by McEvoy et al created oxidative stress by knocking down the cystinosin gene. However, by knocking down the cystinosin gene there was an increase in oxidative stress markers that are also found when cells are exposed to glucolipotoxic conditions, including super oxide (Robertson, 2004). This could mean that the GLT treatment of the pancreatic β-cells could results in a reduction in ATP content due to oxidative stress in type 2 diabetes.

The results demonstrate a reduction in both IDH2 and IDH3 which are both found in the mitochondria and is involved in the citric acid cycle. Following a 5-day incubation ±GLT media the INS-1 showed a reduction of 41.7% of IDH2 protein expression normalised to control and 24% reduction of IDH2 protein expression normalised to control. A reduction of 36.9% was also observed in IDH3 gene expression in response to GLT incubation normalised to control. As the role of IDH2 and IDH3 is to

generate α-ketoglutarate from isocitrate via oxidative carboxylation and in the process IDH2 generates NADPH and IDH3 generates NADH, the reduction in these enzymes suggests that there is a possible dysregulation of mitochondrial metabolites in pancreatic β-cells in response to GLT which could result in a disruption of overall ATP production.

A study conducted by MacDonald et al, 2013 found that when mitochondrial IDH2 and IDH3 were knocked out there was a reduction in α-ketoglutarate by 90%. The work in this research projects builds upon the findings by Macdonald, as despite the fact that both IDH2 and IDH3 are only reduced in response to GLT and not completely knocked out, this will have a negative effect on the production of α-ketoglutarate and hinder the citric acid cycle. This is also supportive of the finding that ATP content is reduced in response to GLT and that the disruption of the citric acid cycle in response to GLT occurs early in the cycle with the excess departure of citrate to the cytosol and reduced IDH2 and IDH3. The same study found that when mitochondrial IDH2 and IDH3 were reduced, IDH1 that is located in the cytosol compensated by producing more metabolites such citrate and α-ketoglutarate to transport back into the mitochondria (MacDonald et al, 2013). This could be a reason for the increased citrate levels that were found in the INS-1 cells that were treated with GLT, however this is unlikely as we found ACLY was increased which functions to convert citrate to acetyl-CoA in the cytosol.

The result in figure 7.7 is supportive of the assumption that glucolipotoxic conditions result in higher levels of acetyl-CoA exiting the citric acid cycle as it shows a significant increase in ACLY gene expression and protein expression both approximately 2.5-fold compared to the untreated control cells using RT-qPCR. Given that the role of ACLY is to convert citrate back to acetyl-CoA and oxaloacetate, the results suggests that ACLY levels increases to meet the demand resulting from increased levels of citrate in GLT conditions.

This finding is consistent with data observed by Zhao et al, 2016, who found that ACLY is the leading supplier of acetyl-coA in standard and nutrient rich conditions. The same research group also found that ACLY is required for glucose-dependent histone acetylation and when ACLY was depleted global histone acetylation was vastly reduced. Their results also showed that following the depletion of ACLY, acetate was used to supply acetyl-coA for histone acetylation, however the level of histone acetylation is much lower than when the acetyl-coA is supplied by ACLY (Zhao et al, 2016). The results in this project build upon the findings of the Zhao lab group as their work was carried in glioblastoma cells, whereas the current project is looking at the effects of nutrient rich conditions (high glucose and fatty acids) on pancreatic β-cells. This means that the effects of GLT treatment on the movement of citrate and the increase in acetyl-CoA are representative of what happens during the onset of type 2 diabetes.

As it has already been established that there is an increase in acetyl-CoA leaving the mitochondria as citrate in GLT conditions, it was then of interest how this increase effects the pathways that occur in the cytosol and utilise the acetyl-coA that is provided by the mitochondrial citric acid cycle. The first metabolite to be observed was the enzyme that is responsible for catalysing acetyl-CoA to malonyl-CoA known as acetyl-coA carboxylase, which is the substrate used as an intermediate in the elongation by the fatty acid synthase enzyme (Wright et al, 2006). The results show in figure 7.4 that there is a significant increase in acetyl-CoA carboxylase gene by 3.9-fold. This result would be suggestive fatty acid synthesis would be increased in GLT conditions resulting from the increase in available in acetyl-CoA and acetyl-CoA carboxylase enzyme. However, fatty acid synthase gene and protein expression was measured in control and GLT conditions. The results were surprising as it was found that both fatty acid synthase gene and protein expression was down regulated in response to GLT. Fatty acid synthase gene expression was reduced by 56.9% in GLT compared to control and fatty acid synthase protein expression was down regulated 52% in GLT conditions compared to control. This finding identifies a potential blockage in the fatty acid synthase pathway of the INS-1 cell in response to GLT conditions. This finding is also similar to results published by Guiu-Jurado et al, 2015 who found that gene expression of enzymes required for fatty acid synthesis was down regulated in both visceral and adipose tissue of obese women. This is relevant as obesity is possibly the main modifiable risk factor for the development of type 2 diabetes (Daousi et al, 2006) and is characterised by high glucose level and free fatty acids.

As it was now apparent that the fatty acid synthesis pathway was blocked following INS-1 β-cell exposure to GLT conditions, another possible route for excess acetyl-CoA was investigated. The cholesterol synthesis pathway is also able to utilise acetyl-CoA. Cholesterol synthesis is an important component of lipid rafts and cell membranes and it is a precursor of steroids, vitamin D and bile (He et al, 2014). The metabolite that was observed was Sterol-C4-Methyl Oxidase-Like (SC4MOL) also known as Methylsterol Monooxygenase 1 (msmo1). SC4MOL is found in the endoplasmic reticulum membrane and is an intermediate enzyme involved in cholesterol biosynthesis (He et al, 2014).

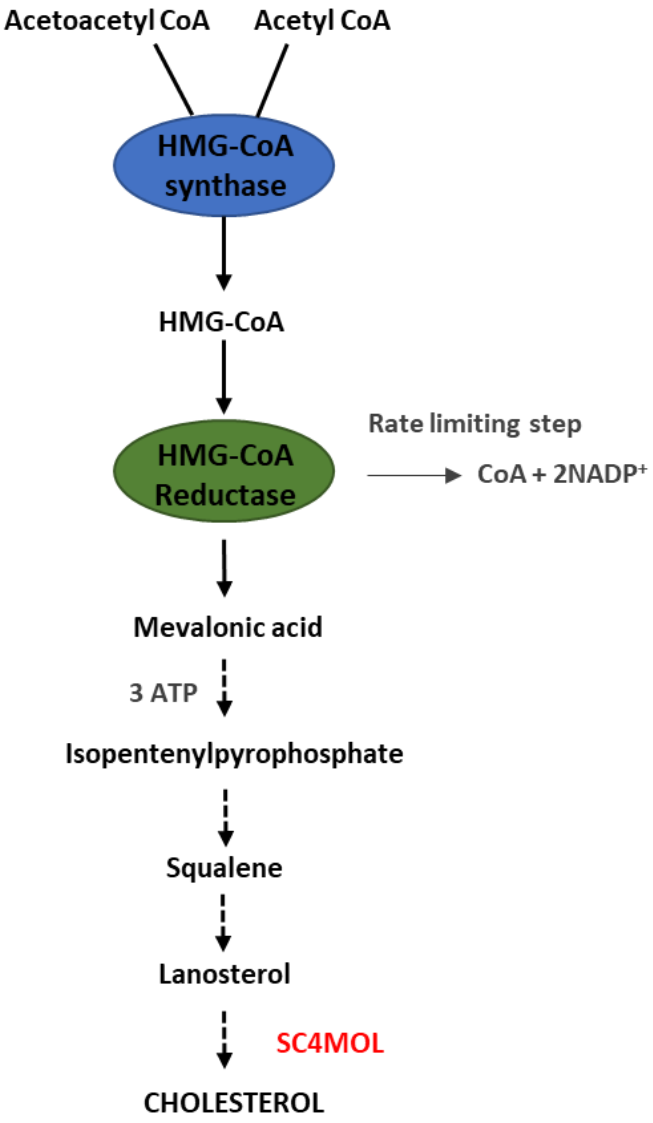

Figure 7.12 Cholesterol biosynthesis pathway. *Pathway identifying steps of the cholesterol synthesis pathway, indicating the location of SC4MOL mechanism of action. Adapted from He et al, 2014.*

Despite, the fact that acetyl-CoA levels are increased in GLT conditions, SC4MOL gene and protein expression were both down regulated. Using RT-qPCR and western blot technology the results showed that SC4MOL was down regulated 77.6% and 57% respectively. This indicates that despite the fact that acetyl-CoA, which is required to begin the cholesterol synthesis pathway, is increased in response to GLT the cholesterol synthesis pathway is disrupted and doesn't utilise the excess acetyl-CoA that is newly available. A similar finding has been reported by Chen et al, in 2012 who identified that SC4MOL was down regulated in an animal model of type 2 diabetes, in a study that was looking at insulin resistance. Reduction in cholesterol synthesis in response to GLT is supported by a publication by Somanath et al, 2009, as they found that in high glucose environments (28mM) cholesterol synthesis

was reduced in rat INS-1 cells. Data published by Somanath et al, suggest the disruption in the cholesterol synthesis occurs early in the pathway as they observed that there was reduction in a key enzyme involved in cholesterol synthesis known as 3-hydroxy-3-methylglutaryl coenzyme A reductase (HMGCR). HMGCR is a key enzyme involved cholesterol synthesis and is responsible for the generation of mevalonate from as 3-hydroxy-3-methylglutaryl coenzyme A (Burg and Espenshade, 2011). The current research project builds upon the findings of the Somanath et al, as we suggest that the excess acetyl-CoA in the cytosol that is unable to be utilised for either fatty acid synthesis or cholesterol synthesis pathways is instead being used for histone acetylation.

The exposure of INS-1 cells to GLT conditions appears to cause a dysregulation of metabolism by disrupting the citric acid cycle. Following 5-day incubation in GLT conditions there is a reduction in overall ATP production (Fig. 7.3). In total there are approximately 38 molecules of ATP formed from glycolysis, citric acid cycle and the electron transport chain (Porter and Brand, 1995). By measuring the amount of ATP using an ATP assay it was found that overall expression of ATP was down-regulated. This finding is supported by Peterson et al, 2004 who found that insulin-resistant individuals produce 30% less ATP than healthy individuals and also by Schmid et al, 2011 who identified that type 2 diabetic patients have reduced levels of hepatic ATP production. As well as reduced ATP production this investigation found lower levels of other citric acid cycle components in GLT conditions, including isocitrate dehydrogenase II. There are three different isoforms of IDH expressed in eukaryotic cells, IDH1, IDH2 and IDH3. Both IDH1 and IDH2 form homodimers and catalyse the formation of alpha-ketoglutarate (AKG) via oxidative decarboxylation of isocitrate. IDH1 catalyses this reaction in the cytosol whereas IDH2 catalyses this reaction in the citric acid cycle in the mitochondria (Keum et al, 2015). The newly formed AKG plays a key role in the citric acid cycle and determines the overall rate of the cycle (Wu et al, 2016). The formation of AKG is considered to be a limiting step of the citric acid cycle, so a down regulation of IDH2 resulting in less AKG could be a key step in the overall reduction of ATP and disruption of the citric acid cycle in GLT conditions.

The results also demonstrated that fatty acid synthesis is down regulated in glucolipotoxic conditions, despite levels of acetyl-coA seemingly increasing. The results showed that using both RT-qPCR and western blot, fatty acid synthesis were down regulated 57% and 48% respectively (Fig. 7.8).

The modification of histone proteins such as acetylation and methylation have crucial roles in epigenetic gene regulation. The addition of an acetyl group to the lysine residue of the histone results in an increased negative charge and reduced affinity between the histone and the negatively charged DNA (Kaelin and McKnight, 2013). The results shown in this thesis identified that both histone H3 and

histone H4 acetylation was upregulated in response to GLT. H3 acetylation increased by more than 2.5-fold and histone H4 acetylation increased by 2.8-fold compared to control. Published data supports these results as a study determined that increased glucose levels were able to acetylate histone H4 in min-6 cells. The same study identified that this acetylation resulted in increased expression of various genes. This study supports the theory put across in this chapter that suggest GLT conditions is able to induce epigenetic changes that alter gene transcription.

In conclusion glucolipotoxic conditions result in mitochondrial metabolism dysfunction and as result this may block cytoplasmic pathways that include fatty acid synthesis and cholesterol synthesis and results in increased histone acetylation.

Chapter 8

General Discussion, Conclusion

and Future Work

8.0 CHAPTER 8: General Discussion, Conclusion and Future Work

8.1 General Discussion

Diabetes mellitus is the term used to describe a group of metabolic diseases that are characterised by hyperglycaemia and arising from defected insulin secretion and/or insulin action. The majority of diabetes cases falls into two broad groups; type 1 diabetes (T1D) and type 2 diabetes (T2D) (Conti et al, 2017). Type 2 diabetes which is the focus of this thesis is characterised by hyperglycaemia arising from insulin resistance. As hyperglycaemia becomes chronic it leads to oxidative stress, which is the central mechanism for glucose toxicity (Karachanak-Yankova et al, 2015). The global prevalence of diabetes is quickly rising. The cause of this rapid increase in prevalence in many countries is due to the rapidly increasing urbanisation and a sedentary lifestyle. However, diabetes may also result from genetic alterations and emerging evidence suggests that environmental factors modulate aberrant expression of several key genes through epigenetic mechanisms in type 2 diabetes (Khullar et al, 2017).

The aim of the thesis was to identify novel mechanisms by which glucolipotoxicity results in the damage and death of pancreatic β-cells. The glucolipotoxic conditions were mimicked by supplementing RPMI-1640 cell media with 28mM glucose, 200µM oleic acid, 200µM palmitic acid and culturing INS-1 rat pancreatic β-cells in these conditions for between 3-5 days. The reason for the use of oleic, a monounsaturated fatty acid and palmitic a saturated fatty acid is because these are the most abundant fatty acids found in the human diet and was therefore representative of human β-cell physiology during the onset of T2D (Orsava et al, 2015). The conditions used to create a glucolipotoxic environment were sufficient to inhibit insulin gene expression and insulin secretion but did not significantly affect cell viability, which meant it was possible to assess mechanisms implicated in glucolipotoxicity with the aim to find therapeutic targets to combat T2D. Based on data gathered via microarray and RNA sequencing by a former PhD student of the Turner Group, the initial investigation of this thesis was focussed on the inflammatory process of the β-cell that occurs in response to GLT. The results showed that both activation and gene expression of NF-κB increased in GLT conditions, this was a significant finding as many of the cellular events resulting for the activation of NF-κB are known, however the initial trigger of activation is poorly defined (Bagnati et al, 2016). The cause of activation was elucidated from network analysis of CD40/TNFR5 signalling using MetaCore™. The network analysis identified genes that are significantly up-regulated in INS-1 cells in response to GLT. The most significantly up-regulated biological networks linked CD40 to both NF-κB and JAK/STAT. Protein and gene expression of CD40 were up-regulated in GLT conditions and following this finding, transient knock down of CD40 was carried out to determine the link between CD40 and NF-κB in β-

cells, which demonstrated that NF-κB activation is dependent on CD40. NF-κB embodies a family of transcription factors that are able to control a large number of genes involved in inflammatory processes (Liu et al, 2016). The finding that NF-κB activation is dependent on CD40 in GLT conditions is important as GLT-induced CD40 is potentially the initiator of inflammation in β-cells and by blocking its action could be a way of preventing β-cell damage in a high glucose and high fat environment. NF-κB is a known transcription factor of iNOS (Morris et al, 2003). When cells were exposed to GLT conditions there was a significant up-regulation in iNOS expression. iNOS produces nitric oxide by utilising L-arginine as a substrate (Förstermann and Sessa, 2012). Despite NO not specifically being measured, it was determined that NO levels increased in INS-1 cells based on evidence of down-stream peroxynitrite activity, which is a nitrating agent that results from the combination of NO with superoxide. 3-NT is a post-translational modification which was significantly increased in response to GLT. 3-NT modifications occur via the action of peroxynitrite and have been used as a marker for nitrosative and oxidative stress mediated by peroxynitrite, resulting in the addition of a $-NO_2$ group (Ahsan, 2013. Cruz and Fardiha, 2016). 4-HNE adducts were also significantly increased, which is a marker of lipid peroxidation which also results from peroxynitrite and forms adducts during oxidative stress (Hogg and Kallyanaraman, 1999. Castro et al, 2017). Therefore, the resulting damage that was evident in the presence of the 3-NT and 4-HNE adducts demonstrated that the initiation of CD40 resulting from exposure of INS-1 cells to GLT conditions concludes in β-cell damage.
The next part of the investigation was to determine whether the activation of CD40 in GLT conditions is responsible for the reduction in insulin gene expression that is observed. It was first established that CD40 is also expressed in the human β-cell line CM and various genes were identified and a network generated that showed a gene in a human β-cell that were negatively regulated by expression of CD40. This was tested by knocking down CD40 using siRNA and measuring the change in expression of 6 of the genes. The results showed that the absence of CD40 resulted in a significant increase of these genes at low glucose level (0.8mM), and therefore demonstrated that CD40 has suppressive effects on various genes. This was followed up using INS-1 cells ±GLT that demonstrated a decrease in SC4MOL and IDH2 at protein level. This was a significant finding as it showed that GLT-induced CD40 was able to affect cellular function by down regulating genes as well as stimulating genes. Despite a human cell line being more physiologically relevant, it was not possible to use the CM cell line in GLT conditions. Publications state that the CM cell line can be used as a beta cell model to study the pathogenesis of T2D (Jonnakuty and Gragnoli, 2007), however, the capacity of CM cells to respond to glucose stimulation is lost if passaged in 'normal' glucose concentrations. If CM cells are cultured at low concentrations for a long period of time (8 weeks), they re-acquire their response to glucose

(Baroni et al, 1999). This proved them to be an un-reliable cell line and research with the rat INS-1 cells resumed.

A major part of this thesis was to identify whether carnosine possessed any therapeutic potential against the CD40-induced inflammation that was shown in chapter 3. Carnosine is a naturally occurring dipeptide that is synthesised from β-alanine and L-histidine. It has previously been shown to exhibit both anti-oxidant and anti-carbonyl properties. A Study claimed that the dietary carnosine was able to reduce fasting plasma glucose levels, but there has been no published data on its beneficial effects again glucolipotoxicity in pancreatic β-cells (Liu et al, 2015). The results demonstrated that the addition of carnosine was able to reduce GLT-induced induction of NF-κB activation, iNOS protein expression, 3-NT species and 4-HNE adducts (Data published in Cripps et al, 2017), demonstrating the protective action of carnosine against glucolipotoxic reactive species in pancreatic beta cells as all inflammatory components down stream of CD40 activation were inhibited. This highlights the potential for carnosine as a therapeutic strategy in T2D, this theory enhanced more so by the finding that carnosine supplementation is also able to reverse the GLT-mediated reduction in insulin secretion (Cripps et al, 2017). However, dietary carnosine has rapid turnover due to the plasma enzyme known as carnosinase 1. Therefore, it may be necessary to administer carnosine in high doses to overcome this problem, or a more realistic approach may be to inhibit carnosinase 1.

The results in this chapter showed for the first time that carnosine synthase, the enzyme responsible for catalysing the synthesis of carnosine was present in β-cells. This suggests that pancreatic β-cells have the potential to generate carnosine when exposed to the necessary conditions.

Mass spectrometry data of INS-1 cells incubated ±GLT, ± carnosine identified numerous proteins that were adducted with 4-HNE or developed 3-NT species in GLT conditions, but these markers of cell damage were removed or prevented by the addition by the additional of carnosine. This further identifies the biological functions and or cellular processes that are affected by GLT, and also the areas which are rescued by the addition of carnosine. This is beneficial as it can help in the specificity of drug development.

Another gene linked to insulin secretion is hepatocyte nuclear factor 4 alpha (HNF4α). This was identified using MetaCore™ that showed HNF4α to be a key gene that is down regulated in response to GLT. HNF4α was shown to be a 'hub' and the effects of GLT on HNF4α showed to have a negative knock on effect on other genes. The HNF4α gene has a role in the development and maintenance of pancreatic β-cell function. The P2 promoter region is associated with associated with T2D susceptibility and mutations in the HNF4α gene or the P2 region cause a type of diabetes known as maturity-onset diabetes of the young (MODY) (Harries et al, 2008). In order to validate the finding of

MetaCore™, siRNA was used to perform a transient knock down of HNF4α, subsequent to this qPCR was used to observe the effects this had on Rab genes. All four of the Rab genes that were observed were down regulated in the absence of HNF4α, therefore validating the MetaCore™ results. Rab proteins act as a vesicle trafficking molecular switch and couple with GTP-binding and hydrolysis they are involved in different stages of vesicle transport (Xiong et al, 2017). Results shown in chapter 4, identify that GTP-binding proteins are down regulated in GLT conditions as a result of CD40 up-regulation, therefore this could be an additional reason for the Rab genes are down regulated in GLT conditions, However, there is not yet a link between the up regulation of CD40 and the suppression of HNF4α gene expression. The down regulation of HNF4α shown in this chapter is also associated with the reduction of both insulin gene expression and insulin secretion. A supporting study also found that INS-1 cells that were dominant negative for HNF4α showed a blunted insulin secretion in response to GLT, however they did not link this to reduced Rab expression as we did in the present study (Wang et al, 2000). Various Rab proteins are associated with insulin secretion however, there are not vast amounts published literature, however a research group examined an insulin secretory granule and identified via proteomic analysis that it contained 3 of the 4 tested in this project (Rab 1b, 2A, and 10) (Brunner et al, 2007). Therefore, if the Rab proteins are negatively affected by GLT down stream of HNF4α, then it likely that the insulin secretory granule will experience dysfunction.

This thesis also concludes that GLT results in increased histone acetylation via the dysregulation and/or blockage of the cholesterol and fatty acid synthesis pathways resulting from GLT-induced dysfunction in the citric acid cycle. Histone acetylation is a well-studied post translation modification, where acetylation of the lysine residue results in the neutralisation of the charge on the histone, which increases chromatin accessibility (Verdone et al 2006). GLT-induced mitochondria damage is not a surprising phenomenon as it has been reported that the mitochondria are a primary target for oxidative stress (Bensellam et al, 2001). GLT initiates the dysregulation via up-regulating citrate, which is evidence that increased acetyl-coA is exiting the mitochondria into the cytoplasm. Acetyl-CoA is not able to leave the mitochondria as acetyl-CoA so it combines with oxaloacetate to form citrate, it is then converted back to acetyl-coA by ATP-citrate lyase once in the cytoplasm (Fan et al, 2015). The results in this chapter also showed that ATP-citrate lyase is up-regulated in response to GLT. The increase in citrate and ATP-lyase are suggestive that in GLT conditions there is increased acetyl-CoA in the cytoplasm, which the location of the fatty acid synthase dependent-fatty acid synthesis pathway and cholesterol synthesis pathway (Mashima et al, 2009. Miller and Bose, 2011).

The results of this chapter of this chapter showed that ATP levels were reduced which is indicative of GLT-induced dysregulation in the mitochondria. The majority of ATP is synthesised in the mitochondria during glucose metabolism via oxidative phosphorylation (Bertram et al, 2006), however, this is not

the only site where ATP is found, therefore a limitation to this investigation is that ATP was measured in the whole cell lysate rather than the mitochondrial extract. As the ATP content down regulation does not represent the mitochondria is not possible to determine whether the overall ATP production of the citric acid cycle is affected by GLT. However, further proof of GLT-induced disruption to the citric acid cycle is observed in the down regulation of IDH2 and IDH3. IDH2 and IDH3 are localised to the mitochondria and are a critical part of the citric acid cycle, they have the responsibility of catalysing isocitrate to α-ketoglutarate via oxidative decarboxylation (Madeiros et al, 2017. Hartong et al, 2008). Therefore, as both of these key citric acid cycle components are down regulated at gene and protein level, suggests that there will be less α-KG generated and will disrupt the next stages of the citric acid cycle.

As previously mentioned, the results showed that there was an increase in acetyl-CoA translocating from the mitochondria, where the citric acid cycle takes places to cytoplasm where it can be utilised in both the fatty acid synthase and cholesterol synthesis pathway. However, the despite the increased cytoplasmic acetyl-CoA there does not appear to be an increase in either fatty acid synthesis or cholesterol synthesis. The results showed a GLT-induced reduction of fatty acid synthase, the enzyme responsible for catalysing the synthesis of fatty acids and the results also showed a reduction in SC4MOL, a key component of the cholesterol synthase pathway. Therefore, it was then hypothesised that the exposure of the INS-1 to GLT conditions resulted in a blockage or disruption of those pathways. It was then believed that the increased acetyl-coA was being transferred to the nucleus and utilised in histone acetylation. The results showed that a significant increase in acetylation of histones H3 and H4. Therefore, the exposure of INS-1 cells to GLT is sufficient to cause disruption to key components of the citric acid cycle and result in increased histone acetylation, which can therefore result in epigenetic changes.

8.2 Conclusion

This thesis elucidates novel mechanisms of GLT-induced damage to pancreatic β-cells that are associated with the onset of T2D. It has been shown that GLT-induced CD40 expression is responsible for activating β-cell inflammation, as well as suppressing insulin gene expression. This thesis also identified novel genes that are associated with insulin secretion and which are regulated by the exposure to GLT. GLT-induced disruption of the citric acid cycle is also shown, which ultimately leads to potential epigenetic alterations. This thesis also demonstrated a potential therapeutic strategy via a naturally occurring dipeptide known as carnosine that is able to reverse the damage caused in the CD40-dependent inflammatory pathway.

8.3 Future Work

8.3.1 CD40 Work: Modulating CD40 signalling

The identification of CD40 as the GLT-induced trigger that results in initiation of the β-cell inflammatory pathway and ultimately cell damage and death give rise for the potential development of a class of drugs based on the antagonism of CD40. One strategy for modulating CD40 signalling would be through Ab-based therapies that target CD40. However, immune cell interactions with the Fc region could potentially lead to either opsonisation of β-cells or antibody-dependent cell cytotoxicity. Therefore, the Fc region of antagonistic CD40 antibody would first need be removed using either pepsin or papain enzymatic IgG cleavage. Pepsin cleavage would result in one bivalent $F(ab)_2$ molecule and then this would be process into two monovalent Fab molecules. Papain cleavage would result in two monovalent Fab molecules. The removal of the Fc region would result in fragmented antibodies that are still able to antagonise CD40 signalling, however the original antibody's Fc portion would no longer be in the fragments and therefore would no longer be able to promote agglutination, precipitation, opsonisation, or cell lysis.

An alternative strategy to achieve modulation of CD40 signalling would be via phage display, which also requires an antagonistic CD40 antibody (Turner MD, 2017). Phage display is already considered a robust technique used in drug discovery and is a technique that uses bacteriophage as a platform to display peptide/polypeptides (Rami et al, 2017). Through utilising the mechanism of phage display it is possible to generate multiple different antibody fragments including $F(ab')_2$ or monovalents Fab, scFv, or Fv domains. This can be achieved for CD40 by amplifying the immunoglobulin heavy and light chains via PCR, ligating with a linker region followed by subcloning into a phagemid vector in order to produce a recombinant phage capable of expressing the desired antibody fragment (Turner MD, 2017)

Finally, inhibition of CD40 signalling could be achieved through CD40 small molecule inhibitors, as reported by Chen et al (2017). The principle behind this is the development of small molecules that are able to interfere with the CD40-CD40L interaction. It has been reported that the development of dye was able to disrupt the interaction in human B cells. A similar pharmacological investigation would need to be carried out to development/identify small molecules that are able to disrupt the CD40-CD40L interaction in pancreatic β-cells, but in theory this should also prevent the initiation of GLT-induced inflammation and the resulting cell damage or death.

8.3.2 Carnosine-based therapeutics

Preliminary studies (Fig.8.1) have shown that supplementing pancreatic β-cells with 100µM β-alanine and L-histidine both separately and combined was able to increase intracellular β-cell carnosine content. Supplementing RPMI-1640 media with 100µM β-alanine was able to increase carnosine content by over 4-fold. This therefore demonstrates that β-alanine supplementation would be beneficial for increasing carnosine content of type 2 diabetic patients and suggests a novel therapeutic application for β-alanine/carnosine supplementation. Future work would highlight the entry mechanism of β-alanine and L-histidine into the pancreatic β-cell and determine an adequate concentration to combat the diabetes associated inflammation.

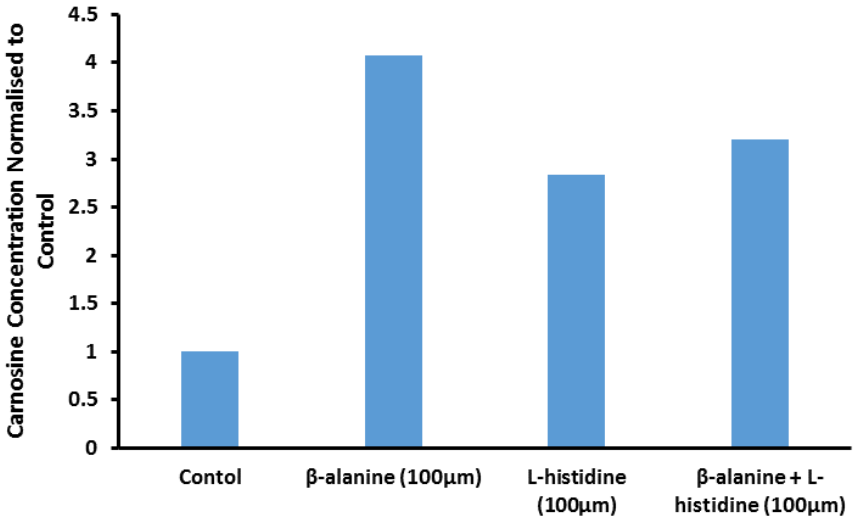

Figure 8.1 Carnosine content in response to beta-alanine and L-histidine supplementation. *INS-1 cells were incubated ±beta-alanine ± L-histidine both individually and combined for 5-days. Amino acid analysis was used to measure carnosine content.*

Despite carnosine content increasing with β-alanine and L-histidine supplementation this does not address the potential for enzyme degradation of carnosine via carnosinase. Therefore, a future research possibility would be the generation of pharmacological carnosinase inhibitors. The reason for this would be to prevent the degradation of carnosine that is seen in individuals with type 2 diabetes. An alternative strategy would be to synthesise non-hydrolysable carnosine mimetics. This approach would also be beneficial as these compounds theoretically function in the same way as carnosine and possess identical scavenging capability. However, their changed molecular structure should in theory be less recognisable, and hence prevent or slow down their natural rate of degradation.

8.3.3 ID4 experiments- Insulin secretion

It has been shown that by reducing ID4 gene expression, there is an increase in inulin gene expression. Therefore, in addition to targeting CD40 to modulate islet inflammation and insulin gene expression, future work should also focus on mechanisms to enhance insulin expression and secretion through strategies that target inhibition of ID4.

8.3.4 HNF4α experiments- Association to CD40

HNF4α gene expression is down regulated in GLT conditions, and this in turn leads to downregulation of a number of genes that are known to function as mediators of endomembrane transport and autophagy. Therefore, further work should investigate whether we can prevent HNF downregulation by GLT, perhaps by interfering with CD40 signalling? Should such an approach prove successful, then this should in turn increase the β-cell's capacity for insulin secretion.

References

Abe, H. Role of histidine-related compounds as intracellular proton buffering constituents in vertebrate muscle. Biochem. (Mosc). 65:757-765, 2000.

Ahsan H. 3-Nitrotyrosine: A biomarker of nitrogen free radical species modified proteins in systemic autoimmunogenic conditions. Human Immunology. 2013;74(10):1392-1399. doi.org/10.1016/j.humimm.2013.06.009

Aggarwal BB. Tumour necrosis factors receptor associated signalling molecules and their role in activation of apoptosis, JNK and NF-kB. Ann Rheum Dis 2000;59(suppl I):i6–i16

Agustı´ A, Morla M, Sauleda J, Saus C, Busquets X. NF-kB activation and iNOS upregulation in skeletal muscle of patients with COPD and low body weight. Thorax 2004; 59:483–487

Akiyama M, Liew CW, Lu S, et al. X-Box Binding Protein 1 Is Essential for Insulin Regulation of Pancreatic α-Cell Function. Diabetes. 2013;62(7):2439-2449. doi:10.2337/db12-1747.

Akram M. Citric acid cycle and Role of its Intermediates in Metabolism. Journal of Biochemistry and Biophysics. 2014; 68(3): 475-478

Al-Sharafi BA, Gunaid AA. Prevalence of Obesity in Patients With Type 2 Diabetes Mellitus in Yemen. International Journal of Endocrinology and Metabolism. 2014;12(2):e13633. doi:10.5812/ijem.13633.

Alejandro EU, Gregg B, Blandino-Rosano M, Cras-Méneur C, Bernal-Mizrachi E. Natural history of β-cell adaptation and failure in type 2 diabetes. Mol Aspects Med. 2015; 42: 19–41.

Aquilante CL. Sulfonylurea pharmacogenomics in Type 2 diabetes: the influence of drug target and diabetes risk polymorphisms. Expert review of cardiovascular therapy. 2010;8(3):359-372. doi:10.1586/erc.09.154

Arya VB, Rahman S, Senniappan S, Flanagan SE, Ellard S, Hussain K. HNF4A mutation: switch from hyperinsulinaemic hypoglycaemia to maturity-onset diabetes of the young, and incretin response. Diabetic Medicine. 2014;31(3):e11-e15. doi:10.1111/dme.12369.

Atkinson MA, Eisenbarth GS, Michels AW. Type 1 diabetes. Lancet. 2014;383(9911):69-82. doi:10.1016/S0140-6736(13)60591-7.

Aquilante CL. Sulfonylurea pharmacogenomics in Type 2 diabetes: the influence of drug target and diabetes risk polymorphisms. Expert review of cardiovascular therapy. 2010;8(3):359-372. doi:10.1586/erc.09.154

Bachar E, Ariav Y, Ketzinel-Gilad M, Cerasi E, Kaiser N, Leibowitz G. Glucose Amplifies Fatty Acid-Induced Endoplasmic Reticulum Stress in Pancreatic β-Cells via Activation of mTORC1. PLoS ONE. 4(3): e4954

Bae J-S, Kim T-H, Kim M-Y, Park J-M, Ahn Y-H. Transcriptional Regulation of Glucose Sensors in Pancreatic β-Cells and Liver: An Update. Sensors (Basel, Switzerland). 2010;10(5):5031-5053. doi:10.3390/s100505031.

Bagnati M, Ogunkolade BW, Marshall C, et al. Glucolipotoxicity initiates pancreatic β-cell death through TNFR5/CD40-mediated STAT1 and NF-κB activation. Cell Death & Disease. 2016;7(8):e2329-. doi:10.1038/cddis.2016.203.

Baguet A, Everaert I, De Naeyer H, Reyngoudt H, Stegen S, Beeckman S, Achten E, Vanhee L, Volkaert A, Petrovic M, Taes Y, Derave W. Effects of sprint training combined with vegetarian or mixed diet on muscle carnosine content and buffering capacity. Eur J Appl Physiol. 2011;111:2571–2580

Ball AJ, Flatt PR, McClenaghan NH. Acute and long-term effects of nateglinide on insulin secretory pathways. British Journal of Pharmacology. 2004;142(2):367-373. doi:10.1038/sj.bjp.0705766

Bagwell AM, Bento JL, Mychaleckyj JC, Freedman BI, Langefeld CD, Bowden DW. Genetic Analysis of HNF4A Polymorphisms in Caucasian-American Type 2 Diabetes. Diabetes 2005; 54(4): 1185-1190.doi.org/10.2337/diabetes.54.4.1185

Barbé-Tuana FM, Klein D, Ichii H, Berman DM, Coffey L, Kenyon NS, Ricordi C, Pastori RL. CD40-CD40 ligand interaction activates proinflammatory pathways in pancreatic islets. Diabetes. 2006;55(9):2437-45.

Barbé-Tuana FM, Cardozo AK, Cnop M. The Role for Endoplasmic Reticulum Stress in Diabetes Mellitus. Endocrine Reviews.2008;29(1):42–61. doi.org/10.1210/er.2007-0015

Baroni MG, Cavallo MG, Mark M, Monetini L, Stoehrer B, Pozzilli P. Beta-cell gene expression and functional characterisation of the human insulinoma cell line CM. J Endocrinol. 1999;161(1):59-68.

Barrera G, Pizzimenti S, Ciamporcero ES, Daga M, Ullio C, Arcaro A, Cetrangolo GP, Ferretti C, Dianzani C, Lepore A, Gentile F. Role of 4-hydroxynonenal-protein adducts in human diseases. Antioxid Redox Signal. 2015;22(18):1681-702. doi: 10.1089/ars.2014.6166.

Barski OA, Xie Z, Baba SP, et al. Dietary Carnosine Prevents Early Atherosclerotic Lesion Formation in ApoE-null Mice. Arteriosclerosis, thrombosis, and vascular biology. 2013;33(6):10.1161/ATVBAHA.112.300572. doi:10.1161/ATVBAHA.112.300572.

Batrukova MA, Rubtsov AM. Histidine-containing dipeptides as endogenous regulators of the activity of sarcoplasmic reticulum Ca-release channels. Biochim Biophys Acta. 1997;1324(1):142-50. doi.org/10.1016/S0005-2736(96)00216-7

Bauchart C, Savary-Auzeloux I, Patureau Mirand P, Thomas E, Morzel M, Rémond D. Carnosine Concentration of Ingested Meat Affects Carnosine Net Release into the Portal Vein of Minipigs. The Journal of Nutrition. 2007;137(3): 589–593. doi.org/10.1093/jn/137.3.589

Bellia F, Vecchio G, Rizzarelli E. Carnosinases, Their Substrates and Diseases. Molecules 2014, 19(2), 2299-2329; doi:10.3390/molecules19022299

Bensellam M, Montgomery MK, Luzuriaga J, Yie JG, Ross Laybutt D. Inhibitor of differentiation proteins protect against oxidative stress by regulating the antioxidant–mitochondrial response in mouse beta cells. Diabetologia. 2015;58(4):758–770. doi.org/10.1007/s00125-015-3503-1

Berg JM, Tymoczko JL, Stryer L. Biochemistry. 5th edition. New York: W H Freeman; 2002. Chapter 17, The Citric Acid Cycle.

Bertram R, Gram Pedersen M, Luciani DS, Sherman A. A simplified model for mitochondrial ATP production. J Theor Biol. 2006;243(4):575-86. doi: 10.1016/j.jtbi.2006.07.019

Boldyrev AA, Aldini G, Derave W. Physiology and Pathophysiology of Carnosine. Physiol Rev 93: 1803–1845, 2 013; doi:10.1152/physrev.00039.2012

Boj SF., Párrizas M, Maestro MA., Ferrer J. A transcription factor regulatory circuit in differentiated pancreatic cells. Proc Natl Acad Sci U S A. 2001; 98(25): 14481–14486

Brunner Y, Couté Y, Iezzi M, Foti M, Fukuda M, Hochstrasser DF, Wollheim CB, Sanchez JC. Proteomics analysis of insulin secretory granules. Mol Cell Proteomics. 2007;6(6):1007-17. doi: 10.1074/mcp.M600443-MCP200

Burg JS, Espenshade PJ. Regulation of HMG-CoA reductase in mammals and yeast. Progress in lipid research. 2011;50(4):403-410. doi:10.1016/j.plipres.2011.07.002.

Calabrese V, Colombrita C, Guagliano E, Sapienza M, Ravagna A, Cardile V, Scapagnini G, Santoro AM, Mangiameli A, Butterfield DA, Giuffrida Stella AM, Rizzarelli E. Protective Effect of Carnosine During Nitrosative Stress in Astroglial Cell Cultures. Neurochemical Research 2005;30(7):797–807.doi: 10.1007/s11064-005-6874-8

Camastra S, Manco M, Mari A, Baldi S, Gastaldelli A, Greco AV, Mingrone G, Ferrannini E. β-Cell Function in Morbidly Obese Subjects During Free Living Long-Term Effects of Weight Loss. Diabetes. 2005; 54(8): 2382-2389. doi.org/10.2337/diabetes.54.8.2382.

Camastra S, Manco M, Mari A, Baldi S, Gastaldelli A, Greco AV, Mingrone G, Ferrannini E. β-Cell Function in Morbidly Obese Subjects During Free Living Long-Term Effects of Weight Loss. Diabetes 2005 Aug; 54(8): 2382-2389. doi.org/10.2337/diabetes.54.8.2382.

Cao SS, Kaufmann RJ. Unfolded Protein Response. Current Biology. 2012;22(16): R622-R626. doi.org/10.1016/j.cub.2012.07.004

Carrer A, Parris JDL, Trefely S, Henry RA, Montgomery DC, Torres A, Viola JM, Kuo YM, Blair IA, Meier JL, Andrews AJ, Snyder NW, Wellen KE. Impact of High Fat Diet on Tissue Acyl-CoA and Histone Acetylation Levels. Journal of Biological chemistry. (2017). M116.750620.

Castro JP, Jung T, Grune T, Siems W. 4-Hydroxynonenal (HNE) modified proteins in metabolic diseases. Free Radical Biology and Medicine. 2017;111: 309-315. doi.org/10.1016/j.freeradbiomed.2016.10.497

Cerqueira NMFSA, Oliveira EF, Gesto DS, Martins DS, Moreira C, Moorthy HN, Ramos MJ, Fernandes PA. Perspective Cholesterol Biosynthesis. A mechanistic overview. Biochemistry, (2016), 55 (39), pp 5483–5506

Chandra RK. Excessive intake of zinc impairs immune responses. JAMA. 1984;252(11):1443-6.

Chen C, Li C, Wang Y, Renaud J, Tian G, Kambhampti S, SaatianB, Nguyen V, Hannoufa A, Mansolais F, Yuan Z, Yu K, Austin RS, Liu J, Kohalmi SE, Wu K, Huang S, Cui Y. Cytosolic Acetyl-CoA Promotes Histone Acetylation Predominantly at H2K27 in Arabidpsis. Nature Plants. (2017); 3:814-824

Chen G, Bentley A, Adeyemo A, et al. Genome-wide association study identifies novel loci association with fasting insulin and insulin resistance in African Americans. Human Molecular Genetics. 2012;21(20):4530-4536. doi:10.1093/hmg/dds282.

Chen J, Song Y, Bojadzic D, Tamayo-Garcia A, Landin AM, Blomberg BB, Buchwald P. Small-Molecule Inhibitors of the CD40-CD40L Costimulatory Protein-Protein Interaction. J Med Chem. 2017;60(21):8906-8922. doi: 10.1021/acs.jmedchem.7b01154.

Chen R, Kang R, Fan XG, Tang D. Release and activity of histone in diseases. Cell Death Dis. 2014; 5(8): e1370

Chen SS, Claus R, Lucas DM, Yu L, Qian J, Ruppert AS, West DA, Williams KE, Johnson AJ, Sablitzky F, Plass C, Byrd JC. Silencing of the inhibitor of DNA binding protein 4 (ID4) contributes to the pathogenesis of mouse and human CLL. Blood.2011;117:862-871; doi:10.1182/blood-2010-05-284638

Chen Y, Lippincott-Schwartz J. Insulin triggers surface-directed trafficking of sequestered GLUT4 storage vesicles marked by Rab10. Small GTPases. 2013;4(3):193-197. doi:10.4161/sgtp.26471.

Cheng K, Andrikopoulos S, Gunton JE. First Phase Insulin Secretion and Type 2 Diabetes. Curr Mol Med. 2013;13(1):126-39.

Cnop M, Toivonen S, Igoillo-Esteve M, Salpea P. Endoplasmic reticulum stress and eIF2α phosphorylation: The Achilles heel of pancreatic β cells. Molecular Metabolism. 2017;6(9):1024-1039. doi:10.1016/j.molmet.2017.06.001.

Collin-Osdoby P, Nickols GA, Osdoby P. Bone cell function, regulation, and communication: a role for nitric oxide. J Cell Biochem. 1995 Mar;57(3):399-408.

Conti C, Mennitto C, Di Francesco G, Fraticelli F, Vitacolonna E, Fulcheri M. Clinical Characteristics of Diabetes Mellitus and Suicide Risk. Frontiers in Psychiatry. 2017;8:40. doi:10.3389/fpsyt.2017.00040.

Corthall JT. Immunoprecipitation. Basic Molecular Protocols in Neuroscience: Tips, Tricks, and Pitfalls. 2014; 8: 77-81. doi.org/10.1016/B978-0-12-801461-5.00008-3

Cosby K, Partovi KS, Crawford JH, Patel RP, Reiter CD, Martyr S, Yang BK, Waclawiw MA, Zalos G, Xu X, Huang KT, Shields H, Kim-Shapiro DB, Schechter AN, Cannon RO, Gladwin MT. Nitrite reduction to nitric oxide by deoxyhemoglobin vasodilates the human circulation. Nat Med. 2003 Dec;9(12):1498-505. Epub 2003 Nov 2.

Cripps MJ, Hanna K, Lavilla C, et al. Carnosine scavenging of glucolipotoxic free radicals enhances insulin secretion and glucose uptake. Scientific Reports. 2017;7:13313. doi:10.1038/s41598-017-13649-w.

Cruz DF, Fardilha M. Relevance of peroxynitrite formation and 3-nitrotyrosine on spermatozoa physiology. Porto Biomedical Journal. 2016;1(4):129-135. doi.org/10.1016/j.pbj.2016.07.004

Culbertson JY, Kreider RB, Greenwood M, Cooke M. Effects of Beta-Alanine on Muscle Carnosine and Exercise Performance:A Review of the Current Literature. Nutrients. 2010;2(1):75-98. doi:10.3390/nu2010075.

Dadgostar H, Zarnegar B, Hoffmann A, Qin X, Truong U, Rao G, Baltimore D, Cheng G. Cooperation of multiple signaling pathways in CD40-regulated gene expression in B lymphocytes. PNAS. 2002; 99 (3) 1497-1502.doi.org/10.1073/pnas.032665099

Dalleau S, Baradat M, Guéraud F, Huc L. Cell death and diseases related to oxidative stress:4-hydroxynonenal (HNE) in the balance. Cell Death and Differentiation. 2013;20(12):1615-1630. doi:10.1038/cdd.2013.138.

Daousi C, Casson IF, Gill GV, MacFarlane IA, Wilding JPH, Pinkney JH. Prevalence of obesity in type 2 diabetes in secondary care: association with cardiovascular risk factors. Postgraduate Medical Journal. 2006;82(966):280-284. doi:10.1136/pmj.2005.039032.

Dardano A, Penno G, Del Prato S, Miccoli R. Optimal therapy of type 2 diabetes: a controversial challenge. Aging. 2014;6(3):187-206.

Darville MI, Eizirik DL. Cytokine Induction of Fas Gene Expression in Insulin-Producing Cells Requires the Transcription Factors NF-κB and C/EBP. Diabetes 2001;50(8): 1741-1748.

Das SLM, Kennedy JIC, Murphy R, Phillips ARJ, Windsor JA, Petrov MS. Relationship between the exocrine and endocrine pancreas after acute pancreatitis. World Journal of Gastroenterology : WJG. 2014;20(45):17196-17205. doi:10.3748/wjg.v20.i45.17196.

Davies SS, Zhang LS. Reactive Carbonyl Species Scavengers—Novel Therapeutic Approaches for Chronic Diseases. Current pharmacology reports. 2017;3(2):51-67. doi:10.1007/s40495-017-0081-6.

De Filippo K, Henderson RB, Laschinger M, Hogg N. Neutrophil Chemokines KC and Macrophage-Inflammatory Protein-2 Are Newly Synthesized by Tissue Macrophages Using Distinct TLR Signaling Pathways. J Immunol, 2008;180 (6) 4308-4315.

De Vos A, Heimberg B, Quartier E, Huypens P, Bouwens L, Pipeleers D, Schuit F. Human and Rat Beta Cells Differ in Glucose Transporter but Not in Glucokinase Gene Expression. The American Society for Clinical Investigation, Inc. 1995; 96:2489-249

Derave W, Everaert I, Beeckman S, Baguet A. Muscle Carnosine Metabolism and β-Alanine Supplementation in Relation to Exercise and Training. Sports Medicine. 2010; 40(3):247-263. doi.org/10.2165/11530310-000000000-00000

Devi SM, Balachandar V, Lee SI, Kim IH. An Outline of Meat Consumption in the Indian Population - A Pilot Review. Korean Journal for Food Science of Animal Resources. 2014;34(4):507-515. doi:10.5851/kosfa.2014.34.4.507.

Donath MY, Böni-Schnetzler M, Ellingsgaard H, Ehses JA. Islet Inflammation Impairs the Pancreatic β-Cell in Type 2 Diabetes. Physiology.2009;24(6), 325-331 doi: 10.1152/physiol.00032.2009.

Drozak J, Veiga-da-Cunha M, Vertommen D, Stroobant V, Van Schaftingen E. Molecular Identification of Carnosine Synthase as ATP-grasp Domain-containing Protein 1 (ATPGD1). The Journal of Biological Chemistry. 2010;285(13):9346-9356. doi:10.1074/jbc.M109.095505.

Dubois M, Vacher P, Roger B, Huyghe D, Vandewalle B, Kerr-Conte J, Pattou F, Moustaïd-Moussa N, Lang J. Glucotoxicity Inhibits Late Steps of Insulin Exocytosis. Endocrinology. 2007; 148(4):1605–1614. doi.org/10.1210/en.2006-1022

Duckworth WC, Bennett RG, Hamel FG. Insulin Degradation: Progress and Potential. Endocrine Reviews.1998; 19(5):608–624.doi.org/10.1210/edrv.19.5.0349

Duez H, Cariou B, Staels B. DPP-4 inhibitors in the treatment of type 2 diabetes. Biochem Pharmacol. 2012;83(7):823-32. doi: 10.1016/j.bcp.2011.11.028.

Eeckhoute J, Formstecher P, Laine B*. Hepatocyte Nuclear Factor 4a enhances the Hepatocyte Nuclear Factor 1a-mediated activation of transcription. 2586±2593 Nucleic Acids Research, 2004;32(8) DOI: 10.1093/nar/gkh581

Eeckhoute J, Moerman E, Bouckenooghe T, Lukoviak B, Pattou F, Formstecher P, Kerr-Conte J, Vandewalle B, Laine B. Hepatocyte Nuclear Factor 4α Isoforms Originated from the P1 Promoter Are Expressed in Human Pancreatic β-Cells and Exhibit Stronger Transcriptional Potentials than P2 Promoter-Driven Isoforms. Endocrinology.2003;144(5); 1686–1694

El-Assaad W, Buteau J, Peyot ML, Nolan C, Roduit R, Hardy S, Joly E, Dbaibo G, Rosenberg L, Prentki M. Saturated fatty acids synergize with elevated glucose to cause pancreatic beta-cell death. Endocrinology. 2003;144(9):4154-63. doi: 10.1210/en.2003-0410

Elgueta R, Benson MJ, de Vries VC, Wasiuk A, Guo Y, Noelle J. Molecular mechanism and function of CD40/CD40L engagement in the immune system. Immunol Rev. 2009; 229(1): 10.1111/j.1600-065X.2009.00782.x.

El Hokayem J, Brittain JC, Nawaz Z, Bethea JR. Tumor Necrosis Factor Receptor Associated Factors (TRAFs) 2 and 3 Form a Transcriptional Complex with Phosho-RNA Polymerase II and p65 in CD40 Ligand Activated Neuro2a Cells. Mol Neurobiol.2017;54:1301–1313.

Ellard S, Colclough K. Mutations in the genes encoding the transcription factors hepatocyte nuclear factor 1 alpha (HNF1A) and 4 alpha (HNF4A) in maturity-onset diabetes of the young. Hum Mutat. 2006 (9):854-69.

Everaert I, Mooyaart A, Baguet A, Zutinic A, Baelde H, Achten E, Taes Y, De Heer E, Derave W. (2011). Vegetarianism, female gender and increasing age, but not CNDP1 genotype, are associated with reduced muscle carnosine levels in humans. Amino acids. 40. 1221-9. 10.1007/s00726-010-0749-2.

Fan J, Krautkramer KA, Feldman JL, Denu JM. Metabolic regulation of histone post-translational modifications. ACS Chem Biol. 2015; 10(1): 95–108

Farris W, Mansourian S, Chang Y, et al. Insulin-degrading enzyme regulates the levels of insulin, amyloid β-protein, and the β-amyloid precursor protein intracellular domain in vivo. Proceedings of the National Academy of Sciences of the United States of America. 2003;100(7):4162-4167. doi:10.1073/pnas.0230450100.

Fernie AR, Carrari F, Sweetlove LJ. Respiratory metabolism: glycolysis, the TCA cycle and mitochondrial electron transport. Current Opinion in Plant Biology 2004, 7:254–261.

Fosmire GJ. Zinc toxicity. Am J Clin Nutr. 1990;51(2):225-7.

Förstermann U, Sessa WC. Nitric oxide synthases: regulation and function. European Heart Journal. 2012;33(7):829-837. doi:10.1093/eurheartj/ehr304.

Free RB, Hazelwood LA, Sibley DR. Identifying Novel Protein-Protein Interactions Using Co-Immunoprecipitation and Mass Spectroscopy. Current protocols in neuroscience / editorial board, Jacqueline N Crawley . [et al]. 2009;0 5:Unit-5.28. doi:10.1002/0471142301.ns0528s46.

Fu Z, Gilbert ER, Liu D. Regulation of Insulin Synthesis and Secretion and Pancreatic Beta-Cell Dysfunction in Diabetes. Current diabetes reviews. 2013;9(1):25-53.

Galdieri G, Zhang T, Rogerson D, Lleshi R, Vancura A. Protein Acetylation and Acetyl Coenzyme A Metabolism in Budding Yeast. Eukaryot Cell. 2014; 13(12): 1472–1483.

Gardner DS, Tai ES. Clinical features and treatment of maturity onset diabetes of the young (MODY). Diabetes, Metabolic Syndrome and Obesity: Targets and Therapy. 2012;5:101-108. doi:10.2147/DMSO.S23353.

Gardner KE, Zhou L, Parra MA, Chen X, Strahl BD. Identification of Lysine 37 of Histone H2B as a Novel Site of Methylation. Bryk M, ed. PLoS ONE. (2011);6(1):e16244. doi:10.1371/journal.pone.0016244.

Gardner ML, Illingworth KM, Kelleher J, Wood D. Intestinal absorption of the intact peptide carnosine in man, and comparison with intestinal permeability to lactulose. The Journal of Physiology. 1991; 439:411-422.

Gautier C, van Faassen E, Mikula I, Martasek P, Slama-Schwok A. Endothelial nitric oxide synthase reduces nitrite anions to NO under anoxia. Biochem Biophys Res Commun. 2006;341(3):816-21. doi: 10.1016/j.bbrc.2006.01.031

Gerber PA, Rutter GA. The Role of Oxidative Stress and Hypoxia in Pancreatic Beta-Cell Dysfunction in Diabetes Mellitus. Antioxidants & Redox Signaling. 2017;26(10):501518. doi:10.1089/ars.2016.6755.

Gerich JE. Role of the kidney in normal glucose homeostasis and in the hyperglycaemia of diabetes mellitus: therapeutic implications. Diabetic Medicine. 2010;27(2):136-142. doi:10.1111/j.1464-5491.2009.02894.x.

German MS, Wang J. The insulin gene contains multiple transcriptional elements that respond to glucose. Molecular and Cellular Biology. 1994;14(6):4067-4075.

Gibbons GF. Regulation of fatty acid and cholesterol synthesis: co-operation or competition? Progress in Lipid Research (2003) 42; 479–497

Giulio Vistoli G, Orioli M, Pedretti A, Regazzoni L, Canevotti R, Negrisoli G, Carini M, Aldini G. Design, Synthesis, and Evaluation of Carnosine Derivatives as Selective and Efficient Sequestering Agents of Cytotoxic Reactive Carbonyl Species. ChemMedChem 2009, 4, 967 – 975 doi: 10.1002/cmdc.200800433

Golson ML, Misfeldt AA, Kopsombut UG, Petersen CP, Gannon M. High Fat Diet Regulation of β-Cell Proliferation and β-Cell Mass. Open Endocrinol J. 2010; 4: 10.2174/1874216501004010066.

Graier WF, Malli R, and Kostner GM. Mitochondrial protein phosphorylation: instigator or target of lipotoxicity? Trends Endocrinol Metab. 2009; 20(4): 186–193. doi:10.1016/j.tem.2009.01.004.

Gu S, Shi J, Tang Z, et al. Comparison of Glucose Lowering Effect of Metformin and Acarbose in Type 2 Diabetes Mellitus: A Meta-Analysis. Gong Y. PLoS ONE. 2015;10(5):e0126704. doi:10.1371/journal.pone.0126704.

Gualano B, Everaert I, Stegen S, Artioli GG, Taes Y, Roschel H, Achten E, Otaduy EC, Lancha Junior AH, Harris R, Derave W. Reduced muscle carnosine content in type 2, but not in type 1 diabetic patients. Amino Acids (2012) 43:21–24. doi:10.1007/s00726-011-1165-y

Guiu-Jurado E, Auguet T, Berlanga A, et al. Downregulation of de Novo Fatty Acid Synthesis in Subcutaneous Adipose Tissue of Moderately Obese Women. Arai T, ed. International Journal of Molecular Sciences. 2015;16(12):29911-29922. doi:10.3390/ijms161226206.

Guillausseau PJ, Meas T, Virally M, Laloi-Michelin M, Médeau V, Kevorkian JP. Abnormalities in insulin secretion in type 2 diabetes mellitus. Diabetes Metab. 2008;34(2):S43-8. doi: 10.1016/S1262-3636(08)73394-9.

Gupta RK, Gao N, Gorski RK, et al. Expansion of adult β-cell mass in response to increased metabolic demand is dependent on HNF-4α. Genes & Development. 2007;21(7):756-769. doi:10.1101/gad.1535507.

Gupta RK., Vatamaniuk MZ., Lee CS., Flaschen RC., Fulmer JT., Matschinsky FM., Duncan SA., Kaestner KH. The MODY1 gene HNF-4α regulates selected genes involved in insulin secretion. J Clin Invest 2005; 115(4): 1006–1015

Haines RJ, Pendleton LC, Eichler DC. Argininosuccinate synthase: at the center of arginine metabolism. International Journal of Biochemistry and Molecular Biology. 2011;2(1):8-23.

Han J, Seo H, Choi Y, Lee C, Kim M, Jeon Y, Lee J, Hong M, Hyun SH, Lee E, Ka H. Expression and regulation of inhibitor of DNA binding proteins ID1, ID2, ID3, and ID4 at the maternal-conceptus interface in pigs. Theriogenology. 2018;108:46e55. doi.org/10.1016/j.theriogenology.2017.11.029

Harding HP, Ron D. Endoplasmic reticulum stress and the development of diabetes: a review. Diabetes. 2002;51 Suppl 3:S455-61. doi.org/10.2337/diabetes.51.2007.S455

Harries LW, Locke JM, Shields B, Hanley NA, Hanley KP, Steele A, Njølstad PR, Ellard S, Hattersley AT. The diabetic phenotype in HNF4A mutation carriers is moderated by the expression of HNF4A isoforms from the P1 promoter during fetal development. Diabetes. 2008;57(6):1745-52. doi: 10.2337/db07-1742.

Harris RC, Wise JA, Price KA, Kim HJ, Kim CK, Sale C. Determinants of muscle carnosine content. Amino Acids. 2012;43(1):5-12. doi:10.1007/s00726-012-1233-y.

Hartong DT, Dange M, McGee TL, Berson EL, Dryja TP, Colman RF. Novel insights into the contributions of isocitrate dehydrogenases to the Krebs cycle from patients with retinitis pigmentosa. Nature genetics. 2008;40(10):1230-1234. doi:10.1038/ng.223.

Hayden MS, Ghosh S. Regulation of NF-κB by TNF Family Cytokines. Seminars in immunology. 2014;26(3):253-266. doi:10.1016/j.smim.2014.05.004.

Hayhurst G,.P, Lee Y, Lambert G, Ward J,.M, Gonzalez F,.J. Hepatocyte Nuclear Factor 4α (Nuclear Receptor 2A1) Is Essential for Maintenance of Hepatic Gene Expression and Lipid Homeostasis. Mol Cell Biol. 2001;21(4): 1393–1403

He M, Kratz LE, Michel JJ, Vallejo AN, Ferris L, Kelley RI, Hoover JJ, Jukic D, Gibson KM, Wolfe LA, Ramachandran D, Zwick ME, Vockley J . Mutations in the human SC4MOL gene encoding a methyl sterol oxidase cause psoriasiform dermatitis, microcephaly, and developmental delay. The Journal of Clinical Investigation. 2011;121(3):976-984. doi:10.1172/JCI42650.

He M, Smith LD, Chang R, Li X, Vockley J. The role of sterol-C4-methyl oxidase in epidermal biology. Biochimica et biophysica acta. 2014;1841(3):331-335. doi:10.1016/j.bbalip.2013.10.009.

Hehlgans T, Pfeffer K. The intriguing biology of the tumour necrosis factor/tumour necrosis factor receptor superfamily: players, rules and the games. Immunology. 2005;115(1):1-20. doi:10.1111/j.1365-2567.2005.02143.x.

Heppner KM, Perez-Tilve D. GLP-1 based therapeutics: simultaneously combating T2DM and obesity. Frontiers in Neuroscience. 2015;9:92. doi:10.3389/fnins.2015.00092.

Hogg N, Kalyanaraman B. Nitric oxide and lipid peroxidation. Biochimica et Biophysica Acta. 1999; 1411:378-384. doi.org/10.1016/S0005-2728(99)00027-4

Hoppa MB, Collins S, Ramracheya R, et al. Chronic Palmitate Exposure Inhibits Insulin Secretion by Dissociation of Ca2+ Channels from Secretory Granules. Cell Metabolism. 2009;10(6):455-465. doi:10.1016/j.cmet.2009.09.011.

Hostager BS, Bishop GA. CD40-Mediated Activation of the NF-κB2 Pathway. Front Immunol. 2013; 4: 376. doi: 10.3389/fimmu.2013.00376

Hostalek U, Gwilt M, Hildemann S. Therapeutic Use of Metformin in Prediabetes and Diabetes Prevention. Drugs. 2015;75(10):1071-1094. doi:10.1007/s40265-015-0416-8.

Hu FB, Manson JE, Meir SJ, Stampfer J, Colditz G, Liu S, Solomon C, Willett C. Diet, Lifestyle, and the risk of type 2 diabetes mellitus in women. N Engl J Med; 2001 345(11).

Huang J, Karakucuk V, Levitsky L,.L, Rhoads D,.B. Expression of HNF4α variants in pancreatic islets and Ins-1 β cells. Diabetes Metab Res Rev (2008) 24: 533–543.

Huang P, Altshuller YM, Hou JC, Pessin JE, Frohman MA. Insulin-stimulated Plasma Membrane Fusion of Glut4 Glucose Transporter-containing Vesicles Is Regulated by Phospholipase D1. Mol Biol Cell. 2005; 16(6): 2614–2623.

Huang S, Czech MP. The GLUT4 Glucose Transporter. Cell Metabolism. 2007; 5(4):237-252

Hulse RE, Ralat LA, Tang W-J. Structure, Function, and Regulation of Insulin-Degrading Enzyme. Vitamins and hormones. 2009;80:635-648. doi:10.1016/S0083-6729(08)00622-5.

Hwang SW, Lee Y, Aldini G, Yeum K. Targeting Reactive Carbonyl Species with Natural Sequestering Agents. Molecules 2016, 21, 280; doi:10.3390/molecules21030280

Ijuin T, Takenawa T. Regulation of Insulin Signaling and Glucose Transporter 4 (GLUT4) Exocytosis by Phosphatidylinositol 3,4,5-Trisphosphate(PIP3) Phosphatase, Skeletal Muscle, and Kidney Enriched Inositol Polyphosphate Phosphatase (SKIP). THE JOURNAL OF BIOLOGICAL CHEMISTRY. 2012;287(10):6991–6999

Jacobsen MLB, Rønn SG, Bruun C, Larsen CM, Eizirik DL, Mandrup-Poulsen T, Billestrup N. IL-1β-induced chemokine and Fas expression are inhibited by suppressor of cytokine signalling-3 in insulin-producing cells. Diabetologia (2009) 52:281–288.

Jen Y, Manova K, Benezra R. Expression patterns of Id1, Id2, and Id3 are highly related but distinct from that of Id4 during mouse embryogenesis. Dev Dyn. 1996;207(3):235-52.

Jewell JL, Oh E, Thurmond DC. Exocytosis mechanisms underlying insulin release and glucose uptake: conserved roles for Munc18c and syntaxin 4. Am J Physiol Regul Integr Comp Physiol. 2010; 298(3): R517–R531.

Ježek P, Jabůrek M, Holendová B, Plecitá-Hlavatá L. Fatty Acid-Stimulated Insulin Secretion vs. Lipotoxicity. Molecules 2018; 23(6): 1483. doi.org/10.3390/molecules23061483

Jiang G, Nepomuceno L, Hopkins K, Sladek FM. Exclusive homodimerization of the orphan receptor hepatocyte nuclear factor 4 defines a new subclass of nuclear receptors. Molecular and Cellular Biology. 1995;15(9):5131-5143.

Jones RL, Barnett CT, Davidson J, et al. β-alanine supplementation improves in-vivo fresh and fatigued skeletal muscle relaxation speed. European Journal of Applied Physiology. 2017;117(5):867-879. doi:10.1007/s00421-017-3569-1.

Jonnakuty C, Gragnoli C. Karyotype of the human insulinoma CM cell line- Beta cell model in vitro. Journal of cellular Physiology. 2007; 213(3): 661-662 doi:10.1002/jcp.21135

Jourd'heuil D,Jourd'heuil FL, Kutchukian PS, Musah RA, Wink‖DA, Grisham MB. Reaction of Superoxide and Nitric Oxide with Peroxynitrite. The Journal of Biological Chemistry. 2001; 276, 28799-28805. doi: 10.1074/jbc.M102341200

Kaddai V, Gonzalez T, Keslair F, et al. Rab4b Is a Small GTPase Involved in the Control of the Glucose Transporter GLUT4 Localization in Adipocyte. Calbet JAL, ed. PLoS ONE. 2009;4(4):e5257. doi:10.1371/journal.pone.0005257.

Kaelin WG, McKnight SL. Influence of Metabolism on Epigenetics and Disease. Cell. 2013;153(1):56-69. doi:10.1016/j.cell.2013.03.004.

Karachanak-Yankova S, Dimova R, Nikolova D, et al. Epigenetic alterations in patients with type 2 diabetes mellitus. Balkan Journal of Medical Genetics: BJMG. 2015;18(2):15-24. doi:10.1515/bjmg-2015-0081.

Karin M. How NF-kB is activated: the role of the IkB kinase (IKK) complex. Oncogene.1999; 18: 6867-6874.

Kaveeshwar SA, Cornwall J. The current state of diabetes mellitus in India. The Australasian Medical Journal. 2014;7(1):45-48. doi:10.4066/AMJ.2013.1979.

Kawahito S, Kitahata H, Oshita S. Problems associated with glucose toxicity: Role of hyperglycemia-induced oxidative stress. World Journal of Gastroenterology: WJG. 2009;15(33):4137-4142. doi:10.3748/wjg.15.4137.

Keane NK, Cruzat VF, Carlessi R,Homem de Bittencourt Jr PI, Newsholme P. Molecular Events Linking Oxidative Stress and Inflammation to Insulin Resistance and β-Cell Dysfunction. Oxidative Medicine and Cellular Longevity. 2015;181643:15 .doi.org/10.1155/2015/181643

Keklikoglu N, Akinci S. The role of iNOS in beta cell destruction in diabetes. Oxid Antioxid Med Sci. 2013; 2(4): 251-254doi: 10.5455/oams.081113.rv.010

Kelpe CL, Moore PC, Parazzoli SD, Wicksteed B, Rhodes CJ, Poitout V. Palmitate Inhibition of Insulin Gene Expression Is Mediated at the Transcriptional Level via Ceramide Synthesis. The Journal of Biological Chemistry. 2003; 278, 30015-30021. doi: 10.1074/jbc.M302548200

Kempf K, Rose B, Herder C, Kleophas U, Martin S, Kolb H. Inflammation in metabolic syndrome and type 2 diabetes: Impact of dietary glucose. Ann N Y Acad Sci. 2006;1084:30-48. DOI: 10.1196/annals.1372.012

Kennedy-Martin T, Boye KS, Peng X. Cost of medication adherence and persistence in type 2 diabetes mellitus: a literature review. Patient preference and adherence. 2017;11:1103-1117. doi:10.2147/PPA.S136639.

Keum Y-S, Choi BY. Isocitrate dehydrogenase mutations: new opportunities for translational research. BMB Reports. 2015;48(5):266-270. doi:10.5483/BMBRep.2015.48.5.021.

Kim N-H, Yu T, Lee DH. The Nonglycemic Actions of Dipeptidyl Peptidase-4 Inhibitors. BioMed Research International. 2014; 368703. doi:10.1155/2014/368703.

Kirkpatrick CL, Wiederkehr A, Baquié M, et al. Hepatic Nuclear Factor 1α (HNF1α) Dysfunction Down-regulates X-box-binding Protein 1 (XBP1) and Sensitizes β-Cells to Endoplasmic Reticulum Stress. The Journal of Biological Chemistry. 2011;286(37):32300-32312. doi:10.1074/jbc.M111.247866.

Klein D, Barbé-Tuana A. Puglies H. Ichii D. Garza M. Gonzalez R. D. Molano C. Ricordi R. L. Pastori. A functional CD40 receptor is expressed in pancreatic beta cells. 2005;48(2): 268–276

Klip M, Marette A. Acute and Chronic Signals Controlling Glucose transport in Sketetal Muscle. Journal of Cell Biochemistry.I 1992; (48): 51-60.

Kohen R, Yamamoto Y, Cundy KC, Ames BN. Antioxidant activity of carnosine, homocarnosine, and anserine present in muscle and brain. Proceedings of the National Academy of Sciences of the United States of America. 1988;85(9):3175-3179.

Kruse A, Fattah-Hosseini S, Saha S, Johnson R, Warwick ER, Sturgeon K, Mueller L, et al, . Combining 'omics and microscopy to visualize interactions between the Asian citrus psyllid vector and the Huanglongbing pathogen Candidatus Liberibacter asiaticus in the insect gut. Combining 'omics and microscopy to visualize interactions between the Asian citrus psyllid vector and the Huanglongbing pathogen Candidatus Liberibacter asiaticus in the insect gut. PLoS ONE. 2017;12(6): e0179531. doi.org/10.1371/journal.pone.0179531

Kulkarni RN. The islet β-cell. The International Journal of Biochemistry & Cell Biology.2004 (36): 365–371

Kwon G, Corbett JA, Rodi CP, Sullivan P, McDaniel ML. Interleukin-lP-Induced Nitric Oxide Synthase Expression by Rat Pancreatic P-Cells: Evidence for the Involvement of Nuclear Factor KB in the Signaling Mechanism*. Endocrinology 1995. Vol. 136. No. 11

Lawrence T. The Nuclear Factor NF-κB Pathway in Inflammation. Cold Spring Harbor Perspectives in Biology. 2009;1(6):a001651. doi:10.1101/cshperspect.a001651.

Lechner M, Lirk P, Rieder J. Inducible nitric oxide synthase (iNOS) in tumor biology: the two sides of the same coin. Semin Cancer Biol. 2005;15(4):277-89. doi: 10.1016/j.semcancer.2005.04.004

Leney SE, Tavaré JM. The molecular basis of insulin-stimulated glucose uptake: signalling, trafficking and potential drug targets. Journal of Endocrinology.2009; 203: 1–18.

Lenzen S, Drinkgern J, Tiedge M. Low antioxidant enzyme gene expression in pancreatic islets compared with various other mouse tissues. Free Radical Biology and Medicine. 1996;20(3):463-466. doi.org/10.1016/0891-5849(96)02051-5.

Leo E, Welsh K, Matsuzawa SI, Zapata JM, Kitada S, Mitchell RS, Ely KR, Reed JC. Differential Requirements for Tumor Necrosis Factor Receptor-associated Factor Family Proteins in CD40-mediated Induction of NF-κB and Jun N-terminal Kinase Activation. The Journal of Biological Chemistry 274, 22414-22422.

Li H, Cui H, Kindu T.K, Alzawahra W, Zweier J.L. Nitric Oxide Production from Nitrite Occurs Primarily in Tissues Not in the Blood CRITICAL ROLE OF XANTHINE OXIDASE AND ALDEHYDE OXIDASE. THE JOURNAL OF BIOLOGICAL CHEMISTRY, 2008 VOL. 283, NO. 26, pp. 17855–17863

Li Q, Sadhukhan S, Berthiaume JM, et al. HNE catabolism and formation of HNE adducts are modulated by beta oxidation of fatty acids in the isolated rat heart. Free radical biology & medicine. 2013;58:35-44. doi:10.1016/j.freeradbiomed.2013.01.005.

Li Q, Tomcik K, Zhang S, Puchowicz MA, Zhang G-F. Dietary-regulation of catabolic disposal of 4-hydroxynonenal analogs in rat liver. Free radical biology & medicine. 2012;52(6):1043-1053. doi:10.1016/j.freeradbiomed.2011.12.022.

Li J, Yin Q, Wu H. Structural Basis of Signal Transduction in the TNF Receptor Superfamily. Advances in immunology. 2013;119:135-153. doi:10.1016/B978-0-12-407707-2.00005-9.

Liu T, Zhang L, Joo D, Sun S-C. NF-κB signaling in inflammation. Signal transduction and targeted therapy. 2017;2:17023. doi:10.1038/sigtrans.2017.23.

Liu X, Wang Z, Yang Y, et al. Rab1A mediates proinsulin to insulin conversion in β-cells by maintaining Golgi stability through interactions with golgin-84. Protein & Cell. 2016;7(9):692-696. doi:10.1007/s13238-016-0298-x.

Liu Y, Cotillard A, Vatier C, et al. A Dietary Supplement Containing Cinnamon, Chromium and Carnosine Decreases Fasting Plasma Glucose and Increases Lean Mass in Overweight or Obese Pre-Diabetic Subjects: A Randomized, Placebo-Controlled Trial. Song Y, ed. PLoS ONE. 2015;10(9):e0138646. doi:10.1371/journal.pone.0138646.

Liu Y, Xu G, Sayre LM. Carnosine Inhibits (E)-4-Hydroxy-2-nonenal-Induced Protein Cross-Linking: Structural Characterization of Carnosine−HNE Adducts. Chem. Res. Toxicol., 2003, 16 (12), pp 1589–1597 doi: 10.1021/tx034160a

Long EK, Olson DM, Bernlohr DA. High Fat Diet Induces Changes in Adipose Tissue trans-4-Oxo-2-Nonenal and trans-4-Hydroxy-2-Nonenal Levels in a Depot-Specific Manner. Free radical biology & medicine. 2013;63:390-398. doi:10.1016/j.freeradbiomed.2013.05.030.

Lopez-Castejon G, Borough D.Understanding the mechanism of IL-1β secretion. Cytokine Growth Factor Rev. 2011; 22(4): 189–195.

Lorenzo O, Picatoste B, Ares-Carrasco S, Ramírez E, Egido J, Tuñón J. Potential Role of Nuclear Factor κB in Diabetic Cardiomyopathy. Mediators of Inflammation. 2011;2011:652097. doi:10.1155/2011/652097.

Low Wang CC, Hess CN, Hiatt W, Goldfine AB. Atherosclerotic Cardiovascular Disease and Heart Failure in Type 2 Diabetes – Mechanisms, Management, and Clinical Considerations. Circulation. 2016; 133(24): 2459–2502.

Lundberg JO, Weitzberg E, Gladwin MT. The nitrate–nitrite–nitric oxide pathway in physiology and therapeutics.

Lyubitelev AV, Nikitin DV, Shaytan AK, Studitsky VM, Kirpichnikov MP. Structure and functions of linker histones. Biochemistry. 2015; 81(3): 213-223.

MacDonald MJ, Brown LJ, Longacre MJ, Stoker SW, Kendrick MA, Hasan NM. Knockdown of Both Mitochondrial Isocitrate Dehydrogenase Enzymes In Pancreatic Beta Cells Inhibits Insulin Secretion. Biochimica et biophysica acta. 2013;1830(11):5104-5111. doi:10.1016/j.bbagen.2013.07.013.

Maedler K, Sergeev P, Ris F, Oberholzer J, Joller-Jemelka HI, Spinas GA, Kaiser N, Halban PA, Donath MY. Glucose-induced β cell production of IL-1β contributes to glucotoxicity in human pancreatic islets. J Clin Invest. 2002 Sep 15; 110(6): 851–860. doi: 10.1172/JCI15318

Mahmood T, Yang P-C. Western Blot: Technique, Theory, and Trouble Shooting. North American Journal of Medical Sciences. 2012;4(9):429-434. doi:10.4103/1947-2714.100998.

Mailloux RJ, Bériault R, Lemire J, Singh R, Chénier DR, Hamel RD, Appanna VD. The Tricarboxylic Acid Cycle, an Ancient Metabolic Network with a Novel Twist. PLoS ONE 2007; 2(8): e690. doi:10.1371/journal.pone.0000690

Manhiani PS, Northcutt JK, Han I, Bridges WC, Scott TR, Dawson PL. Effect of stress on carnosine levels in brain, breast, and thigh of broilers. Broiler. Poultry Science.2011; 90 :2348–2354 doi: 10.3382/ps.2011-01426

Mano J, Biswas MS. Analysis of Reactive Carbonyl Species Generated Under Oxidative Stress. Methods Mol Biol. 2018;1743:117-124. doi: 10.1007/978-1-4939-7668-3_11.

Marín-Peñalver JJ, Martín-Timón I, Sevillano-Collantes C, del Cañizo-Gómez FJ. Update on the treatment of type 2 diabetes mellitus. World Journal of Diabetes. 2016;7(17):354-395. doi:10.4239/wjd.v7.i17.354.

Marinis JM, Hutti JE, Homer CR, Cobb BA, Cantley LC , McDonald C, Abbott DW. κB Kinase α Phosphorylation of TRAF4 Downregulates Innate Immune Signaling. Mol. Cell. Biol.2012;32(13): 2479-2489. doi:10.1128/MCB.00106-12

Mashima T, Seimiya H, Tsuruo T. De novo fatty-acid synthesis and related pathways as molecular targets for cancer therapy. British Journal of Cancer. 2009;100(9):1369-1372. doi:10.1038/sj.bjc.6605007.

Mason TM, Goh T, Tchipashvili V, Sandhu H, Gupta N, Lewis GF, Giacca A. Prolonged Elevation of Plasma Free Fatty Acids Desensitizes the Insulin Secretory Response to Glucose In Viv o in Rats. Diabetes.1999; 48:524–530

Massari ME, Murre C. Helix-Loop-Helix Proteins: Regulators of Transcription in Eucaryotic Organisms. Molecular and Cellular Biology. 2000;20(2):429-440.

McCulloch LJ, van de Bunt M, Braun M, Frayn KN, Clark A, Gloyn AL. GLUT2 (SLC2A2) is not the principal glucose transporter in human pancreatic beta cells: Implications for understanding genetic association signals at this locus. Molecular Genetics and Metabolism. 2011; (104):4 648-653

McEvoy B, Sumayao R, Slattery C, McMorrow T, Newsholme P. Cystine accumulation attenuates insulin release from the pancreatic β-cell due to elevated oxidative stress and decreased ATP levels. The Journal of Physiology. 2015;593(23):5167-5182. doi:10.1113/JP271237.

Medeiros BC, Fathi AT, DiNardo CD, Pollyea DA, Chan SM, Swords R. Isocitrate dehydrogenase mutations in myeloid malignancies. Leukemia. 2017;31:272–281. doi:10.1038/leu.2016.275

Melloul D, Marshak S, Cerasi E. Regulation of insulin gene transcription. Diabetologia. 2002;45(3):309-26. doi: 10.1007/s00125-001-0728-y

Miceli V, Pampalone M, Frazziano G, Grasso G, Rizzarelli E, Ricordi C, Casu A, Iannolo G, Conaldi PG. Carnosine protects pancreatic beta cells and islets against oxidative stress damage. Molecular and Cellular Endocrinology. 2018. doi.org/10.1016/j.mce.2018.02.016

Michel NA, Zirlik A, Wolf D. CD40L and Its Receptors in Atherothrombosis-An Update. Front Cardiovasc Med. 2017;4:40. doi:10.3389/fcvm.2017.00040

Miller WL, Bose HS. Early steps in steroidogenesis: intracellular cholesterol trafficking: Thematic Review Series: Genetics of Human Lipid Diseases. Journal of Lipid Research. 2011;52(12):2111-2135. doi:10.1194/jlr.R016675.

Miura A, Yamagata K, Kakei M, Hatakeyama H, Takahashi N, Fukui K, Nammo T, Yoneda K, Inoue Y, Sladek FM., Magnuson MA., Kasai H, Miyagawa J, Gonzalez FJ., Shimomura I. Hepatocyte Nuclear Factor-4α Is Essential for Glucose-stimulated Insulin Secretion by Pancreatic β-Cells. The Journal of Biological Chemistry (2006); 281, 5246-5257.

Monetta P, Slavin I, Romero N, Alverez C. Rab1b interacts with GBF1 and modulates both ARF1 dynamics and COPI association. Mol Biol Cell. (2007); 18(7):2400-2410

Moore B, Jin R.U, Lo H, Jung M, Wang H, Battle MA, Wollheim CB, Urano F, Mills JC. Transcriptional Regulation of X-Box-binding Protein One (XBP1) by Hepatocyte Nuclear Factor 4α (HNF4A) Is Vital to Beta-cell Function. J Biol Chem. 2016; 291(12): 6146–6157

Moore BD, Jin RU, Lo H, et al. Transcriptional Regulation of X-Box-binding Protein One (XBP1) by Hepatocyte Nuclear Factor 4α (HNF4A) Is Vital to Beta-cell Function. The Journal of Biological Chemistry. 2016;291(12):6146-6157. doi:10.1074/jbc.M115.685750.

Morris KR, Lutz RD, Choi H, Kamitani T, Chmura K, Chan ED. Role of the NF-κB Signaling Pathway and κB cis-Regulatory Elements on the IRF-1 and iNOS Promoter Regions in Mycobacterial Lipoarabinomannan Induction of Nitric Oxide. Infect. Immun. 2003 (71)3:1442-1452. doi: 10.1128/IAI.71.3.1442-1452.2003

Nadkarni P, Chepurny OG, Holz GG. Regulation of Glucose Homeostasis by GLP-1. Progress in molecular biology and translational science. 2014;121:23-65. doi:10.1016/B978-0-12-800101-1.00002-8.

Nauck MA. Update on developments with SGLT2 inhibitors in the management of type 2 diabetes. Drug Design, Development and Therapy. 2014;8:1335-1380. doi:10.2147/DDDT.S50773.

Nazaret C, Heiske M, Thurley K, Mazat JP. Mitochondria Energetic Metabolism: A Simplified Model of TCA cycle with ATP production. Journal of theoretical biology. (2009); 258(3):455-464

Ni CZ, Welsh K, Leo E, Chiou CK, Wu H, Reed JC, Ely KR. Molecular basis for CD40 signaling mediated by TRAF3. Proc Natl Acad Sci U S A. 2000; 97(19): 10395–10399.

Nikolaidou-Neokosmidou V, Zannis VI, Kardassis D. Inhibition of hepatocyte nuclear factor 4 transcriptional activity by the nuclear factor κB pathway. Biochemical Journal. 2006;398:439-450. doi:10.1042/BJ20060169.

Odashima M, Otaka M, Jin M, Wada I, Horikawa Y, Matsuhashi T, Ohba R, Hatakeyama N, Oyake Y, Watanabe S. Zinc l-carnosine protects colonic mucosal injury through induction of heat shock protein 72 and suppression of NF-κB activation. Life Sciences. 2006; 79(24): 2245-2250 doi.org/10.1016/j.lfs.2006.07.032

Oeckinghaus A, Ghosh S. The NF-κB Family of Transcription Factors and Its Regulation. Cold Spring Harbor Perspectives in Biology. 2009;1(4):a000034. doi:10.1101/cshperspect.a000034.

Ogata M, Awaji T, Iwasaki N, Fujimaki R, Takizawa M, Maruyama K, Bell G,.I, Iwamoto Y, Uchigata Y. Localization of hepatocyte nuclear factor-4α in the nucleolus and nucleus is regulated by its C-terminus. J Diabetes Investig.2012; 3(5): 449–456

Ogihara T, Mirmira RG. An islet in distress: β cell failure in type 2 diabetes. J Diabetes Invesig.2010;1(4):123-133

Ogryzko V, Schiltz RL, Russanova V, Howard BH, Nakatani Y. The Transcriptional Coactivators p300 and CBP Are Histone Acetyltransferases. Cell. 1996;87(5): 953-959 doi.org/10.1016/S0092-8674(00)82001-2

Oh YS. Mechanistic insights into pancreatic beta-cell mass regulation by glucose and free fatty acids. Anat Cell Biol. 2015 Mar; 48(1): 16–24.

Olokoba AB, Obateru OA, Olokoba LB. Type 2 Diabetes Mellitus: A Review of Current Trends. Oman Medical Journal. 2012;27(4):269-273. doi:10.5001/omj.2012.68.

O'Neill LA, Adinarello C. The IL-1 receptor/toll-like receptor superfamily: crucial receptors for inflammation and host defense. Immunology Today. 2000; 21(5):206-209.

Ormerod AD, Copeland P, Hay I, Husain A, Ewen SW. The inflammatory and cytotoxic effects of a nitric oxide releasing cream on normal skin. J Invest Dermatol. 1999;113(3):392-7. doi: 10.1046/j.1523-1747.1999.00692.x

Orsavova J, Misurcova L, Vavra Ambrozova J, Vicha R, Mlcek J. Fatty Acids Composition of Vegetable Oils and Its Contribution to Dietary Energy Intake and Dependence of Cardiovascular Mortality on Dietary Intake of Fatty Acids. Suphioglu C, ed. International Journal of Molecular Sciences. 2015;16(6):12871-12890. doi:10.3390/ijms160612871.

Ortega A, Berná G, Rojas A, Martín F, Soria B. Gene-Diet Interactions in Type 2 Diabetes: The Chicken and Egg Debate. Int J Mol Sci. 2017; 18(6): 1188.

Otani H, Okumura A, Nagai K, Okumura N. Colocalization of a carnosine-splitting enzyme, tissue carnosinase (CN2)/cytosolic non-specific dipeptidase 2 (CNDP2), with histidine decarboxylase in the tuberomammillary nucleus of the hypothalamus. Neurosci Lett. 2008;445(2):166-9. doi: 10.1016/j.neulet.2008.09.008.

Pacher P, Beckam JS, Liaudet L. Nitric Oxide and Peroxynitrite in Health and Disease. Physiological reviews. 2007;87(1):315-424. doi:10.1152/physrev.00029.2006.

Paul E. Squires, Tracey E. Harris, Shanta J. Persaud, Susan B. Curtis, Alison M.J. Buchan, and Peter M. Jones. The Extracellular Calcium-Sensing Receptor on Human β-Cells Negatively Modulates Insulin Secretion. DIABETES, VOL. 49, MARCH 2000.

Párrizas M, Maestro MA, Boj SF, et al. Hepatic Nuclear Factor 1-α Directs Nucleosomal Hyperacetylation to Its Tissue-Specific Transcriptional Targets. Molecular and Cellular Biology. 2001;21(9):3234-3243. doi:10.1128/MCB.21.9.3234-3243.2001.

Peleg S, Feller C, Ladurner AG, Imhof A. The metabolic impact on histone acetylation and transcription in ageing. Trends in Biochemical Sciences. 2016; 41(8):700-711. doi.org/10.1016/j.tibs.2016.05.008

Pepper ED, Farrell MJ, Nord G, Finkel SE. Antiglycation Effects of Carnosine and Other Compounds on the Long-Term Survival of Escherichia coli . Applied and Environmental Microbiology. 2010;76(24):7925-7930. DOI 10.1128/AEM.01369-10.

Peters V, Zschocke J, Schmitt CP. Carnosinase, diabetes mellitus and the potential relevance of carnosinase deficiency. J Inherit Metab Dis. 2018 Jan;41(1):39-47. doi: 10.1007/s10545-017-0099-2.

Petersen KF, Dufour S, Befroy D, Garcia R, Shulman GI. Impaired Mitochondrial Activity in the Insulin-Resistant Offspring of Patients with Type 2 Diabetes. The New England journal of medicine. 2004;350(7):664-671. doi:10.1056/NEJMoa031314.

Phipps RP. Atherosclerosis: The emerging role of inflammation and the CD40–CD40 ligand system. Proceedings of the National Academy of Sciences of the United States of America. 2000;97(13):6930-6932.

Pi J, Bai Y, Zhang Q, Wong V, Floering LM, Reece JM, et al. Reactive Oxygen Species as a Signal in Glucose-Stimulated Insulin Secretion. Diabetes 2007; 56(7): 1783-1791. doi:org/10.2337/db06-1601.

Poitout V, Amyot J, Semache M, Zarrouki B, Hagman D, Fontésa G. Glucolipotoxicity of the Pancreatic Beta Cell. Biochim Biophys Acta. 2010; 1801(3): 289–298.

Pitocco D, Tesauro M, Alessandro R, Ghirlanda G, Cardillo C. Oxidative Stress in Diabetes: Implications for Vascular and Other Complications. International Journal of Molecular Sciences. 2013;14(11):21525-21550. doi:10.3390/ijms141121525.

Pivovarova O, von Loeffelholz C, Ilkavets I, et al. Modulation of insulin degrading enzyme activity and liver cell proliferation. Cell Cycle. 2015;14(14):2293-2300. doi:10.1080/15384101.2015.1046647.

Plaisance V, Waeber G, Regazzi R, Abderrahmani A. Role of MicroRNAs in Islet Beta-Cell Compensation and Failure during Diabetes. J Diabetes Res. 2014; 2014: 618652

Plunter H, Cox A.,D, Pind S, Khosarvi-Far R, Bourne J.,R, Schwaninger R, Der C.,J, Balcg W.,E. Rab1B Regulates Vesicular Transport Between the Endoplasmic Reticulum and Successive Golgi Compartments. The journal of Cell Biology.1995; 115(1); 31-43

Poitout V, Amyot J, Semache M, Zarrouki B, Hagman D, Fontés G. Glucolipotoxicity of the Pancreatic Beta Cell. Biochimica et biophysica acta. 2010;1801(3):289-298. doi:10.1016/j.bbalip.2009.08.006.

Pomerantz J, Baltimore D. NF-κB activation by a signalling containing TRAF2, TANK, and TBK1, a novel IKK-related kinase. The EMBO Journal 1999; 18(23): 6694-6704.

Porter RK, Brand MD. Mitochondrial proton conductance and H+/O ratio are independent of electron transport rate in isolated hepatocytes. Biochemical Journal. 1995;310(Pt 2):379-382.

Portillo J-AC, Greene JA, Okenka G, Yangling M, Sheibani N, Kern TS, Subauste CS. CD40 promotes the development of early diabetic retinopathy in mice. Diabetologia. 2014;57(10):2222-2231. doi:10.1007/s00125-014-3321-x.

Prause M, Christensen DP, Billestrup N, Mandrup-Poulsen T. JNK1 Protects against Glucolipotoxicity-Mediated Beta-Cell Apoptosis. Abderrahmani A, ed. PLoS ONE. 2014;9(1):e87067. doi:10.1371/journal.pone.0087067.

Prokopieva VD, Yarygina EG, Bokhan NA, Ivanova SA. Use of Carnosine for Oxidative Stress Reduction in Different Pathologies. Oxidative Medicine and Cellular Longevity. 2016; 2939087, 8. doi:10.1155/2016/2939087

Pryor R, Cabreiro F. Repurposing metformin: an old drug with new tricks in its binding pockets. Biochemical Journal. 2015;471:307-322. doi:10.1042/BJ20150497.

Rami A,Behdani M, Yardehnavi N, Habibi-Anbouhi M, Kazemi-Lomedasht F. An overview on application of phage display technique in immunological studies. Asian Pacific Journal of Tropical Biomedicine. 2017;7(7):599-602. doi.org/10.1016/j.apjtb.2017.06.001

Regazzi R, Wollheim CB, Lang J, Theler JM, Rossetto O, Montecucco C, Sadoul K, Weller U, Palmer M, Thorens B. VAMP-2 and cellubrevin are expressed in pancreatic -cells and are essential for Ca2+- but not for GTPyS-induced insulin secretion. The EMBO Journal 1995;(14):12 2723-2730

Reinehr T. Type 2 diabetes mellitus in children and adolescents. World Journal of Diabetes. 2013;4(6):270-281. doi:10.4239/wjd.v4.i6.270.

Rizvi M, Pathak D, Freedman JE, Chakrabarti S. CD40–CD40 ligand interactions in oxidative stress, inflammation and vascular disease. 2008;14(12):530-538. doi.org/10.1016/j.molmed.2008.09.006

Roberts LD, Ashmore T, Kotwica AO, Murfitt SA, et al. Inorganic Nitrate Promotes the Browning of White Adipose Tissue Through the Nitrate Nitrite-Nitric Oxide Pathway. Diabetes 2015;64:471–484. DOI: 10.2337/db14-0496

Robertson, R.P. 2004. Chronic oxidative stress as a central mechanism for glucose toxicity in pancreatic islet beta cells in diabetes. J. Biol. Chem. 279:42351-42354.

Robertson RP, Harmon JS. Pancreatic Islet β-cell and Oxidative Stress: the Importance of Glutathione Peroxidase. FEBS letters. 2007;581(19):3743-3748. doi:10.1016/j.febslet.2007.03.087.

Robertson RP, Harmon J, Tran PO, Poitout V. Beta-cell glucose toxicity, lipotoxicity, and chronic oxidative stress in type 2 diabetes. Diabetes. 2004;53 1:S11924. doi.org/10.2337/diabetes.53.2007.S119

Röder PV , Wu B, Liu Y, Han W. Pancreatic regulation of glucose homeostasis. Experimental & Molecular Medicine 2016, 48, e219; doi:10.1038/emm.2016.6

Rogers C, Davis B, Neufer PD, Murphy MP, Anderson EJ, Robidoux J. A transient increase in lipid peroxidation primes preadipocytes for delayed mitochondrial inner membrane permeabilization and ATP depletion during prolonged exposure to fatty acids. Free radical biology & medicine. 2014;67:330-341. doi:10.1016/j.freeradbiomed.2013.11.012.

Rorsman P, Eliasson L, Renström E, Gromada J, Barg S, Göpel S. The Cell Physiology of Biphasic Insulin Secretion. News Physiol. Sci. 2000 15: 72-77

Rosenbloom AL, Silverstein JH, Amemiya S, Zeitler P, Klingensmith GJ. ISPAD Clinical Practice Consensus Guidelines 2006-2007. Type 2 diabetes mellitus in the child and adolescent. Pediatr Diabetes. 2008;9(5):512-26. doi: 10.1111/j.1399-5448.2008.00429.x.

Sadaccaa L, Bruno J, Wena J, Xionga W. McGraw T.E. Specialized sorting of GLUT4 and its recruitment to the cell surface are independently regulated by distinct Rabs. Mol Biol Cell. (2013) 24(16): 2544–2557.

Sauerhöfer S, Yuan G, Braun GS, Deinzer M, Neumaier M, Gretz N, Floege J, Kriz W, van der Woude F, Moeller MJ. L-Carnosine, a Substrate of Carnosinase-1, Influences Glucose Metabolism. Diabetes 2007 Oct; 56(10): 2425-2432. doi.org/10.2337/db07-0177

Schmid AI, Szendroedi J, Chmelik M, Krššák M, Moser E, Roden M. Liver ATP Synthesis Is Lower and Relates to Insulin Sensitivity in Patients With Type 2 Diabetes. Diabetes Care. 2011;34(2):448-453. doi:10.2337/dc10-1076.

Seijkens. Kusters P, Engel D, Lutgens E. CD40-CD40L: Linking Pancreatic, adipose tissue and vascular inflammation in type 2 diabetes and its complications. Diabetes & Vascular Disease Research. 2012; 10(2) 115–122. doi: 10.1177/1479164112455817

Semchyshyn HM. Reactive Carbonyl Species In Vivo: Generation and Dual Biological Effects. The Scientific World Journal. 2014;2014:417842. doi:10.1155/2014/417842.

Sepp E, Kolk H, Lõivukene K, Mikelsaar M. Higher blood glucose level associated with body mass index and gut microbiota in elderly people. Microbial Ecology in Health and Disease. 2014;25:10.3402/mehd.v25.22857. doi:10.3402/mehd.v25.22857.

Sharma M, Nazareth I, Petersen I. Trends in incidence, prevalence and prescribing in type 2 diabetes mellitus between 2000 and 2013 in primary care: a retrospective cohort study. BMJ Open 2016;6:e010210. doi:10.1136/bmjopen-2015-010210

Sharma P, Chinaranagari S, Chaudhary J. Inhibitor of Differentiation 4 (ID4) Acts as an Inhibitor of ID-1, -2 and -3 and Promotes basic Helix Loop Helix (bHLH) E47 DNA Binding and Transcriptional Activity. Biochimie. 2015;112:139-150. doi:10.1016/j.biochi.2015.03.006.

Shih VF, Tsui R, Caldwell A, Hoffmann A. A single NFκB system for both canonical and non-canonical signaling. Cell Res. 2010;21(1):86-102.

Shin J-S, Park S-J, Ryu S, et al. Potent anti-inflammatory effect of a novel furan-2,5-dione derivative, BPD, mediated by dual suppression of COX-2 activity and LPS-induced inflammatory gene expression via NF-κB inactivation. British Journal of Pharmacology. 2012;165(6):1926-1940. doi:10.1111/j.1476-5381.2011.01670.x.

Simon PS, Sharman SK, Lu C, et al. The NF-κB p65 and p50 homodimer cooperate with IRF8 to activate iNOS transcription. BMC Cancer. 2015;15:770. doi:10.1186/s12885-015-1808-6.

Ślebioda TJ, Kmieć Z. Tumour Necrosis Factor Superfamily Members in the Pathogenesis of Inflammatory Bowel Disease. Mediators of Inflammation. 2014;2014:325129. doi:10.1155/2014/325129.

Smolkova K, Jezek P. The Role of Mitochondrial NADPH-Dependent Isocitrate Dehydrogenase in Cancer Cells. International Journal of Cell Biology. 2012; 273947. doi:10.1155/2012/273947

Sola D, Rossi L, Schianca GPC, et al. Sulfonylureas and their use in clinical practice. Archives of Medical Science : AMS. 2015;11(4):840-848. doi:10.5114/aoms.2015.53304

Solinas G, Becattini B. JNK at the crossroad of obesity, insulin resistance, and cell stress response. Molecular Metabolism. 2017;6(2):174-184. doi:10.1016/j.molmet.2016.12.001.

Somanath S, Barg S, Marshall C, Silwood CJ, Turner MD. High extracellular glucose inhibits exocytosis through disruption of syntaxin 1A-containing lipid rafts. Biochemical and Biophysical Research Communications. 2009; 389(2): 241–246. doi.org/10.1016/j.bbrc.2009.08.126

Somesh BP, Verma MK, Sadasivuni MK, Mammen-Oommen A, et al. Chronic glucolipotoxic conditions in pancreatic islets impair insulin secretion due to dysregulated calcium dynamics, glucose responsiveness and mitochondrial activity. BMC Cell Biol. 2013; 14: 31.

Song ES, Rodgers DW, Hersh LB. Insulin-degrading enzyme is not secreted from cultured cells. Scientific Reports. 2018; 8:2335. doi:10.1038/s41598-018-20597-6

Stein R, Henderson E, Cordle SR. Analysis of an insulin gene transcription control element. Positive and negative regulation appears to be mediated by different element sequences. FEBS Lett. 1994:31;338(2):187-90.

Stoffel M, Duncan SA. The maturity-onset diabetes of the young (MODY1) transcription factor HNF4a regulates expression of genes required for glucose transport and metabolism. Proc. Natl. Acad. Sci. USA. 1997;94(24): 13209–13214

Striegel DA , Hara M, Periwa V. The Beta Cell in Its Cluster: Stochastic Graphs of Beta Cell Connectivity in the Islets of Langerhans. PLOS Computational Biology; 2015. doi:10.1371/journal.pcbi.1004423

Struhl K. Histone acetylation and transcriptional regulatory mechanisms. Genes & Dev. 1998; 12: 599-606.

Stuerenburg HJ, Kunze K. Concentrations of free carnosine (a putative membrane-protective antioxidant) in human muscle biopsies and rat muscles. Arch Gerontol Geriatr. 1999;29(2):107-13. DOI 10.1016/S0167-4943(99)00020-5

Stützer I, Esterházy D, Stoffel M. The pancreatic beta cell surface proteome. Diabetologia. 2012;55(7):1877-89.

Sugawara T, Kane F, Murata M. Rab2A is a pivotal switch protein that promotes either secretion or ER-associated degradation of (pro)insulin in insulin secreting cells. SciRep. (2014); 4:6952

Summers SA, Whiteman W, Birnbaum MJ. Insulin signaling in the adipocyte. International Journal of Obesity. 2000;24(4): S67-S70.

Squires PE, Harris TE, Persaud SJ, Curtis SB, Buchan AMJ, Jones PM. The Extracellular Calcium-Sensing Receptor on Human β-Cells Negatively Modulates Insulin Secretion. DIABETES, VOL. 49, 2000.

Tak PP, Firestein GS. NF-κB: a key role in inflammatory diseases. Journal of Clinical Investigation. 2001;107(1):7-11.

Takahashi H, McCaffery JM, Irizarry RA, Boeke JD. Nucleocytosolic Acetyl-Coenzyme A Synthetase Is Required for Histone Acetylation and Global Transcription. Molecular Cell. (2006) 23, 207–217

Tang W-J. Targeting insulin-degrading enzyme to treat type 2 diabetes. Trends in endocrinology and metabolism: TEM. 2016;27(1):24-34. doi:10.1016/j.tem.2015.11.003.

Targher G, Zenari L, Bertolini L, Muggeo M, Zoppini G. Elevated levels of interleukin-6 in young adults with type 1 diabetes without clinical evidence of microvascular and macrovascular complications. Diabetes Care. 2001;24(5):956-7.

Terauchi Y, Takamoto I, Kubota N, Matsui J, Suzuki R, Komeda K, Hara A, et al. Glucokinase and IRS-2 are required for compensatory β cell hyperplasia in response to high-fat diet–induced insulin resistance. J Clin Invest. 2007;117(1):246–257. doi:10.1172/JCI17645.

Tian C, Alomar F, Moore CJ, et al. Reactive carbonyl species and their roles in sarcoplasmic reticulum ca2+ cycling defect in the diabetic heart. Heart failure reviews. 2014;19(1):101-112. doi:10.1007/s10741-013-9384-9.

Tiedge M, Lortz S, Drinkgern J, Lenzen S. Relation between antioxidant enzyme gene expression and antioxidative defense status of insulin-producing cells. Diabetes. 1997 Nov;46(11):1733-42.

Tisdale EJ, Kelly C, Artalejo CR. Glyceraldehyde-3-phosphate Dehydrogenase Interacts with Rab2 and Plays an Essential Role in Endoplasmic Reticulum to Golgi Transport Exclusive of Its Glycolytic Activity. The Journal of Biological Chemistry. (2004); 279, 54046-54052.

Tiso M, Schlechter AN. Nitrate Reduction to Nitrite, Nitric Oxide and Ammonia by Gut Bacteria under Physiological Conditions. PLoS ONE 10(3): e0119712. doi:10.1371/journal.pone.0119712

Tone M, Tone Y, Babik JM, Lin C, Waldmann H. The Role of Sp1 and NF-κB in Regulating CD40 Gene Expression. The Journal of Biological Chemistry 2001; 277, 8890-8897.

Tone M, Tone Y, Fairchild PJ, Wykes M, Waldmann H. Regulation of CD40 function by its isoforms generated through alternative splicing. PNAS; 2001. 98 (4) 1751-1756. doi.org/10.1073/pnas.98.4.1751

Tong DL, Boocock DJ, R. Dhondalay GK, Lemetre C, Ball GR. Artificial Neural Network Inference (ANNI): A Study on Gene-Gene Interaction for Biomarkers in Childhood Sarcomas. Pappalardo F, ed. PLoS ONE. 2014;9(7):e102483. doi:10.1371/journal.pone.0102483.

Triplitt C, Cersosimo E, DeFronzo RA. Pioglitazone and alogliptin combination therapy in type 2 diabetes: a pathophysiologically sound treatment. Vascular Health and Risk Management. 2010;6:671-690.

Tundo GR, Sbardella D, Ciaccio C, Bianculli A, Orlandi A, Desimio MG, Arcuri G, Coletta M, Marini S. Insulin-degrading Enzyme (IDE) A NOVEL HEAT SHOCK-LIKE PROTEIN. The Journal of Biological Chemistry. 2012; 288, 2281-2289. doi: 10.1074/jbc.M112.393108.

Turner BM. Histone acetylation and control of gene expression. Journal of cell science. (1991); 99: 13-20.

Turner MD. The identification of TNFR5 as a therapeutic target in diabetes, Expert Opinion on Therapeutic Targets. 2017;21:4, 349-351. DOI:10.1080/14728222.2017.1297426

Urazaev AKH, Naumenko NV, Nikolsky EE, Vyskocil F. Carnosine and other imidazole-containing compounds enhance the postdenervation depolarization of the rat diaphragm fibres. Physiol Res. 1998;47(4):291-5.

Van Kooten C, Banchereau J. CD40-CD40 ligand. J Leukoc Biol. 2000;67(1):2-17. doi.org/10.1002/jlb.67.1.2

Varanoske AN, Hoffman JR, Church DD, et al. Influence of Skeletal Muscle Carnosine Content on Fatigue during Repeated Resistance Exercise in Recreationally Active Women. Nutrients. 2017;9(9):988. doi:10.3390/nu9090988.

Veiga-da-Cunha M, Chevalier N, Stroobant V, Vertommen D, Van Schaftingen E. Metabolite Proofreading in Carnosine and Homocarnosine Synthesis: MOLECULAR IDENTIFICATION OF PM20D2 AS β-ALANYL-LYSINE DIPEPTIDASE. The Journal of Biological Chemistry. 2014;289(28):19726-19736. doi:10.1074/jbc.M114.576579.

Verdone L, Agricola E, Caserta M, Di Mauro E. Histone acetylation in gene regulation, Briefings in Functional Genomics.2006;5(3):209–221. doi.org/10.1093/bfgp/ell028

Véret J, Bellini L, Giussani P, Ng C, Magnan C, Le Stunff H. Roles of Sphingolipid Metabolism in Pancreatic β Cell Dysfunction Induced by Lipotoxicity. Journal of Clinical Medicine. 2014;3(2):646-662. doi:10.3390/jcm3020646.

Vidal N, Cavaille JP, Graziani F, et al. High throughput assay for evaluation of reactive carbonyl scavenging capacity. Redox Biology. 2014;2:590-598. doi:10.10 16/j.redox.2014.01.016.

Vosters O, Beuneu C, Nagy N, Movahedi B, Aksoy E, Salmon I, Pipeleers D, Goldman M, Verhasselt V. CD40 expression on human pancreatic duct cells: role in nuclear factor-kappa B activation and production of pro-inflammatory cytokines. Diabetologia.2004; 47:660–668.

Wang H, Maechler P, Antinozzi PA, Hagenfeldt KA, Wollheim CB. Hepatocyte Nuclear Factor 4α Regulates the Expression of Pancreatic β-Cell Genes Implicated in Glucose Metabolism and Nutrient-induced Insulin Secretion. The Journal of Biological Chemistry. 2000;275:35953-35959. doi: 10.1074/jbc.M006612200

Wang J, Wang H. Oxidative Stress in Pancreatic Beta Cell Regeneration. Oxidative Medicine and Cellular Longevity. 2017;2017:1930261. doi:10.1155/2017/1930261.

Wang X, Misawa R, Zielinski MC, Cowen P,Jo J, Periwal V, Ricordi C, Khan A, Szust J, Shen J, Millis JM, Witkowski P, Hara M. Regional Differences in Islet Distribution in the Human Pancreas - Preferential Beta-Cell Loss in the Head Region in Patients with Type 2 Diabetes. PLoS One. 2013; 8(6): e67454.

Watson, J. B., Coulter, P. M., II, Xia, Y.-R., Lusis, A. J. Mouse chromosomal localization of the cortexin (Ctxn) gene. Genomics. 1994; 22: 251-252.

Weber D, Milkovic L, Bennett SJ, Griffiths HR, Zarkovic N, Grune T. Measurement of HNE-protein adducts in human plasma and serum by ELISA—Comparison of two primary antibodies. Redox Biology. 2013;1(1):226-233. doi:10.1016/j.redox.2013.01.012.

Wellen KE, Hatzivassiliou G, Sachdeva UM, Bui TV, Cross JR, Thompson CB. ATP-citrate lyase links cellular metabolism to histone acetylation. Science (New York, NY). 2009;324(5930):1076-1080. doi:10.1126/science.1164097.

Weir GC, Bonner-Weir S. A dominant role for glucose in β cell compensation of insulin resistance. J Clin Invest. 2007;117(1):81–83. doi:10.1172/JCI30862.

White K, Kim M-J, Han C, Park HJ, Ding D, Boyd K, Walker L, Linser P, Meneses Z, Slade C, Hirst J, Santostefeno K, Terada N, Miyakawa T, Tanokura M, Salvi R, Someya S. Loss of IDH2 Accelerates Age-related Hearing Loss in Male Mice. Scientific Reports. 2018;8:5039. doi:10.1038/s41598-018-23436-w.

Wice BM, Bernal-Mizrachi E, Permutt MA. Glucose and other insulin secretagogues induce, rather than inhibit, expression of Id-1 and Id-3 in pancreatic islet beta cells. Diabetologia. 2001;44(4):453-63. doi.org/10.1007/s001250051643

Woodman P. Vesicle transport: More work for the Rabs? Current Biology. 1998;8(6):R199–R201 doi.org/10.1016/S0960-9822(98)70124-1

Wolin MS, Gupte SA, Oeckler RA. Superoxide in the vascular system. J Vasc Res. 2002;39(3):191-207. doi: 10.1159/000063685

Wright TC, Cant JP, Brenna JT, McBride BW. Acetyl-CoA Carboxylase Shares Control of Fatty Acid Synthesis with Fatty Acid Synthase in Bovine Mammary Homogenate. Journal of Dairy Science; 2006 (89) 7;2552-2558 doi:10.3168/jds.S0022-0302(06)72331-1

Wu H, Arron JR. TRAF6, a molecular bridge spanning adaptive immunity, innate immunity and osteoimmunology. Bioessays. 2003;25(11):1096-105. doi: 10.1002/bies.10352

Wu N, Yang M, Gaur U, Xu H, Yao Y, Li D. Alpha-Ketoglutarate: Physiological Functions and Applications. Biomolecules & Therapeutics. 2016;24(1):1-8. doi:10.4062/biomolther.2015.078.

Xiong QY, Yu C, Zhang Y, Ling L, Wang L, Ga J. Key proteins involved in insulin vesicle exocytosis and secretion. Biomedical Reports. 2017; 6: 134-139. doi.org/10.3892/br.2017.839

Xu Y, Chang L, Huang A, et al. Functional Detection of TNF Receptor Family Members by Affinity-Labeled Ligands. Scientific Reports. 2017; 7:6944. doi:10.1038/s41598-017-06343-4.

Yang Q, Yamagata K, Fukui K, Cao Y, Nammo T, Iwahashi H, Wang H, Matsumura I, Hanafusa T, Bucala R, Wollheim CB, Miyagawa J-I, Matsuzawa Y. Hepatocyte Nuclear Factor-1α Modulates Pancreatic β-Cell Growth by Regulating the Expression of Insulin-Like Growth Factor-1 in INS-1 Cells. Diabetes 2002; 51(6): 1785-1792. doi.org/10.2337/diabetes.51.6.1785

Yamagata K. Roles of HNF1a and HNF4a in Pancreatic b-Cells: Lessons from a Monogenic Form of Diabetes (MODY). Vitamins and Hormones. 2014; 95: 407-423

Yamagata K, Furuta H, Oda N, Kaisaki P,.J, Menzel S, Cox N,.J, Fajans S,.S, Signorini S, Stoffel M, Bell G,.I. Mutations in the hepatocyte nuclear factor-4α gene in maturity-onset diabetes of the young (MODY1). Nature (1996) 384(5) 458-460.

Yao X, Wu J, Lin M, et al. Increased CD40 Expression Enhances Early STING-Mediated Type I Interferon Response and Host Survival in a Rodent Malaria Model. Gazzinelli RT, ed. PLoS Pathogens. 2016;12(10):e1005930. doi:10.1371/journal.ppat.1005930.

Ye J, DeBose-Boy RA. Regulation of Cholesterol and Fatty Acid Synthesis. Cold Spring Harb Perspect Biol. (2011); 3(7): a004754.

Yu W, Dittenhafer-Reed KE, Denu JM. SIRT3 Protein Deacetylates Isocitrate Dehydrogenase 2 (IDH2) and Regulates Mitochondrial Redox Status. The Journal of Biological Chemistry. 2012;287(17):14078-14086. doi:10.1074/jbc.M112.355206.

Zamora R, Vodovotz Y, Billiar TR. Inducible nitric oxide synthase and inflammatory diseases. Molecular Medicine. 2000;6(5):347-373.

Zhang T, Kim DH, Xiao X, Lee S, Gong Z, Muzumdar R, Calabuig-Navarro V, Yamauchi J, Harashima H, Wang R, Bottino R Alvarez-Perez JC, Garcia-Ocaña A, Gittes G, Dong HH. FoxO1 Plays an Important Role in Regulating β-Cell Compensation for Insulin Resistance in Male Mice. Endocrinology. 2016; 157(3): 1055–1070.

Zhang Q, Didonato JA, Karin M, Mckeithan TW. BCL3 Encodes a Nuclear Protein Which Can Alter the Subcellular Location of NF-KB Proteins. Molecular and Cellular Biology. 1994;(4)6:3915-3926

Zhang Q, Xiao X, Li M, et al. Acarbose Reduces Blood Glucose by Activating miR-10a-5p and miR-664 in Diabetic Rats. Ahmad R, ed. PLoS ONE. 2013;8(11):e79697. doi:10.1371/journal.pone.0079697.

Zhao S, Torres A, Henry RA, et al. ATP-citrate lyase controls a glucose-to-acetate metabolic switch. Cell reports. 2016;17(4):1037-1052. doi:10.1016/j.celrep.2016.09.069.

Zhou BR, Jiang J, Feng H, Ghirlando R, Xiao TS, Bai Y. Structural Mechanisms of Nucleosome Recognition by Linker Histones. Mol Cell. 2015; 59(4): 628–638..

Zhuang X, Adipietro KA, Datta S, Northup JK, Ray K. Rab1 Small GTP-Binding Protein Regulates Cell Surface Trafficking of the Human Calcium-Sensing Receptor. Endocrinology. 2010;151(11):5114-5123. doi:10.1210/en.2010-0422.

Zotti T, Vito P, Stilo R. The Seventh Ring: Exploring TRAF7 Functions J Cell Physiol. 2012;227(3):1280-4. doi: 10.1002/jcp.24011

Webpage references

Abcam. 2018. NF-κB inhibitors and activators. < https://www.abcam.com/reagents/nf-kb-small-molecule-guide> 11.02.2018

American Diabetes Association. 2018. Complications. < http://www.diabetes.org/living-with-diabetes/complications/>. 08.02.2018

Creative Diagnostic. 2017. The NF-kB Signaling Pathway. < https://www.creative-diagnostics.com/The-NF-kB-Signaling-Pathway.htm>. 11.02.2018

Diabetes UK. 2017. Type 2 Diabetes. < https://www.diabetes.org.uk/diabetes-the-basics/what-is-type-2-diabetes>. 10.02.2018

Medical Dictionary. Pancreas. < https://medical-dictionary.thefreedictionary.com/pancreas> 21.06.2018

Public Health England. 2001. National service framework: diabetes. < https://www.gov.uk/government/publications/national-service-framework-diabetes> 10.02.2018

Superfoodly. 2017. 40 Highest Food Sources of Carnosine and Benefits Studied. < https://www.superfoodly.com/carnosine-benefits-and-natural-food-sources/> 01.06.2018

Whatisepigenetics. Histone Modifications. < https://www.whatisepigenetics.com/histone-modifications/> 20.03.2018

World Health Organization. 2011. Use of glycated haemoglobin (HbA1c) in the diagnosis of diabetes mellitus. United Nations. < http://www.who.int/diabetes/publications/diagnosis_diabetes2011/en/> 10.02.2018